Recent advances in high-temperature solid looping processes toward commercial application

International Journal of Greenhouse Gas Control 155 (2026) 104718

Contents lists available at ScienceDirect

International Journal of Greenhouse Gas Control

journal homepage: www.elsevier.com/locate/ijggc

Recent advances in high-temperature solid looping processes toward commercial application

Martin Greco-Coppi [a,*], Xiaoyun Li [b], Falko Marx [a], Borja Arias [c], Gemma Grasa [d], Alberto Abad [d], Francisco García-Labiano [d], Tobias Mattisson [b], Jochen Ströhle [a,*]

[a] Technical University of Darmstadt, Department of Mechanical Engineering, Institute for Energy Systems and Technology, Otto-Berndt-Str. 2, Darmstadt, 64287, Germany
[b] Division of Energy Technology, Department of Space, Earth and Environment, Chalmers University of Technology, Gothenburg, 412 96, Sweden
[c] Instituto de Ciencia y Tecnología del Carbono (INCAR-CSIC), C/Francisco Pintado Fe, N26, Oviedo, 33011, Spain
[d] Instituto de Carboquímica (ICB-CSIC), C/Miguel Luesma Castán, 4, Zaragoza, 50018, Spain

ARTICLE INFO

Keywords:
Carbonate looping
Calcium looping
Chemical looping
Combustion
Gasification
Reforming
CO_2 capture
High-temperature solid looping

ABSTRACT

Over the last ten years, *high-temperature solid looping* (HTSL) technologies have received considerable interest from industry and academia, with important progress toward commercialization. There are three main HTSL concepts: (i) *carbonate looping*, based on the reversible carbonation of a metal oxide for separating CO_2 from a gas stream; (ii) *chemical looping*, which utilizes the reversible oxidation and reduction of a metal for separating oxygen from air; and (iii) *indirect gasification* that uses the sensible heat contained in a hot solid to drive gasification (an endothermic reaction). Different HTSL process variants are used for various CO_2 capture applications, such as post-combustion capture, oxyfuel combustion, or pre-combustion capture through gasification and reforming. In this review, we focus on HTSL processes that have reached a high level of maturity, so that commercialization could be expected within the next 5–10 years. This implies that the processes have already been validated in industrially relevant environments, such as pilot testing in continuous operation. Throughout this work, we explain the basic principles of the different HTSL processes and discuss recent advances in arrangements and materials toward reducing costs and energy requirements for CO_2 capture from industrial sources. Furthermore, our review provides an overview of existing HTSL pilot plants and the main results from the last 10 years, as well as the latest developments in modeling of HTSL reactors. Lastly, we review the most relevant techno-economic and environmental studies of HTSL processes for various industrial sectors and propose next research steps toward commercial applications in the near future.

1. Introduction

The IPCC Special Report on Carbon dioxide Capture and Storage (IPCC, 2005) pointed out the large energy penalties and costs associated with the most mature CO_2 capture technologies, such as amine scrubbing or oxyfuel combustion. The report also stated that these costs could potentially be reduced by new technologies. Two innovative technologies specifically mentioned in the report were the use of regenerable solid sorbents to remove CO_2 at relatively high temperatures and chemical looping combustion to avoid the need for an air separation unit in oxyfuel combustion. These two technologies have in common that they are based on solid materials circulating between two (or more) reactors operating at high temperatures. Hence, they are called *high-temperature solid looping* (HTSL) processes.

Depending on their basic operating principle, HTSL processes can be classified into three categories (see Fig. 1): (i) *carbonate looping*, (ii) *chemical looping*, and (iii) *indirect gasification*, although combinations are also possible. Carbonate looping processes utilize the reversible reaction of a metal oxide with CO_2 (e.g., $CaO + CO_2 \leftrightarrow CaCO_3$). The CO_2 contained in a gas is absorbed by a metal oxide to form a metal carbonate. In the reverse reaction, the metal carbonate is decomposed into the metal oxide and a highly pure stream of CO_2. Due to thermodynamic constraints, the decomposition reaction occurs at a higher temperature or lower pressure than the absorption reaction. Chemical looping processes utilize the reversible oxidation and reduction of a metal between different oxidation degrees (e.g. Fe_2O_3 and Fe_3O_4). Here, the oxygen

* Corresponding authors.
E-mail addresses: contact@greco-coppi.com (M. Greco-Coppi), jochen.stroehle@est.tu-darmstadt.de (J. Ströhle).

https://doi.org/10.1016/j.ijggc.2026.104718
Received 15 January 2026; Received in revised form 3 June 2026; Accepted 12 June 2026
Available online 29 June 2026

contained in air reacts with a metal oxide to form a metal oxide with a higher oxidation degree. This highly oxidized metal then reacts with combustible gases (e.g. hydrocarbons, CO, or H_2), acting as an oxygen carrier that avoids direct contact between fuel and air and ensures a CO_2 stream inherently free of N_2. Indirect gasification utilizes the sensible heat contained in a hot solid, which is heated by an exothermal reaction (e.g., combustion), to provide the energy to drive an endothermic reaction (e.g., gasification). The principles of these three categories can be used in processes for different CO_2 capture applications, such as post-combustion capture, oxyfuel combustion, or gasification/reforming for pre-combustion capture.

HTSL processes can be realized by various types of reactor systems. The most straightforward concept employs the continuous transfer of solids between coupled fluidized bed reactors. Fluidized beds have the benefit of very good gas-solid mixing and good temperature control. They are very flexible with respect to the feedstock, allowing the conversion of cheap residues and wastes. Fluidized beds are scalable to large sizes, which has been proven for fluidized bed combustion technology with power plants larger than 600 MW_e (Leckner, 2016). Also, the coupling of two fluidized bed reactors is commercially proven for fluid catalytic cracking and indirect gasification (Thunman et al., 2019). However, fluidized beds have some limitations with respect to particle size, residence time, temperature, and pressure, where other reactor types have some distinct advantages. Entrained flow reactors allow the use of very fine particles that are difficult to fluidize (<100 μm), and they can be operated at very high temperatures (above the ash melting temperature). Moving beds realize a plug-flow type behavior of the particles enabling longer residence times. Fixed bed reactors allow a batchwise cyclic operation at changing pressure (so-called pressure swing), which is difficult to realize with coupled fluidized beds. However, all these alternatives are associated with challenges related to poor mixing and temperature control. In this respect, moving and fixed beds have certain restrictions in scalability that can be overcome by designing a system of multiple reactors operating in parallel.

In the last 20 years, various HTSL process variants have been developed and tested. The most important developments until 2015 were summarized by Abanades et al. (2015) as part of the Special Issue commemorating the 10th year anniversary of the publication of the IPCC Special Report on CCS. At that time, the focus was mainly on CO_2 capture from coal-fired power plants, which were (and are still) by far the main emitters of CO_2 worldwide. However, recent advances in power production from renewable sources such as wind and solar suggest that these renewable sources could potentially decarbonize the entire power sector at reasonable cost. Several countries, particularly in Europe, have already placed laws on the phase-out of coal. Hence, the focus in the development of HTSL processes (and other capture technologies) has shifted toward the capture of so-called unavoidable CO_2 emissions, i.e. capture of CO_2 that is generated within a process and cannot be avoided by a shift to renewable fuels or electrical heating. Examples are lime or cement plants, where CO_2 is formed through decomposition of $CaCO_3$, and waste incineration plants, where the main purpose is to manage waste by thermal treatment whereby the carbon contained in the waste is converted to CO_2. Furthermore, the shift away from fossil fuels has put the spotlight on the use of feedstocks that contain a certain fraction of biogenic carbon, such as biomass or waste, thereby lowering the carbon footprint of the HTSL process. In contrast to woody biomass, biogenic residues as well as municipal and industrial wastes have the advantage of a relatively low cost. However, they often have a low ash melting temperature and high chlorine content, which poses challenges related to particle agglomeration, ash deposition, and corrosion on the processes.

The present work aims to review the progress in the development of HTSL processes within the last 10 years. The focus is on processes that have reached a certain level of maturity, so that commercialization could be expected within the next 5–10 years. This implies that the processes have already been validated in an industrially relevant environment, such as pilot testing in continuous operation. Section 2 explains the basic principles of the different HTSL processes and summarizes recent advances in development of improved processes or materials that could reduce energy requirements and costs for CO_2 capture from industrial sources. Section 3 provides an overview of existing HTSL pilot plants and the main results achieved within the last 10 years. Section 4 presents recent developments in modeling the conversion of solids and gases in HTSL reactors. Section 5 reviews recent studies on techno-economic and environmental assessment of HTSL processes for various industrial sectors. Section 6 gives conclusions and an outlook on potential developments in the near future.

2. Process development

2.1. Carbonate looping processes

Carbonate looping (CaL) refers to a group of processes that removes CO_2 from a gas stream through carbonation with the objective of either capturing CO_2 (CaL for carbon capture) or improving the yield of reforming and gasification products (sorption-enhanced CaL), as illustrated in Fig. 2. The different CaL processes vary in technical maturity, complexity, and economic feasibility. These systems generally rely on calcium oxide (CaO) as a regenerable sorbent. Hence, carbonate looping is also referred to as *calcium looping* (Greco-Coppi et al., 2025b). Other CaL concepts using MgO and synthetic lime-based materials have been also proposed, but they have lower technology readiness level (TRL).

The working principle of CaL is summarized in Fig. 3. At high temperatures, a metal oxide (sorbent, typically CaO) reacts with CO_2 to form

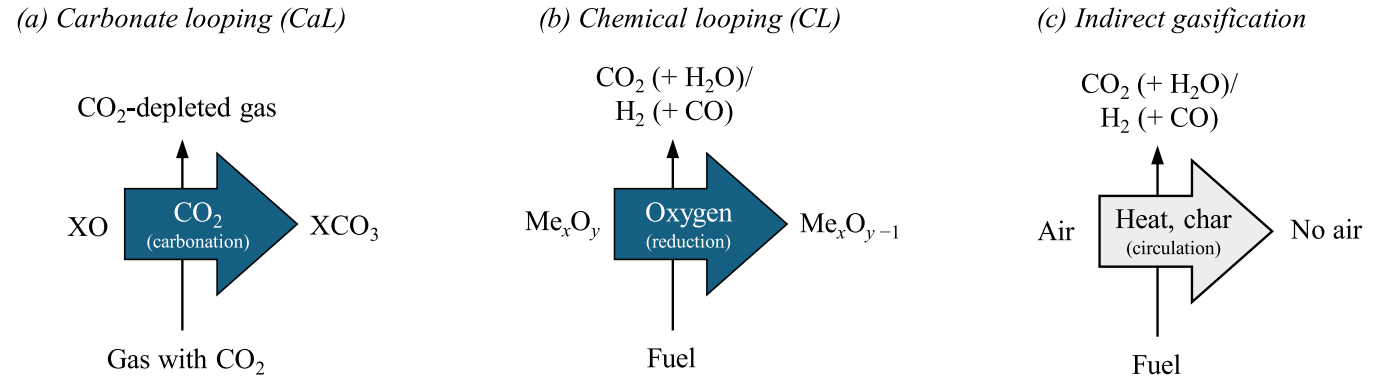

Fig. 1. Overview of the high-temperature solid looping (HTSL) cycles based on their operating principle: (a) in carbonate looping (CaL), an active metal (X, e.g., Ca) is used to remove CO_2 from a gas stream via carbonation; (b) in chemical looping, a metal oxygen carrier (Me_xO_y) is reduced, oxidizing a fuel for combustion, gasification, or reforming; and (c) in indirect gasification, solids circulate between two reactors, enabling heat and char transfer for gasification of a solid fuel in an air-free atmosphere.

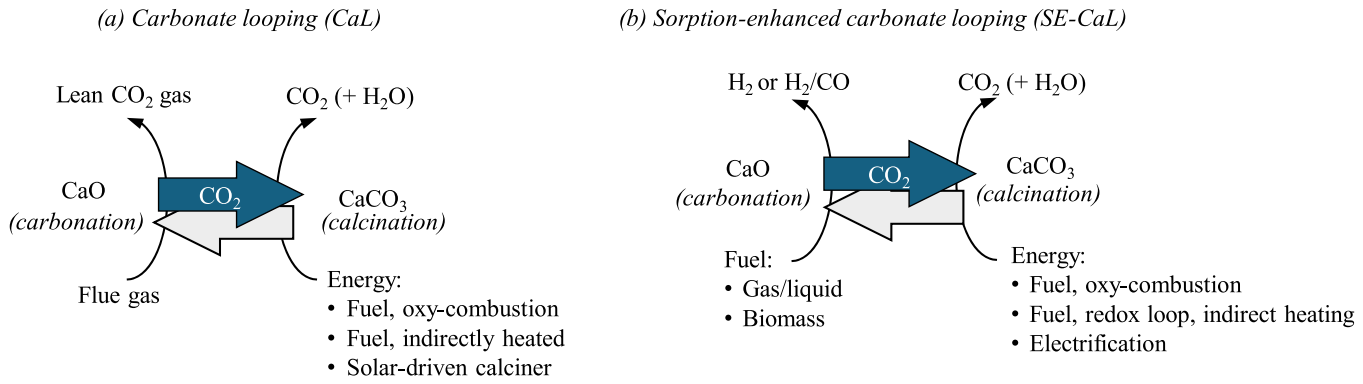

Fig. 2. Overview of carbonate looping (CaL) processes. In the standard CaL process (a), a metal oxide (typically, CaO) is used to remove CO_2 from a gas stream via carbonation for carbon capture. The heat for calcination can be provided by oxy-combustion (oxy-CaL), by indirectly heating from an external combustion chamber (IHCaL), or by solar heating (solar-driven CaL). Sorption-enhanced CaL (b) uses a metal oxide to remove CO_2 from a gas stream via carbonation to enhance the production of H_2 and CO by shifting reaction equilibria.

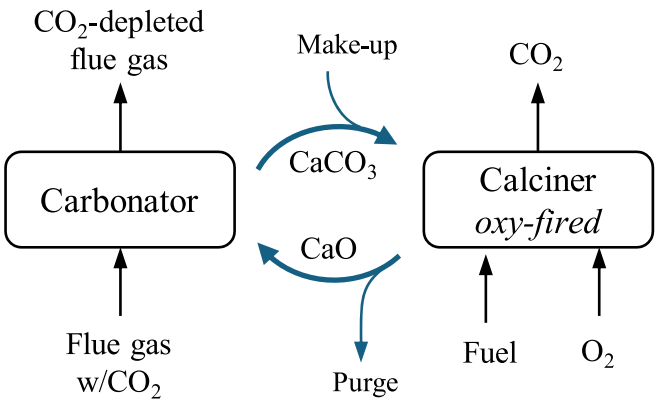

Fig. 3. Scheme of the oxy-fired carbonate looping (CaL) process.

a carbonate (generally, $CaCO_3$), which is then decomposed via calcination in a CO_2-rich environment to regenerate the sorbent via calcination and complete the cycle. When using CaO as the sorbent for CaL, the $CaCO_3$-CaO equilibrium curve defines the temperature ranges suitable for both steps: carbonation at temperatures around 650 °C, so CO_2 concentrations in flue gas can be lowered below 1.2% vol at atmospheric pressure; while calcination temperatures above 900 °C are needed to reach full calcination for high CO_2 concentrations (Greco-Coppi et al., 2025b). These values are based on the equilibrium limitations governed by temperature and CO_2 partial pressure. A key challenge lies in supplying the substantial heat required for $CaCO_3$ decomposition, as the reaction enthalpy is high (168 kJ/mol at 900 °C). Delivering this heat efficiently to a high-temperature reactor remains a critical design issue. There are different strategies to achieve this, such as through in-situ oxy-fire combustion (see Section 2.1.1), indirect-heating from an external combustion chamber (see Section 2.1.2), or by means of solar heating (see Section 2.1.3), or chemical looping (see examples in Section 2.1.4 and Section 2.2.3). The first sections of this chapter focus on CaL for CO_2 capture, and Section 2.1.4 is dedicated to Sorption Enhanced CaL (SE-CaL) for fuel conversion.

2.1.1. *Oxy-fired carbonate looping*

Among the different oxy-fired options (e.g., bubbling bed, entrained flow, rotary kiln), the most advanced approach for the calcination step in CaL systems is oxy-fuel circulating fluidized bed combustion (CFBC). This technology provides high thermal input in compact reactors, uniform combustion temperatures, and extensive solid circulation, making it particularly suitable for large-scale carbonate looping (CaL) applications. Oxy-fuel CFB combustion has already reached a high level of technological maturity (TRL 7–8) (Lupion et al., 2013; Stanger et al., 2015; Yadav and Mondal, 2022; Chen et al., 2023; Kuhn et al., 2025b) and has enabled the scale-up of CaL systems. One of the main advantages of this type of combustor is its fuel flexibility, including the use of biomass and other alternative fuels (e.g., solid recovered fuel, SRF), while simultaneously enabling the capture of acid gases such as SO_2, HCl, and HF (Schakel et al., 2018; Martínez et al., 2018; Haaf et al., 2020d; Neto et al., 2021; Lim et al., 2023; Hanak, 2024). CaL systems are therefore a relevant option for capturing CO_2 from WtE plant exhaust gases due to their inherent capacity to remove these acid species (Haaf et al., 2020a; Lim et al., 2023). Moreover, the use of carbon-neutral fuels can render CFB-CaL systems carbon-negative when the CO_2 released from the calciner is permanently stored or alternatively provide a renewable CO_2 source for the production of CO_2-based synthetic products (IPCC, 2005; IEA, 2020b; Styles et al., 2025).

Nevertheless, one of the main drawbacks of the oxy-fired CFB calciner is the significant energy penalty associated with the air separation unit, which is directly linked to the heat demand of the calciner. As discussed in the following sub-sections, alternative calcination methods to oxy-fuel combustion are being developed to mitigate this penalty. The thermal input to the calciner is primarily determined by the heat of calcination—directly related to the CO_2 captured in the carbonator and the make-up flow of fresh limestone—as well as by the sensible heat of the gas and solid streams entering the reactor. Several approaches have been proposed in recent years to reduce the heat demand in the calciner, mainly by decreasing the circulation of solids (i.e., increasing sorbent activity), lowering the calciner temperature, integrating heat between high-temperature gas and solid streams entering and leaving the reactors, and minimizing CO_2 recycle to the calciner (Perejón et al., 2016; Martínez et al., 2016; Sun et al., 2018; Hanak et al., 2018).

Regarding the carbonation step, the circulating fluidized bed (CFB) configuration is considered the most appropriate due to its ability to handle large gas and solid throughputs. These reactors operate with gas velocities of 3–5 m/s and solid circulation rates of 3–10 kg/m^2·s, values typical of commercial CFB combustors used at large scale in power plants. This configuration has been demonstrated in large-scale pilot plants (TRL 6–7), achieving capture efficiencies above 90% (Kremer et al., 2013; Arias et al., 2013; Dieter et al., 2014). More recently, a CFB carbonator design incorporating a cooled upper section and the injection of $Ca(OH)_2$ as an additional sorbent has been developed to overcome the constraints imposed by the CaO–CO_2 equilibrium, achieving capture efficiencies above 99% (Secomandi et al., 2024; Arias et al., 2024).

The use of turbulent non-circulating fluidized beds has also been tested experimentally (Hornberger et al., 2021). However, these reactors

require larger footprints compared with the fast-fluidized CFB configuration. Turbulent fluidization has been associated with better CO_2 capture efficiencies, which makes it an attractive alternative, as long as high-enough entrainment can be achieved to operate them as CFBs (Greco-Coppi et al., 2024d). Other carbonator concepts analyzed are entrained-flow carbonators. This reactor type can handle fine particles and facilitate their use in cement applications (Spinelli et al., 2018). Nevertheless, their main drawbacks are the reactor length required to achieve sufficient carbonation conversion and the challenges associated with heat extraction. Entrained-flow reactors have also been proposed for CO_2 capture using $Ca(OH)_2$ as a sorbent, taking advantage of its fast carbonation kinetics and high carbonation conversion (Phalak et al., 2013; Criado et al., 2022; Mader et al., 2025). In addition, moving-bed reactor configurations have been analyzed for CO_2 capture that can also benefit from the use of $Ca(OH)_2$ (Abanades et al., 2023; Cui et al., 2025).

As with other capture technologies, the early development of carbonate looping focused on the power sector and on CO_2 removal from large stationary sources operating in base-load mode. However, with the increasing penetration of renewable energy, flexible operation and process configurations that improve techno-economic performance under variable conditions have become critical. Carbonate looping based on fluidized bed reactors offers a certain degree of flexibility, being able to handle flue-gas fluctuations and operate at partial loads down to 40% (Diego and Arias, 2020; Moreno et al., 2021b).

The use of solid storage has also been proposed for CO_2 capture in the steel sector, particularly to manage the fluctuating flue gases produced by Electric Arc Furnaces (EAFs). Configurations incorporating intermediate solids storage offer operational advantages, such as enhanced process stability. Under these conditions, specific fuel consumption as low as 5.85 MJ per kg of CO_2 captured has been reported, with capture efficiencies of around 91% for EAF off-gas (Montiel-Bohórquez et al., 2025). For the more common steelmaking route based on blast furnaces combined with basic oxygen furnaces (BF-BOF), conventional post-combustion CaL process schemes can be applied (Cormos, 2016; Tian et al., 2018).

Carbonate looping is particularly well suited for CO_2 capture in cement plants. Two main approaches have been proposed based on an oxy-fired calciner: the tail-end process and the integrated process (Voldsund et al., 2019; Gardarsdottir et al., 2019; Lena et al., 2019; Amorim et al., 2025). In the tail-end configuration, CO_2 is captured directly from the flue gas emitted at the stack, with no integration between the cement process and the CaL system beyond the use of the CaO-rich purge stream. This option can be retrofitted to existing cement plants and can achieve capture efficiencies of around 90% under conditions similar to those demonstrated in power plants (Atsonios et al., 2015a; Lena et al., 2017). A drawback of this approach is the higher fuel demand—typically 2–3 times that of a benchmark cement plant. However, the excess heat recovered can be used to generate decarbonized electricity, covering plant needs and even allowing export to the grid. Fuel consumption can be reduced by increasing the level of integration, for example by diverting a larger fraction of $CaCO_3$ to the CaL unit instead of the clinker burning line. The specific primary energy consumption for CO_2 avoided (SPECCA) depends on the reference power technology, ranging from 2.7 to 3.7 MJ_{LHV}/kg CO_2 in coal-fired scenarios (Lena et al., 2017).

In the integrated configuration, the oxy-fired calciner produces the calcined material for the kiln and simultaneously supplies a stream of calcined solids to the carbonator, which captures the CO_2 released in the kiln. This setup reduces the overall energy demand of the plant. Two main approaches have been proposed for this configuration. The first involves entrained-flow CaL reactors integrated into the preheater and precalciner of the cement kiln. In this case, calcined raw meal rich in CaO, with particle sizes of 10–20 μm, is used as the CO_2 sorbent in the carbonator loop (Spinelli et al., 2018; Lena et al., 2019). This approach allows a reduction in SPECCA of 15–26% compared with the tail-end configuration (Lena et al., 2019). The second approach is based on circulating fluidized bed (CFB) reactors, which may use either a mixture of limestone and correctives as raw meal in the clinker line or a single raw meal if separation is not feasible. In the first case, particle sizes are adjusted for each stream (Lena et al., 2022). Limestone is ground to 100–200 μm for CFB operation, taking advantage of its natural tendency to undergo attrition and fragmentation during calcination. The coarse calcined fraction is recirculated to the CFB carbonator to capture CO_2 from kiln flue gases, while the finer fraction is fed directly into the kiln. Correctives, by contrast, are ground to 10–20 μm and exit the oxy-fired CFB calciner in a once-through flow. The performance of this configuration depends on the ratio of calcium entering the CaL process relative to the total calcium input of the cement plant and is also affected by the level of fragmentation. Under favorable conditions, specific primary energy consumption for CO_2 avoided values as low as 2.8 MJ/kg CO_2 have been reported (Lena et al., 2022).

Recently, novel CaL configurations employing moving-bed carbonators have been proposed to capture CO_2 from smaller and more dispersed emission sources (Lisbona et al., 2021; Abanades et al., 2023). In this concept, the carbonator and calciner are physically separated, with CO_2 transported between them as $CaCO_3$ at ambient temperature, taking advantage of its high molar density. The moving-bed carbonator design is specifically tailored for decoupled CaL (d-CaL) applications, operating with Ca-solid feeds close to ambient temperature, flue gases at stack conditions, and requiring limited space and auxiliary equipment. The carbonated material is then conveyed to a centralized calciner, where the sorbent is regenerated and returned to the carbonator. High sorbent conversions (up to 0.6–0.8 mol CO_2/mol Ca) can be achieved due to the long residence times in the reactors (Criado et al., 2024), which further reduces the costs associated with solid handling and transport.

2.1.2. *Indirectly heated carbonate looping*

One of the main limitations of the traditional carbonate looping (CaL) process is the high amount of oxygen required for the oxy-fired calciner. This increases operating costs due to electricity requirements in the air separation unit (ASU), as well as investment costs due to the capital expenditures (CAPEX) associated with the ASU (Junk et al., 2013). It has been estimated that this unit accounts for around 15% of the CAPEX (Lena et al., 2022; Fu et al., 2021) and over 40% of the electricity demand (Lena et al., 2022; Haaf et al., 2020a) of a commercial CaL facility.

The disadvantages associated with the ASU can be avoided by providing heat indirectly into the calciner, which removes the requirement of pure oxygen for the in-situ combustion. There are many approaches to indirectly heat the calciner of a CaL process, classified according to the source of the heat: (i) via electrification, using plasma burners, induction, or resistances (Svensson et al., 2021; Jacob and Tokheim, 2023a, 2023b; Bajamundi et al., 2026; and the ELECTRA project, https://www.electra-horizon.eu/); (ii) through addition of steam (Wang et al., 2010; Fan et al., 2012; Ramkumar and Fan, 2010); (iii) using solar heating (discussed in Section 2.1.3); and (iv) from combustion in an external chamber.

The process configuration, in which the heat is provided from an external combustor, is usually referred to as the *indirectly heated carbonate looping* (IHCaL) process (Greco Coppi, 2025). The IHCaL process is illustrated in Fig. 4. Fuel is burnt in an external combustor (indicated in a gray shading) using air. Different fuels can be used, including propane, coal, and refuse-derived fuels (Hofmann et al., 2024b). The off-gas with CO_2 leaves the combustor toward the carbonator for carbon capture. Different strategies have been provided to transfer heat from the external combustor to the calciner. Abanades et al. (2005) proposed transferring heat to a fluidized bed calciner using metallic walls (see also Grasa and Abanades, 2007) or solid heat carriers (see also Diego et al., 2016b, and Martínez et al., 2011). Epple and Seeber (2014) introduced a promising approach that consists in transferring heat via heat

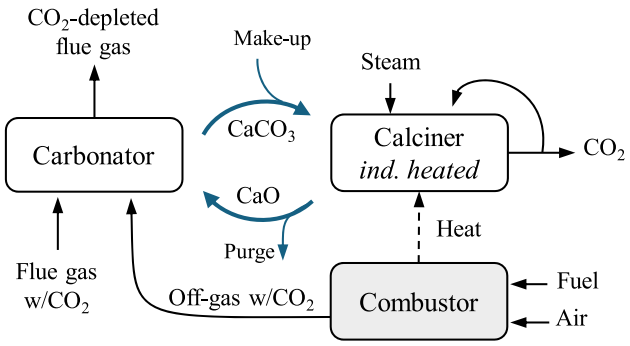

Fig. 4. Scheme of the indirectly heated carbonate looping (IHCaL) process. The external combustor, indicated in a gray shading, provides the heat for the calcination through a heat pipes heat exchanger.

pipes immersed in fluidized beds. IHCaL heat pipes transfer heat through evaporation and condensation of sodium in a closed metal alloy tube with an internal mesh (Höftberger and Karl, 2016; Höftberger, 2016). They offer excellent performance, which explains why this is the only approach that could be validated in pilot operations (Reitz et al., 2016). Thus, the IHCaL process using heat pipes is considered the most advanced version of this technology.

Originally, the IHCaL process has been proposed for CO_2 capture from power plants (Junk et al., 2016a). This approach was studied within the CARINA project (Epple et al., 2016), including pilot tests in the 300-kW_{th} scale. However, the research efforts of the last years have focused on integrating IHCaL technology in cements and lime plants, where synergies in terms of integration of spent sorbent and heat recovery can be exploited, mainly within the ANICA project (Greco-Coppi et al., 2024b; Ströhle et al., 2021). Greco-Coppi et al. (2021a) introduced two concepts for integrating the IHCaL process in lime plants for CO_2 capture (cf. Greco-Coppi et al., 2023a; Greco-Coppi et al., 2021b): (i) a tail-end concept, suitable for retrofitting; and (ii) a fully integrated concept for greenfield projects. Based on a study that considered a 600-tonnes-per-day lime plant in Germany, they indicated that high degrees of heat integration are necessary to keep the heat requirements within reasonable boundaries, inducing the use of a solid-solid heat exchanger and combustion air preheating. The highly integrated concept exhibited significantly lower heat requirements than the tail-end configuration (>30% reduction). Similar results were presented by Peloriadi et al. (2021) for a lime plant in Greece, comprising a double-shaft kiln with a capacity of 150 tonnes of lime per day; thus confirming the observations of Greco-Coppi et al. (2021a). Furthermore, IHCaL configurations can achieve net negative CO_2 emissions in the lime production of more than -1.8 t_{CO2}/t_{CaO} when fuels with a significant biogenic fraction (e.g., SRF) are used in the external combustor (Greco-Coppi et al., 2023b). These CO_2 capture approaches are highly competitive in terms of CO_2 avoidance costs, compared to other capture technologies for the same applications (Greco-Coppi et al., 2024c).

In general, the application of the IHCaL process for lime and cement production is promising in terms of economic indicators, as discussed in Section 5.3. However, the integration of the spent sorbent in the production (cf. Greco-Coppi et al., 2024b), as well as the high heat requirements (cf. Greco-Coppi et al., 2021a) are challenges for the implementation. Furthermore, practical issues related with the operation of the indirectly heated calciner and the heat pipes heat exchanger need to be further addressed prior to commercialization (see Section 3.2.2).

2.1.3. Solar heating and new reaction pathways

In recent years, the integration of solar energy to supply the heat required for the $CaCO_3$ calcination reaction has been proposed within carbonate looping systems. Several technological development pathways have been explored, including *tail-end* CO_2 capture solutions via carbonate looping integrated into cement production (Rincon Duarte et al., 2022; Ferrario et al., 2023), as well as applications in Thermochemical Energy Storage (TCES) systems (see recent reviews by Raganati and Ammendola, 2023; Khan et al., 2024).

The $CaCO_3$/CaO pair has emerged as a promising candidate for TCES due to its high theoretical energy density (3–4 GJ m^{-3}), which enables maximization of storage capacity (Ortiz et al., 2019). In the basic concept of this technology, the endothermic calcination of $CaCO_3$ is carried out in a solar-driven calciner that concentrates solar power, producing CaO and CO_2 as separate stored products. When energy is required, these products are fed into the carbonator, where the exothermic carbonation of CaO releases the stored energy, which can then be harnessed in a power cycle (typically integrated into a combined cycle, CC). Similarly, CaO/$Ca(OH)_2$ hydration-dehydration systems have also been widely investigated for thermochemical energy storage and are based on similar materials and operating temperatures (Rougé et al., 2017; Criado et al., 2017).

Most studies to date rely on process simulations, highlighting the critical role of process integration in adapting carbonate looping technology to Concentrated Solar Power (CSP) plants (Ortiz et al., 2019). Proposed process schemes involve complex networks of high-temperature heat exchangers (gas/gas, gas/solid, and solid/solid), which can theoretically achieve efficiencies of up to 45% when coupled with regenerative CO_2 closed Brayton cycles—excluding the efficiency of the solar receiver acting as the calciner (Chacartegui et al., 2016).

Initially, integration between CSP-CC and carbonate looping was proposed through an indirect coupling of the power block with the carbonator reactor, where energy is released (Ortiz et al., 2017). More recently, direct integration of the carbonate loop into Solar Combined Cycles (SCC-TCES) has been proposed within the SOCRATCES H2020 project (https://www.socratces.com/). In this novel scheme, a thermal fluid (CO_2 or CO_2/H_2O) is heated to 1200°C by solar radiation. Part of this energy is stored in the carbonate looping TCES, while the remainder drives the combined cycle. When solar radiation is unavailable, the TCES provides the necessary energy to operate the power block under the same conditions as during solar operation (Ortiz et al., 2021).

Despite significant progress in component development and lessons learned from different carbonate looping configurations, solar-driven carbonate looping (whether for TCES or *tail-end* CO_2 capture) remains at a relatively low level of technological maturity compared to other processes. While the carbonator reactor for CaL TCES has been successfully demonstrated in an entrained flow reactor at kW scale (Chacartegui et al., 2025), the solar calciner (also referred to as a particle receiver) continues to represent the main technological challenge (Ortiz et al., 2019). Solar-driven calciners can be broadly classified into direct solid particle receivers (SPRs), where particles are directly exposed to concentrated sunlight, and indirect SPRs, where an intermediate heat transfer surface absorbs solar radiation and transfers heat to the particles (Khan et al., 2024).

Novel reactor concepts for solar calciners suitable for coupling with CSP have been reported in the literature, including cyclonic, free-falling particle systems, fixed, fluidized, and moving beds, as well as rotary receivers, in both direct and indirect configurations, for chemical reactions relevant to TCES (Tregambi et al., 2021b).

A series of processes that integrate the decomposition of $CaCO_3$ within CaL systems with the production of valuable products have been proposed in the recent years (Han et al., 2022). In CaL-based CCU processes, the CO_2 generated by decomposition of $CaCO_3$ is converted in situ, thus reducing the CO_2 concentration in the calcination atmosphere and allowing for a lower calcination temperature. Intense work has been reported on the development of dual functional materials acting as CO_2 sorbent and conversion catalyst in CO_2 capture systems, where transition metals act as RWGS or methanation catalysts (Jin et al., 2024). While CH_4 production requires the presence of a methanation catalyst together with $CaCO_3$ (Han et al., 2022), CaO itself has been proved to

exhibit catalytic activity toward the RWGS reaction (Giammaria and Lefferts, 2020; Sun et al., 2021). In this context and aiming at the integration of renewable energy with the production of syn-fuels from captured CO_2, it has been recently proposed the desorption-enhanced reverse water–gas shift process aiming to produce CO/H_2 from $CaCO_3$ decomposition in H_2 (Abanades and Grasa, 2024).

2.1.4. Sorption-enhanced carbonate looping

Sorption-enhanced carbonate looping (SE-CaL) refers to a family of processes that integrate CO_2 capture with fuel conversion reactions to produce hydrogen-rich syngas. The core principle relies on the presence of CaO in a gasifier, or a reformer, which removes CO_2 from the gas phase and shifts the equilibrium of reactions such as steam reforming, reverse water–gas shift, and gasification toward higher hydrogen yields. This approach enables the production of syngas with high H_2 content and minimal CO/CO_2 concentrations and limits coke deposition. The $CaO/CaCO_3$ equilibrium determines the operating temperature and pressure in the reformer to maximize reaction displacement while maintaining high CO_2 capture efficiency. The calciner operates at elevated temperatures and/or reduced pressure to regenerate CaO by calcining the $CaCO_3$ formed during reforming, producing a concentrated CO_2 stream suitable for carbon capture and storage (CCS) or utilization (CCU). This family of processes can be classified as: sorption-enhanced reforming (SER-CaL), when CO_2 removal enhances the steam reforming of CH_4 or another fuel/process gas; sorption-Enhanced Water Gas Shift (SEWGS-CaL) when CaO enhances WGS reaction in a CO/CO_2 rich gas stream or sorption-enhanced Gasification, (SEG-CaL) when the presence of CaO enhances char gasification, reforming and WGS reactions in steam gasification of a solid fuel. Reactor configuration depends on fuel type: solid fuels (e.g., biomass, residues) typically require interconnected fluidized bed reactors (Karl and Pröll, 2018), whereas packed-bed configurations operating in parallel (Martínez et al., 2019) or fluidized systems (Farooqi et al., 2025) have been proposed for liquid and gaseous fuels. See Fig. 5, where the schematic general description of sorption-enhanced CaL processes are depicted.

Hydrogen production via methane steam sorption-enhanced reforming (SER) in interconnected fluidized beds has been experimentally validated, and is currently at TRL 4 (Masoudi Soltani et al., 2021). Development has progressed steadily (Meyer et al., 2014), and the Gas Technology Institute (GTI) achieved 71 kW of H_2 with >80 vol.% purity (Mays, 2017). The technology has been scaled to 1 MW_{th} in the HyPER pilot plant at Cranfield University (Lesemann et al., 2022), although results have not yet been reported. Various process configurations have been proposed to deliver concentrated CO_2 at the regenerator outlet. For example, Martínez et al. (2013a) evaluated oxy-combustion of auxiliary fuel and/or PSA off-gas in a circulating fluidized bed (CFB), achieving 74.2–76.6% equivalent hydrogen production efficiency and >98% CO_2 capture. The HyPER project proposed an indirectly heated entrained-bed calciner (HyPER, 2025), while (Yan et al., 2020b) combined SER with chemical looping combustion (CLC), eliminating the air separation unit and achieving theoretical hydrogen production efficiency of 75.5% with nearly complete carbon capture. An adaptation of this sorption-enhanced chemical looping reforming process scheme operating with three interconnected fluidized beds is under development and described in more detail in section 2.2.3.

Recent research has focused on the development of synthetic CaO-based sorbents, catalysts, and bifunctional materials (Farooqi et al., 2025). However, fluidized-bed SER faces a major limitation: the need for low pressure differences between reactors, which restricts operation at elevated pressures, as the calcination equilibrium imposes challenging temperatures for sorbent regeneration. As an alternative, packed-bed SER reactors operating in parallel enable pressure swing between reforming and regeneration stages (Martínez et al., 2019). The main challenge for the packed-bed configuration still remains on efficiently providing the energy required for regeneration of the $CaCO_3$ formed during the H_2 production stage. The most developed option is the Ca-Cu process that proposes the integration of a Cu/CuO redox loop with the calcination of the $CaCO_3$ (Abanades and Murillo, 2009). The process has been typically proposed to be operated in parallel pressurized fixed-bed reactors, configuration that allows the functional materials to remain steady whereas the reacting gases are repetitively switched between SER and redox conditions. It has been validated in different pilot plants where the performance of individual process stages was assessed with commercial functional materials: reforming catalyst, Cu-based material and sorbent. The feasibility of the overall process was brought to TRL 5 in a packed-bed set up located at Eindhoven University. In this set-up, the SER process via Ca-Cu was run for more than 285 consecutive cycles producing a 95.6% vol. H_2 stream at an S/C=3.2, maximum bed temperature of 668 °C and 2 bar (Martínez et al., 2019). Through technoeconomic analysis, a 74.1% hydrogen production efficiency was estimated, with a carbon capture ratio of 95.6% and a levelized cost of hydrogen of around 0.178 € per Nm^3_{H2} for a standalone H_2 production plant operating at 25 bar (Riva et al., 2018). Process versatility was assessed through modeling work adapted to diverse industrial applications (ammonia production, power generation, pre-combustion CO_2 capture in NGCC and steel production) whose principal results are compiled in the work of Martínez et al. (2019). A variant of the Ca-Cu process has recently achieved TRL 7 integrated in the steel

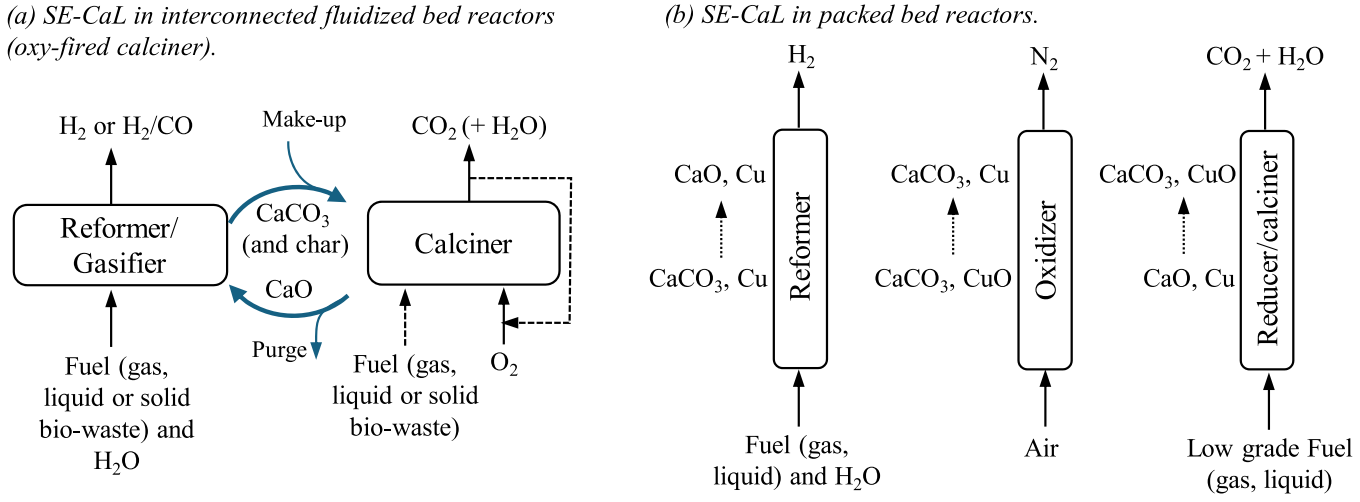

Fig. 5. Schemes of the sorption-enhanced carbonate looping (SE-CaL: SER-CaL or SEG-CaL) process: (a) SE-CaL in interconnected fluidized bed reactors, using an oxy-fired calciner; and (b) SE-CaL(SER-CaL) in packed bed reactors, where a redox loop provides the energy for $CaCO_3$ calcination.

production sector within the C4U project (https://c4u-project.eu/). The process named Calcium Assisted Steel-mill Off-gas Hydrogen production process (CASOH) was designed to decarbonize blast furnace gas (BFG) in steel plants, producing a valuable hydrogen-rich gas and nearly pure CO_2 (Fernández et al., 2020). The main stage of the process is the CASOH itself, where the CO contained in the BFG (20–25% vol.) reacts with steam to produce a H_2/N_2 gas, catalyzed by the Cu-based material. The majority of the CO_2 (both produced via WGS, and that present in BFG) reacts with CaO, allowing for very high CO conversion in a range of temperatures between 550 and 650 °C (i.e., over 97% vol. at 550 °C and 1 bar, and 90% vol. at 650 °C and 10 bar). The CASOH process was first experimentally demonstrated at TRL $\leq$ 4 (Abbas et al., 2022; Grasa et al., 2023) and then scaled up to 1 MW_{th}, TRL 7, where the proof of concept was achieved, treating real BFG from an ArcelorMittal factory located in Asturias (Spain). The plant entered in operation in the first half of 2024 and the results produced were relevant for all gas-solid reactions involved in the process, producing a gas with 40% H_2 with CO_2 capture efficiency over 95% and accumulating over 550 h of operation (Fernández et al., 2025). Efforts have been done through simulation to optimize BFG decarbonization strategies balancing thermal output, efficiency and CO_2 capture (Khallaghi et al., 2025) and enhanced versions of the CASOH process are under investigation by implementing vacuum pressures to the calcination stage (Fernández et al., 2025).

Focusing on solid fuels, biomass steam sorption-enhanced gasification (SEG) has been developed in interconnected fluidized bed reactor systems. In a first reactor the solid fuel (biomass, residues) is gasified with steam in presence of CaO that removes CO_2 from gas phase displacing gasification, reforming and WGS reactions (typical temperatures between 675-750 °C). Unconverted char and the $CaO/CaCO_3$ stream exiting this reactor is directed to the calciner unit where $CaCO_3$ is calcined thanks to the combustion (or oxy-combustion) of char (and additional fuel if needed). The energy required to sustain the endothermic gasification process is provided by the hot regenerated sorbent stream and the exothermic CaO carbonation reaction in the gasifier. SEG was successfully achieved with wood pellets at the 100-kW scale in interconnected fluidized bed systems under autothermal conditions, at the Vienna (Pfeifer et al., 2007) and Stuttgart (Hawthorne et al., 2012). Despite the different geometries of the pilots and operation conditions, in terms of solid circulation rate and bed composition, the consistency of the process producing a gas with around 70% vol. H_2 in dry basis was proved and cold gas efficiencies between 60% and 77% were reported (Parvez et al., 2021). Relevant differences were observed in the reported tar contents, with lower amount at the tests in Vienna, mainly due to the presence of a tar reforming catalyst in bed in their tests, and to the higher reforming temperature.

Recent progress in this technology has been oriented to prove its fuel-flexibility through the use of low-cost fuels as residual or waste materials known to present important challenges due to their ash and/or contaminants content. Although the core of the gasification process might not be affected by fuel composition, all the peripheric equipment dedicated to fuel dosing and/or syngas cleaning (from tars and contaminants) would need to be adapted. Redesigning the upper part of the gasifier as a countercurrent column with hot bed material flowing down and product gas streaming upwards was the strategy adopted in the advanced 100-kW pilot at Vienna to enhance gas-solid contact, residence time, and promote fuel and tar conversion and the WGS reaction in presence of CaO (Müller et al., 2017). The benefit of this design led to an improvement in gas cold efficiency (GCE) up to 74% on wood pellets gasification, and a reduction in tar content (as low as 4.8 g/Nm^3 gas d.b. for GCMS and 0.9 g/Nm^3 gas d.b. for gravimetric tar). Due to the technical challenges of low-grade fuels, scarce experimental campaigns have been performed in dual fluidized bed systems under autothermal conditions. Results from single runs of diverse residual fuels reported by Benedikt et al. (2018) served to prove the feasibility of SEG in DFB to process waste fuels. Recently, the technology has been scaled-up with the construction and commissioning of a 1-MW_{th} (fuel power input) DFB pilot plant (Kadlez et al., 2025).

The ability of the SEG process in DFB systems to produce syngas with an adequate composition for a downstream catalytic syn-fuel synthesis process, was proved in the 200-kW DFB pilot plant at IFK Stuttgart for woody biomass (Hafner et al., 2021). Plant configuration allowed controlling the mass flow of solids between gasifier and combustor. The continuous feeding of limestone to the calciner allowed the modulation of CO_2 capture as function of operating parameters. In this pilot plant, product gas composition with H_2/CO ratios between 8 and 1 were obtained at gasification temperatures between 650 and 775 °C, with low tar contents (as low as 1 g/m^3 d.b., STP of gravimetric tar at 771 °C). Increasing CaO circulation rate was beneficial to improve H_2 content and to reduce CH_4 and light HC contents, in line with results obtained at lower-scale pilot plants (Martínez et al., 2020). In this plant, the feasibility of the SEG configuration with oxy-fired calciner/combustor (oxy-SEG) was confirmed (Parvez et al., 2021).

Although gasification of residues with high ash content (i.e., municipal solid waste, chicken manure, sludge) was already proved in the DFB systems described above (Fürsatz et al., 2021), studies in smaller pilot plants allowed for a deeper analysis of the effect that gasification conditions had on the fate of contaminants (Schmid et al., 2021b; Martínez et al., 2022). Therefore, it was corroborated that CaO has an excellent ability to retain S from fuel, bringing H_2S emissions down to the equilibrium at gasification temperature, with very low amounts of COS and no CH_4S in the gas (Martínez et al., 2022; Schmid et al., 2018). With respect to N-rich fuels (mainly sewage sludge), it was observed that under SEG conditions a relevant fraction of the N in the fuel ends as NH_3 in the produced gas. The ratio Ca/C had a positive effect reducing the NH_3 in the gas, but the fraction of NH_3 released was higher compared with oxy-steam biomass gasification at higher temperatures (Moles et al., 2024).

2.2. Chemical looping processes

Chemical looping technologies have emerged as promising approaches to facilitate the energy transition toward a low-carbon energy conversion. These processes represent a versatile platform for the efficient and clean production of heat/power, synthesis gas (syngas), or hydrogen from various hydrocarbon fuels, offering significant advantages over conventional methods. The fundamental principle involves using a solid oxygen carrier, typically a metal oxide, to transfer oxygen from air to a feedstock, thus avoiding the direct contact between them and enabling an efficient conversion with inherent CO_2 separation (Adanez et al., 2012). The operating principle of the chemical looping processes are summarized in Fig. 6. Three broad families in fuel conversion can be differentiated among the chemical looping technologies: (i) chemical looping combustion (CLC) was formerly developed for heat/power with CO_2 capture; (ii) chemical looping gasification (CLG) extends this concept to gasify solid carbonaceous feedstocks; and (iii) chemical looping reforming (CLR), which offers a route to reform gaseous and liquid hydrocarbons. Both in CLG and CLR, the product is a high-quality synthesis gas (syngas) from an efficient and auto-thermal process while limiting CO_2 emissions to the atmosphere (Zafar et al., 2005). For that, a partial oxidation of the fuel is performed but without direct contact between fuel and air, preventing nitrogen dilution of the produced syngas. The produced syngas is a key intermediate for chemical and energy sectors, and the indirect oxygen transfer in CLG/CLR enables its integration with simplified downstream processes for the syngas managing, which emerges as a major advantage for low-emission hydrogen/syn-fuels manufacture (Ramezani et al., 2023). In the novel sub-class sorption-enhanced CLR (SE-CLR), a solid CO_2 sorbent (e.g., CaO, Li-based, Li_2ZrO_3) is added to shift equilibrium toward H_2 by removing CO_2 in-situ; this can yield very high H_2 purity and simplify downstream separation (Masoudi Soltani et al., 2021). The SE-CLR process is illustrated in Fig. 6.c. In addition, chemical looping

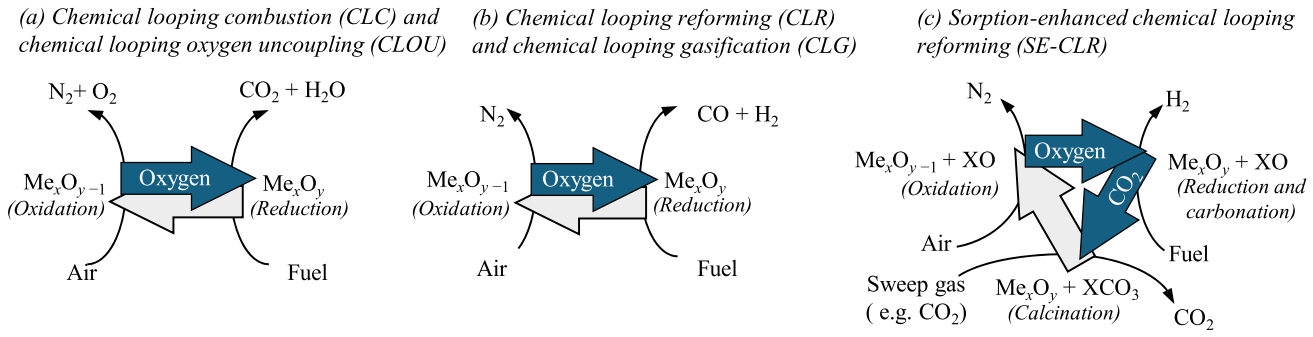

Fig. 6. Operating principle of chemical looping processes: (a) chemical looping combustion (CLC), (b) chemical looping reforming (CLR) and gasification (CLG), and (c) sorption-enhanced chemical looping reforming (SE-CLR). The thick arrows represent the transport of oxygen carrier (OC) (a and b), and OC and sorbent (c). The reactions between brackets refer to the OC and the sorbent. The abbreviation "Me" indicates the active metal for the oxygen carrier (e.g., Fe), and the letter "X", the active element for CO_2 sorption (e.g., Ca).

technology has expanded its application significantly (Zeng et al., 2018) to include processes like H_2O splitting (Voitic and Hacker, 2016), CO_2 splitting (García-Domínguez et al., 2025), and even ammonia synthesis (Han et al., 2025), leveraging the same fundamental redox principles. However, these processes are not covered by this review. For further applications of chemical looping technology in the chemical industry, the reader is referred to the work of Zhu et al. (2020).

Recent studies in chemical looping have focused on developing robust oxygen carriers to enhance performance and durability, optimizing reactor configurations, and integrating chemical looping with renewable energy sources to achieve autothermal operation and efficient heat transfer (Ramezani et al., 2023). These innovations align with global decarbonization goals and the transition toward hydrogen-based energy systems, making them highly relevant in advancing carbon-neutral energy systems.

Recently, metal-based open-loop redox concepts for energy storage and transport have gained much attention (Bergthorson, 2018). Reduced metals such as iron and aluminum can serve as low-carbon energy carriers by undergoing oxidation to release heat, after which they are regenerated through reduction in off-site facilities powered by abundant renewable energy. This "open-loop" chemical looping approach is beyond the scope of this review.

2.2.1. *Chemical looping combustion*

In its most basic form, *chemical looping combustion* (CLC) involves two interconnected reactors, the Air Reactor (AR) and the Fuel Reactor (FR), as shown in Fig. 7. In the FR, the fuel is converted to CO_2 and H_2O in a nitrogen-free environment through the overall reaction of fuel with oxygen carrier (OC):

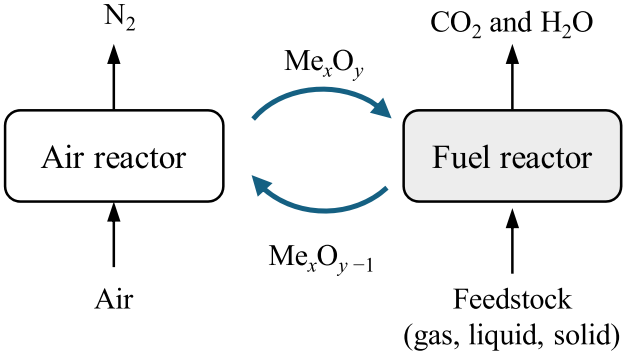

Fig. 7. Scheme of the chemical looping combustion (CLC) process.

$$(2n+m)\ Me_xO_y + C_nH_{2m} \rightarrow (2n+m)Me_xO_{y-1} + n\ CO_2 + m\ H_2O \quad (R1)$$

Here, Me_xO_y and Me_xO_{y-1} are the fully oxidized and reduced forms of the oxygen carrier and C_nH_{2m} is the fuel, which could be in gaseous, liquid or solid form. The reduced oxygen carrier is transported to the air reactor, where it is reoxidized with the combustion air according to:

$$2\ Me_xO_{y-1} + O_2 \rightarrow 2\ Me_xO_y \quad (R2)$$

After condensation of H_2O, a highly concentrated stream of CO_2, suitable for CCS, can be obtained. Implementing CCS with CLC is advantageous, as all the converted carbon is obtained in the concentrated stream from the FR without the need for any downstream gas separation process. This should result in lower costs for carbon capture, a claim which has been supported by a number of techno-economic studies (Lyngfelt and Leckner, 2015; Haaf et al., 2020c). The economic aspect is further discussed in Section 5.1.

Chemical looping with oxygen uncoupling (CLOU) is a variation of CLC (Mattisson et al., 2009; Adánez-Rubio et al., 2012; Rydén et al., 2014). Here, the oxygen carrier releases significant fractions of oxygen to the gas phase in the FR through decomposition of a metal oxide to a reduced solid oxide and gaseous oxygen, according to reverse reaction of (R2). The released oxygen can react directly with the fuel in FR through normal combustion. The reduced oxygen carrier then needs to be oxidized via reaction (R2), in a similar way to normal CLC. In order to be a viable route, oxygen carriers with "uncoupling" properties need to have special thermodynamic and kinetic requirements in comparison to oxygen carriers used in normal CLC, explained hereafter. This mechanism has been shown to be highly advantageous for converting solid fuels or char in the FR, as the slow char gasification step can be fully or partially "replaced" with normal fuel combustion (Adánez et al., 2018). Further, utilization of CLOU should provide advantages also for gaseous and liquid fuels (Jing et al., 2014).

The underlying concept of chemical-looping was introduced more than 70 years ago when Lewis et al. (1949) proposed a method for production of syngas or carbon dioxide from a carbonaceous fuel using iron and copper-based oxygen carriers. Originally, the aim of the proposed methodology had little to do with sustainable energy conversion. To our best knowledge, this process was forgotten until the pioneering research conducted by Ishida et al. (1987). There was only limited research in the 90's on the process, most of it performed at the Tokyo Institute of Technology (Ishida and Jin, 1994; Ishida et al., 1996). It was first in 1994 when the technology was proposed as a combustion option for efficient CO_2 capture (Ishida and Jin, 1994). At the start of the millennium, the research around CLC accelerated, spurred by increased interest in carbon capture, where this emerging technology had a significant advantage with respect to efficiencies and costs in comparison

to other technologies, such as post-combustion capture.

There has been a significant number of review papers on chemical looping processes in the past two decades—see, for instance, the work from Zhao et al. (2017). Comprehensive reviews have been performed by the researchers of the ICB-CSIC (Adánez et al., 2018; Adanez et al., 2012; Mendiara et al., 2018a). There is currently intense and continuous production of review papers on various aspects of chemical looping (Zhou et al., 2025; Seyyedattar and Zendehboudi, 2026; Zhao et al., 2026). The present review elaborates on the development of CLC, with focus on trends and operations in the past decade, including (i) process configurations, (ii) oxygen carrier development, (iii) pilot-operations and (iv) ash species pathways, with the latter two sections covered in section 3.3.1.

2.2.1.1. Process configurations for CLC

2.2.1.1.1. Inter-connected fluidized beds. CLC was demonstrated for the first time in 2003 at Chalmers University of Technology using a reactor based on inter-connected fluidized beds (Lyngfelt et al., 2005), as proposed a few years earlier (Lyngfelt et al., 2001). The unit resembles that of a conventional circulating fluidized bed boiler (CFB) with the addition of a fuel reactor on the return side of the main combustor. Since inception, several alternative variations have been proposed, including the use of CFBs for both the air and the fuel reactor, which is the design utilized by the two largest dedicated CLC units in Europe, i.e., at Technical University of Vienna (Pröll et al., 2009) and Technical University of Darmstadt (Ströhle et al., 2014b). Other configurations use spouted beds (Shen et al., 2010), pressurized systems (Xiao et al., 2012), and novel configurations for CLOU (Zylka et al., 2025). As was shown in review papers by Mattisson et al. (2018) and Adánez et al. (2018), up to 2018, most pilot operations have been conducted in interconnected fluidized beds using gaseous, solid, and liquid fuels. As explained in Section 3.3.1, this is also the case for more recent operations.

Gaseous and liquid fuels are normally introduced from the bottom of the fluidized fuel reactor, with the fuel reacting directly or through intermediates with the fluidized oxygen carrier particles to CO_2 and H_2O via the reaction of (R1). Solid fuels, like coal or biomass, are normally fed to the bed via auxiliary feeding systems. In the bed, the fuel devolatilizes to char and volatiles. The latter can react directly with OC particles (Eq. (R1)) in a similar way as with gaseous fuels. However, the char needs to be converted to a gaseous intermediate, such as CO or H_2, via in-situ gasification before reacting with the oxygen carriers and completing the combustion process. The fuel reactor is normally fluidized with H_2O or CO_2, hence there is a significant driving force for in-situ gasification processes to proceed in the FR. In order to achieve complete conversion of solids in the fuel reactor and hence to prevent unburnt fuel from reaching the air reactor, it is not uncommon to use a carbon stripper that recirculates unburnt fuel from the outlet of FR back to the main bed (Markström and Lyngfelt, 2012; Kramp et al., 2012). The burnable gaseous components also need to be converted to a high extent in order to avoid costly separation processes at the outlet. Staničić et al. (2021) found that significant fractions of combustibles are present in the outlet of the FR for a range of pilot units using solid fuels and Fe-based oxygen carriers. This is evidently a major challenge, and there have been several strategies employed to address it and increase carbon burnout in the FR:

- Use of a separate chamber after the FR where pure O_2 is introduced in order to react with the residual unburned components. This *oxy-polishing* step can likely achieve a high degree of burnout, but at the cost of additional components and of pure O_2 requirements (Gayán et al., 2013; Mei et al., 2025).
- Use of oxygen carriers with uncoupling or CLOU properties. The release of pure oxygen to the gas phase could promote burnout, especially if oxygen is released by the OC near the gas outlet of the FR or in sections where there may be insufficient gas-solid contact (Mendiara et al., 2016; Ohlemüller et al., 2019).
- Use of novel arrangements in the fuel reactor in order to enhance contact between gas and oxygen carriers (Nemati et al., 2024; Li et al., 2022a; Li et al., 2022b).

Most recent operations have been conducted in interconnected fluidized beds (see Section 3.3.1). The broad range of units and the wide range of utilized oxygen carriers demonstrate that the technology is robust and flexible. The similarity of the concept to conventional circulating fluidized beds also opens up the opportunity for flexible systems which can operate in normal combustion mode as well as a chemical-looping combustor, depending upon market conditions. This is a concept which is currently being explored in a major European integrated project "Bio-FlexCLC" (https://www.bioflexclcproject.eu/).

2.2.1.1.2. Moving bed configurations for CLC. Some research groups utilize a moving bed configuration in the fuel reactor (Kim et al., 2013; Fan, 2010). When used for solid fuels, the fuel is introduced in the middle of a moving bed of oxygen carriers moving axially downwards. The reactive gases generated from devolatilization and char gasification move countercurrent to the downward moving oxygen carriers, enabling good contact between the gases and the oxygen carriers. This concept has primarily been developed and explored by the Fan research group at Ohio State University (Tong et al., 2014; Zhang et al., 2021). Here, mainly Fe-based oxygen carriers have been used and high fuel conversion has been reported. The main challenge is related to maintaining a non-fluidized FR while still having reasonable cross-sectional areas of the FR. This is mainly achieved by increasing the particle size of the oxygen carriers, something which entails the need for high velocities in the air reactor in order to entrain particles back to the fuel reactor. Other configurations have been proposed, for instance, the use of a bubbling bed air reactor with connected riser (Schwebel et al., 2012). As is shown in the Table in Section 3.3.1, currently moving beds have been demonstrated to 250 kW size using solid fuels (Zhang et al., 2021).

2.2.1.1.3. Packed or fixed bed reactors. There have been a significant number of studies which explore the use of fixed or packed bed configurations of CLC (Naqvi and Bolland, 2007; Nordness et al., 2016; Hua et al., 2016). The basic idea here is to use a packed bed of oxygen carrier particles which react with the fuel (which needs to be in a gaseous state). When the oxygen in the bed is depleted, the gas is switched to oxygen, thereby oxidizing the oxygen carriers back to the original state. This sequence is similar to the overall reactions from (R1) and (R2), but with the main difference to the fluidized or moving-bed concept being that gases are alternatingly switched and exposed to the oxygen carriers rather than transport of oxygen carriers between the reactors. Advantages would be that attrition likely is minimized and that the process is more amiable for pressurization. The drawbacks would likely be the problems related to gas switching at high temperatures as well as heat management and local hotspots. Finally, conversion of solid fuels would entail a prior gasification step, as it is likely that only gaseous or liquid fuels would work with this concept.

2.2.1.2. Oxygen carriers for CLC.

The cornerstone of the CLC technology is finding oxygen carrier particles which are sufficiently reactive with fuel and oxygen while at the same time having high enough oxygen transport capacity to transfer oxygen from air to fuel and high resistance toward attrition over many redox cycles. It is desirable that the oxygen carrier material be produced by low-cost and facile synthesis methods to eventually be produced at an industrial scale. The synthesis method must produce particles suitable for the reactor in which they will be used. Thus, micronized particles (e.g. 100-500 μm) are demanded for fluidized bed reactors, but pelletized particles in different shapes (e.g. spherical or cylindrical) may be required for packing configurations to reduce the pressure drop in the reactor but minimizing mass and heat

transport issues inside the particles. As hundreds or even thousands of papers have been published around CLC and oxygen carriers, it would be a monumental task to give a precise and all-encompassing overview of all materials tested in the laboratory, but there are a number of more detailed reviews where more specific information can be found regarding oxygen carrier development (e.g., Li et al., 2017; Luo et al., 2015). These, and other general review papers on CLC, give a broad view of the different materials which have been investigated for CLC. In this section we focus on recent developments based on pilot operations. The pilot operations themselves are described in Section 3.3.1. Below we also briefly discuss two promising and recent trends within oxygen carrier science and development: (i) the use of high order complex materials as oxygen carriers for CLC and CLOU and (ii) the use of computational methods for oxygen carrier discovery and understanding.

2.2.1.2.1. Oxygen carrier materials: from mono-metallic to high-entropy oxides. Early research on oxygen carriers focused on mono-metallic oxide systems, primarily utilizing transition metals such as Nickel (Ni), Iron (Fe), Copper (Cu), Manganese (Mn), and Cobalt (Co) (Cho et al., 2004). Among these, NiO initially demonstrated superior oxidizing capacity for hydrocarbon fuels, attributed to its combination of good surface catalysis and rapid oxygen transfer. This property made NiO particularly effective for gaseous fuels like natural gas, where no solid char is involved in the reaction mechanism. At Chalmers University of Technology in Sweden, a Ni-based oxygen carrier with enhanced attrition resistance, successfully demonstrating its stability over 1000 hours in a dedicated test unit (Linderholm et al., 2009). However, as the focus of chemical-looping research shifted from gaseous to solid fuels, such as petroleum coke and coal, the advantages of Ni-based carriers diminished. This is because, in solid-fuel combustion, the reactive species are CO and H_2, rather than hydrocarbons, and other metal oxides than Ni are also highly reactive with these gaseous compounds. Furthermore, concerns regarding Ni's toxicity, cost, and sensitivity to impurities led to increased interest in more environmentally benign alternatives, particularly Cu-, Mn-, and Fe-based oxygen carriers. The problem generally seen with Mn- and Fe-based materials was a combination of low reactivity with hydrocarbons and high degrees of attrition and fragmentation, often resulting in less than perfect gas conversion and low lifetime values of the particles. It has been observed that the degree of particle breakdown is enhanced by the chemical stress when operation demands a high variation of the oxygen carrier conversion.

The introduction of oxygen carriers with uncoupling capabilities fifteen years ago was a breakthrough (Mattisson et al., 2009). The oxygen released in the fuel reactor can react directly with the fuel through combustion. CLOU materials are characterized by (i) the ability to release gaseous oxygen at a sufficient equilibrium partial pressure of oxygen at relevant combustion temperatures, and (ii) exhibiting an equilibrium partial pressure of O_2 low enough for oxidation to be possible at the oxygen concentration level in the outlet of the air reactor. Typically, an equilibrium concentration somewhat below 5% is advantageous at the usual operating temperatures of the AR (i.e., 900–1050°C). There are several benefits of utilizing oxygen carriers with so-called uncoupling properties: (i) the combination of uncoupling and combustion of solid fuels means that the gasification reactions could be partially or fully eliminated; (ii) oxygen release from particles on the freeboard could help convert combustible components; and (iii) the oxygen release could compensate for imperfect gas solid mixing.

For the CLOU process, it is important to consider the interplay between oxygen partial pressure of the metal oxide system, the heats of reaction, and the temperature in the reactors. Both Mn and Cu have oxide systems which could be utilized for CLOU at certain temperatures and partial pressures of O_2. However, Mn oxides do not usually show the oxygen uncoupling capability at the relevant operating conditions in CLOU regarding oxygen concentration in the air reactor and temperature (800-1000 °C). Thus, CuO seems to be the only monometallic oxide with suitable thermodynamic and kinetic properties to be used in CLOU. Still, simple Cu-based materials are burdened with low melting temperatures, high attrition, and high cost. Pure Mn_2O_3 could release O_2 in the fuel reactor, but the kinetics are insufficient. Hence, major efforts have been performed in the last decade to improve performance of Cu- and Mn-based oxygen carriers (Mei et al., 2015; Fan et al., 2015; Filsouf et al., 2026; Lysowski and Ksepko, 2025). The common denominator for all of these investigated materials is that they contain manganese or copper in the structure. For Mn-based material the oxides are normally combined with Ca, Mg, Fe, Ni, Ti and/or Si (Schmitz et al., 2016; Li et al., 2024a; Mattisson et al., 2016; Galinsky et al., 2016; Adánez-Rubio et al., 2016). Normally, these combined oxides have an equilibrium partial pressure of O_2 which is somewhat higher than for pure CuO or Mn_2O_3, meaning that higher temperatures can be used in the combustion process, i.e., 850–1000°C. Also, natural Mn-ores can contain significant quantities of the above-mentioned species, and several researchers have found clear uncoupling properties (Sundqvist et al., 2015; Li et al., 2024a). Recently, the use of so-called high-entropy oxides was demonstrated for use as oxygen carrier for CLC (Adánez-Rubio et al., 2024). Here, an oxygen carrier material containing equimolar amounts of Fe, Mn, Cu, Ti and Mg was found to have suitable chemical and mechanical properties as an oxygen carrier. The fact that this sort of material can be oxidized and reduced in the same phase through oxygen transfer in vacancies could have significant implications for oxygen carrier development, and this new class of materials opens up for an almost infinite compositional space and possibilities to optimize performance of oxygen carriers.

2.2.1.2.2. Computational methods for increased understanding and oxygen carrier discovery. Although the CLC community has come a long way, with many promising oxygen carriers developed, there are many compelling reasons to continue exploration: (i) limited work with biomass with significant fractions of reactive ash species, (ii) attrition and stability needs to be improved, (iii) the rapid expansion of other applications using oxygen carriers, and (iv) recent advances with respect to multi-component and entropy-stabilized oxides. The recent advance of computing power, artificial intelligence, and machine learning opens up a new frontier for oxygen carrier exploration, and there have been some recent interesting efforts:

- Use of high-throughput screening methods for oxygen carrier discovery (Yang and Li, 2025; Brorsson et al., 2023).
- Use of machine learning for establishing oxygen carrier performance (Yan et al., 2020a).
- Use of Density Functional Theory (DFT) to predict thermodynamic stability (Gastaldi et al., 2025).
- Use of electronic structure methods to improve fundamental understanding of materials oxygen transport and chemical reactions (Li et al., 2023; Xing et al., 2024).

These are just some examples of recent computational studies using different types of computational tools for oxygen carrier development. It is likely that such methods will continue to be used more frequently in the coming years with respect to oxygen carrier development. Considering the interesting properties of higher-order and entropy stabilized oxides discussed above, artificial intelligence and machine learning algorithms could be instrumental tools for rapid prediction of viable compositions. The compositional space increases exponentially with the number of elements in the oxygen carrier, and traditional thermodynamic and "trial-and-error" approaches may be intractable for prediction and optimization purposes. Machine learning and AI-algorithms could be established to propose a manageable number of oxygen carrier candidates in the cosmically large compositional space, which can then be investigated experimentally.

2.2.2. Chemical looping gasification

The aim of *chemical looping gasification* (CLG, Fig. 8) is to produce a high-calorific, nitrogen-free syngas from a solid feedstock that retains most of the feedstock energy, while avoiding the requirement for air

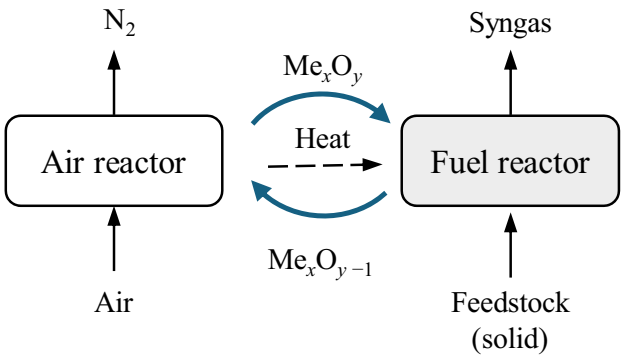

Fig. 8. Scheme of the chemical looping gasification (CLG) process.

separation as in oxygen-blown gasification. Therefore, the chemical looping principle is adapted to transfer only enough oxygen to balance endothermic gasification reactions in the fuel reactor (FR) with exothermic oxidation reactions in the air reactor (AR). Consequently, solid transportation—and thus heat transportation—between the reactors plays a crucial role in the process (Dieringer et al., 2020; Marx et al., 2023b). Mechanistically, circulating oxygen carriers transport both lattice oxygen and sensible heat from the AR to the FR, and chemical energy (in the form of reduced metal) from the FR to the AR, where exothermic oxidation in the AR supplies the heat required for endothermic reduction and gasification in the FR.

The CLG process concentrates carbon in the syngas stream, which is beneficial for carbon-negative process chains, as a CO_2-separation step is usually required regardless (Kumar et al., 2022b). Because the solid feedstock requires good contact with the oxygen carrier, reactor setups typically use either fluidized or moving beds. However, since incomplete conversion of a solid feedstock is targeted to maintain syngas quality, carbon entrainment from the FR and transport toward the AR, as well as formation of condensable hydrocarbons (tars), are inherent challenges. Operating conditions must therefore balance cold gas efficiency, hydrocarbon production, and carbon slip, with temperatures in excess of 850°C being favored (Dieringer et al., 2020; Marx et al., 2023a).

2.2.2.1. Oxygen carriers for CLG. Oxygen carrier (OC) options for CLG are generally the same as for CLC operation, with additional options of OCs that are unable to fully oxidize syngas species due to thermodynamic limitations. These options reside within the so-called syngas region of the Ellingham diagram (Luo et al., 2015) and consist mainly of ceria (CeO_2), but also include NiO and iron-based OCs. The syngas region represents thermodynamic conditions where oxygen carriers can partially oxidize carbonaceous materials without fully converting CO and H_2 to CO_2 and H_2O, thus preserving syngas quality. However, OCs that can fully oxidize a feedstock are also viable when suitable process control methods for limiting the oxidation of syngas species are utilized (Dieringer et al., 2020). As OCs come into contact with the solid feedstock and its ash, they may undergo interactions that degrade OC performance. Therefore, lower-cost materials are more favorable, which has led to extensive research and OC screening for different waste materials (Goel et al., 2023). Wastes from steel production, particularly steel converter slag (Condori et al., 2021c) have received the most attention due to their low cost and availability. Additionally, steel converter slag shows interesting characteristics in reducing the formation of higher hydrocarbons (Hildor et al., 2023) with experiments reporting C_2 fractions typically below 2.5%, attributed to the OC surface oxidation and catalytic interactions with retained alkali species.

Among natural minerals, ilmenite ($FeTiO_3$) is the most adopted and investigated option (Marx et al., 2023a; Dieringer et al., 2023b; Condori et al., 2021b; Condori et al., 2023; Li et al., 2026; Yuan et al., 2023), with iron ores also receiving significant attention (Shen et al., 2018; Wei et al., 2015a, 2015b; Ge et al., 2016a, 2016b; Condori et al., 2021a). Manganese ores are also considered promising materials for continues operation (Condori et al., 2021a).

2.2.2.2. Feedstocks for CLG. Biomass of various types represents the main focus for CLG feedstock studies, with plastic wastes increasingly coming into focus for continuous applications (Panitz et al., 2025; Falascino et al., 2024) and some publications examining coal as a feedstock (Yuan et al., 2023; e.g., Shen et al., 2018). While conversion of woody biomasses appears to pose no significant issues in CLG (Marx et al., 2023a; Dieringer et al., 2023b; Li et al., 2026) the processing of herbaceous materials involves the risk of agglomeration (Dieringer et al., 2023a; Di Giuliano et al., 2023). The specific problems of agglomeration during biomass chemical looping were addressed in a recent comprehensive review by (Miao et al., 2022) with the main conclusions that agglomeration can be reduced with additives and that OC selection and preparation play critical roles in agglomeration risk. Agglomeration tendency increases with temperature and is influenced by ash chemistry, particularly the presence of alkali metals (K, Na) and low-melting-point eutectics that form between ash components and oxygen carrier materials. Additionally, pretreatment of biomass has a significant effect and can enhance the performance and stability of the CLG process (Lebendig et al., 2022; Lebendig and Müller, 2022; Di Giuliano et al., 2023).

2.2.2.3. Novel concepts. Two notable concepts are being investigated to alleviate the problem of autothermal operation and the required heat transfer between reactors. To enhance the temperature of the FR, external heat can be supplied via solar irradiance or via microwaves, enabling novel process configurations that decouple heat supply from oxygen carrier circulation. Solar-assisted CLG concepts are pursued mainly on a theoretical level (e.g., Sun and Aziz, 2022), with experimental evidence of the concept being very limited (Xu et al., 2024). In contrast, microwave-assisted chemical looping has a larger base of lab-scale validation, with batch experiments demonstrating its feasibility (Fu et al., 2024; Ahmad et al., 2024; Li et al., 2025a). However, keeping the microwave heating contained within the reactor system for large-scale continuous operations has yet to be demonstrated, representing a key challenge for scale-up.

These enhancements make it possible to reoxidize the OC material with steam instead of air, thus generating a syngas stream from the FR and a hydrogen stream from the reoxidation reactor. This dual-product configuration requires the additional heat input (from solar or microwave sources) to close the heat balance but offers the significant advantage of producing two valuable products. The feasibility of continuous operation and scale-up, under cyclic solar or microwave heating require further demonstration and quantification before these concepts can transition from laboratory validation to commercial deployment.

2.2.3. Chemical looping reforming

Chemical looping reforming (CLR) represents a strategic adaptation of the chemical looping principle specifically for the production of low-carbon syngas or high-purity hydrogen from gaseous or liquid fuels. In CLR, the oxygen-to-fuel ratio is controlled to achieve partial oxidation, preventing complete combustion and favoring the formation of H_2 and CO, while enough energy is released to achieve auto-thermal operation following scheme in Fig. 9(a). Typical reactions (example for methane) include partial oxidation, further oxidation of gaseous products and reforming reactions with steam or CO_2 (Herrera et al., 2026). The operating conditions and the properties of the oxygen carrier determine which pathway dominates, but both partial oxidation and catalytic reforming are usually required to achieve a suitable syngas composition.

$$\text{Partial oxidation}: \ CH_4 + Me_xO_y \rightarrow CO + 2H_2 + Me_xO_{y-1} \quad \text{(R3)}$$

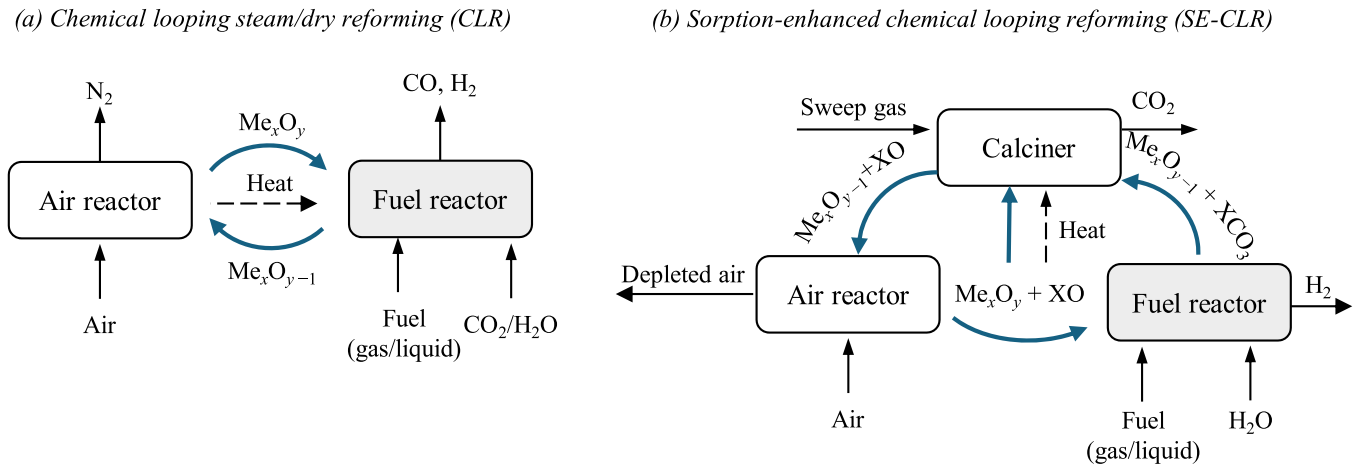

Fig. 9. Schemes of the chemical looping reforming process in two variants: (a) chemical looping steam/dry reforming, and (b) sorption-enhanced chemical looping reforming.

$$\text{Full oxidation}: \ CO/H_2 + Me_xO_y \rightarrow CO_2/H_2O + Me_xO_{y-1} \quad \text{(R4)}$$

$$\text{Steam reforming}: \ CH_4 + H_2O \rightleftarrows CO + 3H_2 \quad \text{(R5)}$$

$$\text{Dry reforming}: \ CH_4 + CO_2 \rightleftarrows 2CO + 2H_2 \quad \text{(R6)}$$

The operating conditions and the properties of the oxygen carrier determine which pathway dominates, but both partial oxidation and catalytic reforming are usually required to achieve a suitable syngas composition. Depending on the specific process emphasis, several CLR-related terminologies are commonly used (Abad, 2015):

- *Chemical looping autothermal reforming* (CLAR or a-CLR): combining exothermic partial oxidation and endothermic steam reforming within a loop to achieve autothermal operation by optimizing the internal heat balance (Ortiz et al., 2011).
- *Chemical looping partial oxidation* (CLPO): focuses on the use of an oxygen carrier both as oxidant and as catalyst (perovskites and Ni-based materials are common) to produce syngas (H_2 + CO) with high heating value.
- *Chemical looping steam reforming* (CLSR): the need to co-feed steam in the fuel to promote steam reforming/water–gas shift reactions, as well as avoiding the carbon deposition (García-Labiano et al., 2015).

The fuel conversion by CLR is characterized by: (i) the production of syngas via a partial oxidation of the fuel; (ii) the potential for autothermal operation, reducing external energy input, (iii) the avoidance of a costly and complex air separation unit, and (iv) significantly lower energy penalties for CO_2 capture compared to conventional reforming processes. Syngas with variable H_2/CO ratio may be achieved, including an optimal H_2/CO ratio for downstream processes like Fischer-Tropsch synthesis. CLR can be further enhanced by incorporating CO_2 sorbents for in-situ carbon removal in the so-called sorption-enhanced chemical looping reforming (SE-CLR, see Fig. 9b). This process combines an oxygen carrier with a CO_2 sorbent which shifts reforming equilibria to higher H_2 yields and purities, sometimes enabling near-pure H_2 streams without hydrogen purification (Masoudi Soltani et al., 2021).

Each variant of CLR requires careful balance of oxygen capacity, oxygen mobility, sorbent reactivity (if used), and reactor heat management. As such, CLR is a pivotal technology for decarbonizing hydrogen production, a crucial energy vector, and for enabling the sustainable production of synthetic fuels and chemicals.

2.2.3.1. Oxygen carriers for CLR. Oxygen carriers are central to CLR performance. In addition to the general properties demanded for an oxygen carrier, catalytic activity for hydrocarbons conversion, e.g., via steam reforming, is required to achieve complete fuel conversion when a partial fuel oxidation is performed. Materials range from Ni-, Fe-, and Cu-based oxides to natural ores and perovskites.

Early oxygen carriers investigated included supported NiO, Fe_2O_3, CuO and Mn-oxides (Hu et al., 2018; Luo et al., 2018b; Antzaras and Lemonidou, 2022; Zheng et al., 2022; Ramezani et al., 2023; Herrera et al., 2026). Also, by ~2010–2015, multifunctional catalysts (e.g., NiO on supports, combined with CO_2 sorbent particulates) had been developed for the sorption-enhanced concept. Ni-based oxygen carriers are often preferred due to good oxygen transport capacity and catalytic activity, while perovskite oxygen carriers, Cu-based, and Fe-based carriers are also frequently evaluated for methane reforming because of oxygen capacity and stability, avoiding or reducing the use of the expensive and environmentally harmful nickel.

Ni-containing oxygen carriers show excellent activity for reforming but are prone to coking and sintering. Many studies explore core–shell structures or Ni-dilution with supports/spinel phases to stabilize Ni and suppress carbon (Ramezani et al., 2023; Hu et al., 2018). CuO and CuO–Ni mixed systems are attractive for reforming and have lower coking than Ni alone.

Fe-based oxygen carriers (Fe_2O_3/$FeAl_2O_4$/spinel/garnet supports) use abundant and cheap materials. Recent work optimized supports and dopants to improve oxygen mobility and cycling stability. Engineering of spinel/perovskite supports reduces sintering and improves cyclic performance (Chang et al., 2023; Ramezani et al., 2023). Also, low-cost iron oxide-rich wastes have been studied to balance cost-effectiveness with performance. In addition, a recent study showed that an iron oxide rich industrial waste can maintain adequate reactivity toward CH_4 in chemical looping transformations and withstand multiple redox cycles, pointing to cost-effective oxygen carrier solutions for large-scale deployment (Zheng et al., 2022).

Cu-based oxygen carriers are also good candidates for CLR. Several supports have been tested for improving performance and avoid agglomeration during operation at high temperature. Good results have been obtained with CuO/Al_2O_3 materials during CLR operation in a continuous unit (Cabello et al., 2022b).

Recent advances include perovskite-based carriers with tunable redox properties and synthetic composites for improved reactivity and attrition resistance. Perovskite structures (ABO_3, e.g., $BaFe_{1-x}Sn_xO_{3-\delta}$, $LaFeO_3$ variants) offer tunable oxygen vacancy concentrations, high oxygen mobility, and intrinsic resistance to coking in many formulations. Recent perovskite studies (e.g., Sn-doped $BaFeO_3$) demonstrate anti-coking behavior and high syngas selectivity in CLR (Zhang et al., 2020).

The recent material engineering trends shift toward multi-functional/dual particles supplying properties to act as oxygen carrier, catalytic reforming function or CO_2 sorbent in structured composites, to be used in new processes such as the SE-CLR. Core–shell particles and dopant-tailored perovskites have been developed in the last decade to improve reactivity, mitigate coking, and enhance cycle life (Ramezani et al., 2023; Hu et al., 2018). For example, adding ceria (CeO_2) to Ni/Cu and perovskite composites can improve oxygen availability at the gas–solid interface and reduce coke by supplying mobile oxygen (Ramezani et al., 2023; Chang et al., 2023).

Although important advances have been done in the development of materials for CLR during the last 10 years, still there are some challenges, including the enhancement of the mechanical and chemical stability of the oxygen carrier material and long term test under relevant conditions; and development of oxygen carriers to be used with some of the fuels contain sulfur-contaminants, which usually produces material deactivation.

2.2.3.2. Fuels for CLR. CLR processes accommodate a wide range of fuels. Gaseous fuels include methane, propane, natural gas, biogas, and biomethane, while liquid fuels such as ethanol, methanol, n-butanol, acetic acid, glycerol, vegetable oils, and pyrolysis oils have been investigated (Luo et al., 2018b). Liquid fuel reforming introduces challenges related to carbon deposition and tar formation, requiring tailored oxygen carrier formulations and optimization of the reactor conditions.

Methane remains the best-developed feedstock due to favorable H/C, low tar formation, and established supply. CLR of methane has been extensively studied in bench-scale fluidized beds and packed beds. Similar to methane but with higher CO_2/impurity content, biogas is also suitable due to the alternative chemical looping dry reforming route (CLDR) in methane conversion (Cabello et al., 2022b; Herrera et al., 2026). In addition, SE-CLR of methane helps achieve high H_2 yield while also enabling in-situ CO_2 sorption (Masoudi Soltani et al., 2021).

The CLR concept has expanded the fuel scope beyond natural gas or biomethane/biogas to include liquid biofuels. These fuels bring variability in reforming behavior and oxygen carrier interaction, necessitating tailored process designs to accommodate complex fuel compositions (Ramezani et al., 2023). Liquid fuel reforming introduces challenges related to carbon deposition and tar formation, requiring optimized oxygen carrier formulations and reactor conditions.

2.2.3.3. Carbon deposition in CLR. Carbon deposition remains a critical challenge, particularly for liquid fuels and operation in packed beds. Hydrocarbon cracking and Boudouard reactions on metal surfaces lead to filamentous and encapsulating carbon (Zhang et al., 2020). Carbon deposition mechanisms include fuel decomposition and Boudouard reactions under low oxygen-availability. The presence of catalytic metals (Ni, Fe) in CLR can accelerate carbon formation if not properly dispersed/oxidized (Nikoo and Amin, 2011).

Mitigation strategies include optimizing steam-to-carbon ratios (e.g., Herrera et al., 2026), incorporating catalytic additives, and designing oxygen carriers with surface properties that inhibit coke formation. Anti-coking oxygen carrier formulations includes the synthesis of perovskites (e.g., Sn-doped $BaFeO_3$) and oxygen-rich carriers with high oxygen mobility to oxidize nascent carbon in situ (Zhang et al., 2020). Zhang et al. (2020) demonstrated Sn-doped BaFe perovskites with significantly reduced coke formation in methane CLPO. Adding second metals (Co, Cu, Sn) can change electronic/structural properties and suppress carbon nucleation (Donat et al., 2022). Also, encapsulating or diluting Ni within a spinel or non-reducible matrix reduces active Ni ensembles that nucleate carbon. Thus, Ni-diluted, Mg-stabilized spinels improved coke resistance (Zhang et al., 2020). The synthesis of core–shell Ni@oxide materials is a valid strategy to reduce the carbon formation.

In addition, sorption-enhanced processes ensure reacting conditions to avoid coke build-up. The use of SE-CLR, by removing CO_2 and shifting reforming equilibrium, reduces the potential for carbon deposition (Antzara et al., 2016; Zhong et al., 2024) and at the same time improves hydrogen yield (las Obras Loscertales et al., 2025a).

2.3. Indirect gasification

Indirect gasification, also known as *dual fluidized bed gasification* (DFBG), represents a promising route to produce nitrogen-free, high-calorific-value syngas without the need for pure oxygen feed, thereby eliminating the requirement for energy-intensive and costly air separation units. Unlike other thermochemical looping technologies, DFBG employs an inert bed material that does not participate significantly in the chemical reactions. Nevertheless, the bed material can be strategically selected or modified to enhance process performance by providing catalytically active sites (Hanchate et al., 2021). Fig. 10 shows a scheme of the indirect gasification process. This process operates through two interconnected fluidized bed reactors: a gasification reactor (GR), where solid feedstock is converted to syngas using steam as the fluidizing agent, and a combustion reactor (CR), where residual char from the GR is combusted to heat the circulating bed material. The endothermic gasification reactions are sustained by the sensible heat carried by the looping bed material from the CR to the GR, creating an autothermal system without direct contact between combustion gases and product syngas. This configuration ensures high syngas quality with minimal nitrogen dilution.

DFBG is a mature and commercially proven technology, with thousands of operating hours documented in industrial-scale facilities utilizing silica sand and olivine as primary bed materials, often supplemented with catalytic additives such as potassium and calcium compounds to enhance tar cracking and optimize syngas composition (Larsson et al., 2021). Consequently, current research efforts have shifted from fundamental process investigation toward targeted optimization and performance enhancement strategies aimed at improving economic viability and overall process efficiency.

A major research focus has been the improvement of gasification performance through enhanced solid-gas contact achieved via novel reactor geometries. Notable work at TU Vienna has explored advanced reactor designs (Benedikt et al., 2017; Schmid et al., 2021a) supported by comprehensive computational modeling efforts to optimize process and process chain integration (Wojnicka et al., 2021; Bartik et al., 2024). In parallel, Mauerhofer et al. (2021) demonstrated the technical feasibility of utilizing CO_2 as an alternative gasification agent in DFBG systems, opening pathways for carbon capture and utilization integration.

Process control and monitoring represent another critical avenue for improvement. Advanced process control systems have been developed and implemented in both commercial-scale installations (Nigitz et al., 2020) and pilot-scale facilities, with model predictive control (MPC) strategies showing particular promise for optimizing dynamic operation

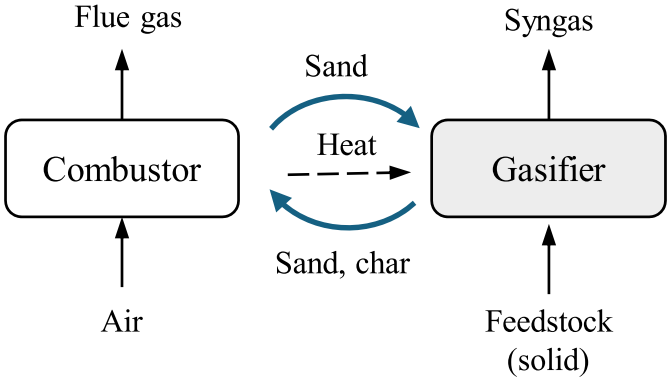

Fig. 10. Scheme of the indirect gasification process.

(Stanger et al., 2023a; Stanger et al., 2024b). Addressing tar formation and accumulation is a persistent challenge across all biomass gasification technologies. Ongoing research has focused on developing online monitoring techniques and predictive models that leverage readily available operational data from commercial plants (Benedikt et al., 2019).

Emerging reactor design concepts are pushing the boundaries of conventional DFBG configurations. Single-vessel unified designs that integrate both gasification and combustion zones within a single reactor vessel have been investigated, although operational data remain limited compared to established dual-reactor configurations (Di Carlo et al., 2022). Solar-assisted gasification has emerged as a theoretical strategy to increase carbon transfer efficiency from feedstock to syngas by replacing combustion-derived heat with concentrated solar energy.

Table 1
Selected pilot plants for testing high-temperature solid looping (HTSL) processes.

No.	Location/owner	Scale (kW_{th})	Reactor type	Specific features	Application	First operation	References
1	Tsinghua, CHEERS	5000	CFB-CFB	Carbon stripper	CLC, CLG	2024	Li et al. (2025b), Li et al. (2026)
2	La Pereda	1700	CFB-CFB	Cone valves	CaL	2012	Arias et al. (2013), Arias et al. (2018)
3	Chalmers	1400	CFB-BFB	Semi-commercial CFB boiler	DFBG, CLC	2009	Berdugo Vilches et al. (2017), Thunman and Seemann (2010)
4	TU Darmstadt	1000	CFB-CFB	J-valve	CaL, CLC, CLG	2010	Haaf et al. (2020b), Ohlemüller et al. (2017), Marx et al. (2023a)
5	ArcelorMittal, Aviles/ CSIC	1000	PB	BFG, in steel plant	SER-CaL	2024	Fernández et al. (2025)
6	BEST, Vienna	1000	CFB-CFB	Internals	DFBG	2024	Kadlez et al. (2025)
7	Buzzi, Vernasca	4 Nm^3/h*	EF-EF	Integrated in cement plant	CaL	2021	Fantini et al. (2021)
8	TU Darmstadt	300	CFB-BFB	Heat pipe heat exchanger	IHCaL	2014	Junk et al. (2016b), Hofmann et al. (2024b)
9	Ohio State Univ., Babcock & Wilcox	250	CFB-MB	–	CLC	2019	Zhang et al. (2021)
10	IFK Stuttgart	200	CFB-BFB; CFB-CFB	–	CaL, SEG-CaL	2010	Hafner et al. (2021); Hornberger et al. (2020)
11	SINTEF	150	CFB-CFB	Lifter	CLC	2011	Bischi et al. (2011), Langørgen et al. (2023)
12	TU Wien	120	CFB-CFB	Bottom loop seal	CLC	2010	Pachler et al. (2020)
13	Chalmers	100	CFB-CFB	Circulation riser	CLC	2012	Linderholm et al. (2017)
14	TU Wien	80	CFB-CFB	Internals	CLC, SEG-CaL	2010	Benedikt et al. (2018)
15	VTT	60	CFB-CFB	–	CLC	2016	Gogolev et al. (2021a), Gogolev et al. (2021b)
16	CSIC	50	CFB-CFB	Carbon stripper	CLC, CLG	2014	Abad et al. (2024)
17	NETL	50	CFB-BFB	–	CLC	2016	Siriwardane et al. (2021)
18	CNRS	50	BFB	Solar driven calciner	CaL	2019†	Esence et al. (2020a)
19	CSIC	30	BFB	–	SEG-CaL	2017	Martínez et al. (2020)
20	Tsinghua	30	CFB-BFB	–	CLC	2018	Chen et al. (2020), Liu et al. (2021b)
21	Hamburg	25	CFB-BFB	Dual-stage BFB	CLC	2012	Haus et al. (2020), Lindmüller et al. (2023)
22	Nanjing	20	CFB-BFB	–	CLC	2016	Wang et al. (2020)
23	Chalmers	10	CFB-BFB	–	CLC	2008	Mei et al. (2021)
24	IFPEN	10	BFB-BFB	–	CLC	2010	Vin et al. (2022)
25	Nanjing	3	BFB-BFB	Multi-stage fuel reactor	CLC	2009	Shen et al. (2020)
26	SINTEF	1–2.1	ICR	–	CLC	2016	Osman et al. (2020)
27	CSIC	1	BFB-BFB	For gaseous fuels	CLC, CLR	2009	Adánez et al. (2009)
28	CSIC	1	BFB-BFB	For liquid fuels	CLC, CLR	2015	García-Labiano et al. (2015), Adánez-Rubio et al. (2021)
29	CSIC	1	BFB-BFB	For solid fuels	CLC, CLG	2011	Cuadrat et al. (2011)
30	CSIC	1	BFB-BFB	Semicontinuous FB, pressurized	CLR	2009	Ortiz et al. (2010)
31	Chalmers	0.3	CFB-BFB	–	CLC	2006	Hedayati et al. (2021), Li et al. (2024b), Lyngfelt et al. (2022a)
32	Eindhoven	0.6	BFB-BFB	Membrane-assisted CLR. Continuous circulation	CLR	2018	Medrano et al. (2018)
33	Eindhoven	N/A	BFB	Membrane-assisted CLR. Gas switched	CLR	2018	Wassie et al. (2018)
34	Univ British Columbia	N/A	FBMR	Membrane-assisted FB	CLR	2011	Andrés et al. (2011)
35	Eindhoven	2	PB		CLR	2017	Spallina et al. (2017)
36	Manchester	Lab scale	PB		CLR	2022	Alexandros Argyris et al. (2022)
37	Ghent	N/A	2 parallel fixed. bed reactors	Super-dry CLR pilot (LCT)	CLR	In construction	Moonshot Flanders (2026)

*No data in terms of heating power available.
†Estimated.
Abbreviations. BEST: Bioenergy and Sustainable Technologies GmbH; BFB: Bubbling fluidized bed; CFB: Circulating fluidized bed; CNRS: National Center for Scientific Research, France; CSIC: Consejo Superior de Investigaciones Científicas, Spain; Chalmers: Chalmers University of Technology, Sweden; Eindhoven: Eindhoven University of Technology, Netherlands; FBMR: Fluidized-bed membrane reformer; Ghent: Ghent University, Belgium; Hamburg: Hamburg University of Technology, Germany; IFPEN: French Institute of Petroleum – New Energies, France; Manchester, The University of Manchester; Nanjing: Southeast University, China; NETL: National Energy Technology Laboratory, USA; PB: Packed-bed; SINTEF: The Foundation for Scientific and Industrial Research at the Norwegian Institute of Technology, Norway; Tsinghua: Tsinghua University, China; TU Darmstadt: Technical University of Darmstadt, Germany; TU Wien: Vienna University of Technology, Austria; VTT: VTT Technical Research Centre of Finland, Finland.

Recent advances have modeled the delivery of high-temperature sensible heat to fluidized bed gasifiers, enabling continuous operation despite solar intermittency through thermal buffering (Suárez-Almeida et al., 2021; Gómez-Barea et al., 2021; Suárez-Almeida et al., 2023) or by replacing the combustor entirely by solar power input (Yakan à Nwai and Patel, 2023). However, experimental validation of these concepts is still missing.

3. Pilot studies

3.1. Existing pilot plants

A large number of HTSL pilot plants with different reactor concepts and varying scale up to 5 MW_{th} have been operated within the last 10 years. The thermal power refers to the fuel input (mass flow times lower calorific value) either into the plant itself or, in the case of post-combustion capture, into a potential upstream plant. Table 1 summarizes the main features of the pilot plants that have been operated under industrially relevant conditions. Here, it should be noted that DFBG has already been operated in commercial plants, which are not included in the table. The type of HTSL process that is tested in each pilot plant will be discussed in the following sections. Some pilot plants can be used for various processes. The different reactors concepts are briefly described below, while referring to the plant numbers defined in Table 1 in brackets.

Most pilot plants utilize a continuous transfer of solids between coupled fluidized bed reactors, which are operated in varying fluidization regimes, i.e., bubbling, turbulent, or fast fluidization. For simplicity, we only differentiate between bubbling fluidized beds (BFB) with only little entrainment of particles and circulating fluidized beds (CFB) with high entrainment of particles. Mostly, at least one reactor is operated as a CFB reactor, enabling entrainment of particles in the riser to the top of the reactor and, after separation in a cyclone, the transfer of these particles by gravity to the second reactor. In some cases, the bottom of the riser is widened to increase the residence time of solids in a bubbling bed regime (13). In other cases, part of the solids separated in the cyclone are fed back to the bottom of the riser to decouple the transfer of solids between the reactors from particle entrainment (2, 4). Here, the control of the solids flow from one reactor to the other can be realized by various means, e.g., double loop seal (16), L-valve (1), J-valve (4), cone valve (2), screw conveyor. The second reactor can be operated as a BFB or a CFB. In the first case, the transfer of solids back to the first reactor is mostly realized by the overflow of particles over a weir, which enables an easy control of the solid circulation through a constant bed height in the second reactor. This approach is sometimes also used for CFB reactors where entrained particles are circulated back to the riser (13), although there exists no distinct bed height in this fluidization regime. An alternative is the coupling via a bottom loop seal where the transfer of solids is controlled by the pressure difference between the two reactors (12, 14). Some plants use specific equipment to control or enhance the solids circulation, such as a circulation riser (13) or a bottom lifter (11). Another option for the second reactor is to use the same principle as in the first reactor, i.e., entrainment in a CFB and transfer by gravity (4, 16). This allows more flexibility regarding the solids inventory in the two reactors, however, at cost of a more difficult control. Mostly, loop seals are used to prevent gas leakages between the reactors. One plant (26) is operated as an Internally Circulating Reactor (ICR). In general, it can be observed that large-scale pilot plants tend to use two coupled CFB reactors, since these are easily scalable and have a low footprint.

Some fluidized bed reactors systems have distinctive features to fulfill specific requirements of a certain process. In chemical looping processes with solid fuels, a carbon stripper separates char from the solids leaving the fuel reactor and transfers the former back to the fuel reactor (1, 13, 16). The separation is mostly achieved by the difference in terminal velocity between char and oxygen carrier particles. Staged reactor systems (21, 25) or internals for narrowing the reactor at certain locations (6, 12) are used to increase the gas-solid contact and thereby improve gas conversion. An indirectly heated calciner utilizes heat pipes immersed in a BFB to enable high heat transfer rates (8). Here, the BFB is divided into two sections to enable a plug-flow-like behavior.

Only few pilot plants make use of other types of reactors than fluidized beds. One chemical looping concept with continuous transfer of solids utilizes the combination of a CFB reactor with a moving bed (MB) reactor (9). The moving bed enables a plug-flow behavior with countercurrent gas-solid flow and a long solids residence time to maximize fuel conversion. This concept requires measures to control the height of the moving bed. Other chemical looping plants employ rotating fixed beds (FB) to enable continuous operation of a chemical looping process. Here, measures are required to minimize gas leakage. A carbonate looping plant for integrated CO_2 capture from cement production applies two coupled entrained flow reactors, thus enabling the use of cement raw meal, which has a rather fine particle size, as the sorbent (7). As an alternative to continuously operating reactor systems, batchwise operation in fixed bed (FB) reactors can be utilized to realize the HTSL processes. This concept allows operation at varying pressures, such as in pressure swing absorption (5).

3.2. Carbonate looping pilot testing

3.2.1. Oxy-fired carbonate looping

Several large pilot facilities have been built to demonstrate oxy-fired carbonate looping. In this subsection, the main activities carried out in these pilots are organized according to the sector of application. A recent review on oxy-fired and indirectly heated carbonate looping facilities has been published by Tan et al. (2024). In the beginning, research on CaL focused on carbon capture for gases related to power generation, validating the technology through many hours of pilot testing at the MW scale (Hilz et al., 2017; Ströhle et al., 2014a; Arias et al., 2013). In the recent years, CaL research has shifted toward industrial applications. These include mainly cement, lime, and waste incineration. Furthermore, many studies of the last years introduced novel CaL configurations that enable higher flexibility and capture rates.

One important aspect of capturing CO_2 from power plants is the flexibility of CaL systems to adapt to flue-gas load changes. Experimental campaigns at the La Pereda pilot plant (see Table 1, no. 2, and Fig. 11) have demonstrated that CaL systems with circulating fluidized bed reactors are highly flexible, handling up to a 50% reduction in flue-gas load (with gas-velocity variations between 2.0 and 5.3 m/s) through the entrainment of solids from the carbonator driven by the solids circulation between reactors (Diego and Arias, 2020). Staging the flue gas entering the carbonator has also been shown to help maintain high capture efficiencies by stabilizing the solids inventory at the reactor bottom during flue-gas load increases (Diego and Arias, 2020). Regarding CaL flexibility, a flexible CaL concept based on a bubbling-bed carbonator with a bottom interlink to a CFB oxy-calciner—allowing the decoupling of both reactors—has been successfully demonstrated with high CO_2 capture efficiency. Carbonator performance has been assessed at partial loads as low as 40%, achieving equilibrium-normalized capture efficiencies of up to 90% in the 200-kW_{th} Stuttgart pilot plant (Moreno et al., 2021b).

Regarding carbonator performance, an alternative strategy to achieve very high CO_2 capture efficiencies in a CFB carbonator has been demonstrated at the La Pereda pilot plant. This approach consists of cooling the upper part of the reactor to create a low-temperature zone while ensuring that sufficient active sorbent is available. Tests were carried out with the calciner operating under typical oxy-fuel conditions and firing biomass at a rate of 2.0 MW_{th}, together with high limestone make-up flows. The results confirm that CO_2 capture efficiencies above 0.99 can be achieved by maintaining a sufficiently low temperature at the carbonator outlet (<550 °C) and ensuring an adequate amount of sorbent in the cooled zone (Arias et al., 2024).

Fig. 11. Photograph of the 1.7-MW_{th} La Pereda pilot plant connected to an existing 50 MW_e power plant. Adapted from Diego et al. (2016a) with permission.

Regarding the calciner, one approach to minimizing its heat demand is to reduce the recycle of CO_2. This recycle is typically used in oxy-combustion systems to dilute the oxygen stream before it enters the combustion chamber, thereby controlling temperature and heat transfer. Operating under higher oxygen concentrations may be feasible in the oxy-fired calciner of a CaL system by taking advantage of the thermal-ballast effect of the cooler solids entering from the carbonator and the endothermic nature of the $CaCO_3$ decomposition reaction. At the 1.7-MW_{th} Pereda pilot plant, tests were conducted with a coal thermal input to the calciner of up to 2.0 MW_{th} and oxygen concentrations in the oxidant reaching 75 vol%, confirming the possibility of operating the oxy-fired CFB calciner without hot spots, provided that sufficient solids circulation and bed inventory were maintained (Arias et al., 2018).

The experimental testing of CaL applied to WtE plants has been carried out in the 1 MW_{th} Darmstadt pilot plant. During these tests, waste-derived fuels in the form of raw fluff were fired in the calciner, and the CO_2 concentration in the flue gas to be decarbonized was maintained at approximately 9.5 vol%, a typical value for WtE plants. Under these conditions, carbonator CO_2 absorption rates of 80–85% and overall CO_2 capture efficiencies above 90% were achieved under representative CaL process conditions. Fuel quality was found to have a significant influence on the operability of the interconnected CFB system. Operation with SRF containing coarse ash fractions led to ash accumulation in the solid phase, which negatively affected system hydrodynamics (Haaf et al., 2020b). In this regard, ash accumulation in the solids inventory has been shown to decrease when coals with smaller particle sizes are used (Hilz et al., 2018). During the SRF tests, chlorine retention exceeded 82% across the experimental points. It was also observed that calciner operating temperatures above 860 °C are desirable to maximize chlorine retention (Haaf et al., 2020d).

The oxyfuel combustion of hard coal, wheat straw, and pelletized SRF was also assessed in the calciner of the 200-kW_{th} CaL pilot plant in Stuttgart to study their impact on NO_x and acidic species (SO_2, HCl), as well as reactor profiles. Fuel blending had little effect on pollutant formation, while biomass substitution altered emissions due to changes in nitrogen and chlorine content. HCl emissions were reduced by Ca-species, achieving chlorine retention above 0.90 mol/mol. High NO_x emissions, however, were measured during oxyfuel calcination tests compared with standard oxyfuel combustion (Moreno et al., 2021a).

Regarding cement applications, the tail-end configuration has been tested in the 200-kW_{th} Stuttgart pilot plant. Different integration levels were assessed with make-up ratios up to 0.9 mol/mol and CO_2 flue-gas concentrations up to 35 vol%. Capture rates close to the equilibrium limit were achieved during these tests thanks to the high CO_2 carrying capacity of CaO (ranging from 0.20 to 0.37 mol CO_2/mol Ca). Tests with low integration levels led to high CO_2 carbonator loads while sorbent activity declined toward its residual level, thus requiring an increase in the sorbent circulation rate between reactors (Hornberger et al., 2020). Moreover, uniform temperature profiles without major hotspots were obtained under operating conditions with recirculation rates as low as 20% and oxygen inlet concentrations up to 56 vol% (Hornberger et al., 2021).

For the integrated configuration in cement applications, a pilot plant connected to a cement facility and based on entrained-flow reactors has been built (Fantini et al., 2021). The calciner is supplied with the same type of raw meal used in the kiln for clinker production, while the carbonator processes the effluents generated by the cement plant. The CaL calciner operates in a recirculated oxy-fuel combustion mode, in which heavy fuel oil is burned with oxygen. More than 200 hours of operation with calcined raw-meal feeding have been achieved. Among the issues encountered during pilot plant operation, the most frequent were related to the strong interconnection of the system and the clogging of discharge pipes due to their small diameter, which could be overcome through scale-up of the plant (Magli et al., 2023).

3.2.2. *Indirectly heated carbonate looping*

The *indirectly heated carbonate looping* (IHCaL) using a *heat pipes heat exchanger* is the most advanced IHCaL configuration, since it is the only one that has been validated in pilot scale (Tan et al., 2024), as explained in Section 2.1.2.

The only existing IHCaL plant is located at the Technical University of Darmstadt (TU Darmstadt) in Germany (Reitz et al., 2014), which is illustrated in Fig. 12. This plant was constructed based on the cold-flow tests and design of Junk et al. (2013), and it was commissioned in 2015 (Reitz et al., 2016). It consists of three reactors: (i) an eight-meter CFB carbonator (ID = 250 mm) to capture CO_2 from synthetic flue gas and combustion gases (from the combustor); (ii) an indirectly heated calciner, operating at ca. 900°C, for sorbent regeneration; and (iii) a combustor, in which fuel is burnt to obtain the heat for the calcination. Both the calciner and the combustor are operated as bubbling fluidized beds and are thermally connected via a heat pipe heat exchanger featuring 72 sodium heat pipes (schematically on Fig. 12, left). The solids circulation is controlled using a cone valve downstream of the carbonator (Fig. 12, right, component no. 5). Here, a sample port is located, which enables discontinuous sampling of solid sorbent leaving the carbonator. More constructive details, as well as operating parameters of this pilot plant, are available in previous publications of the research group (Reitz et al., 2016; Reitz et al., 2014; Hofmann et al., 2022; Reitz, 2017).

Höftberger and Karl (2013) investigated the fluidization of the indirectly heated calciner in a 18-kW bubbling fluidized, using electrically heated heat pipes. They found that the CO_2 release from calcination suffices to fluidize the bed and establish the bubbling fluidization regime without the need of external fluidization gas. However, this could not be replicated in the 300-kW_{th} pilot tests at TU Darmstadt, probably due to the fact that the carbonation degree of the sorbent entering the calciner is generally very low (under 10%).

Starting in 2015, IHCaL pilot tests were performed at the 300-kW_{th} plant at TU Darmstadt to demonstrate the operability of this process for power generation plants (Reitz et al., 2016). A total of 500 hours of operation were achieved, including 340 hours of steady-state CO_2

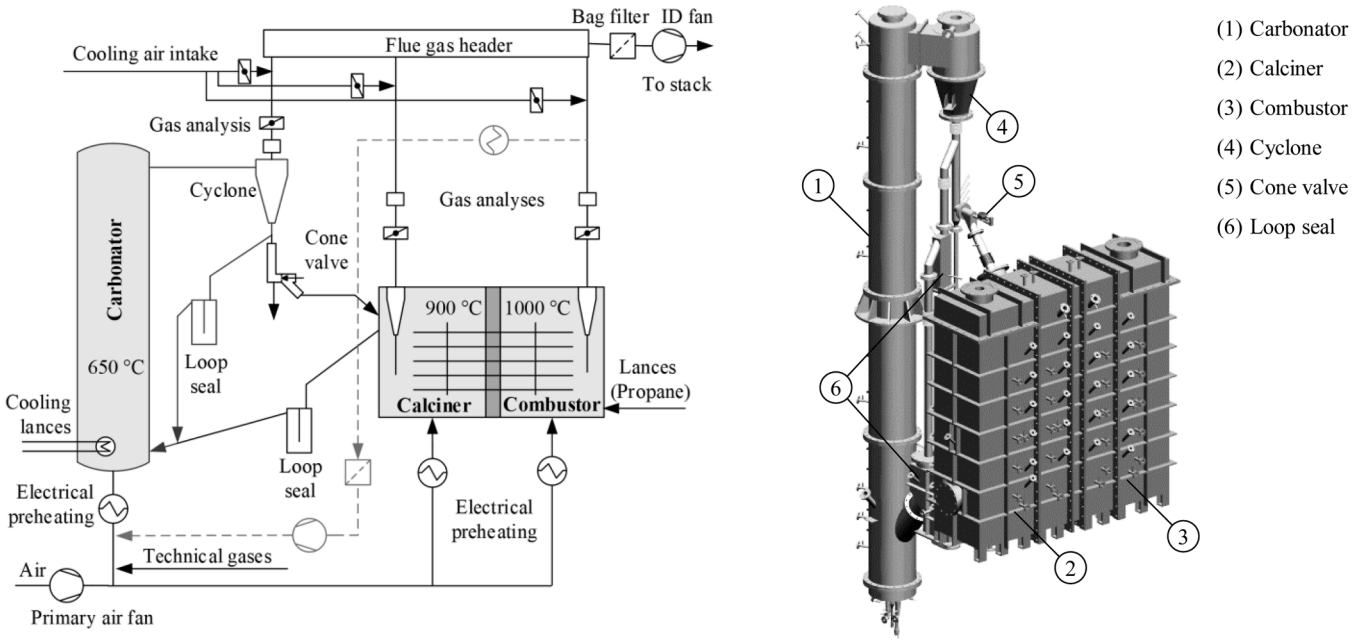

Fig. 12. Indirectly heated carbonate looping (IHCaL) 300-kW_{th} pilot plant at the Technical University of Darmstadt. On the left, the process flow diagram (PFD), adapted from Greco-Coppi et al. (2024d), shows the main components and their interconnections. The three reactors, the carbonator, the calciner, and the combustor, are highlighted with a gray shading. The light-gray broken lines represent the new flue-gas tract that was commissioned in 2022. The sub-figure on the right is the CAD render of the reactors and main solid circulation path, adapted from Reitz et al. (2016). The heat pipe heat exchanger is insider the calciner (2) and the combustor (3), connecting them horizontally. This figure was reproduced from Greco Coppi (2025), licensed under CC BY 4.0.

capture at different operating parameters. CO_2 capture efficiencies of over 90% were achieved in relevant operating conditions, thus validating the concept.

With the shift toward hard-to-abate industries that took place in the last ten years, the IHCaL process has been considered as a promising candidate for the lime and cement industry due to the potential synergies in energy and spent-sorbent integration (see Section 2.1.2). To test the IHCaL for relevant conditions for cement and lime plants, the 300-kW_{th} plant was expanded (Hofmann et al., 2024a, 2024b). The upgrades included a new flue gas tract to circulate the exhaust gases from the combustor into the carbonator (illustrated with broken lines in Fig. 12, left), and a solids fuel feeding system capable of handling coal and pelletized refuse-derived fuel (RDF). The upgraded pilot facility was operated for over 200 hours, including high CO_2 concentrations at the carbonator inlet of up to 18 $vol\%_{db}$, corresponding to operating conditions relevant to lime plants. Coal and RDF were successfully co-fired with propane. However, challenges to achieve complete combustion were reported.

Until now, all the IHCaL pilot tests have used air to fluidize the calciner. However, in real operating conditions, steam, recirculated CO_2, or a combination of both would be required to ensure a high-purity CO_2 stream after the calciner. This would probably require higher temperatures in the calciner, in the order of 900°C (Greco-Coppi et al., 2025b). Furthermore, challenges related with the operation of the IHCaL plant have been reported, which should be addressed before this technology can be safely upscaled. These include, enhancing the combustion efficiency in the external combustor and improving the flue gas circulation into the combustor (Hofmann et al., 2024b), as well as optimizing the entrainment and make-up rates (Greco-Coppi et al., 2025a).

3.2.3. Solar heating and new reaction pathways

Within this section, the review focuses on existing plants on solar-driven $CaCO_3$ calcination. The calcination of $CaCO_3$ is the most challenging step of the solar-driven carbonate looping technology, as explained by Khan et al. (2024).

Fluidized bed reactors have been proposed as particle receivers (Tregambi et al., 2021b), and limestone calcination was successfully achieved in a four-stage horizontal fluidized bed, irradiated on a front metallic wall (1 m long and 0.4 m high) operating with an average of 55 kW, situated inside the 1 MW solar furnace at Centre National de la Recherche Scientifique (CNRS) (Esence et al., 2020b). Up to 20 kg/h of commercial calcium carbonate achieved 95% calcination efficiency.

Alternative reactor designs include the use of rotary kilns (Moumin et al., 2019; Tescari et al., 2020). These reactors were operated at the scale of 14 kW and material flows between 4 and 12 kg/h with calcination degrees between 24 and 99% were obtained. The efficiencies (thermal plus chemical) ranged between 19 and 40%.

3.2.4. Sorption-enhanced carbonate looping

Several pilot plants have been reported in the literature to progress on the demonstration of the SER and SEG technology. This Section focuses on reported experimental results from the recent 5–7 years and their contribution to technology development.

One of the main advantages of the SER based on packed-bed reactors is the rapid scaling-up of the technology, as this has been the case for the 1-MW_{th} plant constructed in the ArcelorMittal GasLab installations in Avilés (Spain), illustrated in Fig. 13. This pilot plant, that entered in operation in the first half of 2024, served to prove the CASOH process at TRL 7 to produce an H_2/N_2 gas stream, and decarbonize, real BFG from ArcelorMittal site (Fernández et al., 2025). One of the reasons of the rapid scale-up of the technology was the use of commercial functional materials (Cu-based solid, and limestone as sorbent precursor) available at the 100-kg scale, whose suitability was previously validated through intense testing at lower TRL (Abbas et al., 2022; Grasa et al., 2023). The pilot plant, that accumulates more than 500 h of operation experience, has been designed to handle a flow of BFG equivalent to approximately 1MW_{th}, divided into 300 Nm^3/h of upgraded BFG and about 0.7 MW_{th} of sensible heat produced at high temperature. During the CASOH stage, the BFG was almost entirely decarbonized and converted into a product gas containing up to 40% vol. H_2 in N_2, with over 95% CO_2 captured in this stage. Experimental results in terms of H_2 yield, CO_2 capture, BFG conversion and even temperature profiles evolution closely matched the

Fig. 13. Photograph of the CASOH pilot plant at ArcelorMittal Gas Lab. This plant uses sorption-enhanced water gas shift (SEWGS) to produce H_2 and decarbonize blast furnace gas (BFG) for the production of steel. Reproduced from Fernández et al. (2025), licensed under CC BY 4.0.

results obtained at lower TRL. Moreover, the TRL 7 pilot operated successfully under dynamic conditions, demonstrating its robustness and adaptability. Future tests in this pilot aim to assess the process's long-term viability paving the way for further scale-up of the technology.

SER pilot plants based on interconnected fluidized bed reactors have been reported in the literature (see, e.g., Hynor or HyPer project). However, no results from their operation have been published to date.

With respect to biomass SEG, DFB steam gasification has been studied in Vienna (100 kW) during the last decade and their more advanced design—adequate to operate with waste fuels—entered into operation in 2014 (Müller et al., 2017). Benedikt et al. (2018) describe the modifications implemented in the upper gasification reactor that was designed as a countercurrent column with hot bed material flowing down and product gas streaming upwards. Results obtained from the gasification of diverse residual fuels indicated that all studied biomasses presented a very similar behavior in terms of gas yield and composition, producing a gas with 11.0–12.5 MJ/Nm^3 db, and the lowest total and gravimetric tar content (around 1 g/m^3 STP, d.b.). Waste-derived fuels produced a syngas with higher lower heating value (14–16 MJ/Nm^3 d.b.), but also with a higher gravimetric tar content 15–20 g/m^3 STP, d.b. gravimetric tar. Overall, cold gas efficiencies ranging from 67% to 74% were reported in these experiments. With the objective of demonstrating the advanced DFB steam gasification close to industrial level, the lessons learned at the 100-kW-scale unit have been incorporated during the design, construction, and commissioning of a 1-MW$_{th}$ (fuel power input) plant at the Syngas Platform Vienna. This installation incorporates a countercurrent column in the upper part of the gasifier, and it has been designed to operate under SEG conditions but also for indirect gasification. It was operated at full load with high-grade wood chips and olivine as bed material, proving the successful operation of the pilot under indirect heating steam gasification. Future tests are expected under SEG conditions (Kadlez et al., 2025).

The 200-kW$_{th}$ plant at IFK Stuttgart served to prove the flexibility of the sorption-enhanced gasification (SEG) in DFB systems (Hafner et al., 2021). The plant configuration allows controlling the mass flow of solids between gasifier and combustor thanks to the rotation speed from a screw feeder and the pressure difference between reactors. Moreover, the continuous feeding of limestone to the calciner allows operating the system with a sorbent with sufficient CO_2 carrying capacity that permits the modulation of CO_2 capture as a function of operating parameters. In this way, for a fixed amount of sorbent feed to the system (0.17 mol CaO per mol of C in the biomass), the effect of temperature, S/C ratio and weight hour space velocity (WHSV) on gas yield and composition—in terms of permanent gases—, production of lower HC, and tar formation was evaluated. The results indicate that gasification temperature is the variable with the highest impact in product gas composition as ratios H_2/CO between 8 and 1 were obtained at gasification temperatures between 650 and 775 °C. High gasification temperatures led to high gas yield and lower tar content (as low as 1 g/m3 d.b., STP for gravimetric tar at 771 °C), but it was disadvantageous regarding H_2 content in the gas. The higher S/C ratio during gasification also improved the H_2 content in the gas and decreased the CO, CO_2, CH_4, and light hydrocarbons and gravimetric tars. With respect to the WHSV (related with the solid circulation between reactors), a lower WHSV (higher circulation rate) was beneficial to improve H_2, and reduce CH_4 and light HC in line with results obtained at lower scale pilot plants (Hafner et al., 2021). In this plant, the feasibility of the Oxy-SEG configuration was proved and an 80% vol. CO_2 gas was obtained at calciner exit operating in oxy-combustion mode without altering the gasifier operation. This indicates that, although sorbent deactivation is increased at severe calcination conditions, stable Oxy-SEG operation was possible confirming the production of identical syngas as those derived from SEG (Parvez et al., 2021).

3.3. Chemical looping pilot testing

Chemical looping technologies have been demonstrated using three reactor groups, namely:

1. Interconnected Circulating Fluidized Bed (CFB): continuous solids circulation between air and fuel reactors. This option is widely used in chemical looping lab pilots, with high confidence in the scale-up due to good solids mixing and heat transfer. For its industrial deployment, attrition-resistant oxygen carriers are required. In general, from the experience on chemical looping units and catalyst performance in the Fluid Catalytic Cracking (FCC) process, limits for crushing strength values higher than 1 N and standardized Air Jet Index (AJI) for attrition (Cabello et al., 2016).
2. Moving Bed: characterized by a continuous flow of solids and gas but avoiding the fluidization of the oxygen carrier particles. It is characterized by a good solids-gas contact with simpler hydrodynamics than CFB, but some limitation may be found in heat transfer during its scale-up.
3. Fixed/Alternating Beds: this is a preferred option at small scale or demonstration reactors alternately regenerated, being useful for proof-of-concept stages. This configuration can be scale-up at pressurized conditions, but it may require several reactors operating in coordinated stages with a complex system of high-temperature valves.

The experience and scope of each one of these options differ depending on the process to be developed, namely CLC, CLG or CLR. This is discussed in the following subsections within Section 3.3.

3.3.1. Chemical looping combustion

Since the landmark 10-kW$_{th}$ gaseous-fuel chemical looping combustion (CLC) pilot operation in 2004 (Lyngfelt et al., 2005), and the first demonstration of solid-fuel CLC in 2008 (Berguerand and Lyngfelt, 2008), CLC has evolved rapidly from proof-of-concept demonstrations toward more application-oriented pilot studies emphasizing comprehensive system performance, i.e., combustion efficiency, carbon capture efficiency, process stability, fuel flexibility, cost reduction, and negative-emission potential. The development of pilot-scale CLC operations has been extensively reviewed in several papers (Adánez et al., 2018; Mattisson et al., 2018; Lyngfelt et al., 2019; Lyngfelt, 2020; Zhao et al., 2020; Qasim et al., 2021; Daneshmand-Jahromi et al., 2023). Building upon these works, Table 2 below provides a comprehensive overview of recent pilot advancements over the past 5 to 10 years. By comparing earlier reviews with current progress, several evolving trends could be identified, particularly regarding scaling-up efforts, reactor configurations (discussed in Section 2.2.1.1), oxygen carrier selection

Table 2
Recent advances on pilot studies of chemical looping combustion (CLC).

No.	Location/ owner	Scale (kW_{th})	Oxygen carrier	Fuel	Operation w/fuel (h)	Reactor type	Fuel/Gas conversion	Carbon Capture	References
1	Tsinghua	5000	Ilmenite	Lignite	20	CFB/BFB	Up to 97.6%	>97%	Li et al. (2025b)
3	Chalmers	1400	Ilmenite; Mn ore	Wood pellets	1000	BFB-CFB	60% (830°C)	N/A	Berdugo Vilches et al. (2017)
4	TU Darmstadt	1000	Ilmenite; Ca-Mn-based	Hard coal; natural gas	153	CFB-CFB	Up to 75%	43-55%	Ohlemüller et al. (2019), Ohlemüller et al. (2017), Ohlemüller et al. (2016)
9	Ohio State Univ., Babcock & Wilcox	250	Fe_2O_3/Ceramic	Coal	288	Moving bed-EF	96%	>98% with >97% CO_2 purity	Zhang et al. (2021)
11	SINTEF	150	Ilmenite; mixture of Ilmenite/ Mn oxide	Woody biomass; SRF; petcoke; waste-derived fuel	67	CFB-CFB	80−81% (SRF); 76.5−79.5% (Biomass)	97.5−98% (SRF); 93.5−95% (Biomass)	Langørgen et al. (2025), Langørgen et al. (2023), Mohn et al. (2025)
12	TU Wien	120	$CaMn_{0.775}Ti_{0.125}Mg_{0.1}O_{3-\delta}$; CuO/Al_2O_3	Natural gas	9	CFB-CFB	88-94%	N/A	Pachler et al. (2020)
13	Chalmers	100	Mixture of Mn ore and ilmenite; Mn ores; synthetic $CaMnO_{3-\delta}$; Ilmenite	Bituminous coals; black pellets; straw pellets; wood char	34	CFB-BFB	Up to 91.5%	Up to 100%	Linderholm et al. (2017), Linderholm et al. (2016), Gogolev et al. (2019)
14	TU Wien	80	Ilmenite; Mn ores; mixture of ilmenite with limestone; synthetic C28	Wood; bark pellets	39	CFB-CFB	89%	>98%	Fleiß et al. (2024), Fleiß et al. (2022)
15	VTT	60	Ilmenite; braunite	Wood pellets; wood char; straw pellets	24	CFB-CFB	Up to 90%	Up to 89%	Gogolev et al. (2021a), Gogolev et al. (2021b)
16	CSIC	50	Cu30MnFe; iron ore	Coal; pine sawdust; pine forest residue; olive stones	130	CFB-CFB	Up to 95.9%	Up to 93%	Abad et al. (2025b), Abad et al. (2024), Abad et al. (2020)
17	NETL	50	$CuFeMnAlO_{4+\delta}$; CuO and Fe_2O_3	Methane; natural gas	65	CFB-BFB	70-90%	N/A	Bayham et al. (2019), Siriwardane et al. (2021)
N/A	SINTEF	50	$CaMnO_{3-\delta}$	CO; H_2	12	Gas Switching/ Pressurized	>90%	>90% CO_2 avoidance	Del Arnaiz Pozo et al. (2019), Ugwu et al. (2022)
20	Tsinghua	30	Ilmenite; Mn ore	Coal; petcock; lignite	260	CFB-BFB	Up to 75%	Up to 95%	Chen et al. (2020), Liu et al. (2021b)
21	Hamburg	25	CuO/Al_2O_3	German hardwood pellets; softwood; coal	8	CFB-dual-stage FR	>98%	93–96%	Haus et al. (2020), Lindmüller et al. (2023)
22	Nanjing	20	Iron ore	Coal	11	CFB-BFB	Up to 95.3%	>97%	Wang et al. (2020)
23	Chalmers	10	Ilmenite; Mn ore; LD slag	Black pellets; Swedish wood char; German wood char; pine forest residue; straw pellet mix	55	CFB-BFB	Up to 95.1%	100% (high-volatile biomass) >94% (low-volatiles biomass)	Gogolev et al. (2021b), Mei et al. (2023), Mei et al. (2021)
24	IFPEN	10	Ilmenite; LY Mn ore	Methane; petcoke	100	BFB-BFB	Up to 88.9%	Up to 90.8%	Vin et al. (2022)
25	Nanjing	3	Fe_2O_3	Lignite coal	9	BFB-BFB	96%	80.3%	Shen et al. (2020)
26	SINTEF	1-2.1	$CaMn_{0.775}Ti_{0.125}Mg_{0.1}O_{3-\delta}$	CO	16	ICR	97%	94%	Osman et al. (2020)
27,29	CSIC	1	Tierga ore; $CaMn_{0.775}Mg_{0.1}Ti_{0.125}O_{2.9-\delta}$; Cu14Al_ICB	Spanish biomass residues (pine sawdust/olive stone/almond shell); methane; simulated biogas	89	BFB-BFB	70–75% (biomass)	90-100%	Mendiara et al. (2018b), Cabello et al. (2023b), Cabello et al. (2021)
31	Chalmers	0.3	Mn ores; LD slag; ilmenite; $CaMnO_{3-\delta}$	Synthetic biomass volatiles; syngas; methane; kerosene	301	CFB-BFB	Up to 97% (CH_4), 85% (kerosene), 99% (syngas), 97.6% (synthetic volatiles)	N/A	Moldenhauer et al. (2018a), Moldenhauer et al. (2018b), Hedayati et al. (2022), Hedayati et al. (2021), Lyngfelt et al. (2022a), Li et al. (2024a), Li et al. (2024b)

Abbreviations. See Table 1.

(discussed in Section 2.2.1.2), fuel choices, and research focuses.

While early studies primarily focused on gaseous fuels for fundamental validation, recent developments exhibit a predominant interest in solid fuels, including coal, biomass, and waste-derived feedstocks. This transition is most likely driven by the urgent need to upscale CLC and decarbonize power generation and heavy industries. A critical milestone in the scaling-up process is the achievement of auto-thermal operation, which is essential for industrial-scale viability. Notable successes have been recorded across various scales, including the SINTEF 150-kW_{th} unit (Langørgen et al., 2025; Langørgen et al., 2023), the Darmstadt 1 MW_{th} pilot plant (Ohlemüller et al., 2016), and the Chalmers 1.4/10 MW_{th} unit (Berdugo Vilches et al., 2017). The details of these plants are available in Table 1, no. 11, 4, and 3. Most recently, the world's largest CLC facility to date,the Tsinghua 5-MW_{th} unit (see Fig. 14 and Table 1, no. 1), has further pushed the boundaries of the technology (Li et al., 2025b). The unit demonstrated exceptional CLC performance using lignite as fuel. Operation achieved a CO_2 capture efficiency exceeding 97% and a remarkably low oxygen demand of 2.45% for unburnt gases. These results, combining high carbon-capture rates with stable thermal performance at up to a multi-megawatt scale, provide conclusive evidence that CLC has reached the technological maturity required for industrial-scale deployment.

As discussed in Section 2.2.1.2, recent years have seen a progression in oxygen carrier development from mono-metallic systems to more complex oxides. When comparing pilot-scale operations reported in earlier investigations, it is clear that a wide range of oxygen carriers has been employed, spanning from natural ores to synthetically produced oxides of varying complexity. NiO was a widely used oxygen carrier during the first decade of oxygen carrier development. However, in recent years, NiO has not been tested in any of the pilot campaigns listed in Table 1. Instead, ilmenite, manganese ores, and mixtures of ilmenite and manganese ores have been used as oxygen carriers in most of the pilot studies summarized in Table 2. In addition, waste-derived oxygen carriers such as LD slag (a steel slag from the Linz–Donawitz process, BOF) have attracted more attention in pilot-scale investigations over the past 5–10 years (Hedayati et al., 2022; Mei et al., 2023). More complex synthetic oxygen carriers—including Cu-based materials (Cu14Al-ICB (Cabello et al., 2023b), Cu30MnFe (Abad et al., 2024), $CuFeMnAlO_{4-\delta}$ (Bayham et al., 2019), Mn-based materials ($CaMnO_3$ made from natural ores (Li et al., 2024b), and synthetic $CaMn_{0.775}Ti_{0.125}Mg_{0.1O3-\delta}$ (Cabello et al., 2021; Osman et al., 2020)—have also been tested at different pilot scales during the last decade to address the limitations of monometallic oxides, such as thermodynamic constraints, attrition, and melting-related issues. Attrition resistance is another key criterion for selecting oxygen carriers for large-scale applications of CLC. Early work showed that commonly used room-temperature mechanical tests, such as crushing strength and jet-cup attrition, do not reliably predict the attrition observed in pilot-scale CLC operation (Lyngfelt et al., 2023). In pilot units, oxygen carriers are exposed to high temperatures, repeated redox cycling, and continuous gas–solid contact, which introduce degradation mechanisms that are not captured by standard mechanical tests. This indicates that pilot-scale testing, especially with solid fuels, in which the attrition of oxygen carriers is recorded, is becoming important. Recent pilot studies with natural, waste-derived, and synthetic oxygen carriers have therefore reported oxygen carrier lifetime directly based on operational data. These studies show that iron- and manganese-based ores generally experience higher attrition rates than benchmark ilmenite, with typical operational lifetimes in the range of

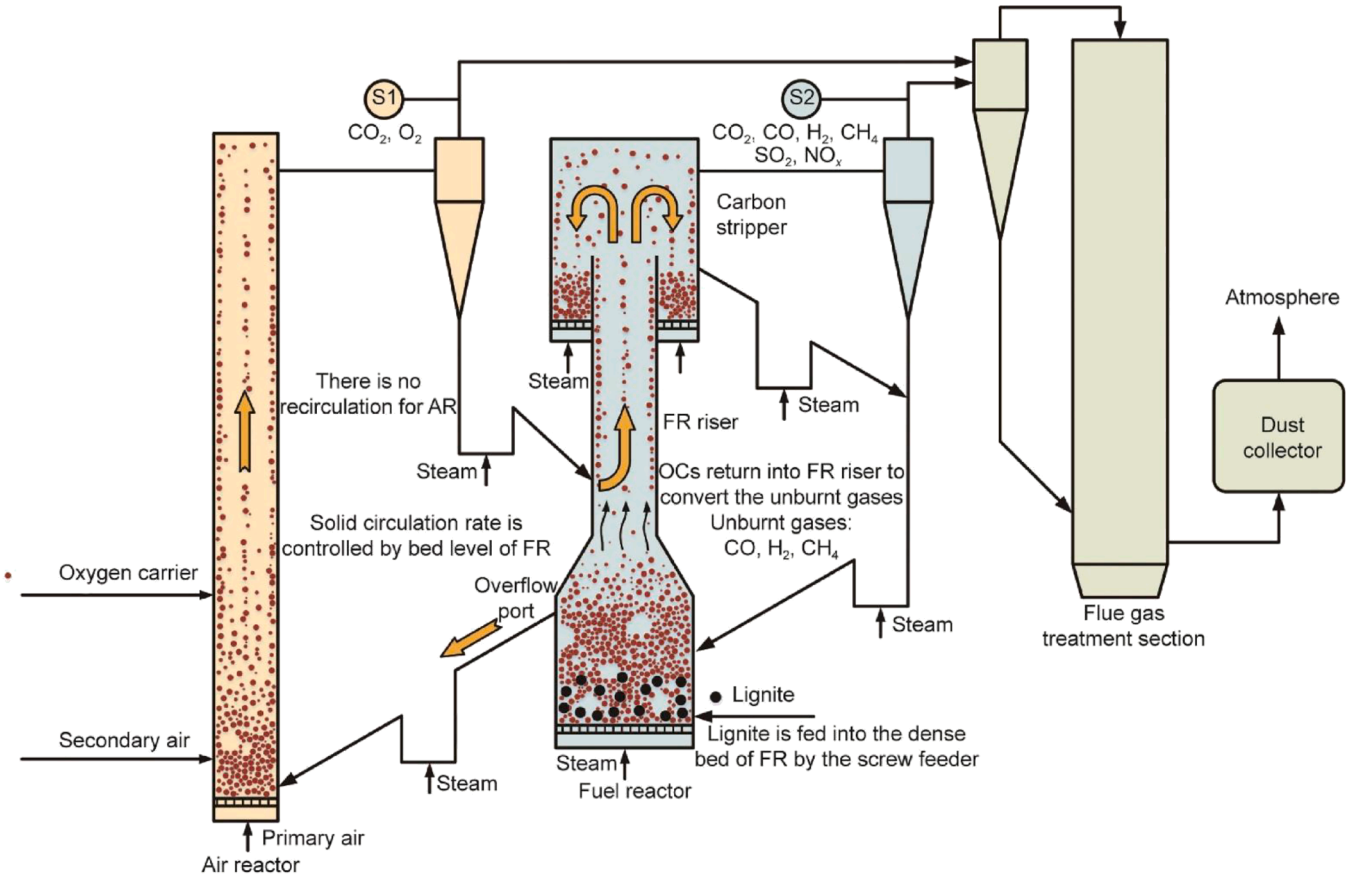

Fig. 14. Schematic representation of the CHEERS pilot plant at Tsinghua. In the figure, the red dots represent the oxygen carrier (ilmenite), and the black, larger dots represent the fuel (lignite). This is the largest pilot plant, in which chemical looping combustion (CLC) has been operated to date (5 MW_{th}). Reproduced from Li et al. (2025b) with permission, licensed under CC BY-NC-ND 4.0.

100–400 hours (Vin et al., 2022; Bayham et al., 2019; Linderholm et al., 2016).

From the operations seen in Table 2, it is clear that CLC has come a long way in the last decade. An additional spin-off concept to CLC worth mentioning is Oxygen carrier aided combustion (OCAC). Here the bed material used in circulation fluidized bed boilers (CFB), i.e., sand, is exchanged with oxygen carriers. This provides an additional mechanism for fuel conversion and has been shown to provide benefits for combustion efficiency and opens up for possibilities to use smaller excess air ratios than done in normal CFB combustion (Störner et al., 2025). OCAC has been successfully demonstrated in pilot-scale units and in more than ten full-scale commercial boilers (Lind et al., 2017; Kuhn et al., 2025a; Staničić et al., 2026). The widespread implementation of OCAC in commercial-scale facilities serves as a crucial indicator of the industrial readiness and mechanical robustness of oxygen carrier materials under rigorous, long-term operating conditions similar to CLC.

Recent pilot-scale CLC studies increasingly focus on biomass and waste-derived fuels in order to enable carbon-neutral or carbon-negative energy systems. Compared to coal, biomass and waste-derived fuels contain higher concentrations of alkali metals, chlorine, and volatile matter, all of which may influence the performance of the CLC process. The high volatile content of biomass has been identified as a primary reason for reduced fuel conversion efficiency in CLC systems (Mohn et al., 2026; Mendiara et al., 2018b). Consequently, various reactor configurations and process concepts—such as multi-stage fuel reactors, fuel reactors equipped with internals, and the use of CLOU oxygen carriers including Ca–Mn-based materials—have been investigated to improve the conversion of high-volatile fuels (Shen et al., 2020; Haus et al., 2020; Lindmüller et al., 2023; Fleiß et al., 2022). As a result, biomass–ash interactions and their impacts on oxygen carrier performance, agglomeration behavior, and gas-phase chemistry have received increasing attention in recent years. Pilot-scale experiments at Chalmers using different oxygen carriers in 10 kW and 100 kW units, as well as at the VTT 60 kW unit, have demonstrated that a substantial fraction of biomass-derived potassium is retained in the bed material rather than released to the gas phase, which can offer advantages such as a reduced corrosion potential of the air-reactor flue gas, allowing for higher steam temperatures (Gogolev et al., 2019; Gogolev et al., 2022; Gogolev et al., 2021a; Gogolev et al., 2021b)..

Overall, the pilot-scale operations summarized in Table 2 show the trends in CLC operation over the past decade. Pilot studies have moved from short-term demonstrations with gaseous fuels and highly reactive model oxygen carriers like Ni-, Fe-, Cu-, and Mn-based monometallic oxides toward extended operation with solid fuels, including biomass and waste-derived fuels, using natural ores such as ilmenite, manganese ores, waste-derived materials like steel slag, and multi-elements synthetic oxygen carriers. As a result, pilot-scale studies have increasingly addressed the performance of these complex oxygen carriers under realistic operating conditions, including both reactivity and attrition, while the introduction of biomass and waste-derived fuels containing high content of ash species open up more detailed investigations of ash interactions. Furthermore, successful auto-thermal operation at scales up to 5 MW_{th} and the widespread commercial deployment of OCAC demonstrate that oxygen carrier materials can withstand long-term circulation under industrially relevant conditions.

3.3.2. *Chemical looping gasification*

Chemical looping gasification (CLG) with intentional partial oxidation has undergone rapid development in recent years, with clear improvements in process control, char conversion, and tar abatement. Most experimental work focuses on circulating or bubbling fluidized bed systems operating with biomass and related residues, typically using natural ores such as ilmenite or hematite as oxygen carriers and bed materials (see Table 3). A key step toward efficient CLG has been the development of strategies to control oxygen transport independently of solids circulation. Larsson et al. (2014) demonstrated in the Chalmers DFB gasifier that adding ilmenite as an oxygen carrier effectively reduces tar yields, but also highlighted that excessive oxygen transport to the gasifier side leads to undesired syngas oxidation and that oxygen transport should be decoupled from bed material circulation. Ge et al. (2016a) tested dilution of hematite with sand in a 25 kW unit, thereby reducing effective oxygen transport capacity, whereas Pissot et al. (2018) later reported that such dilution in a 2–4 MW DFB CLG unit can be operationally sensitive and challenging over longer campaigns.

Dieringer et al. (2020) proposed a complementary strategy based on restricting the air input to the air reactor, thereby limiting the total oxygen made available for circulation while keeping solids flux high. Simulation and pilot-scale data indicate that this approach yields significantly better cold gas efficiencies and char conversion than simply reducing oxygen-carrier circulation. The concept has been experimentally implemented and validated at 20 kW scale by Condori et al. (2023); Condori et al. (2024b), and at 1-MW scale by Marx et al. (2023a) and Dieringer et al. (2023a) (see Fig. 15), all of whom report stable autothermal operation and high flexibility with respect to oxygen-to-fuel ratio control. Dilution of ilmenite with inert sand has likewise been used in a 5-MW CLG pilot by Li et al. (2026) to limit oxygen transport, but long-term operational issues associated with handling two bed materials are not yet fully documented. Recent literature on larger units no longer favors reducing solids circulation as a primary control lever, reflecting a shift toward air-side oxygen restriction and, to a lesser extent, carrier dilution.

From a performance standpoint, enhancing char conversion and

Table 3
Chemical looping gasification (CLG) pilot plants.

No.	Location/ owner	Scale (kW_{th})	Oxygen carrier/Bed Material	Fuel	Operation with fuel (h)	Remark	References
1	Tsinghua, CHEERS	5000	Ilmenite, Ilmenite/ Sand	Wood pellets	45	Air reactor co-feeding, Sand dilution	Li et al. (2026)
3	Chalmers	1400	Ilmenite, Manganese, LD-Slag	Wood pellets	N/A	No process control	Larsson et al. (2014)
4	TU Darmstadt	1000	Ilmenite	Wood pellets, Straw pellets	>400	AR oxygen restriction	Dieringer et al. (2023a), Marx et al. (2023a)
22	Nanjing	25	Hematite, hematite/ sand	Rice husk	N/A	Sand dilution	Ge et al. (2016b), Ge et al. (2016a)
16	CSIC	20	Ilmenite	Wheat straw, pine forest residue, Torrefied wheat straw	85 h	AR oxygen restriction	Condori et al. (2024b), Condori et al. (2024b)
–	Guangzhou	10	Fe-Ni Fe2O3/Al2O3	Pine saw dust	N/A	No process control	Wei et al. (2015b), Wei et al. (2015a)
–	Nanjing	5	hematite	Lignite	N/A		Shen et al. (2018)
–	Ohio	N/A	FeTi based	Biomass	>600	Moving bed gasification reactor	Park et al. (2023)

Abbreviations. See Table 1.

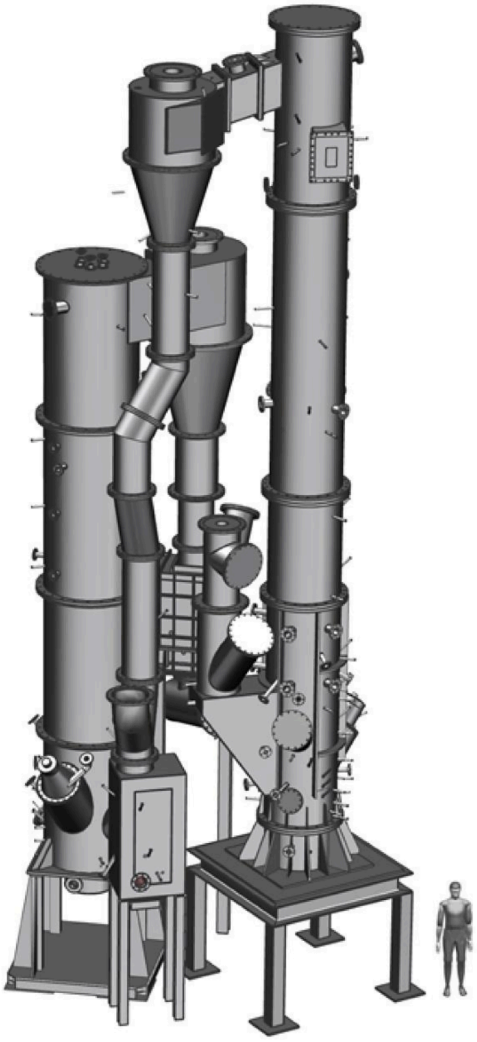

Fig. 15. Reactor configuration of the 1-MW_{th} pilot plant at TU Darmstadt for chemical looping gasification (CLG). The air reactor is on the left, and the fuel reactor is on the right. Reproduced from Marx et al. (2021), licensed under CC BY 4.0.

reducing both carbon slip and tar yield remain central research objectives in CLG. The most consistent levers identified across scales are high fuel-reactor temperatures and the use of catalytically active oxygen carriers. Studies by Wei et al. (2015b) (10 kW), Ge et al. (2016a) (25 kW), and Marx et al. (2023a) (1 MW) show that increasing fuel-reactor temperature systematically improves carbon conversion and reduces carbon leakage, while simultaneously shifting syngas composition toward higher H_2 and CO and lower CO_2.

Oxygen carriers and bed materials are also used as in situ tar-reduction agents. Ilmenite in dual fluidized beds, for example, consistently lowers tar levels relative to units operated with inert bed materials only, while tar concentrations in large CLG pilots (1–5 MW) have been reported below those in comparable non-CLG gasifiers even at similar temperatures. Industrial by-products such as LD slag have emerged as promising low-cost oxygen carriers, combining moderate oxygen transport capacity with strong catalytic activity for tar cracking and reforming, and thus offering a cost-effective alternative to natural ores like ilmenite (Hildor et al., 2023).

Although most CLG demonstrations use woody biomass, more challenging feedstocks such as rice husk and wheat straw have also been investigated in lab and pilot units. Ge et al. (2016a) showed that rice husk can be successfully gasified in CLG with hematite, while Condori et al. (2023) evaluated wheat straw in a 20 kW CLG unit and further studied the impact of torrefaction on syngas yield and char conversion (Condori et al., 2024b). These studies indicate that difficult agricultural residues can be handled reasonably well at smaller scales, but long-term, stable operation with such fuels at larger scales still presents challenges, as highlighted in a 1-MW CLG campaign with biogenic residues (Dieringer et al., 2023a) and in a recent review by Miao et al. (2022) regarding ash, agglomeration, and oxygen-carrier deactivation.

Beyond dual fluidized bed systems, other reactor configurations such as moving-bed–circulating-fluidized-bed hybrids have also been suggested. A notable example is the moving-bed redox-looping biomass-to-syngas system, which has accumulated over 600 h of operation with various biomass feedstocks and produced high-purity syngas with H_2/CO ratios around 2 and very low tar levels, comparable to fluidized-bed CLG units (Park et al., 2023). Despite these promising results, such alternative configurations still receive less attention than DFB-based designs and remain at an earlier stage of technology readiness.

3.3.3. *Chemical looping reforming*

Chemical looping reforming (CLR) typically employs interconnected fluidized bed reactors such as fuel reactor and air reactor (see Fig. 9a). In the FR, the fuel reacts with the oxygen carrier forming syngas. H_2O and/or CO_2 can be introduced with the fuel to assist fluidization and as reforming agent (steam, dry reforming, respectively), which allows adjusting the H_2:CO ratio. In addition, the operation in fixed bed reactors has demonstrated the viability of several oxygen carriers and the pressurized operation of the CLR concept. In general, promising key performance indicators (KPI) values have been reached during the last 10 years with various feedstocks, including gaseous and liquid fuels, which emphasizes the practical application and industrial scalability of this innovative chemical looping approach. The operating experience of CLR in continuous units is summarized in Table 4.

3.3.3.1. Advances in pilot-scale demonstration. The conceptual foundation of chemical looping reforming (CLR) was established in the early 2000s at Chalmers University of Technology, with revolutionary pilot-scale demonstrations marking critical milestones in technology validation (Rydén et al., 2006, 2008; Rydén et al., 2009). Instituto de Carboquímica (ICB-CSIC) demonstrated the CLR feasibility for methane under several operating conditions (Diego et al., 2009). The Vienna University of Technology constructed also one of the first CLR pilot units, a 140-kW dual fluidized bed system operational from 2009, which demonstrated continuous syngas production using natural gas as fuel and nickel-based oxygen carriers (Kolbitsch et al., 2009; Pröll et al., 2010; Bolhàr-Nordenkampf, 2009). Considering the problem of using pressurized, interconnected fluidized beds, Ortiz et al. (2010) presented the first experimental CLR results obtained in a semicontinuous fluidized bed reactor operating at high pressure (up to 10 bar). The use of membranes coupled into the fluidized bed fuel reactor in a CLR process has been also demonstrated (Patil et al., 2007; Gallucci et al., 2008; Andrés et al., 2011; Medrano et al., 2018; Wassie et al., 2018), as well as dynamically operated fixed beds (Karimi et al., 2014). By 2015, interconnected fluidized bed reactors had clearly emerged as a viable configuration for chemical looping applications, while key challenges—including oxygen carrier mechanical stability, carbon formation, and reactor hydrodynamics—were identified. The technology maturity reached TRL 3–4, with limited operation at elevated pressure and scarce data on biogas, liquid fuels, or long-term oxygen carrier degradation, leaving significant uncertainty for industrial deployment.

Over the past 20 years, CLR has progressed from laboratory concept to pilot-scale validation, with recent demonstrations achieving TRL 5 readiness. The last decade has seen a significant push toward optimizing reactor designs and operational strategies to enhance process efficiency. Also, recent studies have emphasized oxygen carrier stability, fuel flexibility, and reactor design, with emerging efforts for flexible fixed-

Table 4
Operating experience on continuous units for chemical looping reforming (CLR).

No.	Location/ owner	Scale (kW)	Configuration	Oxygen carrier	Fuel	Reforming agent	T (°C); p (bar)	KPIs	Operation with fuel (h)	References
Fluidized Beds										
12	TU Wien	120	Dual circulating fluidized bed (DCFB)	Ni-based oxygen carrier (NiO on Al_2O_3/ MgO)	Natural gas	H_2O	750-900; 1	X_f≈100% H_2:CO=2-2.5	18	Bolhàr-Nordenkampf (2009), Pröll et al. (2010)
26	SINTEF	3	Internally circulating reactor (ICR)	NiO65/35 Al_2O_3	CH_4	H_2O	650; 1.7	X_f≈90-98% H_2:CO=2-3.5	N/A	Osman et al. (2019)
27	CSIC-ICB	1	Dual fluidized bed	Ni21-γAl, NiO18-αAl_2O_3	CH_4	H_2O	800-900; 1	X_f≈100% H_2: CO=2.5-3	40	Diego et al. (2009)
				Cu14Al_ICB	CH_4, biogas	H_2O /CO_2	800-900; 1	X_f≈96% H_2: CO=1.2-3	30	Cabello et al. (2022b)
				FerroSorp® DGp	Biogas	CO_2	900; 1	X_f≈55% H_2:CO≈1	N/A	Cabello et al. (2023c)
				Fe residue (Ferrosorp), Mn66FeTi7, Ni added	Biogas	CO_2	900; 1	X_f≈80-90% H_2: CO≈1.2	N/A	Cabello et al. (2024b)
28	CSIC-ICB	1	Dual fluidized bed conical	Ni21-γAl, Ni18-αAl_2O_3	Bioethanol	H_2O	850-950; 1	X_f≈98% H_2: CO≈1.9	50	García-Labiano et al. (2015)
				NiO18-αAl_2O_3	Diesel	H_2O/CO_2 mixtures	900; 1	X_f≈100% H_2: CO≈0.5-2	22	García-Díez et al. (2017)
				NiO18-αAl_2O_3	bio-glycerol	H_2O	750-850; 1	X_f≈100% H_2: CO≈1.5-2	35	Adánez-Rubio et al. (2021)
				NiO18-αAl_2O_3	wood bio-oil	H_2O	650-850; 1	X_f≈100% H_2:CO≈2-3	60	Adánez-Rubio et al. (2022)
30	CSIC-ICB	1	Semicontinuous Fluidized bed	Ni21-γAl, NiO18-αAl_2O_3	CH_4	H_2O	800-900; 1-10	X_f≈100% H_2: CO≈2.5-3	50	Ortiz et al. (2010)
31	Chalmers	0.3	Dual Fluidized bed	NiO60-$MgAl_2O_4$,	Natural gas	H_2O	820-930; 1	X_f≈100% H_2: CO≈1.5-2	41	Rydén et al. (2006)
				Ni20-$MgAl_2O_4$, N18-αAl, Ni21-γAl	Natural gas	H_2O/CO_2	850-950; 1	X_f≈96-100% H_2: CO≈1.3	59 57 42	Rydén et al. (2008)
				Ni40-ZrO2-MgO	Natural gas	H_2O	940; 1	X_f≈100% H_2:CO≈2-2.5	40	Rydén et al. (2009),
				N4MZ-1400 (NiO40-ZrMg)	Kerosene	H_2O	850-950; 1	X_f≈100% H_2: CO≈1.2	20	Moldenhauer et al. (2012)
32	Eindhoven	0.6	Membrane-assisted CLR Continuous circulation	Ni-based, Pd-membranes	CH_4	H_2O	450-600; 1	X_f≈40-90% H_2:CO≈6	100	Medrano et al. (2018)
33	Eindhoven	N/A	Membrane-assisted CLR Gas switched	Ni-based, Pd-Ag membrane	CH_4	H_2O	400-550; 1-4	X_f≈20-50% H_2: CO≈10	N/A	Wassie et al. (2018)
8	Univ British Columbia	N/A	Fluidized-bed reformer with membranes	SE-CLR Pd-Ag membrane, CO_2 capture by limestone	CH_4	H_2O	550; 3	X_f≈50% H_2: CO≈15	5	Andrés et al. (2011)
Packed beds										
35	Eindhoven	2	CLR-PB packed bed	NiO/$CaAl_2O_4$	CH_4	H_2O, CO_2	600-900; 1.1	X_f≈90-92% H_2: CO≈0.25-5	> 400	Spallina et al. (2017)
36	Manchester	lab scale	CLR-PB packed bed	NiO/$CaAl_2O_4$	CH_4	H_2O, CO_2	400-900; 1-5	X_f≈100% H_2: CO≈0.2-0.25	480	Alexandros Argyris et al. (2022)

(*continued on next page*)

Table 4 (*continued*)

No.	Location/ owner	Scale (kW)	Configuration	Oxygen carrier	Fuel	Reforming agent	T (°C); p (bar)	KPIs	Operation with fuel (h)	References
				Fe-Al2O3	CH_4		600-900; 1-3	X_f≈60% H_2: CO≈0.1-2.5	N/A	Leeuwe et al. (2023)
37	Ghent University	Super-dry CLR pilot (LCT)	Two parallel fixed-bed reactors		Biogas/ biomethane + excess CO_2 (super-dry)		High-*T* (design)	N/A		Moonshot Flanders (2026)

Abbreviations. See Table 1. X_f: fuel conversion

bed modules and dual fluidized beds.

Common reactor configurations for chemical looping reforming are categorized into interconnected fluidized bed reactors and batch reactors (fixed /fluidized beds) with gas switching mechanical valves.

Most large-scale chemical looping plants use the configuration of interconnected fluidized beds, operating at nearly atmospheric pressure. Fluidized bed systems offer superior heat transfer and near-isothermal operation, enabling autothermal operation and continuous syngas production and making them attractive for commercial development. Circulating fluidized beds are particularly suitable due to high solids circulation rates. However, it should be considered that CLR does not need so high solid circulation rates as in CLC due to less oxygen needs to be transferred to the fuel, which can make it easier to reach the required entrainment flow of solids from the reactors.

Despite the promising results obtained in CLR units based on fluidized beds, no recent advances in scale-up have been made in interconnected fluidized beds after the demonstration of the CLR process at 140 kW in TUV in 2009, the largest CLR scale ever. This lack of interest in the recent past may be due to several factors, including the energy transition from fossil to renewable energy sources and the smaller market for biogenic or waste fuels, whether gaseous or liquid. However, the increasing interest on the green hydrogen production from also increasing biogenic fuels, such as biogas, could revive the interest in the development of the CLR technology. Also, CLR can be integrated into CO_2 capture processes, allowing to produce H_2 while simultaneously achieving negative CO_2 emissions.

Fixed-bed reactors, typically operated in cyclic mode, have been extensively used for fundamental studies of oxygen carrier kinetics and fuel conversion. This concept has several advantages with respect to the interconnected fluidized beds, including a compact design, better oxygen carrier utilization, and reduced attrition. More recently, dynamically operated packed-bed CLR has gained momentum for TRL 4–6 applications, as it avoids high-temperature solids circulation and is inherently compatible with pressurized operation and downstream pressure swing adsorption (PSA) for high-purity hydrogen production. Thus, syngas production efficiencies can be maintained at elevated pressures relevant for downstream methanol or Fischer–Tropsch synthesis (Spallina et al., 2017; Alexandros Argyris et al., 2022). However, this configuration requires frequent gas switching at high temperature, which is a challenge for large-scale operation. Within the RECYCLE project, more than 480 h of operational experience has been achieved in alternating packed bed CLR reactor pilot located at the University of Manchester. This has been the base for the scale up of the technology up to a 300 $MW_{LHV,H2}$ of blue hydrogen production at pressures above 30 bar and temperatures exceeding 900°C (RECYCLE Consortium, 2022).

3.3.3.2. Operational parameters and performance. Optimal operational windows are critical for maximizing H_2/CO yield and minimizing oxygen carrier degradation. The fuel conversion and syngas/H_2 yield is mainly determined by the oxygen carrier performance and the operating conditions which strongly influence conversion and selectivity. In addition, the syngas composition is influenced by the promotion of either steam or dry reforming in CLR. Thus, chemical looping steam reforming (CLSR) dominates for blue hydrogen, while dry reforming (CLDR) with biogas is emerging for green hydrogen.

Pilot studies report operation predominantly in the 700–950°C range, although lower temperatures are suitable for highly active oxygen carriers. Lower temperatures favor higher H_2/CO ratios in syngas but can lead to incomplete fuel conversion and carbon deposition. Studies have consistently shown that increasing temperature from 800 to 900°C enhances methane conversion from approximately 75% to 95%, though temperatures exceeding 950°C can accelerate oxygen carrier sintering and reduce long-term stability. Also, higher temperatures reduce H_2 selectivity due to the water-gas shift equilibrium. Nevertheless, the H_2/CO ratio may be modified downstream via water-gas shift reaction. Thus, typical operating temperatures are in the range of 850–950°C for Cu-based, Fe-based and perovskites materials to secure high conversion and oxygen-carrier utilization. Nevertheless, lower temperatures (e.g., 600–800°C) may be used with Ni-based oxygen carriers (Adánez-Rubio et al., 2022). Packed bed CLR units have been tested between 400 and 950°C, with higher temperatures favoring CH_4 conversion but increasing sintering and carbon risk (Leeuwe et al., 2023).

Near-atmospheric pressure has been used in fluidized pilots, with the exception of the ICR concept. In fact, pressurization presents significant challenges in reactor sealing and solids circulation but offers major efficiency gains (Osman et al., 2021; Cabello et al., 2023c). On the contrary, packed bed CLR is explicitly developed for elevated pressure (up to ≈ 20–30 bar in design studies and several bar in pilot campaigns) to match synthesis gas downstream requirements (Pröll and Lyngfelt, 2022). Thus, some experience under pressurized conditions can be found for operation in fixed bed reactors. However, tests on continuous units have not yet exceeded 10 bar.

The oxygen-to-fuel ratio may be modified in the interconnected fluidized bed concept, which highly influences the syngas/H_2 yield. The strategy to control the oxygen to fuel ratio varies depending on the reactor variant used. The space velocity, which depends on the bed solids inventory and fuel flow, and the cycle times can be varied in packed beds to achieve target conversions. In interconnected fluidized bed pilots, the oxygen-to-fuel ratio may be set by either controlling the air flow, the solids circulation rate, or the solids inventory. Tuning the solids circulation rate or the solids inventory in the reactors is complex and has low potential for its scale-up (Pröll et al., 2010); thus, the most promising option is to limit the air flow in the air reactor. In this case, concentrated N_2 stream is produced in the air reactor, which can add value to the process. Also, the solids circulation rate is only determined to match the heat demand in the fuel reactor,which simplifies the control of the CLR unit (Diego et al., 2009; Ortiz et al., 2010; García-Labiano et al., 2015; Pröll et al., 2009; Pröll et al., 2010).

While methane and natural gas have dominated CLR pilot studies up to 2015 due to their industrial relevance, recent research has demonstrated successful reforming of diverse fuel sources such as biogas/biomethane (pilots target dry reforming to valorize in-situ CO_2), industrial off-gases and liquid fuels. Thus, a significant trend is the expansion of

CLR beyond natural gas to include a wide range of gaseous and liquid fuels, driven by the need for carbon-neutral or renewable hydrogen.

Biogas and biomethane reforming has been validated at pilot scale, exploiting the inherent CO_2 in the feed for CLDR, sometimes supplemented by steam (combined wet/dry reforming) to tailor syngas composition and mitigate carbon. Studies with biogas feeds (typically 60% CH_4, 40% CO_2) have shown that chemical looping dry reforming can achieve syngas production with H_2/CO ratios near unity, valuable for downstream synthesis applications. In the ICB-CSIC unit, biogas CLDR at 950°C with a Cu-based carrier provided high CH_4 conversion and syngas yields similar to CLSR, using CO_2 as reforming agent (Cabello et al., 2022b). These studies show that CO_2 present in biogas can participate in dry reforming reactions. Other materials used in biogas reforming were a residue based on iron, FerroSorp® DGp, and a synthetic Mn66FeTi7, with some Ni addition (Cabello et al., 2023c; Cabello et al., 2024b).

Liquid fuels, both fossil fuels, including mineral oils and liquid hydrocarbons (diesel, kerosene, heavier fuel oil, vacuum residue), and biogenic fuels -such as ethanol, methanol, glycerol or pyrolysis oils- have been tested at bench and small pilot scales for CLR (García-Díez et al., 2017; Moldenhauer et al., 2012).. Pilot work has reached TRL 4–5, using specially designed fuel injection systems in different chemical looping processes (Moldenhauer et al., 2014). Bioethanol was used as fuel in a 1-kW_{th} CLR unit using Ni-based oxygen carriers to produce a syngas composition closed to the given by the thermodynamic equilibrium and without CO_2 emissions into the atmosphere (García-Labiano et al., 2015). Glycerol, a byproduct of biodiesel production, has been reformed in CLR systems with conversions exceeding 90%. In some cases, challenges with catalyst coking and oxygen carrier stability have limited long-term demonstrations. These issues were solved using highly reactive Ni-based oxygen carriers prepared by incipient wet impregnation on alumina (Adánez-Rubio et al., 2021).

Pyrolysis oils and bio-oils derived from biomass fast pyrolysis represent particularly challenging feedstocks due to their complex composition and high oxygen content. Preliminary studies have shown feasibility but identified significant challenges with tar/coke formation and oxygen carrier deactivation (Adánez-Rubio et al., 2022). Oxygen carriers with high oxygen mobility (e.g., CeO_2-based materials) and co-feeding of steam may be options to limit the formation of carbon deposits (see Section 2.2.3.3). Higher TRL at pilot-scale with liquid fuels remains scarce, most work being still at lab scale, indicating a clear gap in TRL progression for these feedstocks.

3.3.3.3. Oxygen carriers and stability. Pilot reports focus on multi-cycle tests (hundreds of cycles at kW scale) measuring oxygen carrier ageing, attrition, and coke accumulation. Scaled oxygen carrier production is critical for the CLR scale-up, being the practical bottlenecks for TRL progression. Pilot-scale studies have demonstrated that optimized oxygen carriers based on Ni, Cu, Fe, and perovskite formulations can sustain stable redox cycling over several hundred cycles, although attrition and sintering remain key degradation mechanisms for fluidized bed applications. Nevertheless, some relevant advances have been recently achieved in this context. For example, a highly durable material based on CuO has been identified under CLR conditions, including dry reforming of biogas (Cabello et al., 2022b).

Ni-based carriers remain the benchmark due to their high reactivity. Often, pilot CLR operations consistently show that, despite excellent initial fuel conversion, these materials are prone to carbon deposition and sintering. Nevertheless, impregnated Ni-based oxygen carriers using alumina as a support showed excellent stability and reactivity (Diego et al., 2009). Importantly, continuous operation in dual fluidized bed CLR units with these oxygen carriers has proven that coke encapsulation can be effectively mitigated by controlling the steam-to-fuel ratio, demonstrating operational robustness at pilot scale.

While Ni-based carriers exhibit high activity, their high cost, toxicity, and susceptibility to carbon formation and sulfur poisoning limit their scalability and commercial readiness. Consequently, developing oxygen carriers that are low-cost, mechanically stable, and environmentally benign has become a central focus in advancing CLR technology. Recent pilot-scale implementations increasingly target materials that balance redox performance, attrition resistance, and economic feasibility, reflecting a shift from Ni-dominated systems toward Cu, Fe, Mn, and perovskite-based carriers, as well as emerging low-cost, waste-derived materials (Cabello et al., 2023c). These developments indicate a progressive maturation of CLR technology, moving from laboratory studies toward higher TRL demonstrations suitable for industrial application.

Cu-based materials offer improved stability and lower carbon deposition. The ICB-CSIC CLR pilot relies on a synthetic Cu–Al oxygen carrier (Cu14Al), which shows high reactivity and maintains performance over extended campaigns (Cabello et al., 2022b).

Fe-based residues have been also tested with good results in the dry reforming of biogas (Cabello et al., 2023c; Cabello et al., 2024b). Fe-based carriers are particularly attractive for packed-bed CLR due to low cost, environmental benefits and good redox stability but with lower reactivity and catalytic activity (Zheng et al., 2022).

Packed-bed tests with Fe-based beds have reported stable operation at 850°C, with negligible carbon deposition under suitable CH_4/CO_2/H_2O ratios and resilience after episodes of coking. Mid-temperature Fe-based oxygen carriers (≈600°C) show outstanding cyclic stability over hundreds of cycles in lab tests, suggesting possible application in future low-temperature CLR pilots.

Some perovskite oxygen carriers are being evaluated for CLR in pilot-relevant conditions, showing promising redox behavior and long lifetimes, though most testing is still at lab or small pilot scale (Zheng et al., 2022).

3.3.3.4. Carbon formation and mitigation strategies. Carbon deposition on oxygen carriers is a central concern in pilot CLR, particularly for dry reforming and for fuels with higher hydrocarbons or tars (Leeuwe et al., 2023). Thermodynamic analyses indicate that carbon formation is favored at lower temperatures (<750°C) and low oxygen-to-fuel ratios, such as existing in CLR. As explained above, hydrocarbon cracking and Boudouard reactions on metal surfaces (notably Ni ensembles) lead to filamentous and encapsulating carbon (Zhang et al., 2020). However, autothermal CLR pilots report negligible coke formation under controlled stoichiometry. Thus, the intrinsic intermittent oxidation to CLR under optimized air/fuel ratios, steam co-feeding in CLSR and careful thermal management reduce coke in continuous pilots (Piso et al., 2023).

The continuous operation in interconnected fluidized bed reactors minimize the carbon deposition on the oxygen carrier and the avoidance of CO_2 emissions to the atmosphere, which has been proved with methane, ethanol, glycerol, industrial oil and diesel fuel in CLSR, as well as in CLDR with the existing CO_2 to CH_4 ratio in biogas (Diego et al., 2009; García-Labiano et al., 2015; Adánez-Rubio et al., 2022; Cabello et al., 2022b; Cabello et al., 2023c). This fact was confirmed both with Ni-based and Cu-based oxygen carriers in the ICB-CSIC pilot. The exception is when pyrolysis oil was used as fuel, in which case, carbon formation could not be avoided with NiO/Al_2O_3 oxygen carriers, resulting in CO_2 emissions from the air reactor, although oxygen carrier deactivation was not an critical issue (Adánez-Rubio et al., 2022). Nevertheless, the regeneration in air restores oxygen carrier activity by burning coke and prevents excessive carbon buildup that could lead to particle agglomeration and fluidization problems.

3.3.3.5. CLR process intensification. Hydrogen production can be intensified by combining chemical looping reforming with process-enhancement strategies that shift reaction equilibria and improve separation. One approach is SE-CLR, which has been demonstrated in fixed-bed configurations due to their operational simplicity. Early pilot

concepts employed alternating packed beds containing mixed oxygen carrier–CO_2 sorbent materials, operating in cyclic modes comprising sorption-enhanced reforming, sorbent calcination, and oxygen carrier regeneration. Several studies demonstrated high-purity hydrogen production (>95%) in single-bed arrangements (Wang et al., 2015; Antzaras et al., 2020; Masoudi Soltani et al., 2021; Antzaras and Lemonidou, 2022; Zhong et al., 2024).

The SE-CLR concept is also potentially scalable using interconnected fluidized beds (Rydén and Ramos, 2012). Recent studies show that the formulation of the oxygen carrier and CO_2 sorbent, as well as its reactivity and capability to transfer oxygen and CO_2, are key aspects for its proper use in a pilot unit based on three interconnected fluidized bed reactors (las Obras Loscertales et al., 2025a). The construction and operation of a 1 kW SE-CLR unit at the ICB-CSIC, including the complete loop with three interconnected fluidized bed reactors, is planned to demonstrate the proof of concept of this technology to produce highly concentrated hydrogen with inherent CO_2 capture (González-Torrijo et al., 2025).

Super dry reforming (SDR, see Fig. 16) concepts represent a related, though distinct, chemical looping approach focused on CO production. As in SE-CLR, SDR uses also a mixture of oxygen carrier and CO_2 sorbent but from a different perspective. The process involves the following steps: (i) complete fuel oxidation by reaction with an oxygen carrier, the CO_2 being trapped by a sorbent; and (ii) calcination of the sorbent coupled with in-situ CO_2 splitting by the oxygen carrier -which is oxidized- producing CO (Buelens et al., 2016). For that, SDR employs oxygen carriers with CO_2-splitting capability, typically Fe-based materials which may be reduced to Fe or FeO by the fuel and oxidized to Fe_3O_4 by CO_2, producing CO.

In the "super-dry" CLR concept, a high excess of CO_2 is mixed with the fuel, which makes it very attractive for biogas conversion. Recently, the University of Ghent/LCT commissioned an SDR pilot plant (opened in 2024) designed to demonstrate intensified chemical looping dry reforming of biogas/biomethane with CO_2 recycling at pilot scale. The facility features a modular multi-reactor architecture, and kg-scale OC production at TRL ≈ 5 for durability testing representing a bridge toward industrial scale-up (Buelens et al., 2024). The SDR is demonstrated at elevated pressures (up to several bar) to examine industrial conditions (RECYCLE Consortium, 2022). While promising, further evaluation is needed regarding some thermodynamic limitations, namely: (a) complete combustion of fuel by the oxidized Fe_3O_4 is hindered due to the relatively low CO_2/CO ratio (as well as H_2O/H_2) at equilibrium conditions when Fe_3O_4 is being reduced to FeO, which may require an intermediate oxidation step with air to allow fully oxidation to Fe_2O_3; (b) limited conversion of CO_2 evolved in the calcination step via splitting reaction with Fe or FeO, which limits the CO amount produced; and (c) the balance between chemical energy released during fuel combustion and chemical energy in produced CO, which may require additional energy from an external source.

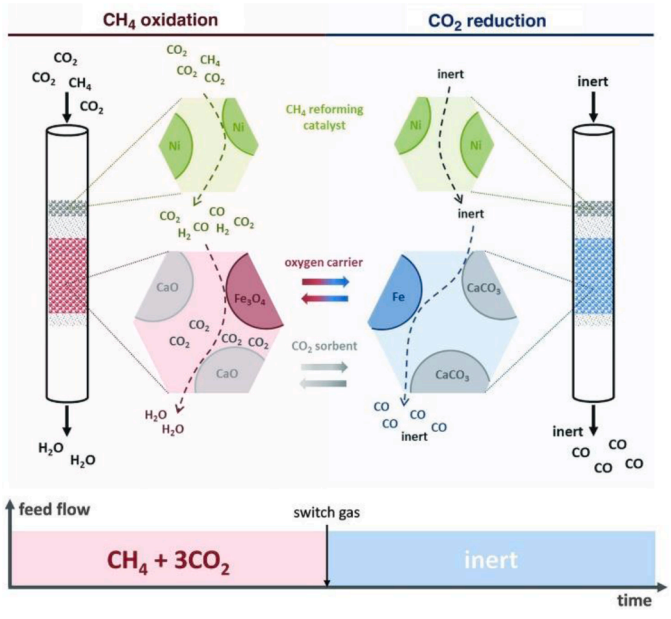

Fig. 16. Super dry reforming (SDR) process for enhanced CO production from CH_4 and CO_2. Reproduced from Buelens et al. (2016) with permission.

Another approach integrates hydrogen-permeable membranes in fluidized-bed reformers to selectively remove hydrogen as a permeate, lowering its partial pressure and driving reactions toward increased CH_4 conversion while producing a high-purity hydrogen stream (Wassie et al., 2018). The membrane assisted CLR has been demonstrated at lab-scale in a continuous operated CLR unit with Pd-based membranes immersed in the fuel reactor bed (Medrano et al., 2018). A high purity H_2 stream was obtained, but the methane conversion was about 60% due to relatively low temperature (<600 °C) which was limited by the membrane specifications.

3.4. Indirect gasification pilot testing

Indirect gasification, also known as dual fluidized bed gasification (DFBG), represents the most mature form of solid looping gasification technology. Several commercial and semi-commercial units with thermal capacities in the range of 8–32 MW have been successfully operated for more than 10,000 hours (see, e.g., Fig. 17). Consequently, a substantial body of real-world operational data exists. These data reveal a high degree of consistency across systems of different sizes and designs, and operation and control concepts, with temperature exerting only a limited effect on syngas quality. In contrast, the choice of bed material and additives—particularly limestone—has a significant influence (Larsson et al., 2021). Most existing DFBG plants primarily utilize wood chips or other wood-derived fuels. However, more challenging feedstocks such as bark (Ahlström et al., 2019) and even plastic wastes (Hongrapipat et al., 2022) are utilized in commercial-scale operation, reflecting the operators' ongoing efforts to reduce feedstock costs. Furthermore, all plants operate with at least olivine, most also with addition of calcium (limestone) or potassium additives to enhance the conversion of the feedstock into syngas, with silica sand being the exception.

In addition to the large-scale operation of DFBG, enhancements in DFBG reactor design have been proposed and investigated in a scale of 0.1–1 MW, notably at TU Wien and the University of L'Aquila. The concept developed by TU Wien features a multi-stage gasification reactor with internal constrictions to enhance gas–solid contact in the gasification reactor and allow axial separation of distinct reaction regimes. Mauerhofer et al. (2019) quantified the evolution of product gas composition along the reactor height for woody biomass, showing that most devolatilization and primary tar release occur in the lower section, while steam reforming, water–gas shift, and tar cracking dominate in the upper stages. They reported increasing H_2 and CO and decreasing hydrocarbons and tars with height, demonstrating that extended gas–solid contact time and staged fluidization substantially improve gas quality and tar conversion. Over the past decade, this configuration has been tested under various conditions, employing a broad range of feedstocks and bed materials. The results have enabled a detailed understanding of key parameters governing gasifier performance, showing the influence of parameters like feedstock feeding location (Bartik et al., 2024; Schmid et al., 2021a; Mauerhofer et al., 2019). In addition to standard DFBG operation, the 100-kW TU Wien unit has been successfully operated with limestone as the bed material at gasification temperatures below 690 °C, thus implementing sorption-enhanced gasification. Building upon the results of this 100-kW advanced DFBG unit, a scale up to 1 MW has been implemented by BEST and early operational data indicate promising performance for further optimization (Kadlez et al., 2025).

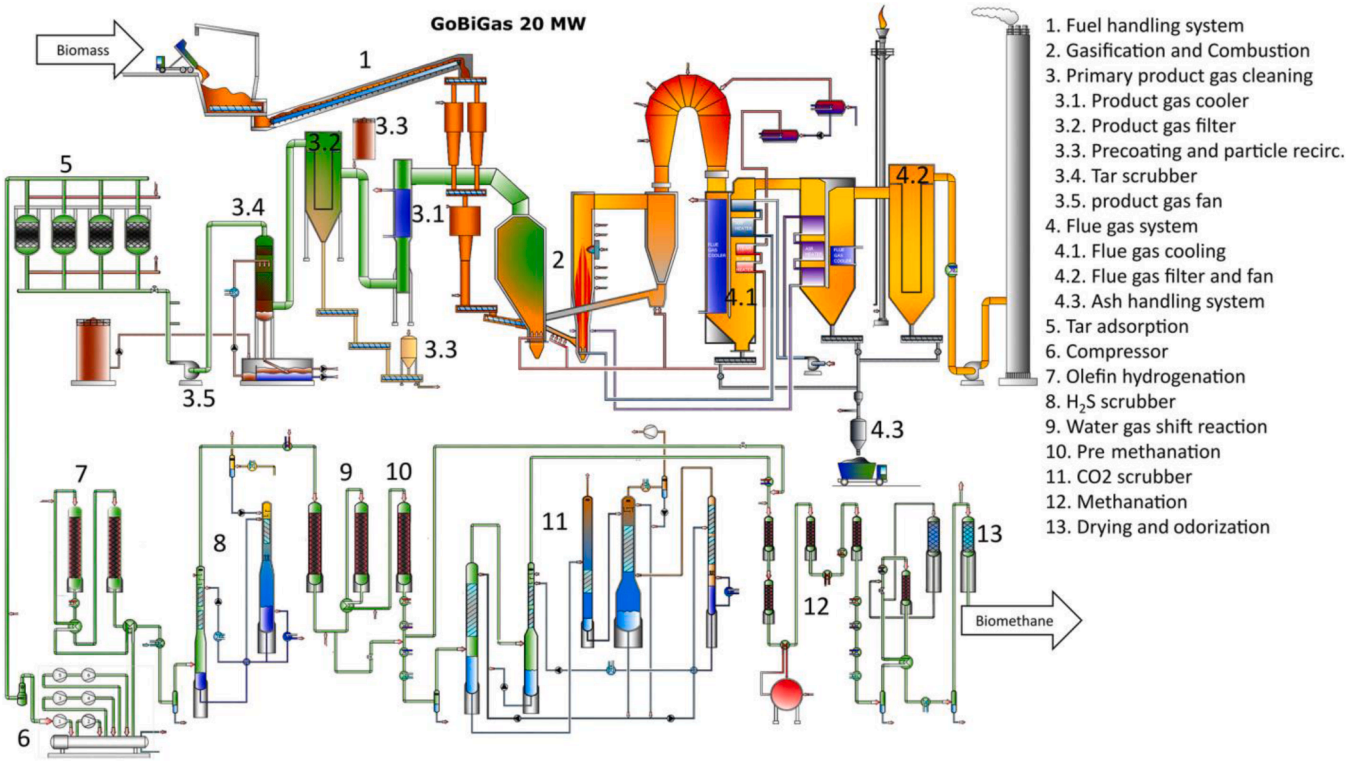

Fig. 17. Scheme of the main process steps in the GoBiGas plant, which is one of the largest indirect gasification facilities worldwide. Reproduced from Thunman et al. (2019), licensed under CC BY 4.0.

A recent innovation has been introduced by the University of L'Aquila, featuring an integrated design in which both reactors are housed within a single vessel. This compact configuration aims to improve the economic and operational efficiency of smaller gasification systems (Di Carlo et al., 2022). However, testing data remains limited (Papa et al., 2023), and its competitiveness relative to conventional DFBG designs with separate reactors is yet to be demonstrated.

4. Model development

4.1. Carbonate looping models

Modeling the carbonate looping (CaL) process is useful for process optimization and assessment, design of reactors, and scale-up. Ten years ago, Martínez et al. (2016) published a detailed review on modeling of the CaL process. Since then, simulation work has focused on improving assumptions using experimental data and developing new models suitable for novel CaL and IHCaL configurations (see Sections 2.1.1 and 2.1.2.). This section focuses on new models and advancements on CaL simulation of the last ten years. However, we also explain the earlier work on which recent publications are based. An overview of the models is available on Table 5.

Modeling CaL involves the consideration of various phenomena in different scales. Thus, reactor models are generally integrated into process-level models to assess the influence of phenomena at the reactor and particle level on process performance. This not only increases the complexity of the simulations but also introduces a necessity for reactor models that can be run with low computational requirements, enabling the integration into larger models. Historically, the focus of reactor modeling was set on the carbonator, which is the main reactor determining the performance of the CaL process. However, recent studies have shown the important of the calciner in terms of sorbent deactivation (Scaltsoyiannes and Lemonidou, 2021) and reduction of sorbent carrying capacity due to incomplete calcination (Greco-Coppi et al., 2025a), motivating more calciner simulations. The carbonator models are discussed in Section 4.1.1 and the calciner models are explained in Section 4.1.2. While previous subsections have been focused on post-combustion applications, Section 4.1.3 has been devoted to describing progress done on modeling of SE-CaL either in FB systems or packed bed configuration.

Process modeling involving some kind of reactor models is generally performed in Aspen Plus (Greco-Coppi et al., 2026b; Martínez et al., 2018; Hejazi and Montagnaro, 2024). Recent studies using process simulations focused on integrating CaL systems to steel mills (Montiel-Bohórquez et al., 2025), and cement (Lena et al., 2019), lime (Greco-Coppi et al., 2024c), and waste incineration plants (Greco-Coppi et al., 2026b, 2024a).

4.1.1. Carbonator models

Carbonator models generally consider: (i) carbonation kinetics, (ii) sorbent deactivation, and (iii) reactor hydrodynamics and solid-gas contact. A review of the most common modeling assumptions for fluidized bed carbonators, using the approach is available in the work of Greco-Coppi et al. (2024d) and Greco-Coppi et al. (2025a).

There are not many experimental studies on carbonation kinetics for the range of temperatures and CO_2 partial pressures relevant for CaL operations. A reason for this is that deriving reliable kinetics data is very challenging (cf. Arcenegui-Troya et al., 2022). In general, two stages are clearly identified within the carbonation reaction: (i) a fast, chemically limited stage, (ii) a much slower stage, limited by diffusion through the $CaCO_3$ product layer. For practical CaL applications in fluidized beds, the slow stage is generally neglected (Greco-Coppi et al., 2025a). The carbonation rate in the first stage is linearly defendant on the specific particle surface. Furthermore, carbonation kinetics are generally considered first-order dependent on CO_2 partial pressure (p_{CO2}) up to 10 kPa offset from equilibrium conditions. There is disagreement whether starting at 10 kPa the first-order dependency on CO_2 continues (e.g., Bhatia and Perlmutter, 1983), or the dependency disappears after this

Table 5
Overview of carbonate looping (CaL) models: recent advances (last 10 years) and most relevant studies of the last 20 years.

Year	Reference	Approach	Reactor model	Reactor type	Main features	Validation
2025	Greco-Coppi et al. (2024d), Greco-Coppi et al. (2025a)	1.5D	Carb	CFB	Improved hydrodynamic parameters; online prediction of sorbent activity (validated); validation with > 60 operating points (pilot).	Pilot data: 300 kW_{th} (Reitz et al. (2016)).
2025	Greco-Coppi et al. (2025b)	1.5D	Calc	CFB,BFB	Non-homogeneous CO_2 concentration; simple yet precise model.	Pilot data: 300 kW_{th} (Reitz et al. (2016)) and 1 MW_{th} Ströhle et al. (2020).
2024	Spyroglou et al. (2024)	1.5D	Calc	EF	CGM w/intraparticle diffusion; radiation and convection from internal walls.	Drop tube reactor (10.5 kW_e) (Fernandez et al. (2019)).
2024	Hejazi and Montagnaro (2024)	Process	–	CFB	Active time approach, considers sorbent sintering.	Pilot data (Hornberger et al. (2020)).
2024	Secomandi et al. (2024)	1.5D	Carb	CFB	Use of $Ca(OH)_2$ to increase E_{carb}. Models vertical temperature profile.	Pilot data: 2 MW_{th} (Arias et al. (2018)). Use of $CaOH_2$ could not be validated.
2024	Tizfahm et al. (2024)	1.5D	Carb	CFB	Fractal-like RPM; Reactor model based on Lasheras et al. (2011); Considers influence of SO_2.	Only kinetics, using a lab-scale FB.
2021	Sattari et al. (2021)	1.5D	Carb	CFB	CaO/Al_2O_3 as sorbent; Considers diffusion phase of carbonation.	Pilot data (Charitos et al. (2010); Dieter et al. (2014)). Partly overpredicted E_{carb}.
2021	Ritvanen et al. (2021)	1D	Coupled system	CFB	Considered hydrodynamic solid profiles and flows between reactors; thermal capacities, temperature-dependent decomposition model	Pilot data from Fuchs et al. (2020)
2018	Martínez et al. (2018)	Process	–	CFB	Calciner under O_2-rich atmosphere and sorbent reactivation.	–
2018	Turrado et al. (2018)	PFM	Carb	DT	EF carbonator for fine particles.	Drop tube reactor (24.5 kW_e). Results showed high dispersion.
2018	Spinelli et al. (2018)	1D	Carb	EF	EF carbonator, for cement applications.	–
2017	Parkkinen et al. (2017)	3D	Calc	CFB	High CO_2 concentration at calciner inlet.	Pilot data: 2 MW_{th} (Arias et al. (2018)).
2015	Atsonios et al. (2015b)	1.5D; 3D; Process	Calc, carb	CFB	CFD model coupled with 1.D and process modeling.	Pilot data: 200 kW_{th} (Dieter et al. (2014)).
2013	Martínez et al. (2013b)	0D	Calc	CFB	CSTR; homogeneous CO_2 concentration.	–
2013	Fernández et al. (2012); (2014) and ((2015))	1D	Ref.-Carb. reactor Oxidation reactor. Reduction reactor	Packed Bed	1D, plug flow with mass and thermal axial dispersion, ideal gas, constant void fraction and perfect mixing of solids in bed with uniform particle size.	Experimental data at different TRL including TRL 7 1MW_{th} (Díez-Martín et al. (2018); Grasa et al. (2023); Fernández et al. (2025))
2012	Romano (2012)	1.5D	Carb	CFB	CSTR; homogeneous temperature; considers influence of SO_2.	Pilot data. In part, the model overpredicted E_{carb}.
2011	Charitos et al. (2011)	0D	Carb	CFB	Introduced the "active time approach".	Pilot data.
2011	Lasheras et al. (2011)	1.5D	Carb	CFB	CSTR; homogeneous temperature.	–

Abbreviations. BFB: Bubbling fluidized bed; Calc: Calciner; Carb: Carbonator; CFB: Circulating fluidized bed; CGM: Changing grain model; CSTR: Ideal continuous stirred-tank reactor operation; DT: Drop tube reactor; E_{carb}: carbonator efficiency; EF: Entrained flow reactor; FB:Fluidized bed; PFM: Plug flow model; RPM: Random pore model.

threshold (e.g., Sun et al., 2008), with more evidence available for the former. The main literature on the topic is summarized in Fig. 18. Most carbonator models utilize the kinetics from Bhatia and Perlmutter (1983), which do not include the influence of the temperature (*T*) on the reaction rate. Notably, Scaltsoyiannes et al. (2021) developed a model based on a large amount of experimental data, including various operating conditions (p_{CO2}, *T*) and four different materials that contained $CaCO_3$.

Fedunik-Hofman et al. (2019) performed a systematic review on particle models for carbonation of CaO particles. One of the main models

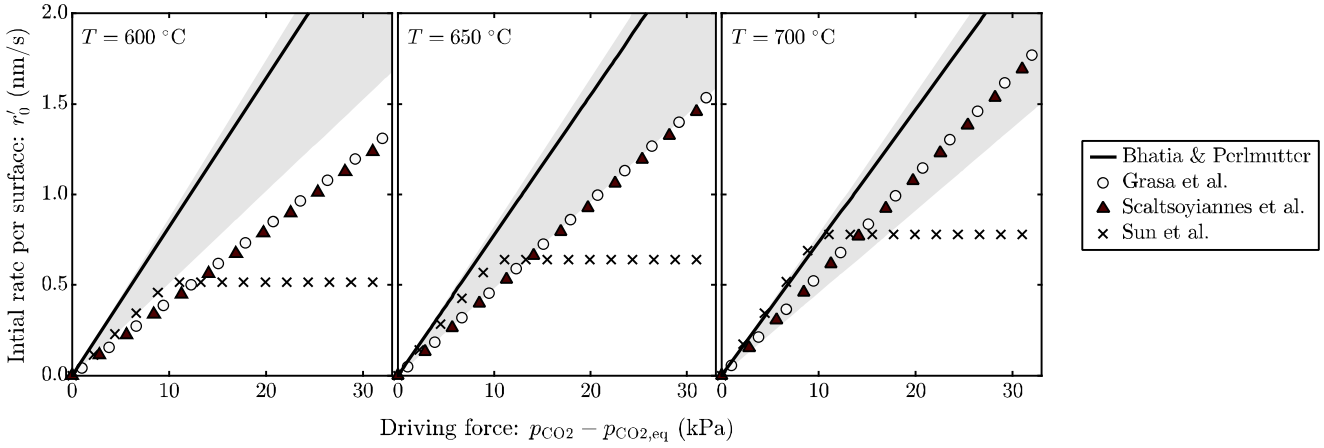

Fig. 18. Comparison of published work carbonation kinetics considering the initial reaction rate per unit surface of a particle of CaO based on experimental data (Bhatia and Perlmutter, 1983; Grasa et al., 2009; Scaltsoyiannes et al., 2021; Sun et al., 2008). The gray area indicates the range of experimental results obtained by Bhatia and Perlmutter (1983). Unlike other studies, Sun et al. (2008) found that the first-order dependency of carbonation kinetics with CO_2 partial pressure ends at ca. 10 kPa. Adapted from Greco-Coppi et al. (2025a), licensed under CC BY 4.0.

used to simulate the chemically controlled carbonation stage was developed by Grasa et al. (2008). The main assumption of this model is that the reaction rate decreases linearly with the reduction in maximum capture capacity, which is explained by the fact that both variables depend on the particle specific surface. The reduction of specific surface and porosity due to sintering is generally considered the main factor for sorbent deactivation (Agnew et al., 2000; Abanades and Alvarez, 2003).

The average activity of the sorbent in the CaL system is usually calculated with the model of Rodríguez et al. (2010). This model requires the input of a particle deactivation model as a function of the number of calcination-carbonation cycles, which is generally obtained using data from thermogravimetric analysis (TGA) (e.g., Grasa and Abanades, 2006). However, some pilot results suggest that the residual activity of the sorbent after many calcination-carbonation cycles may be lower than the one predicted by TGA tests (Greco-Coppi et al., 2025a).

The hydrodynamics model and the simulation of CO_2 conversion in the reactor depend on the reactor type. For circulating fluidized bed (CFB) carbonators, the model of Romano (2012) was one of the most advanced at the time it was published, due to its acceptable accuracy, the large number of input variables considered, and the relative simplicity of the calculations, which enabled integration into process models. However, this model overpredicts carbonator efficiency, especially for relevant operating conditions ($E_{carb} > 60\%$). Recently, Greco-Coppi et al. (2024d) demonstrated that imprecise assumptions in the hydrodynamics model lead to inaccuracies in the prediction of E_{carb}. They provided guidelines to select hydrodynamics assumptions based on a literature review of modeling and experimental investigations of fluidized beds, and introduced an improved model for fluidized bed carbonators based on the work of Romano (2012). Their model is divided into a hydrodynamics sub-model (Greco-Coppi et al., 2024d) and a particle and deactivation sub-model (Greco-Coppi et al., 2025a). It was validated with results from pilot plant operations at the 300-kW_{th} scale.

Many recent carbonator models focus on novel CaL approaches. Spinelli et al. (2018) developed a model for an entrained flow carbonator, suitable for cement applications, using a one-dimensional approach, and Turrado et al. (2018) modelled a drop tube carbonator using a simple plug flow model.

Recently, Secomandi et al. (2024) employed an 1.5D model to simulate a CFB carbonator that uses $Ca(OH)_2$ to increase carbonator efficiency. They could perform a preliminary validation based on previous pilot tests that did not feature the $Ca(OH)_2$ input.

4.1.2. Calciner models

The calciner model from Martínez et al. (2013b), which uses the calcination kinetics obtained by García-Labiano et al. (2002), has been widely utilized for modeling oxy-fired fluidized bed calciners. It is a simple model that assumes homogeneous CO_2 concentration in the calciner but has not been validated with experimental data. Recently, it was shown that this model failed to predict the performance of the indirectly heated calciner in the 300-kW_{th} pilot plant at TU Darmstadt (Hofmann, 2025). Based on the model of Martínez et al. (2013b); Greco-Coppi et al. (2025b) developed an improved model that successfully predicts empirical results from the 300-kW_{th} IHCaL pilot plant (Reitz et al., 2016) and the oxy-fired CaL 1-MW_{th} pilot-scale facility (Ströhle et al., 2020), both at TU Darmstadt. This model has low computational requirements and can be used to design calciners that reach high calcination rates without excessively increasing heat demand due to elevated operating temperatures. Additionally, Greco-Coppi et al. (2025b) presented new guidelines for calciner design and assessment based on two dimensionless numbers: (i) the calcination driving force (DF), and (ii) the dimensionless active time ($\tilde{\tau}_{act}$).

Analogous to carbonator models, recent calciner models have expanded on previous work by adding advanced features corresponding to novel CaL configurations. Parkkinen et al. (2017) developed a 3D model of a CaL calciner operating with high O_2 concentrations at reactor inlet. They validated this model with data from La Pereda pilot plant (Arias et al., 2018) and used the model to design a commercial-scale calciner. Recently, Spyroglou et al. (2024) modeled an entrained flow calciner for storage applications using solar energy. The model was validated with experimental data from a 10.5-kW_e reactor (Fernandez et al., 2019).

4.1.3. SE-CaL models

The most developed among SE-CaL processes for gaseous fuel/process streams is based on packed bed configuration under the so call Ca-Cu process (and its different versions as for example CASOH process). Initial modeling efforts were devoted to determining through basic mass and energy balances the conceptual design of the overall Ca-Cu process for H_2 production from CH_4 sorption-enhanced reforming. A basic reactor model that assumed narrow reaction fronts, plug flow and negligible axial dispersion, was used to describe the dynamic performance of every stage of the process (Fernández et al., 2012). More rigorous reactor models were latterly developed to describe more precisely the dynamic profiles obtained during every stage of the Ca-Cu process. These are basically 1D models in which a moderate axial mass and heat dispersion are considered and mass and heat transfer resistances between the gas and solid phases are neglected (Fernandez et al., 2012). Adequate kinetic expressions for the gas-solid and catalytic reactions occurring on every single stage were incorporated in the reactor models (i.e., CaO carbonation, CH_4 steam reforming and WGS during SER stage; Cu and Ni oxidation during oxidation stage; CuO reduction and $CaCO_3$ calcination during sorbent regeneration stage). The operability windows for each reaction stage were determined from sensitivity analyses of the main operating parameters, and dedicated experimental works served to validate the developed models at laboratory scale for the complete Ca-Cu cycle (Martínez et al., 2019). Such models have demonstrated the ability to reproduce experimentally observed temperature profiles, breakthrough curves, and gas compositions under cyclic operation. Subsequently, the dynamic operation of the overall Ca-Cu process was simulated assuming that the initial conditions of each reaction stage were the result of the previous step, to define a new operation strategy to minimize the number of reactors required and increase the CO_2 capture efficiency and to avoid possible side reactions (Fernández and Abanades, 2017). As experimental programs progressed from laboratory to pilot scale, modeling efforts shifted toward validation and tuning against large-scale data (Martini et al., 2016; Fernández et al., 2025), and to evaluate the integration of Ca-Cu cycle with different gaseous fuel streams (Fernández et al., 2025; Mostafa et al., 2023). Reactor models originally developed at small scale have been adapted to describe non-ideal effects, including heat losses, axial dispersion, and incomplete utilization of the bed. Recent TRL 7 demonstrations of the CASOH process have provided a unique dataset for validating these models under industrially relevant conditions, reinforcing their value as tools for process optimization and commercial scale-up.

At the plant scale, the Ca–Cu and CASOH processes have been extensively modelled using process simulation tools such as Aspen Plus (Khallaghi et al., 2025). In these studies, each reactor stage is represented using a combination of equilibrium, stoichiometric, or kinetic reactor models, along with dedicated heat-exchange blocks to account for solid–gas thermal interactions. Process-level models enable full mass and energy balances, comparison of alternative configurations (e.g., CASOH base versus enhanced concepts), and benchmarking against conventional CO_2 capture technologies such as amine absorption. Results consistently show that CASOH can achieve CO_2 capture efficiencies exceeding 95% while providing competitive or superior energy efficiency compared to benchmark (Khallaghi et al., 2025).

Focusing on solid fuels, biomass steam sorption-enhanced gasification (SEG), early modeling studies were based on thermodynamic equilibrium or quasi-equilibrium approaches, often implemented using Aspen Plus. In these models, gasification and CO_2 capture reactions were

described using Gibbs free energy minimization or restricted equilibrium formulations, enabling rapid evaluation of system-level performance and energy efficiency (Detchusananard et al., 2017; Martínez et al., 2013a). Such process-level models were extensively applied for parametric analyses to assess the influence of gasification temperature, steam-to-carbon ratio and CaO-to-fuel ratio on syngas composition and hydrogen yield. To overcome the limitations of equilibrium-based descriptions, kinetic reactor models incorporating detailed reaction mechanisms were subsequently developed. These models explicitly account for biomass pyrolysis, gas–solid gasification reactions, water–gas shift, tar reforming, and CaO carbonation kinetics (Beirow et al., 2020; Hafner et al., 2021). One-dimensional (1D) hydrodynamic–kinetic models for bubbling and circulating fluidized beds were formulated to resolve axial gradients in temperature, gas composition and solid conversion while considering gas–solid contacting and sorbent deactivation due to cyclic operation. Validation against pilot-scale SEG facilities (≈200 kW_{th}) demonstrated satisfactory agreement, highlighting the critical role of gasification temperature and sorbent make-up rate on CO_2 capture efficiency and syngas quality (Beirow et al., 2020). More recent work has focused on coupled models representing both the gasifier and calciner within dual fluidized bed SEG systems. One-dimensional dynamic models simultaneously describing the interconnected reactors and solid circulation loops have been developed to investigate heat integration, part-load operation and process controllability at industrially relevant scales (Ritvanen et al., 2021). These coupled reactor models enabled the conceptual design of industrial-scale SEG units (≈100 MW_{th}) for synthetic fuel production and allowed systematic assessment of off-design performance and operational flexibility. Such approaches effectively bridge laboratory-scale understanding and techno-economic evaluation of SEG-based fuel pathways.

4.2. Chemical looping models

Modeling of chemical looping processes has evolved from simple shrinking-core kinetics and 0D/1D reactor balances to multiscale models that link detailed redox mechanisms with CFD/CFD–DEM and dynamic process simulators for full plants. More sophisticated models at reactor-scale supports the design and optimization of fluidized-bed and packed-bed systems for different fuels. Over the last decade, research has focused on detailed reaction mechanisms, multi-scale models, rigorous validation against pilot plants, and advanced designs.

4.2.1. Models at the particle level

Sophisticated reactor simulations require reaction models at the particle level. Early research focused on understanding fundamental reaction mechanisms and developing suitable oxygen carriers. Thus, substantial progress has been made in understanding oxygen carrier kinetics in reactions involving a reducing gaseous agent (i.e., a fuel) and the active solid metal oxide, as well as in oxidation with oxygen from air. The unreacted shrinking core model (USCM) emerged as the predominant framework for describing gas-solid reactions in chemical looping systems. García-Labiano et al. (2004) established fundamental kinetic models for copper-based oxygen carriers, determining reaction order and activation energies for both reduction and oxidation phases. Then, Readman et al. (2006) conducted pioneering work on $NiO/NiAl_2O_4$ oxygen carriers using in-situ powder X-ray diffraction and thermogravimetric experiments, elucidating the mechanisms of reduction-oxidation reactions. Recent work has moved from empirical expressions to mechanistic and multi-step redox models. This is especially relevant for processes involving several conversion mechanisms beyond the reduction and oxidation of the oxygen carrier.

The evaluation of the catalytic activity is of paramount importance in processes based on hydrocarbons reforming, such as CLR. In CLR, it is especially relevant the catalytic mechanism catalytic mechanism of the active metal in the oxygen carrier for hydrocarbons reforming. Iliuta et al. (2010) developed a comprehensive mathematical model incorporating both kinetics for the oxygen transference with the oxygen carrier and catalytic activity in methane reforming. Ortiz et al. (2012) determined that the catalytic activity of the oxygen carrier is lower than that of SMR catalysts, and it increases with the reduction degree of NiO, which changes during the oxygen transference process in the fuel reactor. Recently, kinetics studies have been extended to other types of fuels. De las Obras Loscertales et al. (2023) determined the kinetics of relevant reactions in the conversion of ethanol in the presence of a Ni-based oxygen carrier. Interestingly, the main mechanism converting ethanol were dehydration and decomposition, with the last being catalytically improved by the reduced Ni.

In the case of materials with oxygen uncoupling capability, the determination of the kinetics of the decomposition of the metal oxide releasing gaseous oxygen to the reaction environment should also be addressed. For CuO, the equilibrium partial pressure of oxygen, which varies significantly with temperature, was identified as a critical factor affecting both oxygen uncoupling and the subsequent oxidation (Adánez-Rubio et al., 2014). Also, a two-stage combustion sequence has been identified: volatile combustion with solid Co_3O_4 followed by fixed carbon combustion with gas-phase oxygen released from its decomposition (Güleç and Okolie, 2025). This fact is related to the competition between two parallel reactions during fuel conversion: gas-solid reaction and oxygen uncoupling. Adánez-Rubio et al. (2012) and Mei et al. (2015) identified the conditions at which each mechanism is dominant, being the reacting temperature and the gas concentration the more important ones.

For perovskites (mainly Ca–Mn-based), it has been identified both gas-solid reaction and oxygen uncoupling mechanism being relevant for the oxygen transference (Abad et al., 2019). Thus, dedicated kinetics for the reduction, both gas-solid and oxygen uncoupling, and oxidation reactions are relevant for modeling purposes, having been determined and identifying thermochemical restrictions for the oxygen uptake or release (Abad et al., 2015a). Liu et al. (2021a) derived the redox kinetics for Ca-Mn-based perovskite, resolving separate regimes controlled by surface reaction vs internal diffusion. This mechanism may be also applied to mixed oxides with oxygen uncoupling capability, such as CuMn, CuFe or MnTi (Mendiara et al., 2025).

Density functional theory (DFT) is a powerful tool to investigate the reaction mechanism in gas-solid reactions. For example, DFT-based microkinetic studies for CLOU identified the O_2 release/recombination barriers and built a DFT-based kinetic model that replaces empirical Arrhenius parameters, allowing prediction of equilibrium oxygen partial pressure and rate as a function of the reacting temperature (Liu et al., 2025). The oxygen non-stoichiometry, diffusion-controlled oxygen release, and defect chemistry were identified as the basis for kinetic modeling in CLOU.

4.2.2. Models at the reactor level

4.2.2.1. Model development. Reactor models integrate reaction kinetics with the fluid dynamics of the reactors which in turn depend on the reactor type, such as fluidized bed systems or packed beds. Thus, for chemical looping systems based on interconnected fluidized beds, early models used macroscopic based on empirical correlations for solids and gas flows, as well as bubble size. Peltola et al. (2022) summarize macroscopic models where fuel and air reactors are mostly represented by 0D/1D models with plug flow or 1.5D models which includes some dispersion between phases in a bubbling or circulating fluidized bed. These models allow for a quick evaluation of the main design and operating parameters relevant for the performance of the chemical looping processes.

Alternatively, CFD provides a detailed description of the fluid dynamics in a fluidized bed reactor, which allows for a fine definition of the reactor engineering, but at the cost of a great computational effort. CFD models have shifted from purely hydrodynamic studies to

kinetic-embedded models. Shao et al. (2021) review CFD studies on CLC, noting progression from 2D isothermal models with single global reaction to fully coupled 3D non-isothermal CFD with multiple reactions and radiative heat transfer, although computational cost limits use in plant-wide optimization. A cooperating work using macroscopic and CFD models have been suggested as an optimal procedure in the modeling tasks for the scale-up of the chemical looping technology (Abad et al., 2026). Also, alternative approaches may be used to reduce the computing effort of CFD models. A 3D CFD–DEM model of a 1-MW_{th} biomass fuel reactor resolves particle-scale motion and a simplified reaction network (Graf et al., 2024). Interestingly, this CLG model treat solids as discrete particles to capture bubble–particle clusters and mixing, with coarse-graining to keep simulations tractable. This has enabled, for example, accurate prediction of pressure profiles, carbon conversion, oxygen carrier oxidation, and gas composition.

Recently, machine learning methods have also been implemented to predict the behavior of the CLG process using existing experimental results from CLG units (Sison et al., 2023). However, the use of these AI methods should be considered with caution, as they may not reflect aspects relevant to the process due to limitations in the selected base data. For example, the authors identified temperature and steam-to-biomass ratio as being the most relevant parameters affecting the CLG performance, while experimental results showed that FR residence time and oxygen-to-fuel ratio are more relevant on the syngas yield, while steam-to-biomass ratio was of lesser relevance (Condori et al., 2024a).

Recent modeling efforts have emphasized full-reactor simulations capturing both fuel and air reactors simultaneously. Often, the relevance of the air reactor in the chemical looping performance has been understated, as the oxidation reaction is usually a quick process. However, Reinking et al. (2021) highlighted the relevance of the air reactor performance on the global chemical looping unit for the CLOU process, as oxygen uncoupling mechanism is highly temperature-dependent. In fact, the air reactor may limit the oxygen transference rate from air to fuel under certain design and operating conditions, as it was the case for Cu-based oxygen carriers (Abad et al., 2023). Coupling the reactors allows for the evaluation of transient situations. Thus, recent extensions include dynamic models emphasizing time-dependent solids inventory, start-up/transients, and control-relevant formulations (Kataria et al., 2024).

It is highly valuable to validate the developed models which are intended to be used for design purposes. For CLG systems, Qi et al. (2023) validated an Aspen Plus model for hydrogen production from municipal solid waste using $CuFe_2O_4$ spinel oxygen carriers. Gogulancea et al. (2023) and Abad et al. (2025a) validated CLG mathematical models using experimental data from pilot plants, showing excellent agreement for hydrogen and carbon monoxide behavior with pine forest residues and wheat straw. Cold gas efficiency and syngas yield calculations confirmed model reliability for large-scale predictions. Also, recent CFD simulations have achieved remarkable agreement with experimental measurements. For example, validation efforts for CLOU systems on a 200 kW_{th} dual fluidized bed captured basic trends in solids circulation rates, pressure profiles, and particle velocities, enabling design optimization (Reinking et al., 2021).

Regarding the design of chemical looping units, fluidized bed reactors remain the dominant configuration for large-scale applications. Recent development of dual circulating fluidized bed (DCFB) systems has shown superior performance compared to bubbling fluidized bed (BFB) (Abad et al., 2018). Configuration optimization studies using a three-dimensional multiphase particle-in-cell (MP-PIC) method was used to understand the behavior of the full loop CLG unit, which is of paramount relevance for the future design and scale-up of the technology (Wang et al., 2025).

In interconnected fluidized bed systems, the hierarchy of models for design purposes increases as follows: (i) macroscopic 1/1.5/2D models for plant-wide mass/energy integration and CO_2 capture efficiency, (ii) compartment models for risers, bubbling beds, loop seals, and carbon strippers, and (iii) CFD for critical sections (e.g. fuel reactor mixing, flow in cyclones). For example, mathematical models have been used for a basic design of the fuel and/or air reactors for CLC (Abad et al., 2015b), CLR (las Obras Loscertales et al., 2025b), and CLG (Abad et al., 2026).

As stated above, packed beds are also a preferred option for implementing chemical looping technologies, which can be suitable for pressurized operation and combined to gas turbines (Noorman et al., 2007). Conceptual models of fixed/packed-bed were developed employing alternating oxidation–reduction periods. Early packed-bed CLC/CLR models were typically 1D, adiabatic, axially dispersed plug-flow formulations with global redox kinetics and simple effectiveness factors for intra-particle diffusion (Fernández and Alarcón, 2015). 1D CLR packed-bed models resolve radial dispersion when needed and couple multiple reaction stages in cyclic operation (Qayyum et al., 2023). However, dedicated 2D model are more suitable to capture radial temperature gradients, revealing strong thermal fronts and informing design of bed length and cycling strategy (Argyris, 2022).

4.2.2.2. Validation of reactor models. Validating a model is a key step in gaining the necessary confidence in its use for the development of any process, especially in the chemical looping technology since it is not a commercial technology, it is in the process of scaling up and most of the know-how has been obtained from experimental evidence.

Early validation works were performed validating macroscopic models for the fuel reactor with lab-scale units (10–100 kW) for CLC of gaseous fuels (Abad et al., 2010) and solid fuels (Abad et al., 2013). More recently, Qi et al. (2023) validated an Aspen Plus model for hydrogen production for CLG of municipal solid waste using $CuFe_2O_4$ spinel oxygen carriers. Gogulancea et al. (2023) and Abad et al. (2025a) validated CLG macroscopic models using experimental data from pilot plants, showing excellent agreement for hydrogen and carbon monoxide behavior with pine forest residues and wheat straw. Also, recent CFD simulations have achieved remarkable agreement with experimental measurements. For example, validation efforts for CLOU systems on a 200-kW_{th} dual fluidized bed captured basic trends in solids circulation rates, pressure profiles, and particle velocities, enabling design optimization (Reinking et al., 2021). Another validation work involving the oxygen uncoupling capability of perovskite materials revealed the relevance of reaction temperature on the fuel conversion mechanism at the 120-kW_{th} scale (Abad et al., 2019).

As the TRL of the chemical looping technology increases, data becomes available for validating models on a larger scale. This is the case of model validation works using data from the existing 1-MW_{th} chemical looping unit at Darmstadt University of Technology. Thus, combustion efficiency for CLC (Ohlemüller et al., 2018) or cold gas efficiency and syngas yield calculations for CLG (Graf et al., 2024) confirmed model reliability for large-scale predictions.

The prediction of the behavior of the full loop, including the fuel and air reactors, is also highly relevant in order to gain confidence on the design of a chemical looping unit. In this sense, the validation of a CLC model was done using results from the air and fuel reactors in a 120-kW_{th} plant at Vienna University of Technology with Cu- and Fe-based materials. The validated model was able to identify possible causes of the low fuel conversion achieved during the experimental campaign with these highly reactive oxygen carriers, suggesting new approximations to achieve full fuel conversion, e.g. by modifying operating conditions or reactor design (Abad et al., 2023). This methodology has been also presented for the combustion (Gayán et al., 2013) and gasification (Abad et al., 2026) of solid fuels.

In the case of models for packed bed reactors, the inclusion of any relevant mechanism for the fuel conversion is of paramount importance to properly predict the breakthrough curve. Also, temperature profiles, due to heat generation/consumption during the fuel conversion, should be properly predicted. For example, the SE-CLR process was modeled by

Abbas et al. (2017). The 1D dynamic reactor model included detailed kinetics for Ni-based redox behavior as well as catalytic reforming and CaO carbonation. The model quantitatively captured the behavior of the breakthrough curve in a fixed bed, and it was successfully used to evaluate the potential of the SE-CLR process to produce H_2 with near-zero CO_2 emissions.

As an alternative to fixed-bed reactors, moving bed configurations enable counter-current continuous operation between gas and solids, avoiding the use of several out-of-phase reactors while achieving thermodynamically favorable conditions. The counter-current arrangement allows maximum utilization of oxygen carrier capacity; for example, Fe-based systems can achieve higher conversions than co-current fluidized bed operations while maintaining product purity (Fan and Li, 2010). Moving bed reactors for chemical looping hydrogen generation have been validated using CFD-DEM simulations (Teng et al., 2024). This study demonstrated that enhanced particle flux rates and reaction temperatures substantially increase conversion efficiency, with CH_4 conversion identified as the critical factor determining required bed height for complete gas conversion.

4.2.2.3. Applications of the developed models. Mathematical models have been used for determining suitable design parameters or optimal operating conditions for the scale-up of the chemical looping technology. Regarding the design of chemical looping units, fluidized bed reactors remain the dominant configuration for large-scale applications. Recent development of dual circulating fluidized bed (DCFB) systems has shown superior performance compared to bubbling fluidized bed (BFB) (Abad et al., 2018). In interconnected fluidized bed systems, the hierarchy of models for design purposes increases as follows: (i) macroscopic 1/1.5/2D models for plant-wide mass/energy integration and CO_2 capture efficiency, (ii) compartment models for risers, bubbling beds, loop seals, and carbon strippers, and (iii) CFD for critical sections (e.g. fuel reactor mixing, flow in cyclones). For example, mathematical models have been used for a basic design of the fuel and/or air reactors for CLC (Abad et al., 2015b), CLR (las Obras Loscertales et al., 2025b), and CLG (Abad et al., 2026).

A joint modeling of the fuel and air reactors in a chemical looping unit allows for the evaluation of the interaction between the reduction and oxidation processes, which eventually affects fuel conversion. For example, configuration optimization studies using a three-dimensional multiphase particle-in-cell (MP-PIC) method was used to understand the behavior of the full loop CLG unit, which is of paramount relevance for the future design and scale-up of the technology (Wang et al., 2025). In addition, coupling the reactors allows for the evaluation of transient situations. Thus, recent extensions include dynamic models emphasizing time-dependent solids inventory, start-up/transients, and control-relevant formulations (Kataria et al., 2024).

Pressurized systems based on fluidized bed reactors are challenging due to air and fuel reactors should be operated at similar pressure values and a proper management of the pressure fluctuations in the reactors should be done. In addition, both reaction kinetics and fluid dynamics are highly affected by the reactor pressure, which should be considered for a proper design and operation of the reactor (Cabello et al., 2023a).

Fixed-bed concepts in chemical looping often use multiple parallel beds operated in out-of-phase redox cycles, often modeled as adiabatic 1D beds with switching logic to provide quasi-continuous gas, heat or power. For that, modeling of packed-bed has been often used for the optimization of cycle times, also demonstrating the flexibility of chemical looping processes to different fuels, extending the use of methane (Argyris, 2022) to other fuels such as glycerol (Navarro et al., 2024). In this regard, packed-bed CLC/CLR models are now integrated with nonlinear model predictive control (NMPC) to optimize switching times and inlet conditions in large-scale units in real time (Toffolo et al., 2024). Thus, 1D/2D models inform bed length, cycle time, inlet temperature, and pressure to maximize syngas or H_2 yield while respecting material constraints. Due to the dynamic nature of the fixed-bed operation, transient periods should be also modeled using dynamic models, which has been identified as a critical step for the industrial scale-up of this technology (Lucio and Ricardez-Sandoval, 2020).

Despite significant progress on chemical looping modeling, several challenges remain, highlighting scale-up uncertainties and computational efficiency. While validated models exist for laboratory and pilot scales, extrapolation to industrial scale requires improved understanding of heterogeneous flow patterns and particle flow and segregation effects. Also, full-reactor CFD simulations remain computationally expensive, with typical simulations requiring tens/hundreds of hours for some seconds of real-time behavior, limiting their utility for parametric optimization studies.

4.3. Indirect gasification models

Computational fluid dynamics (CFD) has become the dominant reactor-scale modeling approach for dual fluidized bed (DFB) gasification systems. CFD methods provide detailed predictions of gas–solid hydrodynamics, heat transfer, particle circulation, and reaction behavior inside interconnected gasification and combustion reactors. While the hydrodynamic, pyrolysis and gasification mechanisms are the same as for chemical looping gasification, the bed-material particles must not be considered as reactants. Because commercial-sized installations are available, many studies use frameworks in which data from such plants can be used for validation. Therfore, the MP-PIC approach is prominently featured (e.g. Sun et al., 2023a; Kraft et al., 2017; Liu et al., 2015; Sun et al., 2023b; Liu et al., 2016; Sun et al., 2024; Berg et al., 2023). Here the large amount of particles can be computed in an acceptable time, although Graf et al. (2026) showed that also full Euler-Lagrange is in range with GPU acceleration. With increasing computing power, three dimensional semi empiric models (Myöhänen et al., 2018) are only used in very few studies.

Kong et al. (2023) developed a CFD model for an 8 MW industrial DFB gasifier incorporating CO_2 absorption-enhanced reforming (AER), showing a 76.67% reduction in CO_2 mole fraction and a 54.58% increase in H_2 concentration compared with conventional operation. Luo et al. (2019) presented a 3D full-loop CFD model capable of predicting solid circulation rates, pressure distributions, and particle mixing behavior in pilot-scale systems showing benefit of the EMMS drag model over Gidaspow. Kraft et al. (2017) conducted CPFD simulations of an 8 MW industrial-sized DFB steam gasification system, providing detailed predictions of particle mixing, solid circulation, and temperature distributions. The model was validated against operational data from the 8 MW commercial plant in Güssing, Austria.

For process estimation models similar to chemical looping gasification are used which couple hydrodynamic to the gasification and combustion kinetics. Hejazi et al. (2017a, 2017b) developed and validated kinetic models for steam gasification in DFB reactors using pilot-scale experimental data. Their models incorporated char gasification, methane reforming, and water–gas shift kinetics and achieved prediction errors of 5–15% for major gas species.Lundberg et al. (2018) investigated scale-up effects on char conversion and showed that larger reactor sizes reduce conversion efficiency due to broader residence time distributions and temperature non-uniformities. The study emphasized the importance of optimizing solid circulation rates and cyclone separation efficiency to maintain carbon conversion above 95%. In general Aspen Plus is a widely adapted software for the modeling of indirect gasification (e.g. Puig-Gamero et al., 2021; Aghaalikhani et al., 2019; Yan et al., 2016; Alamia et al., 2016; Nicolucci et al., 2025; Rashidi et al., 2025) especially when investigation whole value chains (Wan et al., 2024; Del Grosso et al., 2020).

Tar formation and catalytic cracking were also major focuses of kinetic modeling. Aghaalikhani et al. (2019), used an Aspen Plus model of the TU Wien 100 kW unit to show that gasification temperatures above 850°C combined with catalytic bed materials such as olivine or dolomite

substantially reduced tar concentrations. Liu et al. (2026) investigated the addition of limestone and olivine and demonstrated that catalytic bed materials increased tar cracking rates up to a factor of 3 compared with silica sand.

A comparatively new area of modeling is the modeling of dynamic processes and Model predictive control for runtime plant optimization. These studies recognize that commercial-scale operation requires robust control strategies to maintain stable operation despite disturbances in feedstock properties, load changes, and equipment variations. Stanger et al. (2023b) present a dynamic model intended for use in model-based control design. The model is built on mass and energy balances to predict reactor temperatures in the gasification reactor and combustion reactor, as well as product gas and flue gas mass flows, as a function of manipulable inputs such as fuel, steam, and air flows. Where first-principle modeling is impractical, i.e. the bed material circulation, an artificial neural network is employed. The model was validated using measurement data from a 100 kW pilot plant at TU Wien, with the artificial neural network trained on data from three test runs. Application of this model in a model predictive controller showe that the model achieves errors of approximately 2 kg/h for the gas mass flows and between 8–13°C for the reactor temperatures (Stanger et al., 2024b). The authors conclude that the model reliably predicts plant behavior, is transferable to other fuels and industrial-scale DFB plants via re-estimation of parameters, and is suitable as a foundation for implementing multi-variable model predictive control (Stanger et al., 2024a).

5. Process assessment

To evaluate the potential of HTSL processes for their future deployment, the technical suitability should be proven, as described in the above sections. Furthermore, techno-economic analysis (TEA) and life cycle assessment (LCA) are highly relevant to compare economic and energetic costs as well as environmental benefits/concerns with the performance of alternative options, both commercial and under development. These assessments are based on mass and energy balances of the processes, which generally rely on detailed reactor models to improve accuracy. For TEA, the operating costs, as well as the investments, are computed for the estimated lifetime of the plants. LCAs consider only the environmentally relevant flows in the mass balances to quantify the environmental impact of the processes.

The assessment of HTSL processes is discussed in the present chapter, considering various industrial sectors: power generation (Section 5.1), waste incineration (Section 5.2), lime and cement production (Section 5.3), steel manufacture (Section 5.4), and production of chemicals and fuels from syngas (Section 5.5).

5.1. Power generation

As discussed in Section 3.3.1, numerous continuous CLC units ranging from several kW_{th} to a few MW_{th} have demonstrated stable operation, high-efficiency fuel conversion, and effective inherent CO_2 capture. In particular, the successful operation of the 5-MW_{th} autothermal CLC unit within the CHEERS project demonstrates that CLC can operate under industrially relevant conditions, indicating readiness for system-level demonstration and an approach to TRL 7 (Li et al., 2025b). As stated in the previous sections, the fundamental advantage of CLC lies in its inherent CO_2 capture capability, which avoids the energy-intensive gas–gas separation steps, such as amine scrubbing or air separation, typically required in conventional carbon capture systems. This feature provides a potential pathway toward high-efficiency power generation with reduced CO_2 avoidance costs. Nevertheless, the techno-economic viability of CLC is inherently multifaceted and has strong dependence on reactor and system configuration, oxygen carrier (OC) performance, fuel characteristics, regional policy and market conditions.

When assessed against conventional power plants without carbon capture, which are commonly used as reference systems to quantify the energy and efficiency penalties associated with CO_2 mitigation, CLC systems may exhibit higher system complexity and increased exergy destruction, which can result in reduced net efficiency (Sayeed et al., 2022; Surywanshi et al., 2024; Porrazzo et al., 2016). For instance, Sayeed et al. (2022) reported that a 550-MW_e coal-fired supercritical power plant achieved a net efficiency of 37.88%, compared to 32.11% when operated in CLC mode. This efficiency reduction is primarily attributed to the energy demand for CO_2 compression, which is absent in conventional power plants without capture. However, CLC demonstrates a clear advantage when compared with state-of-the-art CO_2 capture systems by largely eliminating the substantial energy penalty and costs associated with CO_2 separation. This was recognized early on, and has been the main driver for research in the past two decades (Ekström et al., 2009; Lyngfelt and Leckner, 2015). Also, more recent studies of the techno-economics of CLC using both fluidized-bed and packed-bed configurations show that CLC outperforms conventional power plants equipped with post-combustion CO_2 capture. For example, natural-gas-fired CLC systems have been reported to achieve net efficiencies of up to 55.6% and *CO_2 avoidance costs* (*CAC*) as low as 27.5 USD/t_{CO2}, which correspond to 50.6% and 42.9 USD/t_{CO2} in conventional NGCC with CCS (Ogidiama et al., 2018; Oh et al., 2021). In coal-based applications, CLC is widely recognized as one of the most sustainable carbon capture (Zhao et al., 2021; Sayeed et al., 2022). Advanced system configurations may further enhance system performance. Packed-bed CLC system combined with integrated gasification combined cycle (IGCC) can achieve high techno-economic performance, attaining net electric efficiencies of 41–51%, CO_2 capture efficiencies above 95%, and *CAC* of 30–34 €/t_{CO2}, substantially outperforming conventional supercritical pulverized coal and pre-combustion IGCC power systems (Mancuso et al., 2017; Diglio et al., 2018). Multi-stage reactor arrangements integrated with Brayton cycles further improve techno-economic performance, increasing net efficiency from 25% to over 37% and reducing levelized cost of electricity (LCOE) by nearly 50%, primarily through higher turbine inlet temperatures and elimination of external reactant preheating (Tregambi et al., 2021a). However, increased system integration and complexity do not necessarily guarantee improved performance. Luo et al. (2018a) compared coal-direct CLC (CD-CLC) and coal-gasification CLC (CG-CLC), finding that CD-CLC achieved higher net power efficiency (48.45% vs. 38.53%), CO_2 capture efficiency (98.0% vs. 82.4%), and exergy efficiency (49.2% vs. 39.3%). The inferior performance of CG-CLC was mainly attributed to the additional energy penalties associated with oxygen production, syngas decompression, and heat losses in the gasification subsystem.

Beyond the reactor and system configuration, fuel type and oxygen carrier selection is also critical to the techno-economic viability of CLC for power generation, with costs strongly influenced by regional resource availability and market conditions. For example, Zhu et al. (2018) reported that compared to copper-, and ilmenite-based oxygen carriers, nickel-based systems offer the highest net efficiency (50.1%) and lowest LCOE (71.7 €/MWh) among methane-fueled CLC plants, with near-zero CO_2 emissions, outperforming conventional NGCC plants with post-combustion capture. For solid fuels, such as coal and biomass, chemical looping with oxygen uncoupling (CLOU) enhances direct char oxidation, and CLOU systems with oxygen carriers enabling O_2 releasing, show competitive CO_2 capture costs (73–87 €/t CO_2) while maintaining technical feasibility, provided oxygen carriers achieve sufficient durability (~1,000 h) (Cabello et al., 2024a). Keller et al. (2019) reported that biomass supply chain accounts for over 50% of total CO_2 sequestration costs for CLC with biomass in Japan. Further, Haaf et al. (2020c) showed that co-firing negatively priced SRF can improve economics, enabling LCOE comparable to conventional generation with net-negative emissions. The impact of the cost and durability of oxygen carriers highly depends on systems: hematite-based carriers in coal-based CLC have negligible effect on LCOE (Sayeed et al., 2022), whereas NiO-based carriers in gas-fired systems require high durability to maintain economic advantage (Ogidiama et al., 2018;

Porrazzo et al., 2016). Fuel price remains a dominant economic driver, especially for natural gas CLC systems, while CLC of solid fuels with low-cost ores depend more on minimizing capital costs than oxygen carrier longevity.

Despite the clear techno-economic advantages of CLC, these systems generally require supportive policy and market frameworks, such as carbon pricing, CO_2 taxation, or targeted incentives, to achieve more economic competitiveness under current market conditions. This is of course the case for all capture technologies, not only CLC. Given the substantial regional variation in policy environments, additional strategies are required to enhance CLC's adaptability and commercial attractiveness across different locations and market conditions. Poly-generation and advanced system integration represent a strategic pathway to improve the commercial competitiveness of CLC (Del Arnaiz Pozo et al., 2024; Cabello et al., 2022a; Zare et al., 2024; Pankhedkar et al., 2024). These integrated schemes enhance operational flexibility by enabling dynamic allocation of output among electricity, heat, and value-added products such as hydrogen, methanol, ethylene, or high-purity CO_2, depending on regional market demand, for example, through CO_2 utilization in horticultural greenhouse enrichment. Moreover, integration with processes such as plastic waste gasification or solar-assisted CLC integrated with absorption cooling in hot regions significantly enhances overall resource efficiency, with some poly-generation configurations achieving thermal efficiencies of up to 77% (Zare et al., 2024; Ogidiama et al., 2018). Another option, currently being explored in Europe, is the possibility to use a flexible CLC power-generation system. Taking advantage of the fact that CLC has clear similarities to normal CFBs, proposals to design a system which can be operated as either a normal CFB or as a CLC reactor with or without carbon capture have been proposed (Lyngfelt et al., 2022b). Such a system would limit the economic and technical risk for stakeholders, meaning that it could be deployed in current market conditions (Staničić et al., 2025). Collectively, these strategies position CLC as a flexible and multifunctional platform for sustainable energy and industrial applications, reducing energy and capital penalties and enhancing its commercial competitiveness under diverse carbon pricing regimes and market demands.

In spite of the shift of CaL and IHCaL investigations toward industrial applications such as cement production (see Section 5.3) and waste incineration (see Section 5.2), some studies have considered them for decarbonizing power plants. For example, Junk et al. (2016a) calculated *CAC* of 22.6 $€_{2016}/t_{CO2}$ for a hard coal power plant retrofitted with an IHCaL process, without including costs for compression, conditioning, transport, or storage. Recently, Gao et al. (2025) introduced a hybrid CaL with CLC for coal power plants, which does not require an air separation unit for the combustion in the calciner. Instead, oxygen is obtained using a metal energy carrier in an air reactor. The oxygen-depleted air at high temperature is used in turbine to generate power and recover energy. They obtained $CAC = 36.1$ $\$_{2024}/t_{CO2}$ for this solution, which was lower than the value for the traditional CaL using pure oxygen (48.1 $\$_{2024}/t_{CO2}$).

An important consideration for modern power plants is the enhancement of operational flexibility. To address this challenge, several process configurations have been proposed that incorporate solid and energy storage systems into CaL-based schemes for the treatment of flue gases from power generation facilities (Hanak et al., 2016; Astolfi et al., 2019; Cormos, 2020; Arias et al., 2020; Cormos et al., 2021; Criado et al., 2022). This integration enables decoupling of the carbonator and calciner loads, reducing the thermal capacity requirements of the calciner and improving overall economics, with reported reductions in LCOE and CCA of up to 6.6% and 25.5%, respectively, compared with reference cases without storage (Astolfi et al., 2019).

5.2. Waste-to-energy facilities

In general, the costs for capturing CO_2 from waste incineration plants and waste-to-energy (WtE) facilities are higher than for other applications, such as cement production facilities, due to the lower CO_2 flow rates, which negatively impact the economy of scale (Greco-Coppi et al., 2026b). On a recent review of CO_2 capture, utilization, and storage for waste-to-energy plants, Acampora et al. (2025) identified CaL as the technology with lowest *CAC*, compared to other capture processes, including amine scrubbing and membrane separation. Haaf et al. (2020a) calculated the costs of capturing CO_2 from a WtE plant using both CaL and monoethanolamine (MEA) scrubbing. They reported ca. 120 $€_{2017}/t_{CO2,av}$ for the tail-end CaL process, compared to over 280 $€_{2017}/t_{CO2,av}$ for MEA scrubbing.

Lately, studies have compared the utilization of CO_2 from WtE-plant for methanol production (CCU route) to capturing CO_2, transporting it, and storing it in geological sites (CCS route). Hofmann et al. (2021) compared the option of producing methanol and capturing CO_2 using CaL in a generic 60 kW_{th} WtE plant and reported $CAC > 70$ $€_{2018}/t_{CO2,av}$ for the capture and storage option, without including costs for transport and storage. If methanol from CO_2 is produced using H_2 from an electrolyzer, competitive prices can be achieved only for very favorable scenarios with low energy costs and high CO_2 taxes. Similar results were reported by Greco-Coppi et al. (2024a), who showed that the CCU route, in which methanol is produced from green hydrogen and captured CO_2, is only competitive for very low electricity prices of under 25 $€_{2023}$/MWh. For other scenarios, capturing, transporting, and storing CO_2 is the most economically viable option. Thereby, the cost for transport and storage are important drivers of the total costs.

Ströhle (2023) suggested that chemical looping combustion (CLC) may be competitive against post-combustion CO_2 capture technologies for carbon capture from waste incineration plants and reported *CAC* lower than 90 $€/t_{CO2,av}$ (Mohn et al., 2022). However, these results were identified as preliminary. To date, no detailed techno-economic analysis of CLC for waste incineration facilities has been performed. One of the main challenges of applying this technology in waste treatment is that it is only suitable for completely new projects, not being possible to retrofit existing facilities. Furthermore, there are additional limitations that need to be addressed before commercializing CLC for waste incineration, due to the particular nature of the feedstock featuring more impurities and higher variability than conventional fuels. These include incomplete fuel conversion, deactivation of oxygen carrier due to interaction with waste ash, and limited understanding of the influence of phosphorus on the oxygen carrier activity (Yaqub et al., 2023).

Recently, Greco-Coppi et al. (2026b) introduced a novel concept for integrating the CaL process into existing waste incineration plants. This novel concept burns pretreated waste in the calciner using pure oxygen, a viable approach that was demonstrated through pilot operations in the 1-MW_{th} plant at TU Darmstadt by Haaf et al. (2020d). The integration is realized through replacing one existing incineration line, which has reached the end of its operating life, with a CaL unit. The incineration capacity of the entire facility is kept—or even expanded—through the calciner, which acts as an additional oxy-fired incinerator. The economics of the process were compared with the standard back-end retrofitting CaL concept (tail-end). The costs of the tail-end configuration were in agreement with those previously reported by Haaf et al. (2020a). The *CAC* of the novel, integrated concept were 27 $€_{2024}/t_{CO2,av}$ (Greco-Coppi et al., 2026b), —including compression and conditioning but excluding transport and storage—, which is well below current CO_2 prices within the European Trading System (ETS) of the European Union. This represents the lowest cost for CO_2 capture from waste incineration and waste-to-energy plants reported in the literature to date (Greco-Coppi et al., 2026a).

5.3. Lime and cement production

Among the HTSL processes, both the oxy-fired carbonate looping (CaL) and the indirectly heated carbonate looping (IHCaL) have been studied for CO_2 capture from cement plants. The IHCaL process has also

been proposed for lime plants since it allows for cleaner spent sorbent that, unlike in the oxy-fired CaL, is not contaminated by fuel ash (Greco-Coppi et al., 2021a).

Santos and Hanak (2022) reviewed the costs and energy requirements of different CO_2 capture technologies for various industrial applications, including the cement industry. They concluded that CaL and oxy-combustion show the best economic and energy-efficiency indicators. They reported that the mean *CAC* in the literature were 43 €/$t_{CO2,av}$ for CaL and 40 €/$t_{CO2,av}$ for oxy-combustion. They indicated that oxyfuel slightly outperforms CaL in terms of Specific Primary Energy Consumption (SPECCA), with a mean of 1.7 MJ/kg_{CO2} versus a mean of 2.2 MJ/kg_{CO2} for CaL. Yang et al. (2021) combined a literature review with own calculations to assess different technologies to reduce CO_2 emissions in cement plants. They reported that CaL performed better than other technologies when combined with the use of biomass to obtain the energy for the calciner.

Gardarsdottir et al. (2019) compared various CO_2 capture technologies for cement plants: MEA scrubbing, oxyfuel, Chilled Ammonia Process (CAP), membrane separation, and two CaL configurations. They reported that, after oxyfuel (42 $€_{2014}/t_{CO2,av}$), CaL had the lowest *CAC*, with 52 $€_{2014}/t_{CO2,av}$ for a tail-end configuration and 58 $€_{2014}/t_{CO2,av}$ for an integrated concept, in which the pre-calciner of the cement plant is combined with the CaL calciner. These values were similar to those reported by Lena et al. (2019) and Cormos (2020). The results were strongly dependent on electricity prices, with higher prices favoring the tail-end CaL concept due to net CO_2 power generation. The CaL concepts performed better than the other processes in terms of CO_2 emissions abatement potential. Additionally, they showed specific primary energy consumption (SPECCA) values of 3–4 MJ/kg_{CO2}, which were lower than for MEA scrubbing (7.1 MJ/kg_{CO2}) but higher than for oxy-combustion (1.6 MJ/kg_{CO2}) (Voldsund et al., 2019). In contrast, Rolfe et al. (2018) reported that CaL had lower SPECCA (2.4 MJ/kg_{CO2}) than oxyfuel (3.3 MJ/kg_{CO2}) for capturing CO_2 from a cement plant, and indicated that CaL exhibited a lesser environmental impact. The latter observation was associated with the power generation from the recovered heat. Cormos (2022) presented higher costs for CaL in cement production. However, some of their assumptions were unfavorable for CaL: low carbonator operating temperatures (550–625°C), and high calciner temperatures (850–980°C).

In general, CaL is regarded as one of the most promising CO_2 capture technologies for cement plants in terms of low energy consumption and potential for achieving competitive costs. It performs similarly to oxyfuel with better indicators for assumptions that give increased value to electricity (e.g., higher electricity prices, higher specific CO_2 emissions from the grid). This dependance on selected assumptions, as well as the different scales of each study, may explain the different values found throughout the literature.

Greco-Coppi et al. (2023b) evaluated the tail-end IHCaL concept for decarbonizing a German lime plant. They calculated the energy performance for different fuels and various energy scenarios. The process performed better for scenarios corresponding to coal and nuclear power plants. For the scenario Energy mix (2015) EU-28 non-CHP, the SPECCA values were around 3 MJ/kg_{CO2} using lignite in the calciner, and approximately 2 MJ/kg_{CO2} with waste-derived fuels. With a fully integrated concept, even lower SPECCA were achieved (Greco-Coppi et al., 2024a). Additionally, waste-derived fuels enabled negative CO_2 emissions for every scenario (Greco-Coppi et al., 2023b). For lime plants, the *CAC* were lower than 25 $€_{2020}/t_{CO2,av}$ using solid recovered fuel to fire the calciner (Greco-Coppi et al., 2024c).

Rezvani et al. (2025) applied two IHCaL concepts into a cement plant for CO_2 capture. They reported $CAC = 38$ $€_{2020}/t_{CO2,av}$ for the tail-end concept, and $CAC = 30$ $€_{2020}/t_{CO2,av}$ for the integrated concept, in which the pre-calciner and the CaL are merged into a single component. In a similar study, Yin et al. (2024) reported $CAC = 59$ $A\$_{2023}/t_{CO2,av} \approx 34$ $€_{2023}/t_{CO2,av}$, for a cement plant retrofitted with a tail-end IHCaL process.

In general, the IHCaL process presents low *CAC* for both lime and cement applications, compared to other CO_2 capture technologies. The absolute investment costs are higher than for oxy-fired CaL in tail-end applications but are compensated for by the additional production of spent sorbent, which reduces the specific costs. Initial results indicate that the utilization of spent sorbent from IHCaL operation may be possible, but further experimental work is required to demonstrate this (Greco-Coppi et al., 2024b).

One important challenge to integrate CaL and IHCaL into lime and cement plants is the high CO_2 flow rate, which yields elevated fuel requirements (Greco-Coppi et al., 2021a). Additionally, CaL and IHCaL facilities have high CAPEX compared to other post-combustion technologies. Finally, the cost figures presented in the literature depend on energy prices, and the viability of the capture projects is contingent to high CO_2 taxes. Both variables have shown high volatility over the past decade, and it is difficult to predict their evolution over the next 20 years.

5.4. Steel production

Generally, steel is produced through three main routes: blast furnace–basic oxygen furnace (BF-BOF), scrap-based electric arc furnace (EAF), and direct reduced iron–electric arc furnace (DRI-EAF) (Perpiñán et al., 2023). The most common primary production route (from the reduction of iron ore) is the BF-BOF that accounts for 72% of global steel production and represents approximately 90% of the primary production. EAF has undergone a great development in the last decade accounting for 28% global crude steel production in 2019, including approximately 140 Mt crude steel produced by the DRI-EAF (IEA, 2020a).

Focusing on the most common production route, BF-BOF, there are multiple point sources of CO_2 along the steel plant with varied off-gases composition, where conventional post-combustion carbonate looping (CaL) process schemes have been proposed as an alternative for decarbonization. Cormos (2016) presented a technoeconomic analysis comparing the performance of CaL and chemical gas-liquid absorption (amines based) as post-combustion CO_2 capture technologies integrated in a steel-mill. Two alternatives were evaluated for the CaL system: the decarbonization of the gases from the host plant (that uses BF gas and BOF gas), and the decarbonization of the gases from the host plant together with the gases from the rest of the CO_2 sources in the steel-mill. The results indicated better performance for the CaL system in terms of lower specific CO_2 emissions—in kg of CO_2 per tonne of hot rolled coil (HRC)—and lower specific investment cost compared with amine-based technologies. Tian et al. (2018) proposed the integration of the spent material from the post-combustion CaL into the BF, further reducing the emissions associated with lime production.

The direct integration of CaL with the off gas from the blast furnace (BFG), has been recently proposed within the CASOH process (Fernández et al., 2020). The process has been designed to operate in packed bed reactors operating in parallel, where BFG and steam are introduced together during the main process stage (CASOH stage). During the CASOH stage, the sorption-enhanced WGS (SE-WGS) takes place, and a H_2/N_2 rich stream is produced while decarbonizing BFG. The process has been scaled-up to TRL 7 (see Section 3.2.3 for details) and operation strategies have been proposed to overcome the typical decay in activity of natural based CO_2 sorbents (Díaz et al., 2023).. The techno-economics of the process have been recently evaluated, and an enhanced version of the CASOH (CASOH-E), where low steam pressure is used in the system to calcine $CaCO_3$ while producing a highly concentrated CO_2 stream, was proposed (Khallaghi et al., 2025). This was the most favorable alternative in terms of SPECCA, compared with MDEA or conventional CASOH. If the hydrogen-rich stream produced in the CASOH-E is used to meet the energy demand of the regeneration stage, this results in lower specific emissions and better cold gas efficiency (29.8 $kgCO_2/GJ_{LHV}$ and 76% respectively).

Carbone et al. (2023) proposed alternative schemes based on interconnected fluidized bed reactors where the spent purge from the system was used to meet the CaO needs from the BF and/or BOF. In their study, a CaL scheme for the DRI-EAF route was also considered to capture CO_2 from both the reformer and the EAF furnace. However, this study did not address the additional challenge of capturing CO_2 from the fluctuating flue gas streams from the EAFs. In this regard, the use of solid storage has also been proposed for CO_2 capture. Configurations incorporating intermediate solids storage offer operational advantages, such as enhanced process stability. Under these conditions, specific fuel consumption as low as 5.85 MJ per kg of CO_2 captured has been reported, with capture efficiencies of around 91% for EAF off-gas (Montiel-Bohórquez et al., 2025).

5.5. Syngas, fuels, and chemicals production

Among HTSL technologies, chemical looping gasification (CLG) and chemical looping reforming (CLR) are specifically designed to partially oxidize a solid, liquid, or gaseous fuel, producing a high-quality and non-diluted syngas stream suitable for the production of synthetic fuels or chemicals. Downstream processing allows for the production of hydrogen by capturing CO_2. These processes may be intensified by taking advantage of the sorption-enhanced concept (SE-CLG or SE-CLR), producing separated concentrated hydrogen and nearly pure CO_2 streams. Carbonate looping (CaL) in this context usually refers either to CO_2 capture from syngas (Zhang et al., 2022) or to integrated SER/SEG schemes providing high-purity H_2 and a CO_2 stream.

Most TEA and LCA studies consider circulating fluidized-bed (CFB) systems. Fixed- and packed-bed CLR configurations have also been analyzed for decentralized or pressurized hydrogen production, especially at small scales where simpler solids handling is attractive (Bock et al., 2021). Early studies showed the potential of these technologies in reducing CO_2 emissions and H_2 costs from fossil fuels (Nazir et al., 2018), but recent studies mostly consider biogenic or waste materials. Table 6 shows the main KPIs achieved with different HTSL configurations to produce syngas or hydrogen. Although commercial deployment remains limited to pre-commercial demonstration projects, recent TEA studies conclude that CL-based hydrogen and BECCUS concepts can meet or undercut projected cost targets for low-carbon hydrogen when carbon prices exceed moderate thresholds. In general, the captured CO_2 should be considered as a valuable product in the BECCUS concept, highly relevant both for TEA (Cabello et al., 2024a) and LCA (Navajas et al., 2022). In addition, in CLG or CLR process a concentrated N_2 stream is also obtained, which may be also considered as a valuable product from a TEA perspective.

Recent work on techno-economic analysis (TEA) and life cycle assessment (LCA) for the HTSL processes for syngas production are showing competitive costs with strong integration potential with biofuels -mainly biomass- and downstream fuel or chemical synthesis or hydrogen generation after WGS and CO_2 separation. It has been highlighted the flexibility of these processes for the production of different synthetic fuels, as syngas H_2/CO ratios between 1–3 can be achieved.

Indirect gasification allows the generation of high-quality syngas from biomass which may be used to produce synthetic fuel or hydrogen. For example, syngas is suitable for the production of ethanol at a cost of 126 $/MWh (Dutta et al., 2014). If hydrogen is the desired product, a CO_2 separation step should be implemented to the syngas, although high CO_2 emissions are still generated as most CO_2 is produced in the combustor (Gubin et al., 2024). Hydrogen costs in the 4–7 €/kg interval have been reported.

CO_2 emissions are avoided in the chemical looping or carbonate looping concepts. The biomass-to-liquid (BtL) route utilizing CLG has shown promising results. Several EU projects have explored integration of CLG syngas with synthetic fuel production. For example, CLARA project intended the production of sustainable aviation fuel (SAF) via Fischer–Tropsch (FT) synthesis (Gogulancea et al., 2023). The full chain from biomass pretreatment to biofuel synthesis was demonstrated through 1 MW_{th} CLG, syngas cleaning, FT synthesis, and hydrocracking of FT wax, targeting low-carbon liquid biofuels. Specific production costs ranging between €120 and €140 per MWh for FT syncrude were estimated, but it could be as low as 60–80 per MWh if CO_2 credits are included. Major costs are related to capital, feedstock and O&M costs; however, the differential cost of the oxygen carrier has been identified of low relevance for low-cost or highly durable materials. The breakeven specific production (BESP) for FT crude using pine forest residues is €0.82 per liter, while wheat straw achieves €0.78 per liter (Kumar et al., 2022a). The ongoing Bio-MeGaFuel project (https://www.biomegafuelproject.eu/) is focused on the methanol production integrating CLG of bio-based fuels with a dedicated membrane reactor.

These processes have been also evaluated for low-carbon hydrogen production. Integration with carbon capture and renewable energy systems represents an important pathway for future development. CLR systems has been combined with fuel cells and gas turbines, achieving overall efficiencies and H_2 yields superior to conventional SMR-based systems with separate CO_2 capture. CLR in combination with CO_2 capture processes result in high H_2 yields of 70–90% and levelized hydrogen costs in optimized concepts in the range of about 4 $/kg, being about 2 $/kg when carbon pricing is considered, which is considerably lower than the levelized cost of electrolytic hydrogen (~5-10 $/kg). Also, TEA shows competitiveness of the CLR process, compared to other alternatives, improves when co-production of hydrogen, syngas and electricity is considered (Rai et al., 2022). Results forecast a levelized hydrogen

Table 6
Indicative performance ranges in recent TEA/LCA-oriented studies for syngas/H_2 production.

Process	Typical feed	Main solid (s)	Syngas/H_2 characteristics	Inherent CO_2 capture	Costs	References
Indirect gasification	Biomass	Olivine	Cold gas efficiency: 70-80% Syngas H_2/CO ≈1.5-3	-	Ethanol: 0.74 $\$_{2025}$/L (126 $\$_{2025}$/MWh) Hydrogen: 4-7 €/kg	Dutta et al. (2014), Gubin et al. (2024)
CLG	Biomass, wastes	Fe-based OC	Cold gas efficiency 70–80% Syngas H_2/CO ≈ 1–1.5	30-40% with downstream CO_2 separation Up to 90–95% if shift is included	SAF: 120-140 €/MWh (60-80 MWh with CO_2 credit)	Abad et al. (2026), Graf et al. (2024), Kumar et al. (2022b)
CLR	Natural gas, biogas	Ni, Fe, Cu-based OC	Syngas yield 70–85% H_2/CO from 1–3 depending on steam ratio	30-40% with downstream separation of CO_2 Up to 80–95% if shift is included	Hydrogen: 4 $/kg (2 $/kg with CO_2 credits) Electricity H_2 turbines: 75-140 $/MWh	Rai et al. (2022), Ramezani et al. (2023)
SER / SE-CLR	NG, biogas	Ni-based OC / CaO	80–90 vol% H_2; very low CO/CO_2	≳95% via in situ carbonation and calciner regeneration		Ramezani et al. (2023)
CaL-SEG	Biomass	CaO / $CaCO_3$	H_2-rich gas (up to ~70–80 vol %); H_2/CO_2 separation simplified	Near-complete CO_2 capture with appropriate sorbent makeup	Hydrogen: similar cost to electrolytic H_2 (decreased by 35% with CO_2 credit)	Luo et al. (2025), Kopsch et al. (2024)

costs around 3–4 $/kg, with co-product credits substantially improving overall project economics. CLR coupled with combined cycle power generation exhibits net electrical efficiency ranging between 40.0% and 43.4%, with levelized cost of electricity varying between $75.3 and $144.8/MWh depending on fuel costs and contingency rates (Nazir et al., 2018).

Carbonate looping has been demonstrated at the MW_{th} scale with extensive long-term campaigns that validated sorbent management strategies (Hilz et al., 2019; Arias et al., 2024). These results encouraged the development of detailed engineering for the future scale-up to multi-MW_{th} units, including operability studies of a 20-MW_{th} demo unit (Haaf et al., 2018). These studies provided detailed cost and risk data, being also relevant for the sorption-enhanced concepts when the carbonate looping is coupled to gasification and reforming processes. Thus, biomass-based SEG and SER concepts result in hydrogen production costs similar to those for alkaline water electrolysis (levelized to ~3 $/kg), which may be decreased by 35% with a revenue for negative CO_2 emissions of 60 $/t (Luo et al., 2025). In addition, heat storage or solar assistance can reduce overall energy consumption by leveraging high-temperature heat storage and achieve negative or near-zero net CO_2 emissions at hydrogen costs comparable to or slightly above fossil-based CLR (Aragón-García et al., 2025).

Systematic LCA work indicates that chemical looping hydrogen routes generally provide substantial GHG reductions compared with conventional SMR, especially when combined with biomass or biogenic waste feedstocks reaching 75% reductions in CO_2 emissions (Lee et al., 2025). A recent cradle-to-gate LCA for hydrogen production technologies highlighted chemical looping options result in markedly lower global warming impact per kg H_2 relative to SMR without capture (Osman et al., 2024). For biomass-to-H_2 via chemical looping (CLR/CLG) or calcium looping (SEG/SER), integrated TEA–LCA analyses find that carbon-negative operation is possible, with net removals on the order of several kg CO_2 per kg H_2 when biogenic carbon is fully captured and stored (Lundgren et al., 2025).

LCAs also emphasize that oxygen carrier and sorbent production typically contribute only a modest share of life cycle GHG emissions and costs when long solids lifetimes are achieved. Key environmental trade-offs include higher particulate emissions or metal leaching risks if solid wastes are poorly managed. Attrition, agglomeration, sintering, and loss of capacity over many redox or carbonation–calcination cycles increase makeup rates and costs. Solutions include development of mechanically robust, low-cost Fe- or Mn-based carriers, tailored supports and optimized CaO stabilization strategies (Cormos, 2024).

Summarizing, recent TEA and LCA studies position chemical looping as a strong candidate for low-carbon and negative-emission hydrogen and syngas production, particularly in niche applications such as biomass-to-liquids and integrated H_2/power cogeneration. Thermodynamic analyses suggest that pressurized operation (10–30 bar) could improve process economics by reducing compression requirements for downstream applications, though this introduces additional engineering challenges. For example, the hydrodynamics and reaction kinetics of CLR under pressure are not well-understood.

For its deployment at industrial scale, several knowledge gaps must be addressed to advance CLR and CLG to commercial demonstration (TRL >7) despite significant progress. Data from continuous pilot plants operating for >1000 hours is scarce. For CaL applied to hydrogen production, i.e., sorption-enhanced-based processes, demonstration at the MW_{th} scale, together with improved understanding of sorbent behavior, supports the technical feasibility of scaling to commercial plants, although long-term reliability data at industrial scale are still limited. Moreover, more studies are needed on the evolution of oxygen carrier properties (attrition, agglomeration, phase change) and reactor integrity over extended periods in chemical looping. Developing scalable and cheap synthesis routes for high-performance oxygen carriers is essential for economic viability. For the process intensification, mostly when integrated with syngas use, dedicated and scalable pressurized pilot units are required.

6. Conclusions and outlook

Numerous *high-temperature solid looping* (HTSL) processes have been developed and tested for various applications related to CO_2 capture, which include separation of CO_2 from flue gases or syngas, combustion with inherent CO_2 separation, and syngas generation with the potential for downstream CO_2 separation or conversion. This section summarizes the main conclusions for the individual processes and an outlook on potential further developments.

Carbonate looping (CaL) for post-combustion CO_2 capture from power generation has a high potential to reduce the efficiency penalty and CO_2 avoidance costs (*CAC*) compared to conventional scrubbing technologies. Oxyfuel-CaL was already demonstrated under industrially relevant conditions at the megawatt scale more than a decade ago. Recently, improvements in the CO_2 capture efficiency have been achieved by lowering the temperature and by adding $Ca(OH)_2$ at the exit of the carbonator. Concepts for improving the load flexibility of CaL by intermediate storage of the sorbent have been developed and tested. Indirectly heated CaL can further improve efficiency and was tested at pilot scale. However, the huge increase in production of renewable electricity from solar and wind as well as the plans for abandoning power generation from coal in many countries has reduced the interest in post-combustion CO_2 capture from power plants in the last ten years, which has so far hindered the further scale-up of the technology. Instead, the focus has shifted to hard-to-abate industrial flue gases, such as those from the lime and cement industry, steel production, and waste incineration. The *CAC* of CaL for cement and waste-to-energy (WtE) facilities are low compared to other capture processes. The lowest costs reported in the literature for CO_2 capture from WtE plants correspond to a novel integrated CaL process. Several CaL pilot tests have been conducted under the conditions of these industries. However, industrial demonstration of CaL is still pending. Although the knowledge and modeling tools for scale-up are at hand, the large investment costs for a commercial CaL plant with integrated power generation represent a hurdle for companies to invest in a first-of-its-kind plant.

Sorption-enhanced carbonate looping (SE-CaL) in a packed-bed configuration has undergone rapid development over the past decade, culminating in the construction of a 1-MW_{th} pilot plant. This facility has successfully demonstrated the feasibility of decarbonizing blast furnace gas (BFG) while simultaneously producing a hydrogen-rich gas stream. A key factor enabling the fast scale-up of the technology is the use of commercially available functional materials—natural limestone as the CaO precursor and a Cu-based material to supply the heat required for sorbent regeneration. Upcoming tests will focus on evaluating long-term performance and stability, an essential step toward further scale-up and industrial deployment. In parallel, new developments are exploring the use of pressure-swing calcination to enhance overall process efficiency. SE-CaL operated in interconnected fluidized bed reactors for the gasification of solid biogenic fuels has now reached a significant scale of 1 MW_{th}. The technology offers substantial flexibility in both product-gas composition and the range of acceptable feedstocks. However, a major challenge for large-scale deployment remains the handling of residual biomasses with high ash content, particularly those rich in alkali metals. These ash components can interfere with proper fluidization, leading to agglomeration and operational instability. This limitation is a common barrier across most thermochemical conversion technologies processing low-quality biogenic residues.

Chemical looping combustion (CLC) is a novel combustion technology with inherent CO_2 capture, which enables highly efficient power and heat generation at very low CO_2 avoidance costs. CLC of fossil fuels, such as natural gas and coal, was demonstrated around a decade ago at 1-MW_{th} scale. In the meantime, efforts have been made to improve fuel conversion and capture efficiency by novel reactor design or advanced oxygen carriers. However, low-cost oxygen carriers such as ores or

industrial wastes are still most favorable for CLC of solid fuels. Like other capture technologies, the focus of CLC has shifted from fossil fuels to biomass and wastes, which impose challenges related to high volatile release and ash impurities leading to agglomeration or fouling. Recently, the operation of a 5-MW_{th} pilot plant has proven the scalability and improved performance of CLC in an advanced reactor setup. As for CaL, industrial demonstration of CLC is still pending, so far hindered by the large investment costs for a commercial CLC plant with integrated power generation.

Significant progress has been made in the development of *chemical looping gasification* (CLG) over the last five years, involving extensive laboratory operations and autothermal pilot-scale demonstrations of biomass feedstocks at the megawatt scale. This builds on the development of process control schemes that decouple heat from oxygen transport. These schemes provide the necessary endothermic energy for gasification, while also limiting feedstock conversion and maintaining high cold gas efficiency. Other routes involving the supply of external heat via solar or microwave heating are an alternative in the early stages of development to solve this issue. Significant insight has been gained into tar formation and agglomeration, as well as into their dependency on feedstock and oxygen carriers. While woody biomass can be reliably processed, farming residues and waste materials pose a challenge in terms of agglomeration risk and process stability, issues that can be addressed by additives and feedstock pre-treatment. Oxygen carrier development has progressed in laboratory-scale units using low-cost waste materials that demonstrate better tar reduction than natural minerals, while autothermal pilot operation utilizes ilmenite, which is readily available commercially, as bed material.

Chemical looping reforming (CLR) has evolved as a multifunctional platform for highly efficient hydrogen and syngas production, drawing from diverse feedstocks. The conversion of natural gas was demonstrated at 140 kW_{th} scale using interconnected fluidized beds more than a decade ago. During the last years, researchers explored the change from fossil fuels to renewable and waste-derived feedstocks (e.g., biogas and bio-oils) to enable net-negative CO_2 emissions, and the change from fluidized to packed beds to benefit from pressurized operation. Also, the oxygen carriers have moved from Ni-based materials to more environmentally friendly materials such as Cu or Fe, or to special synthetic ones to avoid carbon formation in the process. The sorption-enhanced CLR variants offer a modular route to high-purity H_2 and syngas with intrinsic CO_2 separation potential. The field has progressed strongly in the last decade via improved perovskites, multifunctional OCs, and sorption-enhanced schemes — yet scale-up hurdles (OC durability, coking in long-term operation, manufacturing) must be resolved by targeted materials engineering, pilot testing, and system-level validation. Further research is needed on scale-up, long-term carrier stability, and retrofitting industrial systems. These represent key opportunities in closing knowledge gaps for accelerating commercialization of CLR technologies.

Indirect gasification, with thousands of hours of commercial operation, can be classified as TRL 8, with ongoing research and development efforts focusing on optimizing operation rather than basic phenomena and process parameters. Relevant developments that can easily be retrofitted to existing units include switching to cheaper, albeit more challenging, feedstocks such as residues and plastic waste, and enhanced process control. For newly erected plants, the development of enhanced reactor geometries is an option that will either reduce costs for smaller installations or significantly enhance process efficiency through improved gas-solid contact.

In general, HTSL processes involve relatively high investment costs compared to alternative or state-of-the-art technologies with higher CO_2 emissions. Therefore, larger-scale applications are particularly advantageous due to economies of scale. The minimum plant size required for economic viability depends on several factors, such as the type of application, project lifetime, and energy prices.

Overall, it can be concluded that HTSL processes offer significant potential in reducing energy requirements and costs in comparison with state-of-the-art technologies. The basic working principle of a dual fluidized bed has been proven at commercial scale, showing the potential for fast scale-up of the technology. So far, the commercial adoption has been hindered by the relatively high investment cost associated with HTSL plants integrating efficient power or syngas generation. A further hurdle is the lack of CO_2 infrastructure, which poses challenges related to logistics, particularly in remote locations far from the sea. Hence, regulatory measures are needed to promote investments in CO_2 capture facilities and the surrounding infrastructure.

Licensing and permissions for figures

The details of the CC licenses of the adapted and reproduced figures are available under https://creativecommons.org/licenses. We gratefully acknowledge the authors and editorials that granted us permission to adapt or reproduce figures in this review.

CRediT authorship contribution statement

Martin Greco-Coppi: Writing – original draft, Conceptualization. **Xiaoyun Li:** Writing – original draft. **Falko Marx:** Writing – original draft. **Borja Arias:** Writing – original draft. **Gemma Grasa:** Writing – original draft. **Alberto Abad:** Writing – original draft. **Francisco García-Labiano:** Writing – original draft. **Tobias Mattisson:** Writing – original draft. **Jochen Ströhle:** Writing – original draft, Conceptualization.

Declaration of competing interest

The authors declare that they have no known competing financial interests or personal relationships that could have appeared to influence the work reported in this paper.

Data availability

No data was used for the research described in the article.

References

Abad, A., Adánez, J., García-Labiano, F., Diego, L.F., Gayán, P., 2010. Modeling of the chemical-looping combustion of methane using a Cu-based oxygen-carrier. Combust. Flame 157 (3), 602–615. https://doi.org/10.1016/j.combustflame.2009.10.010.

Abad, A., Adánez, J., Diego, L.F., Gayán, P., García-Labiano, F., Lyngfelt, A., 2013. Fuel reactor model validation: assessment of the key parameters affecting the chemical-looping combustion of coal. Int. J. Greenhouse Gas Control 19, 541–551. https://doi.org/10.1016/j.ijggc.2013.10.020.

Abad, A., 2015. Chemical looping for hydrogen production. Calcium and Chemical Looping Technology for Power Generation and Carbon Dioxide. Elsevier, CO2) Capture, pp. 327–374.

Abad, A., García-Labiano, F., Gayán, P., Diego, L.F., Adánez, J., 2015a. Redox kinetics of CaMg0.1Ti0.125Mn0.775O2.9− for Chemical Looping Combustion (CLC) and Chemical Looping with Oxygen Uncoupling (CLOU). Chem. Eng. J. 269, 67–81. https://doi.org/10.1016/j.cej.2015.01.033.

Abad, A., Adánez, J., Gayán, P., Diego, L.F., García-Labiano, F., Sprachmann, G., 2015b. Conceptual design of a 100 MWth CLC unit for solid fuel combustion. Appl. Energy 157, 462–474. https://doi.org/10.1016/j.apenergy.2015.04.043.

Abad, A., Gayán, P., García-Labiano, F., Diego, L.F., Adánez, J., 2018. Relevance of plant design on CLC process performance using a Cu-based oxygen carrier. Fuel Process. Technol. 171, 78–88. https://doi.org/10.1016/j.fuproc.2017.09.015.

Abad, A., Gayán, P., Diego, L.F., García-Labiano, F., Adánez, J., 2019. Modelling Chemical-Looping assisted by Oxygen Uncoupling (CLaOU): assessment of natural gas combustion with calcium manganite as oxygen carrier. Proc. Combus. Inst. 37 (4), 4361–4369. https://doi.org/10.1016/j.proci.2018.09.037.

Abad, A., Gayán, P., Pérez-Vega, R., García-Labiano, F., Diego, L.F., Mendiara, T., et al., 2020. Evaluation of different strategies to improve the efficiency of coal conversion in a 50 kWth Chemical Looping combustion unit. Fuel 271, 117514. https://doi.org/10.1016/j.fuel.2020.117514.

Abad, A., Gayán, P., García-Labiano, F., Diego, L.F., Izquierdo, M.T., Mendiara, T., Adánez, J., 2023. Relevance of oxygen carrier properties on the design of a chemical looping combustion unit with gaseous fuels. Greenhouse Gases 13 (2), 125–143. https://doi.org/10.1002/ghg.2170.

Abad, A., Filsouf, A., Adánez-Rubio, I., Mendiara, T., Diego, L.F., Izquierdo, M.T., et al., 2024. Chemical looping with oxygen uncoupling of biomass and coal: scaling-up to

50 kWth using a copper-based oxygen carrier. Energy Fuels 38 (21), 21333–21344. https://doi.org/10.1021/acs.energyfuels.4c03173.
Abad, A., Diego, L.F., Izquierdo, M.T., Mendiara, T., García-Labiano, F., 2025a. Modeling chemical looping gasification with agroforestry residues: validation against results in a 20 kWth CLG unit. Ind. Eng. Chem. Res. 64 (38), 18576–18589. https://doi.org/10.1021/acs.iecr.5c01725.
Abad, A., Izquierdo, M.T., Mendiara, T., Diego, L.F., Pérez-Vega, R., García-Labiano, F., 2025b. Assessment of the potential of biomass chemical looping combustion with CO2 capture from experimental results at the 20 kWth scale with olive stone. Appl. Energy Combus. Sci. 23, 100346. https://doi.org/10.1016/j.jaecs.2025.100346.
Abad, A., Diego, L.F., las Obras Loscertales, M., García-Labiano, F., 2026. Designing a 200 MWth biomass chemical looping gasification unit for high-quality syngas production with high CO2 capture rates. Powder. Technol. 470, 121995. https://doi.org/10.1016/j.powtec.2025.121995.
Abanades, J.C, Alvarez, D., 2003. Conversion limits in the reaction of CO2 with lime. Energy Fuels 17 (2), 308–315. https://doi.org/10.1021/ef020152a.
Abanades, J.C., Grasa, G., 2024. Production of a syngas and CaO by desorption-enhanced reverse water–gas shift of CaCO3 with H2. Chem. Eng. J. 493, 152191. https://doi.org/10.1016/j.cej.2024.152191.
Abanades, J.C., Murillo, R. (2009): Method of capturing CO2 by means of CaO and the exothermic reduction of a solid. US8506915 B2.
Abanades, J.C, Anthony, E.J., Wang, J., Oakey, J.E, 2005. Fluidized bed combustion systems integrating CO2 capture with CaO. Environ. Sci. Technol. 39 (8), 2861–2866. https://doi.org/10.1021/es0496221.
Abanades, J.C, Arias, B., Lyngfelt, A., Mattisson, T., Wiley, D.E., Li, H., et al., 2015. Emerging CO2 capture systems. Int. J. Greenhouse Gas Control 40, 126–166. https://doi.org/10.1016/j.ijggc.2015.04.018.
Abanades, J.C, Criado, Y.A., García, R., 2023. Countercurrent moving bed carbonator for CO2 capture in decoupled calcium looping systems. Chem. Eng. J. 461, 141956. https://doi.org/10.1016/j.cej.2023.141956.
Abbas, S.Z., Dupont, V., Mahmud, T., 2017. Modelling of high purity H 2 production via sorption enhanced chemical looping steam reforming of methane in a packed bed reactor. Fuel 202, 271–286. https://doi.org/10.1016/j.fuel.2017.03.072.
Abbas, S.Z., Fernández, J.R, Amieiro, A., Rastogi, M., Brandt, J., Spallina, V., 2022. Lab-scale experimental demonstration of Ca Cu chemical looping for hydrogen production and in-situ CO2 capture from a steel-mill. Fuel Process. Technol. 237, 107475. https://doi.org/10.1016/j.fuproc.2022.107475.
Acampora, L., Grilletta, S., Costa, G., 2025. The integration of carbon capture, utilization, and storage (CCUS) in waste-to-energy plants: a review. Energies (Basel) 18 (8), 1883. https://doi.org/10.3390/en18081883.
Adanez, J., Abad, A., Garcia-Labiano, F., Gayan, P., Diego, L.F., 2012. Progress in chemical-looping combustion and reforming technologies. Prog. Energy Combust. Sci. 38 (2), 215–282. https://doi.org/10.1016/j.pecs.2011.09.001.
Adánez, J., Dueso, C., Diego, L.F., García-Labiano, F., Gayán, P., Abad, A., 2009. Methane combustion in a 500 W th chemical-looping combustion system using an impregnated Ni-based oxygen carrier. Energy Fuels. 23 (1), 130–142. https://doi.org/10.1021/ef8005146.
Adánez, J., Abad, A., Mendiara, T., Gayán, P., Diego, L.F., García-Labiano, F., 2018. Chemical looping combustion of solid fuels. Prog. Energy Combust. Sci. 65, 6–66. https://doi.org/10.1016/j.pecs.2017.07.005.
Adánez-Rubio, I., Abad, A., Gayán, P., Diego, L.F., García-Labiano, F., Adánez, J., 2012. Identification of operational regions in the Chemical-Looping with Oxygen Uncoupling (CLOU) process with a Cu-based oxygen carrier. Fuel 102, 634–645. https://doi.org/10.1016/j.fuel.2012.06.063.
Adánez-Rubio, I., Gayán, P., Abad, A., García-Labiano, F., Diego, L.F., Adánez, J., 2014. Kinetic analysis of a Cu-based oxygen carrier: relevance of temperature and oxygen partial pressure on reduction and oxidation reactions rates in Chemical Looping with Oxygen Uncoupling (CLOU). Chem. Eng. J. 256, 69–84. https://doi.org/10.1016/j.cej.2014.06.102.
Adánez-Rubio, I., Abad, A., Gayán, P., Adánez, I., Diego, L.F., García-Labiano, F., Adánez, J., 2016. Use of hopcalite-derived Cu–Mn mixed oxide as oxygen carrier for chemical looping with oxygen uncoupling process. Energy Fuels 30 (7), 5953–5963. https://doi.org/10.1021/acs.energyfuels.6b00552.
Adánez-Rubio, I., Ruiz, J.A.C., García-Labiano, F., Diego, L.F., Adánez, J., 2021. Use of bio-glycerol for the production of synthesis gas by chemical looping reforming. Fuel 288, 119578. https://doi.org/10.1016/j.fuel.2020.119578.
Adánez-Rubio, I., García-Labiano, F., Abad, A., Diego, L.F., Adánez, J., 2022. Synthesis gas and H2 production by chemical looping reforming using bio-oil from fast pyrolysis of wood as raw material. Chem. Eng. J. 431, 133376. https://doi.org/10.1016/j.cej.2021.133376.
Adánez-Rubio, I., Izquierdo, M.T., Brorsson, J., Mei, D., Mattisson, T., Adánez, J., 2024. Use of a high-entropy oxide as an oxygen carrier for chemical looping. Energy 298, 131307. https://doi.org/10.1016/j.energy.2024.131307.
Aghaalikhani, A., Schmid, J.C., Borello, D., Fuchs, J., Benedikt, F., Hofbauer, H., et al., 2019. Detailed modelling of biomass steam gasification in a dual fluidized bed gasifier with temperature variation. Renew. Energy 143, 703–718. https://doi.org/10.1016/j.renene.2019.05.022.
Agnew, J., Hampartsoumian, E., Jones, J.M., Nimmo, W., 2000. The simultaneous calcination and sintering of calcium based sorbents under a combustion atmosphere. Fuel 79 (12), 1515–1523. https://doi.org/10.1016/S0016-2361(99)00287-2.
Ahlström, J.M., Alamia, A., Larsson, A., Breitholtz, C., Harvey, S., Thunman, H., 2019. Bark as feedstock for dual fluidized bed gasifiers-operability, efficiency, and economics. Int. J. Energy Res. 43 (3), 1171–1190. https://doi.org/10.1002/er.4349.
Ahmad, F., Zhang, Y., Fu, W., Zhao, W., Xiong, Q.;, Li, B., 2024. Microwave-assisted chemical looping gasification of sugarcane bagasse biomass using Fe3O4 as oxygen carrier for H2/CO-rich syngas production. Chem. Eng. J. 501, 157675. https://doi.org/10.1016/j.cej.2024.157675.
Alamia, A., Thunman, H., Seemann, M., 2016. Process simulation of dual fluidized bed gasifiers using experimental data. Energy Fuels 30 (5), 4017–4033. https://doi.org/10.1021/acs.energyfuels.6b00122.
Alexandros Argyris, P., Leeuwe, C., Abbas, S.Z., Amieiro, A., Poultson, S., Wails, D., Spallina, V., 2022. Chemical looping reforming for syngas generation at real process conditions in packed bed reactors: an experimental demonstration. Chem. Eng. J. 435, 134883. https://doi.org/10.1016/j.cej.2022.134883.
Amorim, A., Filipe, R.M., Matos, H.A, 2025. Analysis of integrated calcium looping alternatives in a cement plant. Chem. Eng. Sci. 313, 121709. https://doi.org/10.1016/j.ces.2025.121709.
Andrés, M.-B., Boyd, T., Grace, J.R., Jim Lim, C., Gulamhusein, A., Wan, B., et al., 2011. In-situ CO2 capture in a pilot-scale fluidized-bed membrane reformer for ultra-pure hydrogen production. Int. J. Hydrogen. Energy 36 (6), 4038–4055. https://doi.org/10.1016/j.ijhydene.2010.09.091.
Antzara, A., Heracleous, E., Lemonidou, A.A, 2016. Energy efficient sorption enhanced-chemical looping methane reforming process for high-purity H2 production: experimental proof-of-concept. Appl. Energy 180, 457–471. https://doi.org/10.1016/j.apenergy.2016.08.005.
Antzaras, A.N., Lemonidou, A.A, 2022. Recent advances on materials and processes for intensified production of blue hydrogen. Renewable Sustainable Energy Rev. 155, 111917. https://doi.org/10.1016/j.rser.2021.111917.
Antzaras, A.N., Heracleous, E., Lemonidou, A.A, 2020. Sorption enhanced–chemical looping steam methane reforming: optimizing the thermal coupling of regeneration in a fixed bed reactor. Fuel Process. Technol. 208, 106513. https://doi.org/10.1016/j.fuproc.2020.106513.
Aragón-García, A., Villanueva Perales, A.L., González, W.A., Fuentes-Cano, D., Alonso-Fariñas, B., Gómez-Barea, A., 2025. Impact of solar thermal energy and calcium looping implementation on biomass gasification for low-carbon hydrogen production. Chem. Eng. J. 523, 168635. https://doi.org/10.1016/j.cej.2025.168635.
Arcenegui-Troya, J., Durán-Martín, J.D., Perejón, A., Valverde, J.M., Maqueda, P., Luis, A., Jiménez, S., Pedro, E., 2022. Overlooked pitfalls in CaO carbonation kinetics studies nearby equilibrium: instrumental effects on calculated kinetic rate constants. Alexandria Eng. J. 61 (8), 6129–6138. https://doi.org/10.1016/j.aej.2021.11.043.
Argyris, P.A, 2022. Chemical Looping Reforming in Packed Bed Reactors. Doctoral dissertation. University of Manchester.
Arias, B., Diego, M.E., Abanades, J.C, Lorenzo, M., Diaz, L., Martínez, D., et al., 2013. Demonstration of steady state CO2 capture in a 1.7MWth calcium looping pilot. Int. J. Greenhouse Gas Control 18, 237–245. https://doi.org/10.1016/j.ijggc.2013.07.014.
Arias, B., Diego, M.E., Méndez, A., Alonso, M., Abanades, J.C, 2018. Calcium looping performance under extreme oxy-fuel combustion conditions in the calciner. Fuel 222, 711–717. https://doi.org/10.1016/j.fuel.2018.02.163.
Arias, B., Criado, Y.A., Abanades, J.C, 2020. Thermal integration of a flexible calcium looping CO2 capture system in an existing back-up coal power plant. ACS Omega 5 (10), 4844–4852. https://doi.org/10.1021/acsomega.9b03552.
Arias, B., Yolanda, A.C, Méndez, A., Marqués, P., Finca, I., Abanades, J.C, 2024. Pilot testing of calcium looping at TRL7 with CO2 capture efficiencies toward 99. Energy Fuels 38 (15), 14757–14764. https://doi.org/10.1021/acs.energyfuels.4c02472.
Astolfi, M., Lena, E., Romano, M.C, 2019. Improved flexibility and economics of Calcium Looping power plants by thermochemical energy storage. Int. J. Greenhouse Gas Control 83, 140–155. https://doi.org/10.1016/j.ijggc.2019.01.023.
Atsonios, K., Grammelis, P., Antiohos, S.K., Nikolopoulos, N., Kakaras, E.m., 2015a. Integration of calcium looping technology in existing cement plant for CO 2 capture: process modeling and technical considerations. Fuel 153, 210–223. https://doi.org/10.1016/j.fuel.2015.02.084.
Atsonios, K., Zeneli, M., Nikolopoulos, A., Nikolopoulos, N., Grammelis, P., Kakaras, E., 2015b. Calcium looping process simulation based on an advanced thermodynamic model combined with CFD analysis. Fuel 153, 370–381. https://doi.org/10.1016/j.fuel.2015.03.014.
Bajamundi, C., Leino, T., Kauppinen, J., Louhola, O., Lappalainen, M., 2026. Production of high-concentration CO2 from electrified limestone calcination for carbon capture applications. Int. J. Greenhouse Gas Control 149, 104559. https://doi.org/10.1016/j.ijggc.2025.104559. Article.
Bartik, A., Benedikt, F., Fuchs, J., Hofbauer, H., Müller, S., 2024. Experimental investigation of hydrogen-intensified synthetic natural gas production via biomass gasification: a technical comparison of different production pathways. Biomass Conv. Bioref. 14 (18), 23091–23110. https://doi.org/10.1007/s13399-023-04341-3.
Bayham, S., Straub, D., Weber, J., 2019. Operation of a 50-kWth chemical looping combustion test facility under autothermal conditions. Int. J. Greenhouse Gas Control 87, 211–220. https://doi.org/10.1016/j.ijggc.2019.05.022.
Beirow, M., Parvez, A.M, Schmid, M., Scheffknecht, G., 2020. A detailed one-dimensional hydrodynamic and kinetic model for sorption enhanced gasification. Appl. Sci. 10 (17), 6136. https://doi.org/10.3390/app10176136.
Benedikt, F., Fuchs, J., Schmid, J.C, Müller, S., Hofbauer, H., 2017. Advanced dual fluidized bed steam gasification of wood and lignite with calcite as bed material. Korean J. Chem. Eng. 34 (9), 2548–2558. https://doi.org/10.1007/s11814-017-0141-y.
Benedikt, F., Schmid, J.C., Fuchs, J., Mauerhofer, A.M., Müller, S., Hofbauer, H., 2018. Fuel flexible gasification with an advanced 100 kW dual fluidized bed steam gasification pilot plant. Energy 164, 329–343. https://doi.org/10.1016/j.energy.2018.08.146.

Benedikt, F., Kuba, M., Schmid, J.C, Müller, S., Hofbauer, H., 2019. Assessment of correlations between tar and product gas composition in dual fluidized bed steam gasification for online tar prediction. Appl. Energy 238, 1138–1149. https://doi.org/10.1016/j.apenergy.2019.01.181.

Berdugo Vilches, T., Lind, F., Rydén, M., Thunman, H., 2017. Experience of more than 1000 h of operation with oxygen carriers and solid biomass at large scale. Appl. Energy 190, 1174–1183. https://doi.org/10.1016/j.apenergy.2017.01.032.

Berg, L., Anca-Couce, A., Hochenauer, C., Scharler, R., 2023. Multi-scale modelling of a fluidized bed biomass gasifier of industrial size (1 MW) using a detailed particle model coupled to CFD: proof of feasibility and advantages over simplified approaches. Energy Convers. Manage. 286, 117070. https://doi.org/10.1016/j.enconman.2023.117070.

Bergthorson, J.M., 2018. Recyclable metal fuels for clean and compact zero-carbon power. Prog. Energy Combust. Sci. 68, 169–196. https://doi.org/10.1016/j.pecs.2018.05.001.

Berguerand, N., Lyngfelt, A., 2008. Design and operation of a 10kWth chemical-looping combustor for solid fuels – testing with South African coal. Fuel 87 (12), 2713–2726. https://doi.org/10.1016/j.fuel.2008.03.008.

Bhatia, S.K., Perlmutter, D.D., 1983. Effect of the product layer on the kinetics of the CO2-lime reaction. aIChE J. 29 (1), 79–86. https://doi.org/10.1002/aic.690290111.

Bischi, A., Langørgen, Ø., Saanum, I., Bakken, J., Seljeskog, M., Bysveen, M., et al., 2011. Design study of a 150kWth double loop circulating fluidized bed reactor system for chemical looping combustion with focus on industrial applicability and pressurization. Int. J. Greenhouse Gas Control 5 (3), 467–474. https://doi.org/10.1016/j.ijggc.2010.09.005.

Bock, S., Stoppacher, B., Malli, K., Lammer, M., Hacker, V., 2021. Techno-economic analysis of fixed-bed chemical looping for decentralized, fuel-cell-grade hydrogen production coupled with a 3 MWth biogas digester. Energy Convers. Manage 250, 114801. https://doi.org/10.1016/j.enconman.2021.114801.

Bolhàr-Nordenkampf, J., 2009. Chemical looping for synthesis gas and power generation with CO2 capture - pilot plant study and process modeling. Doctoral dissertation. Technischen Universität Wien, Wien.

Brorsson, J., Rehnberg, V., Arvidsson, A.A., Leion, H., Mattisson, T., Hellman, A., 2023. Discovery of oxygen carriers by mining a first-principle database. J. Phys. Chem. C 127 (20), 9437–9451. https://doi.org/10.1021/acs.jpcc.2c08545.

Buelens, L.C., Galvita, V.V., Poelman, H., Detavernier, C., Marin, G.B., 2016. Super-dry reforming of methane intensifies CO2 utilization via Le Chatelier's principle. Science (New York, N.Y.) 354 (6311), 449–452. https://doi.org/10.1126/science.aah7161.

Buelens, L., van Cauwelaert, M., Poelman, H., Galvita, V., van Geem, K., 2024. Development, installation, and operation of a chemical looping pilot plant for super-dry reforming of methane (plenary lecture). In: Spring24+20th GCPS, 2024 AIChE Spring Meeting & 20th Global Congress on Process Safety, Abstracts. Available online at. https://aiche.confex.com/aiche/s24/meetingapp.cgi/Home/0.

Cabello, A., Gayán, P., García-Labiano, F., Diego, L.F., Abad, A., Adánez, J., 2016. On the attrition evaluation of oxygen carriers in chemical looping combustion. Fuel Process. Technol. 148, 188–197. https://doi.org/10.1016/j.fuproc.2016.03.004.

Cabello, A., Abad, A., Gayán, P., García-Labiano, F., Diego, L.F., Adánez, J., 2021. Increasing energy efficiency in chemical looping combustion of methane by in-situ activation of perovskite-based oxygen carriers. Appl. Energy 287, 116557. https://doi.org/10.1016/j.apenergy.2021.116557.

Cabello, A., Mendiara, T., Abad, A., Adánez, J., 2022a. Techno-economic analysis of a chemical looping combustion process for biogas generated from livestock farming and agro-industrial waste. Energy Convers. Manage 267, 115865. https://doi.org/10.1016/j.enconman.2022.115865.

Cabello, A., Mendiara, T., Abad, A., Izquierdo, M.T., García-Labiano, F., 2022b. Production of hydrogen by chemical looping reforming of methane and biogas using a reactive and durable Cu-based oxygen carrier. Fuel 322, 124250. https://doi.org/10.1016/j.fuel.2022.124250.

Cabello, A., Abad, A., Loscertales, O., de, M., Bartocci, P., García-Labiano, F., Diego, L.F., 2023a. Exploring design options for pressurized chemical looping combustion of natural gas. Fuel 342, 126983. https://doi.org/10.1016/j.fuel.2022.126983.

Cabello, A., Abad, A., Mendiara, T., Izquierdo, M.T., Diego, L.F., 2023b. Outstanding performance of a Cu-based oxygen carrier impregnated on alumina in chemical looping combustion. Chem. Eng. J. 455, 140484. https://doi.org/10.1016/j.cej.2022.140484.

Cabello, A., Mendiara, T.T., Izquierdo, M., García-Labiano, F., Abad, A., 2023c. Energy use of biogas through chemical looping technologies with low-cost oxygen carriers. Fuel 344, 128123. https://doi.org/10.1016/j.fuel.2023.128123.

Cabello, A., Abad, A., las Obras Loscertales, M., Domingos, Y., Mendiara, T., 2024a. Techno-economic analysis of chemical looping processes with biomass resources for energy production and CO2 utilization. Comparison of CLC and CLOU technologies. Energy Convers. Manage 310, 118476. https://doi.org/10.1016/j.enconman.2024.118476.

Cabello, A., Mendiara, T., Izquierdo, M.T, Diego, L., Abad, A., 2024b. Conversion of dry biogas in a chemical looping reforming unit: performance of Fe and FeMn-based oxygen carriers. Int. J. Hydrogen. Energy 76, 281–289. https://doi.org/10.1016/j.ijhydene.2024.05.074.

Carbone, C., Ferrario, D., Lanzini, A., Verda, V., Agostini, A., Stendardo, S., 2023. Calcium looping in the steel industry: GHG emissions and energy demand. Int. J. Greenhouse Gas Control 125, 103893. https://doi.org/10.1016/j.ijggc.2023.103893.

Chacartegui, R., Alovisio, A., Ortiz, C., Valverde, J.M., Verda, V., Becerra, J.A., 2016. Thermochemical energy storage of concentrated solar power by integration of the calcium looping process and a CO2 power cycle. Appl. Energy 173, 589–605. https://doi.org/10.1016/j.apenergy.2016.04.053.

Chacartegui, R., Gravanis, G., Carro, A., Ortiz, C., Pérez-Maqueda, L.A., Amghar, N., et al., 2025. Carbonation tests in a kW-scale entrained flow reactor for thermochemical energy storage using the calcium looping-based system. Chem. Eng. J. 524, 169801. https://doi.org/10.1016/j.cej.2025.169801.

Chang, W., Hu, Y., Xu, W., Huang, C., Chen, H., He, J., et al., 2023. Recent advances of oxygen carriers for hydrogen production via chemical looping water-splitting. Catalysts 13 (2), 279. https://doi.org/10.3390/catal13020279.

Charitos, A., Hawthorne, C., Bidwe, A.R., Sivalingam, S., Schuster, A., Spliethoff, H., Scheffknecht, G., 2010. Parametric investigation of the calcium looping process for CO2 capture in a 10kWth dual fluidized bed. Int. J. Greenhouse Gas Control 4 (5), 776–784. https://doi.org/10.1016/j.ijggc.2010.04.009.

Charitos, A., Rodríguez, N., Hawthorne, C., Alonso, M., Zieba, M., Arias, B., et al., 2011. Experimental validation of the calcium looping CO 2 capture process with two circulating fluidized bed carbonator reactors. Ind. Eng. Chem. Res. 50 (16), 9685–9695. https://doi.org/10.1021/ie200579f.

Chen, H.u, Cheng, M., Liu, L., Li, Y.e, Li, Z., Cai, N., 2020. Coal-fired chemical looping combustion coupled with a high-efficiency annular carbon stripper. Int. J. Greenhouse Gas Control 93, 102889. https://doi.org/10.1016/j.ijggc.2019.102889.

Chen, G.e, Shiyuan, L.i, Linwei, W., 2023. Current investigation status of oxy-fuel circulating fluidized bed combustion. Fuel 342, 127699. https://doi.org/10.1016/j.fuel.2023.127699.

Cho, P., Mattisson, T., Lyngfelt, A., 2004. Comparison of iron-, nickel-, copper- and manganese-based oxygen carriers for chemical-looping combustion. Fuel 83 (9), 1215–1225. https://doi.org/10.1016/j.fuel.2003.11.013.

Condori, O., Diego, L.F, Garcia-Labiano, F., Izquierdo, M.T, Abad, A., Adánez, J., 2021a. Syngas production in a 1.5 kWth biomass chemical looping gasification unit using Fe and Mn Ores as the oxygen carrier. Energy Fuels 35 (21), 17182–17196. https://doi.org/10.1021/acs.energyfuels.1c01878.

Condori, O., García-Labiano, F., Diego, L.F., Izquierdo, M.T., Abad, A., Adánez, J., 2021b. Biomass chemical looping gasification for syngas production using ilmenite as oxygen carrier in a 1.5 kWth unit. Chem. Eng. J. 405, 126679. https://doi.org/10.1016/j.cej.2020.126679.

Condori, O., García-Labiano, F., Diego, L.F., Izquierdo, M.T., Abad, A., Adánez, J., 2021c. Biomass chemical looping gasification for syngas production using LD Slag as oxygen carrier in a 1.5 kWth unit. Fuel Process. Technol. 222, 106963. https://doi.org/10.1016/j.fuproc.2021.106963.

Condori, O., Abad, A., Izquierdo, M.T., Diego, L.F., García-Labiano, F., Adánez, J., 2023. Assessment of the chemical looping gasification of wheat straw pellets at the 20 kWth scale. Fuel 344, 128059. https://doi.org/10.1016/j.fuel.2023.128059.

Condori, O., Abad, A., García-Labiano, F., Diego, L.F., Izquierdo, M.T., Adánez, J., 2024a. Parametric evaluation of clean syngas production from pine forest residue by chemical looping gasification at the 20 kWth scale. J. Clean. Prod. 436, 140434. https://doi.org/10.1016/j.jclepro.2023.140434.

Condori, O., Abad, A., Izquierdo, M.T., Diego, L.F., Funcia, I., Pérez-Vega, R., et al., 2024b. Effect of biomass torrefaction on the syngas quality produced by chemical looping gasification at 20 kWth scale. Energy Fuels. 38 (13), 11779–11792. https://doi.org/10.1021/acs.energyfuels.4c01096.

Greco Coppi, M.N., 2025. Modeling, assessment, and optimization of the indirectly heated carbonate looping process for CO_2 capture from lime plants. Doctoral dissertation. 1. Aufl. Darmstadt. Cuvillier Verlag, Germany. https://doi.org/10.61061/ISBN_9783689528454.

Greco-Coppi, M., Tschiedel, C., Roloff, N., Ströhle, J., Epple, B., 2026a. Post-combustion CO_2 capture in waste incineration plants. Universitäts- und Landesbibliothek Darmstadt. 3. Jahrestreffen der DECHEMA Fachsektion Energie, Chemie und Klima. Frankfurt am Main, Germany. https://doi.org/10.26083/tuda-7937. March 24–25, 2026.

Cormos, C.-C., Dragan, S., Cormos, A.-M., Petrescu, L., Dumbrava, I.-D., Sandu, V., 2021. Evaluation of calcium looping cycle as a time-flexible CO2 capture and thermo-chemical energy storage system. Chem. Eng. Trans. 88, 19–24. https://doi.org/10.3303/CET2188003.

Cormos, C.-C., 2016. Evaluation of reactive absorption and adsorption systems for post-combustion CO2 capture applied to iron and steel industry. Appl. Therm. Eng. 105, 56–64. https://doi.org/10.1016/j.applthermaleng.2016.05.149.

Cormos, C.C., 2020. Techno-economic implications of flexible operation for super-critical power plants equipped with calcium looping cycle as a thermo-chemical energy storage system. Fuel 280, 118293. https://doi.org/10.1016/j.fuel.2020.118293.

Cormos, C.-C., 2022. Decarbonization options for cement production process: a techno-economic and environmental evaluation. Fuel 320, 123907. https://doi.org/10.1016/j.fuel.2022.123907.

Cormos, C.-C., 2024. Decarbonized green hydrogen production by sorption-enhanced biomass gasification: an integrated techno-economic and environmental evaluation. Int. J. Hydrogen. Energy 95, 592–603. https://doi.org/10.1016/j.ijhydene.2024.11.281.

Criado, Y.A., Huille, A., Rougé, S., Abanades, J.C., 2017. Experimental investigation and model validation of a CaO/Ca(OH)2 fluidized bed reactor for thermochemical energy storage applications. Chem. Eng. J. 313, 1194–1205. https://doi.org/10.1016/j.cej.2016.11.010.

Criado, Y.A., Arias, B., Abanades, J.C, 2022. A flexible CO 2 capture system for backup power plants using Ca(OH) 2 /CaCO 3 solid storage. Sustainable Energy Fuels 7 (1), 122–130. https://doi.org/10.1039/d2se01195f.

Criado, Y.A., García, R., Abanades, J.C, 2024. Demonstration of CO2 capture with CaO and Ca(OH)2 in a countercurrent moving bed carbonator pilot. Chem. Eng. J. 494, 152945. https://doi.org/10.1016/j.cej.2024.152945.

Cuadrat, A., Abad, A., García-Labiano, F., Gayán, P., Diego, L.F., Adánez, J., 2011. The use of ilmenite as oxygen-carrier in a 500 Wth chemical-looping coal combustion

unit. Int. J. Greenhouse Gas Control 5 (6), 1630–1642. https://doi.org/10.1016/j.ijggc.2011.09.010.
Cui, P., Dziva, G., Song, T., Dhital, S., Wang, S., Zeng, L., 2025. Dual moving bed calcium looping process: optimizing CO2 capture efficiency and energy utilization. Carbon Capture Sci. Technol. 17, 100535. https://doi.org/10.1016/j.ccst.2025.100535. S.
Díaz, M., Alonso, M., Grasa, G., Fernández, J.R, 2023. The Ca-Cu looping process using natural CO2 sorbents in a packed bed: operation strategies to accommodate activity decay. Chem. Eng. Sci. 273, 118659. https://doi.org/10.1016/j.ces.2023.118659.
Díez-Martín, L., López, J.M., Fernández, J.R., Martínez, I., Grasa, G., Murillo, R., 2018. Complete Ca/Cu cycle for H2 production via CH4 sorption enhanced reforming in a Lab-Scale fixed bed reactor. Chem. Eng. J. 350, 1010–1021. https://doi.org/10.1016/j.cej.2018.06.049.
Daneshmand-Jahromi, S., Sedghkerdar, M.H, Mahinpey, N., 2023. A review of chemical looping combustion technology: Fundamentals, and development of natural, industrial waste, and synthetic oxygen carriers. Fuel 341, 127626. https://doi.org/10.1016/j.fuel.2023.127626.
Del Arnaiz Pozo, C., Cloete, S., Cloete, J.H, Jiménez Álvaro, Á, Amini, S., 2019. The potential of chemical looping combustion using the gas switching concept to eliminate the energy penalty of CO2 capture. Int. J. Greenhouse Gas Control 83, 265–281. https://doi.org/10.1016/j.ijggc.2019.01.018.
Del Arnaiz Pozo, C., Sánchez-Orgaz, S., Navarro-Calvo, A., Jiménez Álvaro, Á, Cloete, S., 2024. Integration of chemical looping combustion in the graz power cycle. Energies (Basel) 17 (10), 2334. https://doi.org/10.3390/en17102334.
Del Grosso, M., Sridharan, B., Tsekos, C., Klein, S., Jong, W., 2020. A modelling based study on the integration of 10 MWth indirect torrefied biomass gasification, methanol and power production. Biomass Bioenergy 136, 105529. https://doi.org/10.1016/j.biombioe.2020.105529.
Detchusananard, T., Ponpesh, P., Saebea, D., Authayanun, S., Arpornwichanop, A., 2017. Modeling and analysis of sorption enhanced chemical looping biomass gasification. Chem. Eng. Trans. 57, 103–108. https://doi.org/10.3303/CET1757018.
Di Carlo, A., Savuto, E., Foscolo, P.U, Papa, A.A, Tacconi, A., Del Zotto, L., et al., 2022. Preliminary results of biomass gasification obtained at pilot scale with an innovative 100 kWth dual bubbling fluidized bed gasifier. Energies (Basel) 15 (12), 4369. https://doi.org/10.3390/en15124369.
Di Giuliano, A., Malsegna, B., Lucantonio, S., Gallucci, K., 2023. Experimental assessments of pyrolytic and fluid-dynamic interactions between pretreated residual biomasses and fluidized beds made up of oxygen carriers for chemical looping gasification. Adv. Powder Technol. 34 (5), 104010. https://doi.org/10.1016/j.apt.2023.104010.
Diego, M.E., Arias, B., 2020. Impact of load changes on the carbonator reactor of a 1.7 MWth calcium looping pilot plant. Fuel Process. Technol. 200, 106307. https://doi.org/10.1016/j.fuproc.2019.106307. Article.
Diego, L.F., Ortiz, M., García-Labiano, F., Adánez, J., Abad, A., Gayán, P., 2009. Hydrogen production by chemical-looping reforming in a circulating fluidized bed reactor using Ni-based oxygen carriers. J. Power Sources 192 (1), 27–34. https://doi.org/10.1016/j.jpowsour.2008.11.038.
Diego, M.E., Arias, B., Méndez, A., Lorenzo, M., Díaz, L., Sánchez-Biezma, A., Abanades, J.C., 2016a. Experimental testing of a sorbent reactivation process in La Pereda 1.7 MWth calcium looping pilot plant. Int. J. Greenhouse Gas Control 50, 14–22. https://doi.org/10.1016/j.ijggc.2016.04.008.
Diego, M.E., Arias, B., Abanades, J.C, 2016b. Analysis of a double calcium loop process configuration for CO2 capture in cement plants. J. Clean. Prod. 117, 110–121. https://doi.org/10.1016/j.jclepro.2016.01.027.
Dieringer, P., Marx, F., Alobaid, F., Ströhle, J., Epple, B., 2020. Process control strategies in chemical looping gasification—a novel process for the production of biofuels allowing for net negative CO2 emissions. Appl. Sci. 10 (12), 4271. https://doi.org/10.3390/app10124271.
Dieringer, P., Marx, F., Lebendig, F., Müller, M., Di Giuliano, A., Gallucci, K., et al., 2023a. Fate of ilmenite as oxygen carrier during 1 MWth chemical looping gasification of biogenic residues. Appl. Energy Combus. Sci. 16, 100227. https://doi.org/10.1016/j.jaecs.2023.100227.
Dieringer, P., Marx, F., Michel, B., Ströhle, J., Epple, B., 2023b. Design and control concept of a 1 MWth chemical looping gasifier allowing for efficient autothermal syngas production. Int. J. Greenhouse Gas Control 127, 103929. https://doi.org/10.1016/j.ijggc.2023.103929.
Dieter, H., Bidwe, A.R., Varela-Duelli, G., Charitos, A., Hawthorne, C., Scheffknecht, G., 2014. Development of the calcium looping CO2 capture technology from lab to pilot scale at IFK, University of Stuttgart. Fuel 127, 23–37. https://doi.org/10.1016/j.fuel.2014.01.063.
Diglio, G., Bareschino, P., Mancusi, E., Pepe, F., 2018. Techno-economic evaluation of a small-scale power generation unit based on a chemical looping combustion process in fixed bed reactor network. Ind. Eng. Chem. Res. 57 (33), 11299–11311. https://doi.org/10.1021/acs.iecr.8b02378.
Donat, F., Kierzkowska, A., Müller, C.R, 2022. Chemical looping partial oxidation of methane: reducing carbon deposition through alloying. Energy Fuels. 36 (17), 9780–9784. https://doi.org/10.1021/acs.energyfuels.2c01345.
Duarte, R., Pablo, J., Kriechbaumer, D., Lachmann, B., Tescari, S., Fend, T., Roeb, M., Sattler, C., 2022. Solar calcium looping cycle for CO2 capturing in a cement plant. Definition of process parameters and reactors selection. Sol. Energy 238, 189–202. https://doi.org/10.1016/j.solener.2022.04.031.
Dutta, A., Hensley, J., Bain, R., Magrini, K., Tan, E.C.D., Apanel, G., et al., 2014. Technoeconomic analysis for the production of mixed alcohols via indirect gasification of biomass based on demonstration experiments. Ind. Eng. Chem. Res. 53 (30), 12149–12159. https://doi.org/10.1021/ie402045q.
Ekström, C., Schwendig, F., Biede, O., Franco, F., Haupt, G., Koeijer, G., et al., 2009. Techno-economic evaluations and benchmarking of pre-combustion CO2 capture and oxy-fuel processes developed in the European ENCAP project. Energy Procedia 1 (1), 4233–4240. https://doi.org/10.1016/j.egypro.2009.02.234.
Epple, B., Seeber, J., 2014. Verfahren und Einrichtung zur Abscheidung von CO2 aus Abgas. Veröffentlichungsnr.: EP 2299176 B1.
Epple, B.; Junk, M.; Ströhle, J.; Reitz, M.; Karl, J.; Höftberger, D. (2016): Carbon capture by means of indirectly heated carbonate looping process (CARINA). Final report. Luxembourg: Publications Office of the European Union (EUR, 27812). Available online at https://bookshop.europa.eu/en/carbon-capture-by-means-of-indirectly-heated-carbonate-looping-process-carina–pbKINA27812/.
Esence, T., Benoit, H., Poncin, D., Tessonneaud, M., Flamant, G., 2020a. A shallow cross-flow fluidized-bed solar reactor for continuous calcination processes. Sol. Energy 196, 389–398. https://doi.org/10.1016/j.solener.2019.12.029.
Esence, T., Guillot, E., Tessonneaud, M., Sans, J.-L.;, Flamant, G., 2020b. Solar calcination at pilot scale in a continuous flow multistage horizontal fluidized bed. Sol. Energy 207, 367–378. https://doi.org/10.1016/j.solener.2020.06.098.
Falascino, E., Joshi, R.K., Kumar, S., Jawdekar, T., Kudva, I.K., Shinde, S.G., et al., 2024. Enabling plastic waste gasification by autothermal chemical looping with >90 % syngas purity for versatile feedstock handling. Appl. Energy Combus. Sci. 19, 100270. https://doi.org/10.1016/j.jaecs.2024.100270.
Fan, L.-S.;, Li, F., 2010. Chemical looping technology and its fossil energy conversion applications. Ind. Eng. Chem. Res. 49 (21), 10200–10211. https://doi.org/10.1021/ie1005542.
Fan, L.-S.; Gupta, H.; Iyer, M. (2012): Separation of carbon dioxide from gas mixtures by calcium based reaction separation.
Fan, Y., Siriwardane, R., Tian, H., 2015. Trimetallic oxygen carriers CuFeMnO 4, CuFeMn 2 O 4, and CuFe 0.5 Mn 1.5 O 4 for chemical looping combustion. Energy Fuels 29 (10), 6616–6624. https://doi.org/10.1021/acs.energyfuels.5b01388.
Fan, L.-S., 2010. Chemical Looping Systems for Fossil Energy Conversions. Wiley.
Fantini, M., Balocco, M., Buzzi, L., Canonico, F., Consonni, S., Cremona, R., et al., 2021. Calcium looping technology demonstration in industrial environment: status of the cleanker pilot plant. SSRN Journal. https://doi.org/10.2139/ssrn.3817346.
Farooqi, A.S, Allam, A.N., Shahid, M.Z, Aqil, A., Fajri, K., Park, S., et al., 2025. Advancements in sorption-enhanced steam reforming for clean hydrogen production: a comprehensive review. Carbon Capture Sci. Technol. 14, 100336. https://doi.org/10.1016/j.ccst.2024.100336.
Fedunik-Hofman, L., Bayon, A., Donne, S.W., 2019. Kinetics of solid-gas reactions and their application to carbonate looping systems. Energies (Basel) 12 (15), 2981. https://doi.org/10.3390/en12152981. Article.
Fernández, J.R., Abanades, J.C., 2017. Optimized design and operation strategy of a Ca Cu chemical looping process for hydrogen production. Chem. Eng. Sci. 166, 144–160. https://doi.org/10.1016/j.ces.2017.03.039.
Fernández, J.R., Alarcón, J.M., 2015. Chemical looping combustion process in fixed-bed reactors using ilmenite as oxygen carrier: conceptual design and operation strategy. Chem. Eng. J. 264, 797–806. https://doi.org/10.1016/j.cej.2014.12.022.
Fernández, J.R., Abanades, J.C., Murillo, R., Grasa, G., 2012. Conceptual design of a hydrogen production process from natural gas with CO2 capture using a Ca–Cu chemical loop. Int. J. Greenhouse Gas Control 6, 126–141. https://doi.org/10.1016/j.ijggc.2011.11.014.
Fernández, J.R, Spallina, V., Abanades, J.C, 2020. Advanced packed-bed Ca-Cu looping process for the CO2 capture from steel mill off-gases. Front. Energy Res. 8, 146. https://doi.org/10.3389/fenrg.2020.00146. Article.
Fernández, J.R, Alonso, M., Mendez, A., Diaz, M., Garcia, R., Cano, M., et al., 2025. Decarbonization of blast furnace gases using a packed bed of Ca-Cu solids in a new TRL7 pilot. Energies (Basel) 18 (3), 675. https://doi.org/10.3390/en18030675.
Fernandez, J.R., Abanades, J.C., Murillo, R., 2012. Modeling of sorption enhanced steam methane reforming in an adiabatic fixed bed reactor. Chem. Eng. Sci. 84, 1–11. https://doi.org/10.1016/j.ces.2012.07.039.
Fernandez, J.R, Turrado, S., Abanades, J.C, 2019. Calcination kinetics of cement raw meals under various CO 2 concentrations. React. Chem. Eng. 4 (12), 2129–2140. https://doi.org/10.1039/C9RE00361D.
Ferrario, D., Stendardo, S., Verda, V., Lanzini, A., 2023. Solar-driven calcium looping system for carbon capture in cement plants: process modelling and energy analysis. J. Clean. Prod. 394, 136367. https://doi.org/10.1016/j.jclepro.2023.136367.
Filsouf, A., Mendiara, T., Adánez-Rubio, I., Izquierdo, M.T., Adánez, J., Gayán, P., Abad, A., 2026. Physicochemical evolution of a Cu/Mn/Fe oxygen carrier in a 50 kWth chemical looping with oxygen uncoupling unit with solid fuels. Fuel 406, 137162. https://doi.org/10.1016/j.fuel.2025.137162.
Fleiß, B., Penthor, S., Müller, S., Hofbauer, H., Fuchs, J., 2022. Holistic assessment of oxygen carriers for chemical looping combustion based on laboratory experiments and validation in 80 kW pilot plant. Fuel Process. Technol. 231, 107249. https://doi.org/10.1016/j.fuproc.2022.107249.
Fleiß, B., Bartik, A., Priscak, J., Benedikt, F., Fuchs, J., Müller, S., Hofbauer, H., 2024. Experimental demonstration of 80 kWth chemical looping combustion of biogenic feedstock coupled with direct CO2 utilization by exhaust gas methanation. Biomass Conv. Bioref. 14 (17), 20973–20990. https://doi.org/10.1007/s13399-023-04311-9.
Fu, C., Roussanaly, S., Jordal, K., Anantharaman, R., 2021. Techno-economic analyses of the CaO/CaCO3 post-combustion CO2 capture from NGCC power plants. Front. Chem. Eng. 2. https://doi.org/10.3389/fceng.2020.596417.
Fu, W., Zhang, Y., Cao, W., Zhao, W., Li, B., 2024. Microwave-assisted chemical looping gasification of plastics for H2-rich gas production. Chem. Eng. J. 499, 156225. https://doi.org/10.1016/j.cej.2024.156225.
Fuchs, J., Schmid, J.C., Müller, S., Mauerhofer, A.M., Benedikt, F., Hofbauer, H., 2020. The impact of gasification temperature on the process characteristics of sorption enhanced reforming of biomass. Biomass Conv. Bioref. 10 (4), 925–936. https://doi.org/10.1007/s13399-019-00439-9.

Fürsatz, K., Fuchs, J., Benedikt, F., Kuba, M., Hofbauer, H., 2021. Effect of biomass fuel ash and bed material on the product gas composition in DFB steam gasification. Energy 219, 119650. https://doi.org/10.1016/j.energy.2020.119650.

Gómez-Barea, A., Suárez-Almeida, M., Ghoniem, A., 2021. Analysis of fluidized bed gasification of biomass assisted by solar-heated particles. Biomass Conv. Bioref. 11 (1), 143–158. https://doi.org/10.1007/s13399-020-00865-0.

Galinsky, N., Sendi, M., Bowers, L., Li, F., 2016. CaMn1−B O3− (B = Al, V, Fe, Co, and Ni) perovskite based oxygen carriers for chemical looping with oxygen uncoupling (CLOU). Appl. Energy 174, 80–87. https://doi.org/10.1016/j.apenergy.2016.04.046.

Gallucci, F., van Sint Annaland, M., Kuipers, J.A.M., 2008. Autothermal reforming of methane with integrated CO2 capture in a novel fluidized bed membrane reactor. Part 1: experimental demonstration. Top. Catal. 51 (1-4), 133–145. https://doi.org/10.1007/s11244-008-9126-8.

Gao, L., He, S., Zheng, Y., Wang, J., Zeng, X., 2025. Decarbonizing and transforming coal-fired power plants into hybrid cycle systems using CaL-CLC process: a comprehensive techno-economic-environmental evaluation. J. Environ. Chem. Eng. 13, 119867. https://doi.org/10.1016/j.jece.2025.119867. S.

García-Díez, E., García-Labiano, F., Diego, L.F., Abad, A., Gayán, P., Adánez, J., Ruíz, J.A. C., 2017. Steam, dry, and steam-dry chemical looping reforming of diesel fuel in a 1 kWth unit. Chem. Eng. J. 325, 369–377. https://doi.org/10.1016/j.cej.2017.05.042.

García-Domínguez, A.O., Cabello, A., García-Labiano, F., Izquierdo, M.T., Diego, L.F., 2025. Agglomeration tendency and CO production capacity of Fe-based oxygen carriers for the chemical looping CO 2 splitting process. Energy Fuels 39 (36), 17410–17422. https://doi.org/10.1021/acs.energyfuels.5c02881.

García-Labiano, F., Diego, L.F., Adánez, J., Abad, A., Gayán, P., 2004. Reduction and oxidation kinetics of a copper-based oxygen carrier prepared by impregnation for chemical-looping combustion. Ind. Eng. Chem. Res. 43 (26), 8168–8177. https://doi.org/10.1021/ie0493311.

García-Labiano, F., García-Díez, E., Diego, L.F., Serrano, A., Abad, A., Gayán, P., et al., 2015. Syngas/H2 production from bioethanol in a continuous chemical-looping reforming prototype. Fuel Process. Technol. 137, 24–30. https://doi.org/10.1016/j.fuproc.2015.03.022.

García-Labiano, F., Abad, A., Diego, L.F., Gayán, P., Adánez, J., 2002. Calcination of calcium-based sorbents at pressure in a broad range of CO2 concentrations. Chem. Eng. Sci. 57, 2381–2393. https://doi.org/10.1016/S0009-2509(02)00137-9.

Gardarsdottir, S.O, Lena, E., Romano, M., Roussanaly, S., Voldsund, M., Pérez-Calvo, J.-F., et al., 2019. Comparison of technologies for CO2 capture from cement production—part 2: cost analysis. Energies (Basel) 12 (3), 542. https://doi.org/10.3390/en12030542.

Gastaldi, J., Brorsson, J., Staničić, I., Hellman, A., Mattisson, T., 2025. First-principles estimation of thermodynamic properties and phase stability of CaMnO 3−δ for chemical-looping combustion. Energy Fuels 39 (19), 9113–9120. https://doi.org/10.1021/acs.energyfuels.5c00267.

Gayán, P., Abad, A., Diego, L.F., García-Labiano, F., Adánez, J., 2013. Assessment of technological solutions for improving chemical looping combustion of solid fuels with CO2 capture. Chem. Eng. J. 233, 56–69. https://doi.org/10.1016/j.cej.2013.08.004.

Ge, H., Guo, W., Shen, L., Song, T., Xiao, J., 2016a. Biomass gasification using chemical looping in a 25 kWth reactor with natural hematite as oxygen carrier. Chem. Eng. J. 286, 174–183. https://doi.org/10.1016/j.cej.2015.10.092.

Ge, H., Guo, W., Shen, L., Song, T., Xiao, J., 2016b. Experimental investigation on biomass gasification using chemical looping in a batch reactor and a continuous dual reactor. Chem. Eng. J. 286, 689–700. https://doi.org/10.1016/j.cej.2015.11.008.

Giammaria, G., Lefferts, L., 2020. Synergy between dielectric barrier discharge plasma and calcium oxide for reverse water gas shift. Chem. Eng. J. 392, 123806. https://doi.org/10.1016/j.cej.2019.123806.

Goel, A., Ismailov, A., Moghaddam, E.M., He, C., Konttinen, J., 2023. Evaluation of low-cost oxygen carriers for biomass chemical looping gasification. Chem. Eng. J. 469, 143948. https://doi.org/10.1016/j.cej.2023.143948.

Gogolev, I., Linderholm, C., Gall, D., Schmitz, M., Mattisson, T., Pettersson, J.B.C., Lyngfelt, A., 2019. Chemical-looping combustion in a 100 kW unit using a mixture of synthetic and natural oxygen carriers – operational results and fate of biomass fuel alkali. Int. J. Greenhouse Gas Control 88, 371–382. https://doi.org/10.1016/j.ijggc.2019.06.020.

Gogolev, I., Pikkarainen, T., Kauppinen, J., Linderholm, C., Steenari, B.-M., Lyngfelt, A., 2021a. Investigation of biomass alkali release in a dual circulating fluidized bed chemical looping combustion system. Fuel 297, 120743. https://doi.org/10.1016/j.fuel.2021.120743.

Gogolev, I., Soleimanisalim, A.H., Linderholm, C., Lyngfelt, A., 2021b. Commissioning, performance benchmarking, and investigation of alkali emissions in a 10 kWth solid fuel chemical looping combustion pilot. Fuel 287, 119530. https://doi.org/10.1016/j.fuel.2020.119530.

Gogolev, I., Pikkarainen, T., Kauppinen, J., Hurskainen, M., Lyngfelt, A., 2022. Alkali emissions characterization in chemical looping combustion of wood, wood char, and straw fuels. Fuel Process. Technol. 237, 107447. https://doi.org/10.1016/j.fuproc.2022.107447.

Gogulancea, V., Rolfe, A., Jaffar, M., Brandoni, C., Atsonios, K., Detsios, N., et al., 2023. Technoeconomic and environmental assessment of biomass chemical looping gasification for advanced biofuel production. Int. J. Energy Res. 2023 2023, 1–17. https://doi.org/10.1155/2023/6101270. S.

González-Torrijo, J., Loscertales, O., de, M., Mendiara, T., Alberto, A., 2025. Diseño y optimización de un sistema de reformado mejorado de CH4 con procesos chemical looping (SE-CLR). XVII Reunión del GEC. Zaragoza, 19-22 octubre 2025.

Graf, C., Coors, F., Marx, F., Dieringer, P., Zeneli, M., Stamatopoulos, P., et al., 2024. Development of a CFD-DEM Model for a 1 MWth chemical looping gasification pilot plant using biogenic residues as feedstock. Energy Fuels 38 (19), 18660–18673. https://doi.org/10.1021/acs.energyfuels.4c02571.

Graf, C., Lichtmannegger, Y., Ströhle, J., Epple, B., 2026. Scale-up of CFD-DEM simulation of chemical looping gasification by GPU acceleration. Particuology 112, 62–73. https://doi.org/10.1016/j.partic.2026.02.020.

Grasa, G.S., Abanades, J.C, 2006. CO2 capture capacity of CaO in long series of carbonation/calcination cycles. Ind. Eng. Chem. Res. 45 (26), 8846–8851. https://doi.org/10.1021/ie0606946.

Grasa, G.S., Abanades, J.C, 2007. Narrow fluidised beds arranged to exchange heat between a combustion chamber and a CO2 sorbent regenerator. Chem. Eng. Sci. 62 (1-2), 619–626. https://doi.org/10.1016/j.ces.2006.09.026.

Grasa, G.S., Abanades, J.C, Alonso, M., González, B., 2008. Reactivity of highly cycled particles of CaO in a carbonation/calcination loop. Chem. Eng. J. 137 (3), 561–567. https://doi.org/10.1016/j.cej.2007.05.017.

Grasa, G., Murillo, R., Alonso, M., Abanades, J.C, 2009. Application of the random pore model to the carbonation cyclic reaction. AIChE J. 55 (5), 1246–1255. https://doi.org/10.1002/aic.11746.

Grasa, G., Díaz, M., Fernández, J.R., Amieiro, A., Brandt, J., Abanades, J.C., 2023. Blast furnace gas decarbonisation through calcium assisted steel-mill off-gas hydrogen production. Experimental and modelling approach. Chem. Eng. Res. Des. 191, 507–522. https://doi.org/10.1016/j.cherd.2023.01.047.

Greco-Coppi, M., Hofmann, C., Ströhle, J., Walter, D., Epple, B., 2021a. Efficient CO2 capture from lime production by an indirectly heated carbonate looping process. Int. J. Greenhouse Gas Control 112, 103430. https://doi.org/10.1016/j.ijggc.2021.103430. Article.

Greco-Coppi, M., Hofmann, C., Ströhle, J., Walter, D., Epple, B., 2021b. Efficient CO2 capture from lime production by an indirectly heated carbonate looping process. In: Proceedings of the 15th International Conference on Greenhouse Gas Control Technologies (GHGT-15). Abu Dhabi, UAE, 15th-18th March 2021.

Greco-Coppi, M., Hofmann, C., Ströhle, J., Epple, B., 2023a. Vorrichtung und Verfahren zum Herstellen von Kalk (patent pending). Deutsches Patent- und Markenamt. https://doi.org/10.5281/zenodo.19135527. Veröffentlichungsnr.: no. 10 2023 114 354.9.

Greco-Coppi, M., Hofmann, C., Walter, D., Ströhle, J., Epple, B., 2023b. Negative CO2 emissions in the lime production using an indirectly heated carbonate looping process. Mitig. Adapt. Strateg. Glob. Change 28 (6). https://doi.org/10.1007/s11027-023-10064-7.

Greco-Coppi, M., Eisenbach, N., Kurkunc, M.-D.;, Sattler, M., Roloff, N., Ströhle, J., Epple, B., 2024a. Carbon-neutral polygeneration in waste-to-energy plants: techno-economic study using carbon capture and utilization. In: Proceedings of the 17th International Conference on Greenhouse Gas Control Technologies. https://dx.doi.org/10.2139/ssrn.5069382, 20–24 Oct.

Greco-Coppi, M.; Hofmann, C.; Ströhle, J. (2024b): Advanced indirectly heated carbonate looping process (ANICA) – Final report: accelerating CCS Technologies (ACT). https://doi.org/10.26083/tuprints-00026729.

Greco-Coppi, M., Seufert, P.M, Hofmann, C., Rolfe, A., Huang, Y.e, Rezvani, S., et al., 2024c. Efficient CO2 capture from lime plants: techno-economic assessment of integrated concepts using indirectly heated carbonate looping technology. Carbon Capture Sci. Technol. 11, 100187. https://doi.org/10.1016/j.ccst.2023.100187. Article.

Greco-Coppi, M., Ströhle, J., Epple, B., 2024d. A carbonator model for CO2 capture based on results from pilot tests. Part I: hydrodynamics and reactor model. Chem. Eng. J. 500, 155119. https://doi.org/10.1016/j.cej.2024.155119. Article.

Greco-Coppi, M., Ströhle, J., Epple, B., 2025a. A carbonator model for CO2 capture based on results from pilot tests. Part II: deactivation and reaction model. Chem. Eng. J. 508, 159041. https://doi.org/10.1016/j.cej.2024.159041. Article.

Greco-Coppi, M., Ströhle, J., Epple, B., 2025b. Modeling and design of a calciner for commercial-scale CO2 capture using stochastic methods and results from pilot tests. Fuel 388, 133931. https://doi.org/10.1016/j.fuel.2024.133931. Article.

Greco-Coppi, M., Eisenbach, N., Kurkunc, M.-D.;, Sattler, M., Roloff, N., Ströhle, J., Epple, B., 2026b. Techno-economic assessment of carbonate looping for cost-effective CO2 capture in waste incineration. Int. J. Greenhouse Gas Control 149, 104558. https://doi.org/10.1016/j.ijggc.2025.104558. Article.

Gubin, V., Benedikt, F., Thelen, F., Hammerschmid, M., Popov, T., Hofbauer, H., Müller, S., 2024. Hydrogen production from woody biomass gasification: a techno-economic analysis. Biofuels Bioprod. Bioref. 18 (4), 818–836. https://doi.org/10.1002/bbb.2647.

Güleç, F., Okolie, J.A., 2025. Chemical looping combustion of low-volatile semi-anthracite coal with Co-based metal oxide: performances, kinetics, and mechanisms. J. Energy Inst. 119, 101993. https://doi.org/10.1016/j.joei.2025.101993.

Höftberger, D., Karl, J., 2013. Self-fluidization in an indirectly heated calciner. Chem. Eng. Technol. 36 (9), 1533–1538. https://doi.org/10.1002/ceat.201300111.

Höftberger, D., Karl, J., 2016. The indirectly heated carbonate looping process for CO2 capture—a concept with heat pipe heat exchanger. J. Energy Resour. Technol. 138 (4), 042211. https://doi.org/10.1115/1.4033302. Article.

Höftberger, D., 2016. Design und Dimensionierung eines indirekt beheizten Carbonate Looping Prozesses. Doctoral dissertation. Friedrich-Alexander-Universitaet Erlangen-Nuernberg, Nuremberg.

Haaf, M., Hilz, J., Helbig, M., Weingärtner, C., Stallmann, O., Ströhle, J., Epple, B., 2018. Assessment of the operability of a 20 MWth calcium looping demonstration plant by advanced process modelling. Int. J. Greenhouse Gas Control 75, 224–234. https://doi.org/10.1016/j.ijggc.2018.05.014.

Haaf, M., Anantharaman, R., Roussanaly, S., Ströhle, J., Epple, B., 2020a. CO2 capture from waste-to-energy plants: Techno-economic assessment of novel integration concepts of calcium looping technology. Resour. Conserv. Recycl. 162, 104973. https://doi.org/10.1016/j.resconrec.2020.104973.

Haaf, M., Hilz, J., Peters, J., Unger, A., Ströhle, J., Epple, B., 2020b. Operation of a 1 MWth calcium looping pilot plant firing waste-derived fuels in the calciner. Powder Technol. 372, 267–274. https://doi.org/10.1016/j.powtec.2020.05.074.

Haaf, M., Ohlemüller, P., Ströhle, J., Epple, B., 2020c. Techno-economic assessment of alternative fuels in second-generation carbon capture and storage processes. Mitig. Adapt. Strateg. Glob. Change 25 (2), 149–164. https://doi.org/10.1007/s11027-019-09850-z.

Haaf, M., Peters, J., Hilz, J., Unger, A., Ströhle, J., Epple, B., 2020d. Combustion of solid recovered fuels within the calcium looping process – experimental demonstration at 1 MWth scale. Exp. Therm. Fluid. Sci. 113, 110023. https://doi.org/10.1016/j.expthermflusci.2019.110023.

Hafner, S., Schmid, M., Scheffknecht, G., 2021. Parametric study on the adjustability of the syngas composition by sorption-enhanced gasification in a dual-fluidized bed pilot plant. Energies (Basel) 14 (2), 399. https://doi.org/10.3390/en14020399.

Han, R., Wang, Y., Xing, S., Pang, C., Hao, Y., Song, C., Liu, Q., 2022. Progress in reducing calcination reaction temperature of Calcium-Looping CO2 capture technology: a critical review. Chem. Eng. J. 450, 137952. https://doi.org/10.1016/j.cej.2022.137952.

Han, Z., Guo, T., Liu, Y., Lu, Y., Ma, J., Hu, X., Guo, Q., 2025. Unraveling the role of CaO and MgO as supports in the vanadium-based nitrogen carrier for chemical looping ammonia production. Chem. Eng. J. 525, 170579. https://doi.org/10.1016/j.cej.2025.170579.

Hanak, D.P., Biliyok, C., Manovic, V., 2016. Calcium looping with inherent energy storage for decarbonisation of coal-fired power plant. Energy Environ. Sci. 9 (3), 971–983. https://doi.org/10.1039/c5ee02950c.

Hanak, D.P., Erans, M., Nabavi, S.A., Jeremias, M., Romeo, L.M., Manovic, V., 2018. Technical and economic feasibility evaluation of calcium looping with no CO2 recirculation. Chem. Eng. J. 335, 763–773. https://doi.org/10.1016/j.cej.2017.11.022.

Hanak, D.P., 2024. Transforming carbon-intensive coal-fired power plants into negative emission technologies via biomass-fired calcium looping retrofit. Clean Energy 8 (6), 263–282. https://doi.org/10.1093/ce/zkae089.

Hanchate, N., Ramani, S., Mathpati, C.S., Dalvi, V.H, 2021. Biomass gasification using dual fluidized bed gasification systems: a review. J. Clean. Prod. 280, 123148. https://doi.org/10.1016/j.jclepro.2020.123148.

Haus, J., Lindmüller, L., Dymala, T., Jarolin, K., Feng, Y.i, Hartge, E.-U., et al., 2020. Increasing the efficiency of chemical looping combustion of biomass by a dual-stage fuel reactor design to reduce carbon capture costs. Mitig Adapt Strateg. Glob. Change 25 (6), 969–986. https://doi.org/10.1007/s11027-020-09917-2.

Hawthorne, C., Poboss, N., Dieter, H., Gredinger, A., Zieba, M., Scheffknecht, G., 2012. Operation and results of a 200-kWth dual fluidized bed pilot plant gasifier with adsorption-enhanced reforming. Biomass Conv. Bioref. 2 (3), 217–227. https://doi.org/10.1007/s13399-012-0053-3.

Hedayati, A., Soleimanisalim, A.H., Linderholm, C.J, Mattisson, T., Lyngfelt, A., 2021. Experimental evaluation of manganese ores for chemical looping conversion of synthetic biomass volatiles in a 300 W reactor system. J. Environ. Chem. Eng. 9 (2), 105112. https://doi.org/10.1016/j.jece.2021.105112.

Hedayati, A., Soleimanisalim, A.H., Mattisson, T., Lyngfelt, A., 2022. Thermochemical conversion of biomass volatiles via chemical looping: comparison of ilmenite and steel converter waste materials as oxygen carriers. Fuel 313, 122638. https://doi.org/10.1016/j.fuel.2021.122638.

Hejazi, B., Montagnaro, F., 2024. A modeling and simulation study to accommodate sorbent sintering in a Ca-looping system coupled with a cement plant. Ind. Eng. Chem. Res. 63 (25), 11069–11081. https://doi.org/10.1021/acs.iecr.4c00941.

Hejazi, B., Grace, J.R., Bi, X., Mahecha-Botero, A., 2017a. Kinetic model of steam gasification of biomass in a bubbling fluidized bed reactor. Energy Fuels 31 (2), 1702–1711. https://doi.org/10.1021/acs.energyfuels.6b03161.

Hejazi, B., Grace, J.R., Bi, X., Mahecha-Botero, A., 2017b. Kinetic model of steam gasification of biomass in a dual fluidized bed reactor: comparison with pilot-plant experimental results. Energy Fuels 31 (11), 12141–12155. https://doi.org/10.1021/acs.energyfuels.7b01833.

Herrera, B., Greco-Coppi, M., Cacua, K., Moreno, A., Suárez, N., Epple, B., 2026. The effects of oxygen carrier, CO2/H2O ratio, temperature, and CO2 content in chemical looping reforming of biogas: a parametric experimental study. Appl. Energy Combus. Sci. 25, 100444. https://doi.org/10.1016/j.jaecs.2025.100444. Article.

Hildor, F., Soleimanisalim, A.H., Seemann, M., Mattisson, T., Leion, H., 2023. Tar characteristics generated from a 10 kWth chemical-looping biomass gasifier using steel converter slag as an oxygen carrier. Fuel 331, 125770. https://doi.org/10.1016/j.fuel.2022.125770.

Hilz, J., Helbig, M., Haaf, M., Daikeler, A., Ströhle, J., Epple, B., 2017. Long-term pilot testing of the carbonate looping process in 1 MWth scale. Fuel 210, 892–899. https://doi.org/10.1016/j.fuel.2017.08.105.

Hilz, J., Helbig, M., Haaf, M., Daikeler, A., Ströhle, J., Epple, B., 2018. Investigation of the fuel influence on the carbonate looping process in 1 MWth scale. Fuel Process. Technol. 169, 170–177. https://doi.org/10.1016/j.fuproc.2017.09.016.

Hilz, J., Haaf, M., Helbig, M., Lindqvist, N., Ströhle, J., Epple, B., 2019. Scale-up of the carbonate looping process to a 20 MWth pilot plant based on long-term pilot tests. Int. J. Greenhouse Gas Control 88, 332–341. https://doi.org/10.1016/j.ijggc.2019.04.026.

Hofmann, C., Haaf, M., Unger, A., Ströhle, J., Epple, B., 2021. Valorizing waste derived fuels for climate change mitigation: techno-economic comparison of CCS and CCU approaches based on the carbonate looping process. SSRN Journal. https://doi.org/10.2139/ssrn.3820501.

Hofmann, C., Greco-Coppi, M., Ströhle, J., Epple, B., 2022. Pilot testing of the indirectly heated carbonate looping process for cement and lime plants. In: Proceedings of the 16th International Conference on Greenhouse Gas Control Technologies. Available online at, 23–24 Oct. https://deliverypdf.ssrn.com/delivery.php?ID=623110115067021007066023016111123092051040069008061028095104015090009064077122031071123059021013106005121070000103073104087031105043041005072087098011113005021113096056082040091095090077092100003123096080010028064110003070025025030119084004018113001087&EXT=pdf&INDEX=TRUE. zuletzt geprüft am 24.01.2023.

Hofmann, C., Greco-Coppi, M., Ströhle, J., Epple, B., 2024a. Adaption of a 300 kWth pilot plant for testing the indirectly heated carbonate looping process for CO2 capture from lime and cement industry. In: 13th European Conference on Industrial Furnaces and Boilers (INFUB-13). Algarve, Portugal.

Hofmann, C., Greco-Coppi, M., Ströhle, J., Epple, B., 2024b. Enhancement of a 300 kWth pilot plant for testing the indirectly heated carbonate looping process for CO2 capture from lime and cement industry. Exp. Therm. Fluid. Sci. 151, 111091. https://doi.org/10.1016/j.expthermflusci.2023.111091. Article.

Hofmann, C., 2025. Bewertung und Optimierung des indirekt beheizten Carbonate-Looping-Prozesses im Pilotmaßstab für die Anwendung in der Kalkindustrie. Doctoral dissertation. Technical University of Darmstadt, Darmstadt, Germany.

Hongrapipat, J., Rauch, R., Pang, S., Liplap, P., Arjharn, W., Messner, M., et al., 2022. Co-gasification of refuse derived fuel and wood chips in the Nong Bua dual fluidised bed gasification power plant in Thailand. Energies (Basel) 15 (19), 7363. https://doi.org/10.3390/en15197363.

Hornberger, M., Moreno, J., Schmid, M., Scheffknecht, G., 2020. Experimental investigation of the carbonation reactor in a tail-end Calcium Looping configuration for CO2 capture from cement plants. Fuel Process. Technol. 210, 106557. https://doi.org/10.1016/j.fuproc.2020.106557.

Hornberger, M., Moreno, J., Schmid, M., Scheffknecht, G., 2021. Experimental investigation of the calcination reactor in a tail-end calcium looping configuration for CO2 capture from cement plants. Fuel 284, 118927. https://doi.org/10.1016/j.fuel.2020.118927.

Hu, J., Galvita, V.V., Poelman, H., Marin, G.B, 2018. Advanced Chemical Looping Materials for CO_2 Utilization: a Review. Materials (Basel, Switzerland) (7), 1187. https://doi.org/10.3390/ma11071187.

Hua, X., Zhu, J., Wu, X., Xia, Z., Deng, Z., Wang, W., 2016. Packed bed chemical looping platform: design and operation of 30kWth pilot unit. Procedia Environ. Sci. 31, 81–90. https://doi.org/10.1016/j.proenv.2016.02.011.

HyPER, 2025. The HyPER project. Available online at. https://hyperh2.co.uk/the-project/.

IEA, 2020a. Iron and Steel Technology Roadmap. Available online at, Paris. https://www.iea.org/reports/iron-and-steel-technology-roadmap.

IEA, 2020b. The role of CCUS in low-carbon power systems. Available online at, Paris. www.iea.org/reports/the-role-of-ccus-in-low-carbon-power-systems.

Iliuta, I., Tahoces, R., Patience, G.S., Rifflart, S., Luck, F., 2010. Chemical-looping combustion process: kinetics and mathematical modeling. aIChE J. 56 (4), 1063–1079. https://doi.org/10.1002/aic.11967.

IPCC, 2005. IPCC special report on carbon dioxide capture and storage. 1. publ. Hg. v. Bert Metz. Cambridge Univ. Press. Available online at, Cambridge. https://www.ipcc.ch/site/assets/uploads/2018/03/srccs_wholereport-1.pdf. zuletzt geprüft am 30.11.2022.

Ishida, M., Jin, H., 1994. A novel combustor based on chemical-looping reactions and its reaction kinetics. J. Chem. Eng. Japan /JCEJ 27 (3), 296–301. https://doi.org/10.1252/jcej.27.296.

Ishida, M., Zheng, D., Akehata, T., 1987. Evaluation of a chemical-looping-combustion power-generation system by graphic exergy analysis. Energy 12 (2), 147–154. https://doi.org/10.1016/0360-5442(87)90119-8.

Ishida, M., Jin, H., Okamoto, T., 1996. A fundamental study of a new kind of medium material for chemical-looping combustion. Energy Fuels 10 (4), 958–963. https://doi.org/10.1021/ef950173n.

Jacob, R.M., Tokheim, L.-A., 2023a. Electrified calciner concept for CO2 capture in pyro-processing of a dry process cement plant. Energy, 126673. https://doi.org/10.1016/j.energy.2023.126673. Article 126673.

Jacob, R.M., Tokheim, L.-A., 2023b. Novel design of a rotary calciner internally heated with electrical axial heaters: experiments and modelling. Results Eng. 17, 100992. https://doi.org/10.1016/j.rineng.2023.100992.

Jin, B.o, Fu, D., Xiang, X., Zhao, H., Zhang, H., Mei, D., Liang, Z., 2024. Integrated metal carbonate thermal decomposition with in-situ CO2 conversion: review and perspective. Gas Sci. Eng. 129, 205416. https://doi.org/10.1016/j.jgsce.2024.205416.

Jing, D., Arjmand, M., Mattisson, T., Rydén, M., Snijkers, F., Leion, H., Lyngfelt, A., 2014. Examination of oxygen uncoupling behaviour and reactivity towards methane for manganese silicate oxygen carriers in chemical-looping combustion. Int. J. Greenhouse Gas Control 29, 70–81. https://doi.org/10.1016/j.ijggc.2014.07.003.

Junk, M., Reitz, M., Ströhle, J., Epple, B., 2013. Thermodynamic evaluation and cold flow model testing of an indirectly heated carbonate looping process. Chem. Eng. Technol. 36 (9), 1479–1487. https://doi.org/10.1002/ceat.201300019.

Junk, M., Reitz, M., Ströhle, J., Epple, B., 2016a. Technical and economical assessment of the indirectly heated carbonate looping process. J. Energy Resour. Technol. 138 (4), 042210. https://doi.org/10.1115/1.4033142. Article.

Junk, M., Reitz, M., Ströhle, J., Epple, B., 2016b. Technical and economical assessment of the indirectly heated carbonate looping process. J. Energy Resour. Technol. 138 (4), 042210. https://doi.org/10.1115/1.4033142. Article.

Kadlez, D., Benedikt, F., Huber, M., Fürsatz, K., Schmid, J.C., Hofbauer, H., Müller, S., 2025. Technology development of advanced dual fluidized bed steam gasification from pilot to demonstration scale – first results from a newly commissioned 1 MW demonstration plant. Fuel 381, 133376. https://doi.org/10.1016/j.fuel.2024.133376.

Karimi, E., Forutan, H.R., Saidi, M., Rahimpour, M.R., Shariati, A., 2014. Experimental study of chemical-looping reforming in a fixed-bed reactor: performance investigation of different oxygen carriers on Al 2 O 3 and TiO 2 support. Energy Fuels 28 (4), 2811–2820. https://doi.org/10.1021/ef5003765.

Karl, J., Pröll, T., 2018. Steam gasification of biomass in dual fluidized bed gasifiers: a review. Renewable Sustainable Energy Rev. 98, 64–78. https://doi.org/10.1016/j.rser.2018.09.010.

Kataria, P., Yeo, W.S, Nandong, J., 2024. Reviewing the dynamic modeling aspects of chemical looping hydrogen production. Int. J. Hydrogen Energy 82, 1282–1299. https://doi.org/10.1016/j.ijhydene.2024.08.033.

Keller, M., Kaibe, K., Hatano, H., Otomo, J., 2019. Techno-economic evaluation of BECCS via chemical looping combustion of Japanese woody biomass. Int. J. Greenhouse Gas Control 83, 69–82. https://doi.org/10.1016/j.ijggc.2019.01.019.

Khallaghi, N., Zapata-Boada, S., Gutierrez, D., Miriam, Wright, A.D, Fernández, J.R, Abanades, J.C, Spallina, V., 2025. Blast furnace gas utilization with calcium-assisted steel mill off-gas hydrogen production (CASOH) technology: technical evaluation. Ind. Eng. Chem. Res. 64 (29), 14616–14627. https://doi.org/10.1021/acs.iecr.5c01422.

Khan, M.I, Mishamandani, A.S, Asfand, F., Fadlallah, S., Kurniawan, T.A, 2025. Solar driven calcium-looping for thermochemical energy storage system and carbon capture in power and cement industry: a review. Process Saf. Environ. Prot. 193, 886–917. https://doi.org/10.1016/j.psep.2024.11.067.

Kim, H.R., Wang, D., Zeng, L., Bayham, S., Tong, A., Chung, E., et al., 2013. Coal direct chemical looping combustion process: design and operation of a 25-kWth sub-pilot unit. Fuel 108, 370–384. https://doi.org/10.1016/j.fuel.2012.12.038.

Kolbitsch, P., Pröll, T., Bolhar-Nordenkampf, J., Hofbauer, H., 2009. Design of a chemical looping combustor using a dual circulating fluidized bed (DCFB) reactor system. Chem. Eng. Technol. 32 (3), 398–403. https://doi.org/10.1002/ceat.200800378.

Kong, D., Wang, S., Luo, K., Xu, Q., Fan, J., 2023. Insights of biomass gasification combined with CO2 absorption enhanced reforming in an 8 MWth dual fluidized bed. Chem. Eng. J. 466, 142981. https://doi.org/10.1016/j.cej.2023.142981.

Kopsch, M., Lebendig, F., Yazhenskikh, E., Amado-Fierro, Á, Centeno, T., Müller, M., 2024. Effect of HTC and water-leaching of low-grade biomasses on the release behavior of inorganic constituents in a calcium looping gasification process at 650°C. Energy Fuels 38 (17), 16504–16519. https://doi.org/10.1021/acs.energyfuels.4c02833.

Kraft, S., Kirnbauer, F., Hofbauer, H., 2017. CPFD simulations of an industrial-sized dual fluidized bed steam gasification system of biomass with 8 MW fuel input. Appl. Energy 190, 408–420. https://doi.org/10.1016/j.apenergy.2016.12.113.

Kramp, M., Thon, A., Hartge, E.-U., Heinrich, S., Werther, J., 2012. Carbon stripping – a critical process step in chemical looping combustion of solid fuels. Chem. Eng. Technol. 35 (3), 497–507. https://doi.org/10.1002/ceat.201100438.

Kremer, J., Galloy, A., Ströhle, J., Epple, B., 2013. Continuous CO 2 capture in a 1-MW th carbonate looping pilot plant. Chem. Eng. Technol. 36 (9), 1518–1524. https://doi.org/10.1002/ceat.201300084.

Kuhn, A., Graf, C., Hülsbruch, D., Ströhle, J., Epple, B., 2025a. Oxygen Carrier Aided Combustion (OCAC) of Solid Recovered Fuel (SRF) and coal in a 1 MWth CFB pilot plant using Ilmenite. Appl. Therm. Eng. 274, 126692. https://doi.org/10.1016/j.applthermaleng.2025.126692.

Kuhn, A., Graf, C., Ströhle, J., Epple, B., 2025b. Experimental study on oxyfuel-combustion of solid recovered fuel using ilmenite as bed material in a 1 MWth fluidized bed reactor. Carbon Capture Sci. Technol. 15, 100436. https://doi.org/10.1016/j.ccst.2025.100436.

Kumar, T.R., Mattisson, T., Rydén, M., 2022a. Techno-economic assessment of chemical looping gasification of biomass for Fischer–Tropsch crude production with net-negative CO 2 emissions: part 2. Energy Fuels 36 (17), 9706–9718. https://doi.org/10.1021/acs.energyfuels.2c01184.

Kumar, T.R., Mattisson, T., Rydén, M., Stenberg, V., 2022b. Process analysis of chemical looping gasification of biomass for Fischer–Tropsch crude production with net-negative CO 2 emissions: part 1. Energy Fuels 36 (17), 9687–9705. https://doi.org/10.1021/acs.energyfuels.2c00819.

Langørgen, Ø, Saanum, I., Khalil, R., Haugen, N., Erland, L., 2023. Evaluation of CLC as a BECCS technology from tests on woody biomass in an auto-thermal 150-kW pilot unit. Int. J. Greenhouse Gas Control 130, 104006. https://doi.org/10.1016/j.ijggc.2023.104006.

Langørgen, Ø, Saanum, I., Khalil, R., 2025. Pilot tests with waste and biomass in a 150 kWth autothermal CLC unit. Ind. Eng. Chem. Res. 64 (44), 21316–21328. https://doi.org/10.1021/acs.iecr.5c01757.

Larsson, A., Israelsson, M., Lind, F., Seemann, M., Thunman, H., 2014. Using ilmenite to reduce the tar yield in a dual fluidized bed gasification system. Energy Fuels 28 (4), 2632–2644. https://doi.org/10.1021/ef500132p.

Larsson, A., Kuba, M., Vilches, B., Teresa, Seemann, M., Hofbauer, H., Thunman, H., 2021. Steam gasification of biomass – typical gas quality and operational strategies derived from industrial-scale plants. Fuel Process. Technol. 212, 106609. https://doi.org/10.1016/j.fuproc.2020.106609.

las Obras Loscertales, M., Abad, A., García-Labiano, F., Ruiz, J.A.C., Adánez, J., 2023. Reaction kinetics of a NiO-based oxygen carrier with ethanol to be applied in chemical looping processes. Fuel 345, 128163. https://doi.org/10.1016/j.fuel.2023.128163.

las Obras Loscertales, M., Mendiara, T., Abad, A., Gayan, P., 2025a. Assessment of hydrogen production from Sorption Enhanced Chemical Looping Reforming (SE-CLR) of methane. Int. J. Hydrogen Energy 142, 674–684. https://doi.org/10.1016/j.ijhydene.2025.01.122.

las Obras Loscertales, M., Abad, A., Diego, L.F., Cabello, A., Ruiz, J.;G., Labiano, F., 2025b. Chemical looping reforming of bioethanol for hydrogen production: Modeling and design of the fuel reactor of a 350 MW unit. Biomass Bioenergy 197, 107830. https://doi.org/10.1016/j.biombioe.2025.107830.

Lasheras, A., Ströhle, J., Galloy, A., Epple, B., 2011. Carbonate looping process simulation using a 1D fluidized bed model for the carbonator. Int. J. Greenhouse Gas Control 5 (4), 686–693. https://doi.org/10.1016/j.ijggc.2011.01.005.

Lebendig, F., Müller, M., 2022. Effect of pre-treatment of herbaceous feedstocks on behavior of inorganic constituents under chemical looping gasification (CLG) conditions. Green. Chem. 24 (24), 9643–9658. https://doi.org/10.1039/D2GC02906E.

Lebendig, F., Funcia, I., Pérez-Vega, R., Müller, M., 2022. Investigations on the effect of pre-treatment of wheat straw on ash-related issues in chemical looping gasification (CLG) in comparison with woody biomass. Energies (Basel) 15 (9), 3422. https://doi.org/10.3390/en15093422.

Leckner, B.o, 2016. Developments in fluidized bed conversion of solid fuels. Therm. Sci. 20 (suppl. 1), 1–18. https://doi.org/10.2298/TSCI150703135L.

Lee, J., Lee, M., Shin, Y., Kim, D., Lee, J.W, 2025. Techno-economic and environmental impact assessment of feasible alternatives to steam methane reforming for hydrogen production: dry and chemical looping reforming routes. Sustainable Energy Technol. Assess. 82, 104512. https://doi.org/10.1016/j.seta.2025.104512.

Leeuwe, C., Abbas, S.Z, Argyris, P.A, Zaidi, A., Amiero, A., Poultson, S., et al., 2023. Thermochemical syngas generation via solid looping process: an experimental demonstration using Fe-based material. Chem. Eng. J. 453, 139791. https://doi.org/10.1016/j.cej.2022.139791.

Lena, E., Spinelli, M., Martínez, I., Gatti, M., Scaccabarozzi, R., Cinti, G., Romano, M.C., 2017. Process integration study of tail-end Ca-Looping process for CO2 capture in cement plants. Int. J. Greenhouse Gas Control 67, 71–92. https://doi.org/10.1016/j.ijggc.2017.10.005.

Lena, E., Spinelli, M., Gatti, M., Scaccabarozzi, R., Campanari, S., Consonni, S., et al., 2019. Techno-economic analysis of calcium looping processes for low CO2 emission cement plants. Int. J. Greenhouse Gas Control 82, 244–260. https://doi.org/10.1016/j.ijggc.2019.01.005.

Lena, E., Arias, B., Romano, M.C., Abanades, J.C, 2022. Integrated calcium looping system with circulating fluidized bed reactors for low CO2 emission cement plants. Int. J. Greenhouse Gas Control 114, 103555. https://doi.org/10.1016/j.ijggc.2021.103555.

Lesemann, M., Mays, J., Clough, P.T., Oakey, J., Adedipe, T., Duncan, A., 2022. Hydrogen production with integrated CO2 capture via sorbent enhanced reforming. In: Proceedings of the 16th Greenhouse Gas Control Technologies Conference (GHGT-16), 23-24 Oct 2022.

Lewis, W.K., Gilliland, E.R., McBride, G.T., 1949. Gasification of carbon by carbon dioxide in fluidized powder bed. Ind. Eng. Chem. 41 (6), 1213–1226. https://doi.org/10.1021/ie50474a017.

Li, J., Zhang, H., Gao, Z., Fu, J., Ao, W., Dai, J., 2017. CO 2 capture with chemical looping combustion of gaseous fuels: an overview. Energy Fuels 31 (4), 3475–3524. https://doi.org/10.1021/acs.energyfuels.6b03204.

Li, X., Lyngfelt, A., Linderholm, C., Leckner, B.o, Mattisson, T., 2022a. Performance of a volatiles distributor equipped with internal baffles under different fluidization regimes. Powder. Technol. 409, 117807. https://doi.org/10.1016/j.powtec.2022.117807.

Li, X., Lyngfelt, A., Pallarès, D., Linderholm, C., Mattisson, T., 2022b. Investigation on the performance of volatile distributors with different configurations under different fluidization regimes. Energy Fuels 36 (17), 9571–9587. https://doi.org/10.1021/acs.energyfuels.1c04159.

Li, Z., Tang, H., Sun, Z., Chen, C., Duan, L., 2023. Unraveling the structure–reactivity relationship of CuFe 2 O 4 oxygen carriers for chemical looping combustion: a DFT study. Energy Fuels 37 (14), 10521–10530. https://doi.org/10.1021/acs.energyfuels.3c01101.

Li, X., Faust, R., Lyngfelt, A., Knutsson, P., Mattisson, T., 2024a. Noncalcined manganese ores as oxygen carriers for chemical looping combustion with oxygen uncoupling in a circulating fluidized bed reactor system. Energy Fuels 38 (17), 16657–16677. https://doi.org/10.1021/acs.energyfuels.4c02406.

Li, X., Faust, R., Purnomo, V., Mei, D., Linderholm, C., Lyngfelt, A., Mattisson, T., 2024b. Performance of a perovskite-structured calcium manganite oxygen carrier produced from natural ores in a batch reactor and in operation of a chemical-looping combustion reactor system. Chem. Eng. J. 497, 154516. https://doi.org/10.1016/j.cej.2024.154516.

Li, G., Fu, W., Zhao, W., Zhang, Y., 2025a. Microwave-assisted chemical looping gasification of lignite coal for CO-rich syngas production. J. Energy Inst. 120, 102108. https://doi.org/10.1016/j.joei.2025.102108.

Li, Z., Wang, Y., Li, W., Wei, G., Liu, X., Lin, et al., 2026. Demonstration of a 5-MWth chemical looping combustion unit fueled by lignite. Engineering 59, 168–177. https://doi.org/10.1016/j.eng.2025.07.017.

Li, Z., Li, J.;, Wang, Y., Li, W.;, Wei, G., Liu, X., et al., 2026. Demonstration of biomass chemical looping gasification in a 5 MWth pilot unit using ilmenite as oxygen carrier. Fuel 405, 136472. https://doi.org/10.1016/j.fuel.2025.136472.

Lim, L.H, Tan, P., Chan, W.P, Veksha, A., Lim, T.-T., Lisak, G., Liu, W., 2023. A techno-economic assessment of the reutilisation of municipal solid waste incineration ash for CO2 capture from incineration flue gases by calcium looping. Chem. Eng. J. 464, 142567. https://doi.org/10.1016/j.cej.2023.142567.

Lind, F., Corcoran, A., Thunman, H., 2017. Validation of the oxygen buffering ability of bed materials used for OCAC in a large scale CFB boiler. Powder. Technol. 316, 462–468. https://doi.org/10.1016/j.powtec.2016.12.048.

Linderholm, C., Mattisson, T., Lyngfelt, A., 2009. Long-term integrity testing of spray-dried particles in a 10-kW chemical-looping combustor using natural gas as fuel. Fuel 88 (11), 2083–2096. https://doi.org/10.1016/j.fuel.2008.12.018.

Linderholm, C., Schmitz, M., Knutsson, P., Lyngfelt, A., 2016. Chemical-looping combustion in a 100-kW unit using a mixture of ilmenite and manganese ore as oxygen carrier. Fuel 166, 533–542. https://doi.org/10.1016/j.fuel.2015.11.015.
Linderholm, C., Lyngfelt, A., Rydén, M., Schmitz, M., 2017. Chemical-looping combustion of biomass in a 100 kW pilot. In: 25th European Biomass Conference and Exhibition. Stockholm, Sweden, pp. 12–15. June 2017.
Lindmüller, L., Haus, J., Heinrich, S., 2023. Experiments on the dynamic behavior of the chemical looping combustion process. Chem. Ing. Tech. 95 (1-2), 136–142. https://doi.org/10.1002/cite.202200155.
Lisbona, P., Gori, R., Romeo, L.M., Desideri, U., 2021. Techno-economic assessment of an industrial carbon capture hub sharing a cement rotary kiln as sorbent regenerator. Int. J. Greenhouse Gas Control 112, 103524. https://doi.org/10.1016/j.ijggc.2021.103524.
Liu, H., Cattolica, R.J., Seiser, R., Liao, C.-, 2015. Three-dimensional full-loop simulation of a dual fluidized-bed biomass gasifier. Appl. Energy 160, 489–501. https://doi.org/10.1016/j.apenergy.2015.09.065.
Liu, H., Cattolica, R.J., Seiser, R., 2016. CFD studies on biomass gasification in a pilot-scale dual fluidized-bed system. Int. J. Hydrogen Energy 41 (28), 11974–11989. https://doi.org/10.1016/j.ijhydene.2016.04.205.
Liu, L., Li, Z., Li, Z., Larring, Y., Li, Y.e, Cai, N., 2021a. Fast redox kinetics of a perovskite oxygen carrier measured using micro-fluidized bed thermogravimetric analysis. Proc. Combus. Inst. 38 (4), 5259–5269. https://doi.org/10.1016/j.proci.2020.06.160.
Liu, L., Li, Z., Wu, S., Li, D., Cai, N., 2021b. Conversion characteristics of lignite and petroleum coke in chemical looping combustion coupled with an annular carbon stripper. Fuel Process. Technol. 213, 106711. https://doi.org/10.1016/j.fuproc.2020.106711.
Liu, L., Li, K., Liu, H., Sun, Z., 2025. A DFT-based kinetic model for Cu-Al oxygen carrier material in chemical looping with oxygen uncoupling. Fuel 381, 133572. https://doi.org/10.1016/j.fuel.2024.133572.
Liu, R., Li, X., Wu, Z., Zhou, M., Huang, W., 2026. Comprehensive modeling of biomass dual fluidized bed gasification: Integrating reaction kinetics, hydrodynamics, and tar formation. J. Energy Inst. 127, 102566. https://doi.org/10.1016/j.joei.2026.102566.
Lucio, M., Ricardez-Sandoval, L.A., 2020. Dynamic modelling and optimal control strategies for chemical-looping combustion in an industrial-scale packed bed reactor. Fuel 262, 116544. https://doi.org/10.1016/j.fuel.2019.116544.
Lundberg, L., Pallarès, D., Thunman, H., 2018. Upscaling effects on char conversion in dual fluidized bed gasification. Energy Fuels 32 (5), 5933–5943. https://doi.org/10.1021/acs.energyfuels.8b00088.
Lundgren, J., Vreugdenhil, B., Ganjkhanlou, Y., Baldwin, R., 2025. Biomass gasification for hydrogen production. IEA Bioenergy.
Luo, S., Zeng, L., Fan, L.-S., 2015. Chemical looping technology: oxygen carrier characteristics. Annu Rev. Chem. Biomol. Eng. 6, 53–75. https://doi.org/10.1146/annurev-chembioeng-060713-040334.
Luo, M., Yi, Y., Wang, C., Liu, K.e, Pan, J., Wang, Q., 2018a. Energy and exergy analysis of power generation systems with chemical looping combustion of coal. Chem. Eng. Technol. 41 (4), 776–787. https://doi.org/10.1002/ceat.201700495.
Luo, M., Yi, Y., Wang, S., Wang, Z., Du, M., Pan, J., Wang, Q., 2018b. Review of hydrogen production using chemical-looping technology. Renewable Sustainable Energy Rev. 81, 3186–3214. https://doi.org/10.1016/j.rser.2017.07.007.
Luo, H., Lin, W., Song, W., Li, S., Dam-Johansen, K., Wu, H., 2019. Three dimensional full-loop CFD simulation of hydrodynamics in a pilot-scale dual fluidized bed system for biomass gasification. Fuel Process. Technol. 195, 106146. https://doi.org/10.1016/J.FUPROC.2019.106146.
Luo, Q., Li, J., Wang, Y., Chen, R., Chen, S., Xiang, W., 2025. Technoeconomic and life-cycle assessment of biomass-to-hydrogen conversion via a compact fluidized bed calcium looping gasifier. Bioresour. Technol. 434, 132814. https://doi.org/10.1016/j.biortech.2025.132814.
Lupion, M., Alvarez, I., Otero, P., Kuivalainen, R., Lantto, J., Hotta, A., Hack, H., 2013. 30 MWth CIUDEN Oxy-cfb boiler - first experiences. Energy Procedia 37, 6179–6188. https://doi.org/10.1016/j.egypro.2013.06.547.
Lyngfelt, A., Leckner, B.o, 2015. A 1000 MWth boiler for chemical-looping combustion of solid fuels – discussion of design and costs. Appl. Energy 157, 475–487. https://doi.org/10.1016/j.apenergy.2015.04.057.
Lyngfelt, A., Leckner, B.o, Mattisson, T., 2001. A fluidized-bed combustion process with inherent CO2 separation; application of chemical-looping combustion. Chem. Eng. Sci. 56 (10), 3101–3113. https://doi.org/10.1016/S0009-2509(01)00007-0.
Lyngfelt, A., Kronberger, B., Adanez, J., Morin, J., Hurst, P., 2005. The grace project: development of oxygen carrier particles for chemical-looping combustion. Design and operation of a 10 kW chemical-looping combustor. Greenhouse Gas Control Technologies 7. I: Elsevier, pp. 115–123.
Lyngfelt, A., Brink, A., Langørgen, Ø, Mattisson, T., Rydén, M., Linderholm, C., 2019. 11,000 h of chemical-looping combustion operation—where are we and where do we want to go? Int. J. Greenhouse Gas Control 88, 38–56. https://doi.org/10.1016/j.ijggc.2019.05.023.
Lyngfelt, A., Hedayati, A., Augustsson, E., 2022a. Fate of NO and ammonia in chemical looping combustion-investigation in a 300 W chemical looping combustion reactor system. Energy Fuels 36 (17), 9628–9647. https://doi.org/10.1021/acs.energyfuels.2c00750.
Lyngfelt, A., Pallarès, D., Linderholm, C., Lind, F., Thunman, H., Leckner, B.O, 2022b. Achieving adequate circulation in chemical looping combustion-design proposal for a 200 MW th chemical looping combustion circulating fluidized bed boiler. Energy Fuels 36 (17), 9588–9615. https://doi.org/10.1021/acs.energyfuels.1c03615.
Lyngfelt, A., Moldenhauer, P., Biermann, M., Johannsen, K., Wimmer, D., Hanning, M., 2023. Operational experiences of chemical-looping combustion with 18 manganese ores in a 300W unit. Int. J. Greenhouse Gas Control 127, 103937. https://doi.org/10.1016/j.ijggc.2023.103937.
Lyngfelt, A., 2020. Chemical looping combustion: status and development challenges. Energy Fuels 34 (8), 9077–9093. https://doi.org/10.1021/acs.energyfuels.0c01454.
Lysowski, R., Ksepko, E., 2025. Ti doping as an effective strategy for increasing the stability of strontium-copper-iron perovskite-based oxygen carriers. J. Environ. Manage. 393, 127262. https://doi.org/10.1016/j.jenvman.2025.127262.
Müller, S., Fuchs, J., Schmid, J.C., Benedikt, F., Hofbauer, H., 2017. Experimental development of sorption enhanced reforming by the use of an advanced gasification test plant. Int. J. Hydrogen. Energy 42 (50), 29694–29707. https://doi.org/10.1016/j.ijhydene.2017.10.119.
Mader, N., Mack, A., Scheffknecht, G., 2025. CO2 capture for backup power plants: Entrained flow Calcium Looping using Ca(OH)2. Fuel 401, 135855. https://doi.org/10.1016/j.fuel.2025.135855.
Magli, F., De Lena, E., Cremona, R., Spinelli, M., Alonso, M., Mader, N., et al., 2023. Cleanker pilot test results. In: Cleanker Conference. Piacenza, 15 Mar.
Mancuso, L., Cloete, S., Chiesa, P., Amini, S., 2017. Economic assessment of packed bed chemical looping combustion and suitable benchmarks. Int. J. Greenhouse Gas Control 64, 223–233. https://doi.org/10.1016/j.ijggc.2017.07.015.
Markström, P., Lyngfelt, A., 2012. Designing and operating a cold-flow model of a 100kW chemical-looping combustor. Powder. Technol. 222, 182–192. https://doi.org/10.1016/j.powtec.2012.02.041.
Martínez, I., Murillo, R., Grasa, G., Rodríguez, N., Abanades, J.C, 2011. Conceptual design of a three fluidised beds combustion system capturing CO2 with CaO. Int. J. Greenhouse Gas Control 5 (3), 498–504. https://doi.org/10.1016/j.ijggc.2010.04.017.
Martínez, I., Romano, M.C., Chiesa, P., Grasa, G., Murillo, R., 2013a. Hydrogen production through sorption enhanced steam reforming of natural gas: thermodynamic plant assessment. Int. J. Hydrogen. Energy 38 (35), 15180–15199. https://doi.org/10.1016/j.ijhydene.2013.09.062.
Martínez, I., Grasa, G., Murillo, R., Arias, B., Abanades, J.C, 2013b. Modelling the continuous calcination of CaCO3 in a Ca-looping system. Chem. Eng. J. 215-216, 174–181. https://doi.org/10.1016/j.cej.2012.09.134, 215-216.
Martínez, I., Grasa, G., Parkkinen, J., Tynjälä, T., Hyppänen, T., Murillo, R., Romano, M. C, 2016. Review and research needs of Ca-Looping systems modelling for post-combustion CO2 capture applications. Int. J. Greenhouse Gas Control 50, 271–304. https://doi.org/10.1016/j.ijggc.2016.04.002.
Martínez, I., Arias, B., Grasa, G.S., Abanades, J.C, 2018. CO2 capture in existing power plants using second generation Ca-Looping systems firing biomass in the calciner. J. Clean. Prod. 187, 638–649. https://doi.org/10.1016/j.jclepro.2018.03.189.
Martínez, I., Fernández, J.R., Martini, M., Gallucci, F., van Sint Annaland, M., Romano, M.C., Abanades, J.C, 2019. Recent progress of the Ca-Cu technology for decarbonisation of power plants and carbon intensive industries. Int. J. Greenhouse Gas Control 85, 71–85. https://doi.org/10.1016/j.ijggc.2019.03.026.
Martínez, I., Grasa, G., Callén, M.S., López, J.M, Murillo, R., 2020. Optimised production of tailored syngas from municipal solid waste (MSW) by sorption-enhanced gasification. Chem. Eng. J. 401, 126067. https://doi.org/10.1016/j.cej.2020.126067.
Martínez, I., Callén, M.S., Grasa, G., López, J.M., Murillo, R., 2022. Sorption-enhanced gasification (SEG) of agroforestry residues: Influence of feedstock and main operating variables on product gas quality. Fuel Process. Technol. 226, 107074. https://doi.org/10.1016/j.fuproc.2021.107074.
Martini, M., van den Berg, A., Gallucci, F., van Sint Annaland, M., 2016. Investigation of the process operability windows for Ca-Cu looping for hydrogen production with CO2 capture. Chem. Eng. J. 303, 73–88. https://doi.org/10.1016/j.cej.2016.05.135.
Marx, F., Dieringer, P., Ströhle, J., Epple, B., 2021. Design of a 1 MWth pilot plant for chemical looping gasification of biogenic residues. Energies. (Basel) 14 (9), 2581. https://doi.org/10.3390/en14092581.
Marx, F., Dieringer, P., Ströhle, J., Epple, B., 2023a. Process efficiency and syngas quality from autothermal operation of a 1 MWth chemical looping gasifier with biogenic residues. Appl. Energy Combus. Sci. 16, 100217. https://doi.org/10.1016/j.jaecs.2023.100217.
Marx, F., Dieringer, P., Ströhle, J., Epple, B., 2023b. Solid flux measurement in dual fluidized bed processes based on solid samples. Fuel 341, 127589. https://doi.org/10.1016/j.fuel.2023.127589.
Masoudi Soltani, S., Lahiri, A., Bahzad, H., Clough, P., Gorbounov, M., Yan, Y., 2021. Sorption-enhanced steam methane reforming for combined CO2 capture and hydrogen production: a state-of-the-art review. Carbon Capture Sci. Technol. 1, 100003. https://doi.org/10.1016/j.ccst.2021.100003.
Mattisson, T., Lyngfelt, A., Leion, H., 2009. Chemical-looping with oxygen uncoupling for combustion of solid fuels. Int. J. Greenhouse Gas Control 3 (1), 11–19. https://doi.org/10.1016/j.ijggc.2008.06.002.
Mattisson, T., Jing, D., Lyngfelt, A., Rydén, M., 2016. Experimental investigation of binary and ternary combined manganese oxides for chemical-looping with oxygen uncoupling (CLOU). Fuel 164, 228–236. https://doi.org/10.1016/j.fuel.2015.09.053.
Mattisson, T., Keller, M., Linderholm, C., Moldenhauer, P., Rydén, M., Leion, H., Lyngfelt, A., 2018. Chemical-looping technologies using circulating fluidized bed systems: status of development. Fuel Process. Technol. 172, 1–12. https://doi.org/10.1016/j.fuproc.2017.11.016.
Mauerhofer, A.M., Schmid, J.C., Benedikt, F., Fuchs, J., Müller, S., Hofbauer, H., 2019. Dual fluidized bed steam gasification: change of product gas quality along the reactor height. Energy 173, 1256–1272. https://doi.org/10.1016/j.energy.2019.02.025.

Mauerhofer, A.M, Müller, S., Benedikt, F., Fuchs, J., Bartik, A., Hofbauer, H., 2021. CO2 gasification of biogenic fuels in a dual fluidized bed reactor system. Biomass Conv. Bioref. 11 (4), 1101–1116. https://doi.org/10.1007/s13399-019-00493-3.

Mays, J. (2017): One step hydrogen generation through sorption enhanced reforming.

Medrano, J.A., Potdar, I., Melendez, J., Spallina, V., Pacheco-Tanaka, D.A., van Sint Annaland, M., Gallucci, F., 2018. The membrane-assisted chemical looping reforming concept for efficient H2 production with inherent CO2 capture: experimental demonstration and model validation. Appl. Energy 215, 75–86. https://doi.org/10.1016/j.apenergy.2018.01.087.

Mei, D., Abad, A., Zhao, H., Adánez, J., 2015. Characterization of a sol–gel derived CuO/CuAl2O4 oxygen carrier for chemical looping combustion (CLC) of gaseous fuels: relevance of gas–solid and oxygen uncoupling reactions. Fuel Process. Technol. 133, 210–219. https://doi.org/10.1016/j.fuproc.2015.02.007.

Mei, D., Soleimanisalim, A.H., Linderholm, C., Lyngfelt, A., Mattisson, T., 2021. Reactivity and lifetime assessment of an oxygen releasable manganese ore with biomass fuels in a 10 kWth pilot rig for chemical looping combustion. Fuel Process. Technol. 215, 106743. https://doi.org/10.1016/j.fuproc.2021.106743.

Mei, D., Gogolev, I., Soleimanisalim, A.H., Lyngfelt, A., Mattisson, T., 2023. Investigation of LD-slag as oxygen carrier for CLC in a 10 kW unit using high-volatile biomasses. Int. J. Greenhouse Gas Control 127, 103940. https://doi.org/10.1016/j.ijggc.2023.103940.

Mei, D., Lyngfelt, A., Mattisson, T., Linderholm, C., 2025. Oxy-polishing of gas from chemical looping combustion: fuel-nitrogen transformation and model-aided gas purity optimization. Chem. Eng. J. 509, 161267. https://doi.org/10.1016/j.cej.2025.161267.

Mendiara, T., Adánez-Rubio, I., Gayán, P., Abad, A., Diego, L.F., García-Labiano, F., Adánez, J., 2016. Process comparison for biomass combustion: in situ gasification-chemical looping combustion (iG-CLC) versus Chemical Looping with Oxygen Uncoupling (CLOU). Energy Tech 4 (10), 1130–1136. https://doi.org/10.1002/ente.201500458.

Mendiara, T., García-Labiano, F., Abad, A., Gayán, P., Diego, L.F., Izquierdo, M.T., Adánez, J., 2018a. Negative CO2 emissions through the use of biofuels in chemical looping technology: a review. Appl. Energy 232, 657–684. https://doi.org/10.1016/j.apenergy.2018.09.201.

Mendiara, T., Pérez-Astray, A., Izquierdo, M.T., Abad, A., Diego, L.F., García-Labiano, F., et al., 2018b. Chemical looping combustion of different types of biomass in a 0.5 kWth unit. Fuel 211, 868–875. https://doi.org/10.1016/j.fuel.2017.09.113.

Mendiara, T., Filsouf, A., Adánez-Rubio, I., Izquierdo, M.T, Abad, A., 2025. Performance of granulated Ti-dopped manganese oxide oxygen carriers in chemical looping processes. Appl. Sci. 15 (2), 750. https://doi.org/10.3390/app15020750.

Meyer, J., Mastin, J., Pinilla, C.S, 2014. Sustainable hydrogen production from biogas using sorption-enhanced reforming. Energy Procedia 63, 6800–6814. https://doi.org/10.1016/j.egypro.2014.11.714.

Miao, Z., Jiang, E., Hu, Z., 2022. Review of agglomeration in biomass chemical looping technology. Fuel 309, 122199. https://doi.org/10.1016/j.fuel.2021.122199.

Mohn, P., Hofmann, C., Alobaid, F., Ströhle, J., Epple, B., 2022. Application of chemical-looping combustion on waste-to-energy: a techno-economic assessment. In: Proceedings of the 16th International Conference on Greenhouse Gas Control Technologies, 23–24 Oct.

Mohn, P.; Saanum, I.; Langørgen, Ø; Khalil, R.; Ströhle, J.; Epple, B. (2025): Chemical looping combustion of waste-derived fuel at 150 kW pilot-scale: fuel conversion behavior and CO2 capture.

Mohn, P., Saanum, I., Langørgen, Ø, Khalil, R., Ströhle, J., Epple, B., 2026. Chemical looping combustion of waste-derived fuel at 150 kW pilot-scale: fuel conversion behavior and CO2 capture. Fuel Process. Technol. 281, 108379. https://doi.org/10.1016/j.fuproc.2025.108379.

Moldenhauer, P., Rydén, M., Mattisson, T., Lyngfelt, A., 2012. Chemical-looping combustion and chemical-looping reforming of kerosene in a circulating fluidized-bed 300W laboratory reactor. Int. J. Greenhouse Gas Control 9, 1–9. https://doi.org/10.1016/j.ijggc.2012.02.015.

Moldenhauer, P., Rydén, M., Mattisson, T., Hoteit, A., Jamal, A., Lyngfelt, A., 2014. Chemical-looping combustion with fuel oil in a 10 kW pilot plant. Energy Fuels 28 (9), 5978–5987. https://doi.org/10.1021/ef5014677.

Moldenhauer, P., Serrano, A., García-Labiano, F., Diego, L.F., Biermann, M., Mattisson, T., Lyngfelt, A., 2018a. Chemical-looping combustion of kerosene and gaseous fuels with a natural and a manufactured Mn–Fe-based oxygen carrier. Energy Fuels 32 (8), 8803–8816. https://doi.org/10.1021/acs.energyfuels.8b01588.

Moldenhauer, P., Sundqvist, S., Mattisson, T., Linderholm, C., 2018b. Chemical-looping combustion of synthetic biomass-volatiles with manganese-ore oxygen carriers. Int. J. Greenhouse Gas Control 71, 239–252. https://doi.org/10.1016/j.ijggc.2018.02.021.

Moles, S., Martinez, I., Soledad Callén, M., Gómez, J., Manuel López, J., Murillo, R., 2024. Pilot-scale study of sorption-enhanced gasification of sewage sludge. Fuel 360, 130611. https://doi.org/10.1016/j.fuel.2023.130611.

Montiel-Bohórquez, N.D., Gatti, M., Romano, M.C, 2025. Flexible calcium looping for CO2 capture in electric Arc Furnace steelmaking: a techno-economic analysis. Carbon Capture Sci. Technol. 17, 100504. https://doi.org/10.1016/j.ccst.2025.100504.

Moonshot Flanders, 2026. UGent researchers open the groundbreaking super-dry reforming (SDR) pilot plant. News from Moonshot Flanders Industry Innovation. Available online at. https://www.moonshotflanders.be/en/news/ugent-researchers-open-groundbreaking-super-dry-reforming-sdr-pilot-plant. zuletzt geprüft am 15.01.2026.

Moreno, J., Hornberger, M., Schmid, M., Scheffknecht, G., 2021a. Oxy-fuel combustion of hard coal, wheat straw, and solid recovered fuel in a 200 kWth calcium looping CFB calciner. Energies (Basel) 14 (8), 2162. https://doi.org/10.3390/en14082162.

Moreno, J., Hornberger, M., Schmid, M., Scheffknecht, G., 2021b. Part-load operation of a novel calcium looping system for flexible CO 2 capture in coal-fired power plants. Ind. Eng. Chem. Res. 60 (19), 7320–7330. https://doi.org/10.1021/acs.iecr.1c00155.

Mostafa, A., Rapone, I., Bosetti, A., Romano, M.C., Beretta, A., Groppi, G., 2023. Sustainable hydrogen production via sorption enhanced reforming of complex biorefinery side streams in a fixed bed adiabatic reactor. Ind. Eng. Chem. Res. 62 (39), 15884–15896. https://doi.org/10.1021/acs.iecr.3c02401.

Moumin, G., Tescari, S., Sundarraj, P., Oliveira, L., Roeb, M., Sattler, C., 2019. Solar treatment of cohesive particles in a directly irradiated rotary kiln. Sol. Energy 182, 480–490. https://doi.org/10.1016/j.solener.2019.01.093.

Myöhänen, K., Palonen, J., Hyppänen, T., 2018. Modelling of indirect steam gasification in circulating fluidized bed reactors. Fuel Process. Technol. 171, 10–19. https://doi.org/10.1016/j.fuproc.2017.11.006.

Naqvi, R., Bolland, O., 2007. Multi-stage chemical looping combustion (CLC) for combined cycles with CO2 capture. Int. J. Greenhouse Gas Control 1 (1), 19–30. https://doi.org/10.1016/S1750-5836(07)00012-6.

Navajas, A., Mendiara, T., Gandía, L.M., Abad, A., García-Labiano, F., Diego, L.F., 2022. Life cycle assessment of power-to-methane systems with CO2 supplied by the chemical looping combustion of biomass. Energy Convers. Manage. 267, 115866. https://doi.org/10.1016/j.enconman.2022.115866.

Navarro, C., Zaidi, A., Leeuwe, C., Spallina, V., Grasa, G., 2024. Packed-bed chemical looping reforming for renewable syngas production from glycerol with Ni_Fe-based oxygen carriers/catalysts. Energy Fuels 38 (21), 20669–20680. https://doi.org/10.1021/acs.energyfuels.4c02863.

Nazir, S.M, Morgado, J.F, Bolland, O., Quinta-Ferreira, R., Amini, S., 2018. Techno-economic assessment of chemical looping reforming of natural gas for hydrogen production and power generation with integrated CO2 capture. Int. J. Greenhouse Gas Control 78, 7–20. https://doi.org/10.1016/j.ijggc.2018.07.022.

Nemati, N., Pallarès, D., Mattisson, T., Guío-Pérez, D.C, Rydén, M., 2024. Experimental investigation and modeling of the impact of random packings on mass transfer in fluidized beds. Powder. Technol. 440, 119781. https://doi.org/10.1016/j.powtec.2024.119781.

Neto, S., Szklo, A., Rochedo, P.R.R., 2021. Calcium looping post-combustion CO2 capture in sugarcane bagasse fuelled power plants. Int. J. Greenhouse Gas Control 110, 103401. https://doi.org/10.1016/j.ijggc.2021.103401.

Nicolucci, E., Palone, O., Colozzi, M., Borello, D., 2025. A novel model of a double fluidized bed steam gasifier for biomass and solid recovered fuel co-gasification. Int. J. Hydrogen Energy 177, 151620. https://doi.org/10.1016/j.ijhydene.2025.151620.

Nigitz, T., Gölles, M., Aichernig, C., Schneider, S., Hofbauer, H., Horn, M., 2020. Increased efficiency of dual fluidized bed plants via a novel control strategy. Biomass Bioenergy 141, 105688. https://doi.org/10.1016/j.biombioe.2020.105688.

Nikoo, M.K., Amin, N.A.S., 2011. Thermodynamic analysis of carbon dioxide reforming of methane in view of solid carbon formation. Fuel Process. Technol. 92 (3), 678–691. https://doi.org/10.1016/j.fuproc.2010.11.027.

Noorman, S., van Sint Annaland, M., Kuipers, 2007. Packed bed reactor technology for chemical-looping combustion. Ind. Eng. Chem. Res. 46 (12), 4212–4220. https://doi.org/10.1021/ie061178i.

Nordness, O., Han, L.u, Zhou, Z., Bollas, G.M., 2016. High-pressure chemical-looping of methane and synthesis gas with Ni and Cu oxygen carriers. Energy Fuels 30 (1), 504–514. https://doi.org/10.1021/acs.energyfuels.5b01986.

Ogidiama, O.V, Abu-Zahra, M.R.M., Shamim, T., 2018. Techno-economic analysis of a poly-generation solar-assisted chemical looping combustion power plant. Appl. Energy 228, 724–735. https://doi.org/10.1016/j.apenergy.2018.06.091.

Oh, D.H., Lee, C.H.A, Lee, J.C., 2021. Performance and cost analysis of natural gas combined cycle plants with chemical looping combustion. ACS Omega 6 (32), 21043–21058. https://doi.org/10.1021/acsomega.1c02695.

Ohlemüller, P., Busch, J.-P., Reitz, M., Ströhle, J., Epple, B., 2016. Chemical-looping combustion of hard coal: autothermal operation of a 1 MWth pilot plant. J. Energy Resour. Technol. 138 (4), 042203. https://doi.org/10.1115/1.4032357. Article.

Ohlemüller, P., Ströhle, J., Epple, B., 2017. Chemical looping combustion of hard coal and torrefied biomass in a 1 MW th pilot plant. Int. J. Greenhouse Gas Control 65, 149–159. https://doi.org/10.1016/j.ijggc.2017.08.013.

Ohlemüller, P., Alobaid, F., Abad, A., Adanez, J., Ströhle, J., Epple, B., 2018. Development and validation of a 1D process model with autothermal operation of a 1 MW th chemical looping pilot plant. Int. J. Greenhouse Gas Control 73, 29–41. https://doi.org/10.1016/j.ijggc.2018.03.013.

Ohlemüller, P., Reitz, M., Ströhle, J., Epple, B., 2019. Investigation of chemical looping combustion of natural gas at 1 MWth scale. Proc. Combus. Inst. 37 (4), 4353–4360. https://doi.org/10.1016/j.proci.2018.07.035.

Ortiz, M., Diego, L.F., Abad, A., García-Labiano, F., Gayán, P., Adánez, J., 2010. Hydrogen production by auto-thermal chemical-looping reforming in a pressurized fluidized bed reactor using Ni-based oxygen carriers. Int. J. Hydrogen Energy 35 (1), 151–160. https://doi.org/10.1016/j.ijhydene.2009.10.068.

Ortiz, M., Abad, A., Diego, L.F., García-Labiano, F., Gayán, P., Adánez, J., 2011. Optimization of hydrogen production by chemical-looping auto-thermal reforming working with Ni-based oxygen-carriers. Int. J. Hydrogen Energy 36 (16), 9663–9672. https://doi.org/10.1016/j.ijhydene.2011.05.025.

Ortiz, M., Diego, L.F., Abad, A., García-Labiano, F., Gayán, P., Adánez, J., 2012. Catalytic activity of Ni-based oxygen-carriers for steam methane reforming in chemical-looping processes. Energy Fuels 26 (2), 791–800. https://doi.org/10.1021/ef2013612.

Ortiz, C., Chacartegui, R., Valverde, J.M., Alovisio, A., Becerra, J.A., 2017. Power cycles integration in concentrated solar power plants with energy storage based on calcium looping. Energy Convers. Manage 149, 815–829. https://doi.org/10.1016/j.enconman.2017.03.029.

Ortiz, C., Valverde, J.M., Chacartegui, R., Perez-Maqueda, L.A., Giménez, P., 2019. The Calcium-Looping (CaCO3/CaO) process for thermochemical energy storage in concentrating solar power plants. Renewable Sustainable Energy Rev. 113, 109252. https://doi.org/10.1016/j.rser.2019.109252.

Ortiz, C., Chacartegui, R., Valverde, J.M., Carro, A., Tejada, C., Valverde, J., 2021. Increasing the solar share in combined cycles through thermochemical energy storage. Energy Convers. Manage 229, 113730. https://doi.org/10.1016/j.enconman.2020.113730.

Osman, M., Zaabout, A., Cloete, S., Amini, S., 2019. Internally circulating fluidized-bed reactor for syngas production using chemical looping reforming. Chem. Eng. J. 377, 120076. https://doi.org/10.1016/j.cej.2018.10.013.

Osman, M., Zaabout, A., Cloete, S., Amini, S., 2020. Mapping the operating performance of a novel internally circulating fluidized bed reactor applied to chemical looping combustion. Fuel Process. Technol. 197, 106183. https://doi.org/10.1016/j.fuproc.2019.106183.

Osman, M., Khan, M.N., Zaabout, A., Cloete, S., Amini, S., 2021. Review of pressurized chemical looping processes for power generation and chemical production with integrated CO2 capture. Fuel Process. Technol. 214, 106684. https://doi.org/10.1016/j.fuproc.2020.106684.

Osman, A.I., Nasr, M., Mohamed, A.R., Abdelhaleem, A., Ayati, A., Farghali, M., et al., 2024. Life cycle assessment of hydrogen production, storage, and utilization toward sustainability. WIREs Energy Environ. 13 (3), e526. https://doi.org/10.1002/wene.526. Article.

Pachler, R.F., Penthor, S., Mayer, K., Hofbauer, H., 2020. Investigation of the fate of nitrogen in chemical looping combustion of gaseous fuels using two different oxygen carriers. Energy 195, 116926. https://doi.org/10.1016/j.energy.2020.116926.

Panitz, F.; Kaltenmorgen, J.; Siodlaczek, M.; Ströhle, J.; Epple, B. (2025): Fluidized bed gasification of plastic waste and residual biomass – an overview of HTW® and Chemical looping technology development.

Pankhedkar, N., Sartape, R., Singh, M.R., Gudi, R., Biswas, P., Bhargava, S., 2024. System-level feasibility analysis of a novel chemical looping combustion integrated with electrochemical CO 2 reduction. Sustainable Energy Fuels 8 (16), 3688–3703. https://doi.org/10.1039/D4SE00770K.

Papa, A.A, Tacconi, A., Savuto, E., Ciro, E., Hatunoglu, A., Foscolo, P.U, et al., 2023. Performance evaluation of an innovative 100 kWth dual bubbling fluidized bed gasifier through two years of experimental tests: results of the BLAZE project. Int. J. Hydrogen. Energy 48 (70), 27170–27181. https://doi.org/10.1016/j.ijhydene.2023.03.439.

Park, C., Joshi, R.K., Falascino, E., Pottimurthy, Y., Xu, D., Wang, D., et al., 2023. Biomass gasification: sub-pilot operation of >600 h with extensive tar cracking property and high purity syngas production at H2:CO ratio ~2 using moving bed redox looping technology. Fuel Process. Technol. 252, 107966. https://doi.org/10.1016/j.fuproc.2023.107966.

Parkkinen, J., Myöhänen, K., Abanades, J.C, Arias, B., Hyppänen, T., 2017. Modelling a calciner with high inlet oxygen concentration for a calcium looping process. Energy Procedia 114, 242–249. https://doi.org/10.1016/j.egypro.2017.03.1166.

Parvez, A.M, Hafner, S., Hornberger, M., Schmid, M., Scheffknecht, G., 2021. Sorption enhanced gasification (SEG) of biomass for tailored syngas production with in-situ CO2 capture: current status, process scale-up experiences and outlook. Renewable Sustainable Energy Rev. 141, 110756. https://doi.org/10.1016/j.rser.2021.110756.

Patil, C.S., van Sint Annaland, M., Kuipers, J.A.M., 2007. Fluidised bed membrane reactor for ultrapure hydrogen production via methane steam reforming: experimental demonstration and model validation. Chem. Eng. Sci. 62 (11), 2989–3007. https://doi.org/10.1016/j.ces.2007.02.022.

Peloriadi, K., Atsonios, K., Nikolopoulos, A., Intzes, K., Dimitriadis, G., Nikolopoulos, N., 2021. Process integration of indirectly heated carbonate looping in lime plant for enhanced CO2 capture. TCCS-11: CO2 capture, transport and storage, Trondheim, 22nd-23rd June 2021. In: Røkke, N.A., Hanna, K., Knuutila, (Hg.) (Eds.), Short papers from the 11th International Trondheim CCS Conference. Trondheim, Norway. SINTEF. Oslo: SINTEF Academic Press, pp. 515–522. June 21–23SINTEF proceedings, 7.

Peltola, P., Alobaid, F., Tynjälä, T., Ritvanen, J., 2022. Overview of fluidized bed reactor modeling for chemical looping combustion: status and research needs. Energy Fuels 36 (17), 9385–9409. https://doi.org/10.1021/acs.energyfuels.2c01680.

Perejón, A., Romeo, L.M., Lara, Y., Lisbona, P., Martínez, A., Valverde, J.M, 2016. The Calcium-Looping technology for CO2 capture: on the important roles of energy integration and sorbent behavior. Appl. Energy 162, 787–807. https://doi.org/10.1016/j.apenergy.2015.10.121.

Perpiñán, J., Peña, B., Bailera, M., Eveloy, V., Kannan, P., Raj, A., et al., 2023. Integration of carbon capture technologies in blast furnace based steel making: a comprehensive and systematic review. Fuel 336, 127074. https://doi.org/10.1016/j.fuel.2022.127074.

Pfeifer, C., Puchner, B., Hofbauer, H., 2007. In-situ CO2-absorption in a dual fluidized bed biomass steam gasifier to produce a hydrogen rich syngas. Int. J. Chem. Reactor Eng. 5 (1). https://doi.org/10.2202/1542-6580.1395.

Phalak, N., Wang, W., Fan, L.-S., 2013. Ca(OH) 2 -based calcium looping process development at the Ohio state university. Chem. Eng. Technol. 36 (9), 1451–1459. https://doi.org/10.1002/ceat.201200707.

Piso, G.C, Bareschino, P., Brachi, P., Tregambi, C., Ruoppolo, G., Pepe, F., Mancusi, E., 2023. Numerical simulation of biogas chemical looping reforming in a dual fluidized bed reactor. Renew. Energy 212, 350–358. https://doi.org/10.1016/j.renene.2023.05.060.

Pissot, S., Teresa, B.V, Maric, J., Seemann, M., 2018. Chemical looping gasification in a 2-4 MWth dual fluidized bed gasifier. In: 23rd International Conference on Fluidized Bed Conversion. Seoul, South Korea.

Porrazzo, R., White, G., Ocone, R., 2016. Techno-economic investigation of a chemical looping combustion based power plant. Faraday Discuss 192, 437–457. https://doi.org/10.1039/C6FD00033A.

Pröll, T., Lyngfelt, A., 2022. Steam methane reforming with chemical-looping combustion: scaling of fluidized-bed-heated reformer tubes. Energy Fuels 36 (17), 9502–9512. https://doi.org/10.1021/acs.energyfuels.2c01086.

Pröll, T., Mayer, K., Bolhàr-Nordenkampf, J., Kolbitsch, P., Mattisson, T., Lyngfelt, A., Hofbauer, H., 2009. Natural minerals as oxygen carriers for chemical looping combustion in a dual circulating fluidized bed system. Energy Procedia 1 (1), 27–34. https://doi.org/10.1016/j.egypro.2009.01.006.

Pröll, T., Bolhàr-Nordenkampf, J., Kolbitsch, P., Hofbauer, H., 2010. Syngas and a separate nitrogen/argon stream via chemical looping reforming – a 140kW pilot plant study. Fuel 89 (6), 1249–1256. https://doi.org/10.1016/j.fuel.2009.09.033.

Puig-Gamero, M., Pio, D.T., Tarelho, L.A.C., Sánchez, P., Sanchez-Silva, L., 2021. Simulation of biomass gasification in bubbling fluidized bed reactor using aspen plus®. Energy Convers. Manage. 235, 113981. https://doi.org/10.1016/j.enconman.2021.113981.

Qasim, M., Ayoub, M., Ghazali, N.A, Aqsha, A., Ameen, M., 2021. Recent advances and development of various oxygen carriers for the chemical looping combustion process: a review. Ind. Eng. Chem. Res. 60 (24), 8621–8641. https://doi.org/10.1021/acs.iecr.1c01111.

Qayyum, H., Cheema, I.I, Abdullah, M., Amin, M., Khan, I.A, Lee, E.-J., Lee, K.H, 2023. One-dimensional modeling of heterogeneous catalytic chemical looping steam methane reforming in an adiabatic packed bed reactor. Front. Chem. 11, 1295455. https://doi.org/10.3389/fchem.2023.1295455.

Qi, J., Liu, J., Chen, G., Yao, J., Yan, B., Yi, W., et al., 2023. Hydrogen production from municipal solid waste via chemical looping gasification using CuFe2O4 spinel as oxygen carrier: an Aspen Plus modeling. Energy Convers. Manage. 294, 117562. https://doi.org/10.1016/j.enconman.2023.117562.

Raganati, F., Ammendola, P., 2023. Review of carbonate-based systems for thermochemical energy storage for concentrating solar power applications: state-of-the-art and outlook. Energy Fuels 37 (3), 1777–1808. https://doi.org/10.1021/acs.energyfuels.2c03853.

Rai, C., Bhui, B., V, P., 2022. Techno-economic analysis of e-waste based chemical looping reformer as hydrogen generator with co-generation of metals, electricity and syngas. Int. J. Hydrogen Energy 47 (21), 11177–11189. https://doi.org/10.1016/j.ijhydene.2022.01.159.

Ramezani, R., Luca, D.iF., Gallucci, F., 2023. A review of chemical looping reforming technologies for hydrogen production: recent advances and future challenges. J. Phys. Energy 5 (2), 024010. https://doi.org/10.1088/2515-7655/acc4e8.

Ramkumar, S., Fan, L.-S., 2010. Thermodynamic and experimental analyses of the three-stage calcium looping process. Ind. Eng. Chem. Res. 49 (16), 7563–7573. https://doi.org/10.1021/ie100846u.

Rashidi, H., Duffy, A., Doherty, W., 2025. A detailed general model of the gasification zone of a dual fluidised bed gasifier. Biomass Conv. Bioref. 15 (15), 21745–21760. https://doi.org/10.1007/s13399-022-02529-7.

Readman, J.E., Olafsen, A., Smith, J.B., Blom, R., 2006. Chemical looping combustion using NiO/NiAl 2 O 4: mechanisms and kinetics of reduction−oxidation (Red-Ox) reactions from in situ powder X-ray diffraction and thermogravimetry experiments. Energy Fuels 20 (4), 1382–1387. https://doi.org/10.1021/ef0504319.

RECYCLE Consortium, 2022. REthinking low Carbon hYdrogen production by Chemical Looping rEforming, RECYCLE. Feasibility Study Technical Report – Final. Available online at https://assets.publishing.service.gov.uk/media/64679002628371000c3a891f/HYS2137_The_University_of_Manchester_Final_Feasibility_Report_Public_.pdf.

Reinking, Z., Whitty, K.J., Lighty, J.oA.S., 2021. A simulation-based parametric study of CLOU chemical looping reactor performance. Fuel Process. Technol. 215, 106755. https://doi.org/10.1016/j.fuproc.2021.106755.

Reitz, M., Junk, M., Ströhle, J., Epple, B., 2014. Design and erection of a 300 kWth indirectly heated carbonate looping test facility. Energy Procedia 63, 2170–2177.

Reitz, M., Junk, M., Ströhle, J., Epple, B., 2016. Design and operation of a 300 kWth indirectly heated carbonate looping pilot plant. Int. J. Greenhouse Gas Control 54, 272–281. https://doi.org/10.1016/j.ijggc.2016.09.016.

Reitz, M., 2017. Experimentelle Untersuchung und Bewertung eines indirekt beheizten Carbonate-Looping-Prozesses. Doctoral dissertation, 1st ed. Cuvillier Verlag, Göttingen.

Rezvani, S., Rolfe, A., Franco, F., Brandoni, C., Böge, K., Hewitt, N., Huang, Y.e, 2025. Indirectly heated carbonate looping cycles in cement plants for CO2 capture and storage. Appl. Therm. Eng. 263, 125349. https://doi.org/10.1016/j.applthermaleng.2024.125349.

Ritvanen, J., Myöhänen, K., Pitkäoja, A., Hyppänen, T., 2021. Modeling of industrial-scale sorption enhanced gasification process: One-dimensional simulations for the operation of coupled reactor system. Energy 226, 120387. https://doi.org/10.1016/j.energy.2021.120387.

Riva, L., Martínez, I., Martini, M., Gallucci, F., van Sint Annaland, M., Romano, M.C, 2018. Techno-economic analysis of the Ca-Cu process integrated in hydrogen plants with CO2 capture. Int. J. Hydrogen. Energy 43 (33), 15720–15738. https://doi.org/10.1016/j.ijhydene.2018.07.002.

Rodríguez, N., Alonso, M., Abanades, J.C, 2010. Average activity of CaO particles in a calcium looping system. Chem. Eng. J. 156 (2), 388–394. https://doi.org/10.1016/j.cej.2009.10.055.

Rolfe, A., Huang, Y., Haaf, M., Pita, A., Rezvani, S., Dave, A., Hewitt, N.J., 2018. Technical and environmental study of calcium carbonate looping versus oxy-fuel options for low CO2 emission cement plants. Int. J. Greenhouse Gas Control 75, 85–97. https://doi.org/10.1016/j.ijggc.2018.05.020.

Romano, M.C., 2012. Modeling the carbonator of a Ca-looping process for CO2 capture from power plant flue gas. Chem. Eng. Sci. 69 (1), 257–269. https://doi.org/10.1016/j.ces.2011.10.041.
Rougé, S., Criado, A., Yolanda, Soriano, O., Abanades, J.C., 2017. Continuous CaO/Ca(OH) 2 fluidized bed reactor for energy storage: first experimental results and reactor model validation. Ind. Eng. Chem. Res. 56 (4), 844–852. https://doi.org/10.1021/acs.iecr.6b04105.
Rydén, M., Ramos, P., 2012. H2 production with CO2 capture by sorption enhanced chemical-looping reforming using NiO as oxygen carrier and CaO as CO2 sorbent. Fuel Process. Technol. 96, 27–36. https://doi.org/10.1016/j.fuproc.2011.12.009.
Rydén, M., Lyngfelt, A., Mattisson, T., 2006. Synthesis gas generation by chemical-looping reforming in a continuously operating laboratory reactor. Fuel 85 (12-13), 1631–1641. https://doi.org/10.1016/j.fuel.2006.02.004.
Rydén, M., Lyngfelt, A., Mattisson, T., 2008. Chemical-looping combustion and chemical-looping reforming in a circulating fluidized-bed reactor using Ni-based oxygen carriers. Energy Fuels 22 (4), 2585–2597. https://doi.org/10.1021/ef800065m.
Rydén, M., Johansson, M., Lyngfelt, A., Mattisson, T., 2009. NiO supported on Mg–ZrO2 as oxygen carrier for chemical-looping combustion and chemical-looping reforming. Energy Environ. Sci. 2 (9), 970. https://doi.org/10.1039/b904370e.
Rydén, M., Jing, D., Källén, M., Leion, H., Lyngfelt, A., Mattisson, T., 2014. CuO-based oxygen-carrier particles for chemical-Looping with oxygen uncoupling – experiments in batch reactor and in continuous operation. Ind. Eng. Chem. Res. 53 (15), 6255–6267. https://doi.org/10.1021/ie4039983.
Santos, M.P.S., Hanak, D.P, 2022. Carbon capture for decarbonisation of energy-intensive industries: a comparative review of techno-economic feasibility of solid looping cycles. Front. Chem. Sci. Eng. 16 (9), 1291–1317. https://doi.org/10.1007/s11705-022-2151-5.
Sattari, F., Tahmasebpoor, M., Valverde, J.M, Ortiz, C., Mohammadpourfard, M., 2021. Modelling of a fluidized bed carbonator reactor for post-combustion CO2 capture considering bed hydrodynamics and sorbent characteristics. Chem. Eng. J. 406, 126762. https://doi.org/10.1016/j.cej.2020.126762.
Sayeed, I., Kibria, M.A., Bhattacharya, S., 2022. Process modelling and techno-economic analysis of a 550MWe chemical looping power plant with Victorian brown coal. Int. J. Greenhouse Gas Control 113, 103547. https://doi.org/10.1016/j.ijggc.2021.103547.
Scaltsoyiannes, A.A., Lemonidou, A.A, 2021. On the factors affecting the deactivation of limestone under calcium looping conditions: a new comprehensive model. Chem. Eng. Sci. 243, 116797. https://doi.org/10.1016/j.ces.2021.116797. Article.
Scaltsoyiannes, A.A., Antzaras, A., Koilaridis, G., Lemonidou, A., 2021. Towards a generalized carbonation kinetic model for CaO-based materials using a modified random pore model. Chem. Eng. J. 407, 127207. https://doi.org/10.1016/j.cej.2020.127207.
Schakel, W., Hung, C.R, Tokheim, L.A., Strømman, A.H, Worrell, E., Ramírez, A., 2018. Impact of fuel selection on the environmental performance of post-combustion calcium looping applied to a cement plant. Appl. Energy 210, 75–87. https://doi.org/10.1016/j.apenergy.2017.10.123.
Schmid, M., Beirow, M., Schweitzer, D., Waizmann, G., Spörl, R., Scheffknecht, G., 2018. Product gas composition for steam-oxygen fluidized bed gasification of dried sewage sludge, straw pellets and wood pellets and the influence of limestone as bed material. Biomass Bioenergy 117, 71–77. https://doi.org/10.1016/j.biombioe.2018.07.011.
Schmid, J.C, Benedikt, F., Fuchs, J., Mauerhofer, A.M, Müller, S., Hofbauer, H., 2021a. Syngas for biorefineries from thermochemical gasification of lignocellulosic fuels and residues—5 years' experience with an advanced dual fluidized bed gasifier design. Biomass Conv. Bioref. 11 (6), 2405–2442. https://doi.org/10.1007/s13399-019-00486-2.
Schmid, M., Hafner, S., Biollaz, S., Schneebeli, J., Waizmann, G., Scheffknecht, G., 2021b. Steam-oxygen gasification of sewage sludge: Reduction of tar, H2S and COS with limestone as bed additive. Biomass Bioenergy 150, 106100. https://doi.org/10.1016/j.biombioe.2021.106100.
Schmitz, M., Linderholm, C., Hallberg, P., Sundqvist, S., Lyngfelt, A., 2016. Chemical-looping combustion of solid fuels using manganese ores as oxygen carriers. Energy Fuels. https://doi.org/10.1021/acs.energyfuels.5b02440.
Schwebel, G.L., Gipperich, A., Krumm, W., 2012. Design considerations of chemical-looping systems incorporating a moving bed fuel reactor (MBFR). In: 2nd International Conference on Chemical Looping. Darmstadt, Germany.
Secomandi, M., Nikku, M., Arias, B., Ritvanen, J., 2024. A conceptual evaluation of the use of Ca(OH)2 for attaining carbon capture rates of 99% in the calcium looping process. Int. J. Greenhouse Gas Control 139, 104279. https://doi.org/10.1016/j.ijggc.2024.104279.
Seyyedattar, M., Zendehboudi, S., 2026. Carbon capture and storage: a comprehensive review on current trends, techniques, and future prospects in North America. Fuel 407, 137276. https://doi.org/10.1016/j.fuel.2025.137276.
Shao, Y., Agarwal, R.K., Wang, X., Jin, B., 2021. Review of computational fluid dynamics studies on chemical looping combustion. J. Energy Resour. Technol. 143 (8), 080802. https://doi.org/10.1115/1.4048680. Article.
Shen, L., Wu, J., Gao, Z., Xiao, J., 2010. Characterization of chemical looping combustion of coal in a 1kWth reactor with a nickel-based oxygen carrier. Combust. Flame 157 (5), 934–942. https://doi.org/10.1016/j.combustflame.2009.10.009.
Shen, T., Wu, J., Shen, L., Yan, J., Jiang, S., 2018. Chemical looping gasification of coal in a 5 kW th interconnected fluidized bed with a two-stage fuel reactor. Energy Fuels 32 (4), 4291–4299. https://doi.org/10.1021/acs.energyfuels.7b03111.
Shen, T., Wang, S., Yan, J., Shen, L., Tian, H., 2020. Performance improvement of chemical looping combustion with coal by optimizing operational strategies in a 3 kWth interconnected fluidized bed. Int. J. Greenhouse Gas Control 98, 103060. https://doi.org/10.1016/j.ijggc.2020.103060.
Siriwardane, R., Riley, J., Benincosa, W., Bayham, S., Bobek, M., Straub, D., Weber, J., 2021. Development of CuFeMnAlO4+δ oxygen carrier with high attrition resistance and 50-kWth methane/air chemical looping combustion tests. Appl. Energy 286, 116507. https://doi.org/10.1016/j.apenergy.2021.116507.
Sison, A.E., Etchieson, S.A., Güleç, F., Epelle, E.I., Okolie, J.A, 2023. Process modelling integrated with interpretable machine learning for predicting hydrogen and char yield during chemical looping gasification. J. Clean. Prod. 414, 137579. https://doi.org/10.1016/j.jclepro.2023.137579.
Spallina, V., Marinello, B., Gallucci, F., Romano, M.C., van Sint Annaland, M., 2017. Chemical looping reforming in packed-bed reactors: modelling, experimental validation and large-scale reactor design. Fuel Process. Technol. 156, 156–170. https://doi.org/10.1016/j.fuproc.2016.10.014.
Spinelli, M., Martínez, I., Romano, M.C., 2018. One-dimensional model of entrained-flow carbonator for CO2 capture in cement kilns by Calcium looping process. Chem. Eng. Sci. 191, 100–114. https://doi.org/10.1016/j.ces.2018.06.051.
Spyroglou, S.G., Skaltsogiannis, A.A., Yiantsios, S.G., Lemonidou, A.A., 2024. Multiscale modeling of an entrained flow solar calciner for thermochemical energy storage via calcium looping. Chem. Eng. J. 486, 150171. https://doi.org/10.1016/j.cej.2024.150171. Article.
Störner, F., Faust, R., Knutsson, P., Rydén, M., 2025. Oxygen carrier aided combustion with copper smelter slag as bed material in a semi-commercial wood-fired circulating fluidized bed. Biomass Bioenergy 193, 107565. https://doi.org/10.1016/j.biombioe.2024.107565.
Stanger, R., Wall, T., Spörl, R., Paneru, M., Grathwohl, S., Weidmann, M., et al., 2015. Oxyfuel combustion for CO2 capture in power plants. Int. J. Greenhouse Gas Control 40, 55–125. https://doi.org/10.1016/j.ijggc.2015.06.010.
Stanger, L., Schirrer, A., Bartik, A., Kozek, M., 2023a. Minimum-variance model predictive control for dual fluidized bed circulation control. IFAC-PapersOnLine 56 (2), 2701–2706. https://doi.org/10.1016/j.ifacol.2023.10.1364.
Stanger, L., Schirrer, A., Benedikt, F., Bartik, A., Jankovic, S., Müller, S., Kozek, M., 2023b. Dynamic modeling of dual fluidized bed steam gasification for control design. Energy 265, 126378. https://doi.org/10.1016/J.ENERGY.2022.126378.
Stanger, L., Bartik, A., Binder, M., Schirrer, A., Jakubek, S., Kozek, M., 2024a. Gaussian process regression-based control of solids circulation rate in dual fluidized bed gasification. IEEe Access 12, 138535–138546. https://doi.org/10.1109/ACCESS.2024.3466394.
Stanger, L., Bartik, A., Hammerschmid, M., Jankovic, S., Benedikt, F., Müller, S., et al., 2024b. Model predictive control of a dual fluidized bed gasification plant. Appl. Energy 361, 122917. https://doi.org/10.1016/j.apenergy.2024.122917.
Staničić, I., Mattisson, T., Backman, R., Cao, Y.u, Rydén, M., 2021. Oxygen carrier aided combustion (OCAC) of two waste fuels - Experimental and theoretical study of the interaction between ilmenite and zinc, copper and lead. Biomass Bioenergy 148, 106060. https://doi.org/10.1016/j.biombioe.2021.106060.
Staničić, I., Mattisson, T., Brorsson, J., Hellman, A., Rydén, M., Casabella, F., Judit, et al., 2025. Achieving BECCS with chemical looping combustion. In: Lutz, N., de Joannis, P., Alvarado Cummings, C., Schwingshackl, C., von Rothkirch, J., Müller-Hansen, F., et al. (Eds.), (Hg.): 3rd International Conference on Negative CO2 Emissions Conference Proceedings. University of Oxford. Unter Mitarbeit von S. Smith und N. Lutz.
Staničić, I., Rydén, M., Störner, F., Lind, F., Mattisson, T., 2026. Oxygen carrier aided combustion. Chemical Looping Processes. Elsevier, pp. 107–136.
Ströhle, J., Junk, M., Kremer, J., Galloy, A., Epple, B., 2014a. Carbonate looping experiments in a 1MWth pilot plant and model validation. Fuel 127, 13–22. https://doi.org/10.1016/j.fuel.2013.12.043.
Ströhle, J., Orth, M., Epple, B., 2014b. Design and operation of a 1 MWth chemical looping plant. Appl. Energy 113, 1490–1495. https://doi.org/10.1016/j.apenergy.2013.09.008.
Ströhle, J., Hilz, J., Epple, B., 2020. Performance of the carbonator and calciner during long-term carbonate looping tests in a 1 MWth pilot plant. J. Environ. Chem. Eng. 8 (1), 103578. https://doi.org/10.1016/j.jece.2019.103578. Article.
und Ströhle, J., Hofmann, C., Greco-Coppi, M., Epple, B., 2021. CO2 capture from lime and cement plants using an indirectly heated carbonate looping process – The ANICA project, TCCS-11: CO2 capture, transport and storage, Trondheim, 22nd-23rd June 2021. In: Røkke, N.A., Hanna, K.K (Eds.), Short papers from the 11th International Trondheim CCS Conference. Trondheim, Norway. SINTEF. Oslo: SINTEF Academic Press (SINTEF proceedings, pp. 529–535. June 21–237.
Ströhle, J., 2023. Chemical looping combustion of waste-opportunities and challenges. Energy Fuels 37 (3), 1465–1471. https://doi.org/10.1021/acs.energyfuels.2c04297.
Styles, D.; Bishop, G.; Ofori, E.; Hennig, C.; Bang, C.; Bentsen, N.S et al., (2025): BECCUS science & policy. WP7 Summary Report. Hg. v. Christiane Hennig. IEA Bioenergy.
Suárez-Almeida, M., Gómez-Barea, A., Ghoniem, A.F., Pfeifer, C., 2021. Solar gasification of biomass in a dual fluidized bed. Chem. Eng. J. 406, 126665. https://doi.org/10.1016/j.cej.2020.126665.
Suárez-Almeida, M., Gómez-Barea, A., Salinero, J., 2023. Design and performance analysis of a solar dual fluidized bed gasifier. Fuel 338, 127031. https://doi.org/10.1016/j.fuel.2022.127031.
Sun, Z., Aziz, M., 2022. Solar-assisted biomass chemical looping gasification in an indirect coupling: principle and application. Appl. Energy 323, 119635. https://doi.org/10.1016/j.apenergy.2022.119635.
Sun, P., Grace, J.R., Lim, C.J., Anthony, E.J, 2008. Determination of intrinsic rate constants of the CaO–CO2 reaction. Chem. Eng. Sci. 63 (1), 47–56. https://doi.org/10.1016/j.ces.2007.08.055.
Sun, H., Wu, C., Shen, B., Zhang, X., Zhang, Y., Huang, J., 2018. Progress in the development and application of CaO-based adsorbents for CO2 capture—a review. Mater. Today Sustainability 1-2, 1–27. https://doi.org/10.1016/j.mtsust.2018.08.001.

Sun, S., Lv, Z., Qiao, Y., Qin, C., Xu, S., Wu, C., 2021. Integrated CO2 capture and utilization with CaO-alone for high purity syngas production. Carbon Capture Sci. Technol. 1, 100001. https://doi.org/10.1016/j.ccst.2021.100001.
Sun, H., Bao, G., Yang, S., Hu, J., Wang, H., 2023a. Numerical study of the biomass gasification process in an industrial-scale dual fluidized bed gasifier with 8MWth input. Renew. Energy 211, 681–696. https://doi.org/10.1016/j.renene.2023.04.118.
Sun, H., Yang, S., Bao, G., Luo, K., Hu, J., Wang, H., 2023b. CFD investigation of the complex multiphase flow of biomass gasification in industrial-scale dual fluidized bed reactor. Chem. Eng. J. 457, 141312. https://doi.org/10.1016/j.cej.2023.141312.
Sun, H., Bao, G., Yang, S., Hu, J., Wang, H., 2024. Numerical investigation on the influence of immersed tube bundles on biomass gasification in industrial-scale dual fluidized bed gasifier. Fuel 357, 129742. https://doi.org/10.1016/j.fuel.2023.129742.
Sundqvist, S., Arjmand, M., Mattisson, T., Rydén, M., Lyngfelt, A., 2015. Screening of different manganese ores for chemical-looping combustion (CLC) and chemical-looping with oxygen uncoupling (CLOU). Int. J. Greenhouse Gas Control 43, 179–188. https://doi.org/10.1016/j.ijggc.2015.10.027.
Surywanshi, G.D, Leion, H., Soleimanisalim, A.H, 2024. Energy, exergy, economic and exergoeconomic analyses of chemical looping combustion plant using waste bark for district heat and power generation with negative emissions. Energy Tech 12 (2), 2300577. https://doi.org/10.1002/ente.202300577. Article.
Svensson, E., Wiertzema, H., Harvey, 2021. Potential for negative emissions by carbon capture and storage from a novel electric plasma calcination process for pulp and paper mills. Front. Clim. 3, 705032. https://doi.org/10.3389/fclim.2021.705032. Article.
Tan, Y., Liu, W., Zhang, X., Wei, W., Wang, 2024. Conventional and optimized testing facilities of calcium looping process for CO2 capture: a systematic review. Fuel 358, 130337. https://doi.org/10.1016/j.fuel.2023.130337. Article.
Teng, S., Zhou, Y.X, Xv, Y., Zhuang, K.e, Zhou, K., Zhang, Q., et al., 2024. CFD-DEM simulation of chemical looping hydrogen generation in a moving bed reactor. Int. J. Chem. Reactor Eng. 22 (5), 529–546. https://doi.org/10.1515/ijcre-2024-0001.
Tescari, S., Sundarraj, P., Moumin, G., Duarte, J.PR., Agrafiotis, C., Oliveira, L., et al., 2020. Solar rotary kiln for continuous treatment of particle material: Chemical experiments from micro to milli meter particle size. In: SOLARPACES 2019: International Conference on Concentrating Solar Power and Chemical Energy Systems. SOLARPACES 2019: International Conference on Concentrating Solar Power and Chemical Energy Systems. Daegu, South Korea. AIP Publishing (AIP Conference Proceedings, 140007.
Thunman, H., Seemann, M.C., 2010. First experiences with the new chalmers gasifier. In: Yue, G., Zhang, H. (Eds.), Changsui Zhao und Zhongyang Luo (Hg.): Proceedings of the 20th International Conference on Fluidized Bed Combustion. Berlin, Heidelberg. Springer Berlin Heidelberg, pp. 659–663.
Thunman, H., Gustavsson, C., Larsson, A., Gunnarsson, I., Tengberg, F., 2019. Economic assessment of advanced biofuel production via gasification using cost data from the GoBiGas plant. Energy Sci. Eng. 7 (1), 217–229. https://doi.org/10.1002/ese3.271.
Tian, S., Jiang, J., Zhang, Z., Manovic, V., 2018. Inherent potential of steelmaking to contribute to decarbonisation targets via industrial carbon capture and storage. Nat. Commun. 9 (1), 4422. https://doi.org/10.1038/s41467-018-06886-8.
Tizfahm, M., Tahmasebpoor, M., Behtash, H.R, Balsamo, M., Montagnaro, F., 2024. Coupled kinetic and hydrodynamic model for a carbonator reactor of calcium looping process: Sulfur dioxide effect. Process Saf. Environ. Prot. 185, 1205–1218. https://doi.org/10.1016/j.psep.2024.03.065.
Toffolo, K., Meunier, S., Ricardez-Sandoval, L., 2024. Optimal operation of a large-scale packed bed chemical-looping combustion process using nonlinear model predictive control. Fuel 357, 129876. https://doi.org/10.1016/j.fuel.2023.129876.
Tong, A., Bayham, S., Kathe, M.V., Zeng, L., Luo, S., Fan, L.S., 2014. Iron-based syngas chemical looping process and coal-direct chemical looping process development at Ohio State University. Appl. Energy 113, 1836–1845. https://doi.org/10.1016/j.apenergy.2013.05.024.
Tregambi, C., Bareschino, P., Hanak, D.P., Mancusi, E., Pepe, F., 2021a. Technoeconomic analysis of a fixed bed system for single/two–stage chemical looping combustion. Energy Tech 9 (10), 2100538. https://doi.org/10.1002/ente.202100538. Article.
Tregambi, C., Troiano, M., Montagnaro, F., Solimene, R., Salatino, P., 2021b. Fluidized beds for concentrated solar thermal technologies—a review. Front. Energy Res. 9, 618421. https://doi.org/10.3389/fenrg.2021.618421. Article.
Turrado, S., Arias, B., Fernández, J.R, Abanades, J.C, 2018. Carbonation of fine CaO particles in a drop tube reactor. Ind. Eng. Chem. Res. 57 (40), 13372–13380. https://doi.org/10.1021/acs.iecr.8b02918.
Ugwu, A., Del Arnaiz Pozo, C., Zaabout, A., Nazir, S.M, Kalendar, N.U, Cloete, S., et al., 2022. Gas switching technology: economic attractiveness for chemical looping applications and scale up experience to 50 kWth. Int. J. Greenhouse Gas Control 114, 103593. https://doi.org/10.1016/j.ijggc.2022.103593.
Vin, N., Bakoc, K., Lambert, A., Pelletant, W., Bertholin, S., 2022. Chemical looping combustion of petcoke using two natural ores in a 10 kW th continuous pilot plant: a performance comparison. Energy Fuels 36 (17), 9485–9501. https://doi.org/10.1021/acs.energyfuels.2c00439.
Voitic, G., Hacker, V., 2016. Recent advancements in chemical looping water splitting for the production of hydrogen. RSC Adv. 6 (100), 98267–98296. https://doi.org/10.1039/C6RA21180A.
Voldsund, M., Gardarsdottir, S., Lena, E., Pérez-Calvo, J.-F., Jamali, A., Berstad, D., et al., 2019. Comparison of technologies for CO2 capture from cement production—part 1: technical evaluation. Energies (Basel) 12 (3), 559. https://doi.org/10.3390/en12030559.
Wan, H., Feng, F., Yan, B., Liu, J., Chen, G., Yao, J., 2024. Methanation of syngas from biomass gasification in a dual fluidized bed: an Aspen plus modeling. Energy Convers. Manage. 318, 118902. https://doi.org/10.1016/j.enconman.2024.118902.
Wang, W., Ramkumar, S., Li, S., Wong, D., Iyer, M., Sakadjian, B.B., et al., 2010. Subpilot demonstration of the carbonation−calcination reaction (CCR) process: high-temperature CO2 and sulfur capture from coal-fired power plants. Ind. Eng. Chem. Res. 49 (11), 5094–5101. https://doi.org/10.1021/ie901509k.
Wang, C., Chen, Y., Cheng, Z., Luo, X., Jia, L., Song, M., et al., 2015. Sorption-enhanced steam reforming of glycerol for hydrogen production over a NiO/NiAl 2 O 4 catalyst and Li 2 ZrO 3 -based sorbent. Energy Fuels 29 (11), 7408–7418. https://doi.org/10.1021/acs.energyfuels.5b01941.
Wang, X., Wang, X., Kong, Z., Shao, Y., Jin, B., 2020. Auto-thermal operation and optimization of coal-fueled separated gasification chemical looping combustion in a pilot-scale unit. Chem. Eng. J. 383, 123159. https://doi.org/10.1016/j.cej.2019.123159.
Wang, Z., Ku, X., Lin, J., Liu, Z., 2025. Hot-state chemical looping gasification with continuous biomass feeding: a full-loop 3D simulation study. Chem. Eng. J. 524, 169201. https://doi.org/10.1016/j.cej.2025.169201.
Wassie, S.A., Medrano, J.A., Zaabout, A., Cloete, S., Melendez, J., Tanaka, D.A.P, et al., 2018. Hydrogen production with integrated CO2 capture in a membrane assisted gas switching reforming reactor: proof-of-concept. Int. J. Hydrogen Energy 43 (12), 6177–6190. https://doi.org/10.1016/j.ijhydene.2018.02.040.
Wei, G., He, F., Huang, Z., Zheng, A., Zhao, K., Li, H., 2015a. Continuous operation of a 10 kW th chemical looping integrated fluidized bed reactor for gasifying biomass using an iron-based oxygen carrier. Energy Fuels 29 (1), 233–241. https://doi.org/10.1021/ef5021457.
Wei, G., He, F., Zhao, Z., Huang, Z., Zheng, A., Zhao, K., Li, H., 2015b. Performance of Fe–Ni bimetallic oxygen carriers for chemical looping gasification of biomass in a 10 kWth interconnected circulating fluidized bed reactor. Int. J. Hydrogen Energy 40 (46), 16021–16032. https://doi.org/10.1016/j.ijhydene.2015.09.128.
Wojnicka, B., Ściążko, M., Schmid, J.C, 2021. Modelling of biomass gasification with steam. Biomass Conv. Bioref. 11 (5), 1787–1805. https://doi.org/10.1007/s13399-019-00575-2.
Xiao, R., Chen, L., Saha, C., Zhang, S., Bhattacharya, S., 2012. Pressurized chemical-looping combustion of coal using an iron ore as oxygen carrier in a pilot-scale unit. Int. J. Greenhouse Gas Control 10, 363–373. https://doi.org/10.1016/j.ijggc.2012.07.008.
Xing, J., Xia, X., Jin, F., Sun, X., Zhang, H., Xu, C., Ye, F., 2024. Density functional theory study on Support-Promoted CH4 reforming in Ni-based oxygen carriers for chemical-looping conversion. Appl. Surf. Sci. 656, 159691. https://doi.org/10.1016/j.apsusc.2024.159691.
Xu, D., Wang, B.o, Li, X., Cheng, Y.W, Fu, W., Dai, Y., Wang, C.-H., 2024. Solar-driven biomass chemical looping gasification using Fe3O4 for syngas and high-purity hydrogen production. Chem. Eng. J. 479, 147901. https://doi.org/10.1016/j.cej.2023.147901.
Yadav, S., Mondal, S.S., 2022. A review on the progress and prospects of oxy-fuel carbon capture and sequestration (CCS) technology. Fuel 308, 122057. https://doi.org/10.1016/j.fuel.2021.122057.
Yakan à Nwai, C., Patel, B., 2023. Techno-economic study and environmental analysis for the production of bio-methanol using a solar-aided dual-bed gasifier. Waste Biomass Valor 14 (12), 4155–4171. https://doi.org/10.1007/s12649-023-02115-6.
Yan, L., Jim Lim, C., Yue, G., He, B., Grace, J.R, 2016. One-dimensional modeling of a dual fluidized bed for biomass steam gasification. Energy Convers. Manage. 127, 612–622. https://doi.org/10.1016/j.enconman.2016.09.027.
Yan, Y., Mattisson, T., Moldenhauer, P., Anthony, E.J., Clough, P.T, 2020a. Applying machine learning algorithms in estimating the performance of heterogeneous, multi-component materials as oxygen carriers for chemical-looping processes. Chem. Eng. J. 387, 124072. https://doi.org/10.1016/j.cej.2020.124072.
Yan, Y., Thanganadar, D., Clough, P.T., Mukherjee, S., Patchigolla, K., Manovic, V., Anthony, E.J, 2020b. Process simulations of blue hydrogen production by upgraded sorption enhanced steam methane reforming (SE-SMR) processes. Energy Convers. Manage. 222, 113144. https://doi.org/10.1016/j.enconman.2020.113144.
Yang, K., Li, F., 2025. Computationally accelerated discovery of mixed metal compounds for chemical looping combustion and beyond. Energy Environ. Sci. 18 (23), 10036–10047. https://doi.org/10.1039/D5EE02521D.
Yang, F., Meerman, J.C., Faaij, A.P.C., 2021. Carbon capture and biomass in industry: a techno-economic analysis and comparison of negative emission options. Renewable Sustainable Energy Rev. 144, 111028. https://doi.org/10.1016/j.rser.2021.111028.
Yaqub, Z.T., Oboirien, B.O., Leion, H., 2023. Chemical looping combustion (CLC) of municipal solid waste (MSW). J. Mater. Cycles. Waste Manage. 25 (4), 1900–1920. https://doi.org/10.1007/s10163-023-01674-z.
Yin, J., Li, C.', Paicu, G., Su, S., 2024. Techno-economic assessment of retrofitting indirect-heated calcium looping using coal and biomass as fuels into an existing cement plant for CO2 capture. Gas Sci. Eng. 123, 205236. https://doi.org/10.1016/j.jgsce.2024.205236. Article.
Yuan, P., Guo, T., Pan, X., Hu, X., Ma, J., Xu, D., et al., 2023. Process optimization and thermodynamic analysis of autothermal coal chemical looping gasification industrial demonstration system. Fuel 334, 126667. https://doi.org/10.1016/j.fuel.2022.126667.
Zafar, Q., Mattisson, T., Gevert, B., 2005. Integrated hydrogen and power production with CO 2 capture using chemical-looping reformingredox reactivity of particles of CuO, Mn 2 O 3, NiO, and Fe 2 O 3 using SiO 2 as a support. Ind. Eng. Chem. Res. 44 (10), 3485–3496. https://doi.org/10.1021/ie048978i.
Zare, D., Akbar, A., Yari, M., 2024. Techno economic analysis of efficient and environmentally friendly methods for hydrogen, power, and heat production using chemical looping combustion integrating plastic waste gasification and

thermochemical copper chlorine cycles. Energy 289, 129941. https://doi.org/10.1016/j.energy.2023.129941.

Zeng, L., Cheng, Z., Fan, J.A., Fan, L.-S., Gong, J., 2018. Metal oxide redox chemistry for chemical looping processes. Nat. Rev. Chem. 2 (11), 349–364. https://doi.org/10.1038/s41570-018-0046-2.

Zhang, L.i, Hu, Y., Xu, W., Huang, C., Su, Y., Tian, M., et al., 2020. Anti-coke BaFe 1– x Sn x O 3−δ oxygen carriers for enhanced syngas production via chemical looping partial oxidation of methane. Energy Fuels 34 (6), 6991–6998. https://doi.org/10.1021/acs.energyfuels.0c00951.

Zhang, Y., Wang, D., Pottimurthy, Y., Kong, F., Hsieh, T.-L., Sakadjian, B., et al., 2021. Coal direct chemical looping process: 250 kW pilot-scale testing for power generation and carbon capture. Appl. Energy 282, 116065. https://doi.org/10.1016/j.apenergy.2020.116065.

Zhang, C., Li, Y., Yang, L., Fan, X., Chu, L., 2022. Analysis on H2 production process integrated CaO/Ca(OH)2 heat storage and sorption enhanced staged gasification using calcium looping. Energy Convers. Manage. 253, 115169. https://doi.org/10.1016/j.enconman.2021.115169.

Zhao, X., Zhou, H., Sikarwar, V.S, Zhao, M., Park, A.h-H.A., Fennell, P.S., et al., 2017. Biomass-based chemical looping technologies: the good, the bad and the future. Energy Environ. Sci. 10 (9), 1885–1910. https://doi.org/10.1039/C6EE03718F.

Zhao, H., Tian, X., Ma, J., Chen, X.i, Su, M., Zheng, C., Wang, Y., 2020. Chemical looping combustion of coal in china: comprehensive progress, remaining challenges, and potential opportunities. Energy Fuels 34 (6), 6696–6734. https://doi.org/10.1021/acs.energyfuels.0c00989.

Zhao, Y.-, Duan, Y.-, Liu, Q., Cui, Y., Mohamed, U., Zhang, Y.u-, et al., 2021. Life cycle energy-economy-environmental evaluation of coal-based CLC power plant vs. IGCC, USC and oxy-combustion power plants with/without CO2 capture. J. Environ. Chem. Eng. 9 (5), 106121. https://doi.org/10.1016/j.jece.2021.106121.

Zhao, Y., Chen, G., Guo, Y., Min, S., Wang, R., Xu, X., et al., 2026. Recent progress of chemical looping technology for waste plastic conversion. Appl. Energy 404, 127180. https://doi.org/10.1016/j.apenergy.2025.127180.

Zheng, H., Jiang, X., Gao, Y., Tong, A., Zeng, L., 2022. Chemical looping reforming: process fundamentals and oxygen carriers. Discov. Chem. Eng. 2 (1). https://doi.org/10.1007/s43938-022-00012-3.

Zhong, M., Cai, Y.;, Wang, C.;, Li, J., Xiao, B.o, Xu, T.;, Wang, X., 2024. Sorption-enhanced chemical looping steam reforming coupled with water splitting for syngas and H2 coproduction using waste plastic as fuel. Chem. Eng. J. 494, 152927. https://doi.org/10.1016/j.cej.2024.152927.

Zhou, C., Liu, D., Feng, Y., Dou, B., Ma, J., Ma, J., 2025. Structure design and performance of coal-fired chemical looping combustion systems: a review. Chem. Eng. J. 519, 165125. https://doi.org/10.1016/j.cej.2025.165125.

Zhu, L., He, Y., Li, L., Wu, P., 2018. Tech-economic assessment of second-generation CCS: chemical looping combustion. Energy 144, 915–927. https://doi.org/10.1016/j.energy.2017.12.047.

Zhu, X., Imtiaz, Q., Donat, F., Müller, C.R., Li, F., 2020. Chemical looping beyond combustion – a perspective. Energy Environ. Sci. 13 (3), 772–804. https://doi.org/10.1039/C9EE03793D.

Zylka, A., Krzywanski, J., Czakiert, T., Sosnowski, M., Grabowska, K., Skrobek, D., Lasek, L., 2025. Improving CO2 capture efficiency through novel CLOU-based fuel reactor configuration in chemical looping combustion. Energies (Basel) 18 (17), 4640. https://doi.org/10.3390/en18174640.